The application of seismic surveys to the evaluation of shallow coal deposits

Peter John Brabham

Frontispiece

Peter Brabham & John Dent Drilling
Seismic Shot holes at Barley Hill, Northumberland

The Application of Seismic Surveys to the Evaluation of Shallow Coal Deposits

by

Peter John Brabham

A Thesis submitted for the Degree of Doctor of Philosophy at the University of Durham

Department of Geological Sciences

August 1986

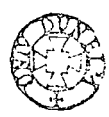

ABSTRACT

The viability of using surface seismic techniques in the exploration of shallow coal deposits in the UK is investigated. The geological factors that affect the economic viability of a prospective site are the overburden ratio and the presence of faulting, drift channels and previous mine workings.

The seismic refraction technique using both compressional (P) waves and shear (S) waves is used and also the P wave reflection technique. The P wave source used is explosive and the shear wave source is a horizontal hammer. Seven site surveys are described, six in North East England, and one in the North West.

The refraction technique using the Plus-Minus and Generalized Reciprocal Methods of interpretation is used to locate faults, estimate drift cover thicknesses and pinpoint areas of previous opencast excavation. Faults are located by a change in refractor velocity, or by a sudden change in refractor depth. Shear waves display a greater ability to image sharp depth anomalies than P waves, due to the greater velocity contrast between consolidated and unconsolidated rocks that S waves exhibit. S waves are better lithological indicators than P waves as there exist distinct ranges of S wave velocities for unconsolidated (150 to 400m/sec) and consolidated (650 to 1400m/sec) rocks.

The fundamental problem with shallow reflection surveys on land is that the shallow reflections occur at the same time as surface waves and ground roll. The reflection technique is used to locate faults and detect the boundaries of old mine workings. No reflections shallower than 70m are recorded, and in areas of thick glacial drift cover no frequencies higher than 100Hz are detected. The results of the survey to locate positions of old mine workings are inconclusive, although some features seen on the final sections could be related to boundaries between unworked and worked strata.

ACKNOWLEDGMENTS

I would like to acknowledge the NERC for providing me with a three year research grant so that I could undertake this research at Durham University, and also the NCB for funding the fieldwork. This project entailed a great deal of fieldwork, all of which was carried out by my supervisor Dr.N.R.Goulty, Mr.J.Dent and myself. I wish to thank Neil for his enthusiasm during the fieldwork and John for his technical assistance, hardwork and friendship, which always made the work an enjoyable experience.

I would also like to express my gratitude to the geologists of the Opencast Executive for their help during this project, particularly Richard Cory, Graham Sylvester, Keith Philpott, Dave Blythe, Roy Blenkinsop, and others too numerous to mention. I thank them for sparing some of their time to explain the geological complexities to me.

The seismic data processing was carried out using the computing facilities available at Durham, thanks go to Richard Hobbs, Mike Smith, and Dave Stevenson for applying their expertise to helping me to solve my computing problems and Naomi for help with all things geophysical.

In compiling this thesis a great deal of time was spent drawing the diagrams. I am grateful to Andy Reid and Karen Gittins for their patience during my constant borrowing of their draughting equipment. Thanks also go to Gerry Dresser and Alan Carr for photo-reducing the numerous diagrams over the past year. I am indebted to Dave Asbery for his helpfulness in solving many problems during my time at Durham.

My gratitude goes to Neil Goulty for his supervision over the past four years, his thorough scrutiny of my text and correction of my spulling !

On the social side, I am indebted to the geology postgraduate students (and big Paul), for making the department a pleasurable place to work and for providing me with many sporting and social highlights during my time spent in Durham.

My great gratitude goes to my parents for their help, encouragement and concern during my postgraduate education, without which this work could not have been completed. I am also indebted to my Aunt and Uncle for providing me with the financial assistance to reproduce this work. Lastly I am grateful to Anne for not only helping in the correction of my grammar, but for her love, patience and understanding during my university career.

CONTENTS

LIST OF ILLUSTRATIONS

PLATES

MAPS

FIGURES

DECLARATION

The content of this thesis is the original work of the author (other people's work, where included, is acknowledged by reference). This work has not been previously submitted for a degree at this or or any other university.

P.J. Brabham

Durham
August 1986

COPYRIGHT

CHAPTER ONE

INTRODUCTION

The basic aim of this research project is to assess the viability of using surface seismic techniques in the exploration of shallow coal deposits, in relation to the opencast coal mining industry in the United Kingdom.

Opencast mining is the process of excavating all the material down to and including the coal seam. It has distinct advantages over underground techniques including greater recovery of the in situ resources, greater safety and greater productivity. The chief disadvantage is its environmental impact (Ward, 1984). The technique is restricted to the removal of relatively thick, shallow lying coal seams or aggregations of coal seams of high quality. Opencast coal is most useful for upgrading deep mined coal because opencast coal is mined carefully, selectively and is of high quality.

Opencast coal mining in the UK began as a wartime measure. Today the UK opencast coal mining industry produces around 15 million tons of coal per annum. In 1983-1984 this accounted for 15% of the total output of the UK. Half the anthracite production in Great Britain comes from opencast mining (Davison, 1977; Barefoot, 1978; Spooner et al., 1985).

The majority of opencast coal sites are worked by civil engineering companies under the supervision of the Opencast Executive of the National Coal Board (NCB). Only 1 million tons

per annum are produced by small private, licensed mines. Opencast coal sites in the urban environment of the UK are small by world standards, site boundaries being restricted by roads, railways and villages etc. Most of the sites have reserves of less than 5 million tons, although one site in Scotland has reserves of 28 million tons. At present in the UK 20 contractors operate 51 sites (Spooner et al., 1985).

When opencast coal production began in 1942, sites were operating at an average depth of only 9m producing poor quality near surface weathered coal. Today the average site depth is 75m, but some large sites exceed 200m in depth. At these sort of depths much of the coal that is being worked was left behind by previous deep mine workings. As stated previously the quality of opencast coal is substantially higher than that of the deep mined counterpart. The basic reason for this is the methods of coal exploitation used, and the high quality coals that are exploited. After the overburden and topsoil has been removed by mechanical diggers, the sandstone and shale horizons are removed by blasting or ripping down to the coal seam, which is then left exposed (plate 1). Prior to extraction the top of the seam is cleaned by men using shovels and brushes. The coal is then carefully lifted by small cranes into waiting lorries. This ensures a 100% coal product that requires no further purification. Individual coal seams down to thicknesses of 10cm can be extracted in this way, although nearly all the sites in the UK exploit many individual seams.

At the end of a site's life the NCB is obliged to restore the land, where it is used for agricultural, industrial or leisure

purposes.

Although the general outline of the geology of the coalfields of Great Britain is well known, the detailed structure required for opencast site planning is not. Therefore exploration is carried out in areas of interest by the Opencast Executive. From the exploration phase the geological structure, coal thickness and quality can be determined at a prospect. A detailed site specification is drawn up and civil engineering companies are invited to tender for the exploitation contract. If the geological information in the specification turns out to be inaccurate, the civil engineering company who won the open tender exercise and begin to exploit the coal, may make a financial claim against the NCB. If there turns out to be more coal on site than the site specification predicted, then the contractor stands to profit. It is in the NCB's interest therefore to make as detailed a site specification as possible.

The preliminary stage of exploration involves the assessment of known geological information about the prospective area. This involves the study of geological maps, old mine plans and results from opencast sites in adjacent areas, along with studies of regional, geographic and economic constraints. From this initial phase the general feasibility of establishing a profitable mining operation can be determined. If a site appears viable then active exploration is carried out (Ward, 1984).

Exploration is undertaken using boreholes, drilling being done by subcontractors using highly mobile rigs. The holes are drilled openhole, using a tricone bit with an airflush system. The

compressed air brings rock fragments up to the surface; these are then logged, along with the hole depth, by the driller. Some holes are cored so that coal quality tests can be carried out. It is unusual to get a 100% recovery rate due to the friable sediments that are encountered. Initially boreholes are drilled on 120m centres to the deepest seam of interest. If the site appears attractive from the results of the initial holes, then a second phase of drilling is carried out to fill in to 60m centres. In areas of structural complexity, or in areas of old mine workings, boreholes may be drilled to 30m centres.

After individual holes have been drilled, the holes are geophysically logged by a geophysical contractor. The usual logs that are taken are natural gamma and gamma-gamma logs. Neutron-neutron logs have also been used, but are not employed in opencast exploration on a regular basis. (Dison & Whitworth, 1985).

The natural gamma log monitors the naturally occurring radiation in the strata. It is particularly useful for monitoring mudstone horizons. The gamma-gamma (density log) uses a Caesium 137 source and measures the flux of backscattered gamma rays at a detector at the top of the sonde. The number of backscattered gamma rays detected is inversely related to the number of electrons per unit volume of the rock. This in turn is related to the rock's bulk density. Coal, having a low density, is picked out using this method. The neutron-neutron log uses a neutron source and detector, the detector response being related to the amount of hydrogen present in the strata. This logging tool can be used to indicate the presence of water; it has also been shown

Plate 1 A dipping coal seam lies exposed at the bottom of an opencast coal site

Plate 2 Coal pillars due to previous pillar & stall mining lie exposed at bottom of cut. Subsidence features related to old mine workings are exposed in cut wall.

to correlate with the fracture density in borehole cores.

The data gathered from the boreholes are combined to give information on drift thickness, horizon lithology, coal seam depth and thickness. Individual coal seams are coded and can be correlated between boreholes. From this data set plans of drift thickness and coal seam structure can be drawn. Normal faults can be inferred by structural anomalies, or when a borehole intersects a fault plane, by direct evidence. From coal seam plans and thickness values the tonnage of coal reserves on site can be estimated. The opencast coal mine can be designed to exploit the coal in the most economic way, in light of the known geological structure.

The main geological factor that affects the economic viability of a prospective opencast coal site is the overburden ratio. The ratio can be defined as the thickness of overburden (topsoil, drift and non-coal strata), to that of the thickness of workable coal (figure 1.1). For each borehole the overburden ratio can be calculated and contoured on a plan. An average value can be calculated for the total prospect. The average figure in the UK is about 15:1. For higher grade coals such as anthracite it may exceed 25:1.

Another geological feature that affects the economic viability of a prospect is the presence of faulting. Severe faulting may make the extraction of the coal difficult. Minor faulting does not usually affect the volume of coal present. Only major faulting, when coal-bearing strata are juxtaposed against barren strata does faulting influence coal volume calculations. Faults

often mark the boundary of old mine workings; it is common to find that mining was abandoned when a fault was encountered. The precise location of the fault plane can only be inferred between two boreholes, unless the borehole intersects the fault plane. Therefore if the fault is a boundary fault, then this can lead to some uncertainty in the coal volume calculations.

The presence of deep glacial channels at a site may have caused some of the coal to have been removed by erosion (figure 1.1). The rockhead topography needs to be known in detail before the exact volume of coal present can be assessed. The drift thickness plans also need to be known for engineering purposes, as the topsoil and drift are stored separately at a working site for the ground restoration at the end of the site's life.

As opencast mines become deeper, they encroach upon coal seam horizons that may have been previously mined by deep mine techniques. The usual method of exploitation was by pillar and stall mining (plate 2). This technique can leave as much as 70% of the coal seam behind, so the presence of old mine workings may not necessarily make a site uneconomic. Exploration of old mine workings is difficult, especially as no old mine plans may exist. The volume of coal left in situ must be estimated from borehole information. The method relies upon the percentage of boreholes that intersect mine workings directly reflecting the percentage of coal left in the ground. For example if every borehole intersects a pillar, then the presence of the old workings is unknown, resulting in coal calculations being based on 100% coal present: obviously this is a very risky calculation.

Some factors affecting the economic viability of an opencast coal site.

Overburden ratio

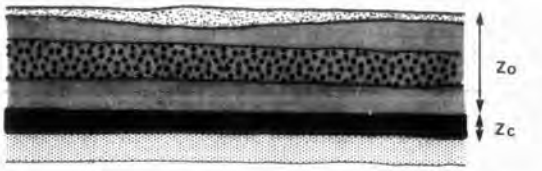

$$\text{Overburden ratio} = \frac{\text{Thickness of overburden } (z_o)}{\text{Thickness of coal seam } (z_c)}$$

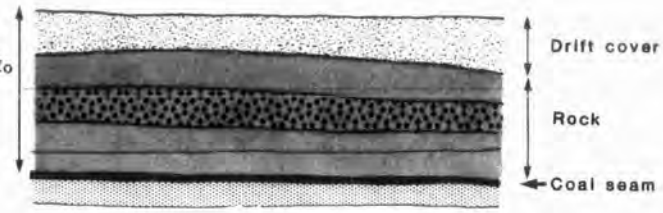

Economic limit typically 15 to 25 : 1

Faulting

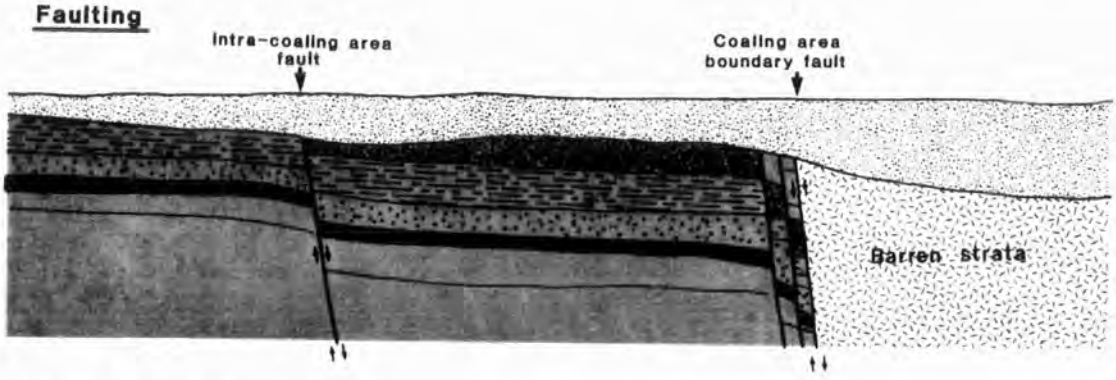

Drift channels

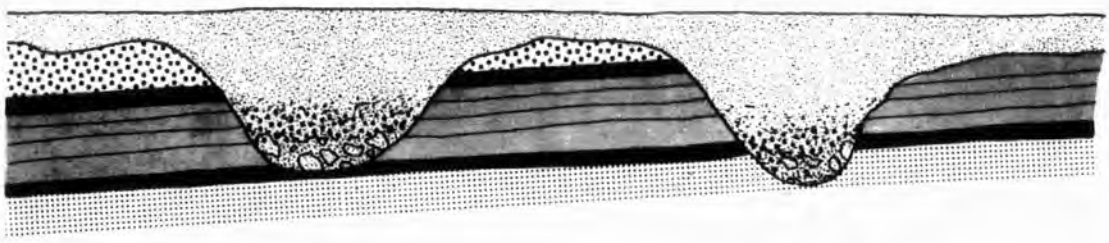

Old mine workings

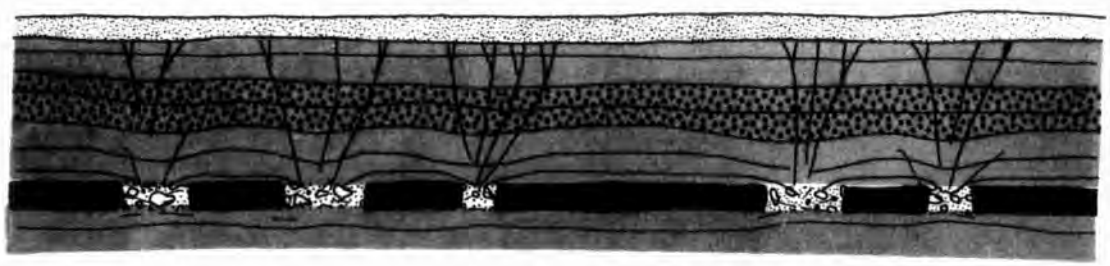

A percentage of coal already lost to old pillar & stall mining

Figure 1.1

The Opencast Executive spends 12 million pounds sterling per annum on drilling and prospecting, which is about 3% of its budget (Bush, 1985). No surface geophysical technique is used on a regular basis in the exploration phase. The objective therefore of this project was to determine the viability of using seismic techniques in the exploration phase, to help determine the detailed geological structure needed for the site specification.

Geophysical methods have been well established as an essential component of oil exploration for over 40 years. They have taken much longer to gain acceptance in the coal industry, mainly because of difficulties in gaining the degree of resolution necessary. Reflection seismology has been used as a tool for coal exploration for deep mines in the UK since 1976, following trials carried out in 1973-1974 (Ziolkowski, 1981). Seismic surveys have been used with success in every active British coalfield. The technique played a vital part in the exploration of the Selby concealed coalfield in Yorkshire (Stephenson, 1985). It has also been used in Western Area of the NCB to site deep exploration boreholes to avoid areas of structural complexity and faulting (Goosens, 1985). Reflection seismology for coalfield exploration has also been carried out in Australia (Harman, 1981), West Germany (Schlicker & Bonning, 1981), The Netherlands (De Voogd & Staudt, 1982) and Wyoming USA (Greaves, 1984).

In October 1980 the NCB undertook a one year co-operative research programme with the US Geological Survey to look into the possible development of using shallow seismic surveys in the detection of old mine workings, faults, washouts and hidden coal subcrops. The work was carried out by Dr.Hasbrouck of the USGS

using a portable seismic acquisition/processing system which he had developed. Both compressional (P), and shear (S) waves were used to explore a variety of geological situations. The results of this programme were encouraging. Success was achieved in detecting the depth to rockhead using refracted waves and locating the outcrop position of a competent sandstone overlying a coal seam. It was also suggested that old mine workings might be detected using surface waves (Hasbrouck & Padget, 1982).

It was from this initial programme that the project which is the subject of this thesis was born. Finance was obtained from the NCB to cover the costs of field work and the salary of one technician for a two year period. The author was funded by a CASE award from the Natural Environmental Research Council. The project was based at the Department of Geological Sciences at the University of Durham under the supervision of Dr.N.R. Goulty.

Some preliminary refraction work was carried out by Chester (1982) as an M.Sc. project. The major fieldwork began in September 1982. The field work was carried out in three summer seasons, (Sept.to Nov. 1982, April to Oct. 1983 and April to Sept. 1984).

In total during the course of this project, fifteen survey sites were visited, at some of which only a reconnaissance survey was carried out. The seven site surveys included in this thesis involve multiple seismic lines, and cover a wide variety of geological targets investigated using the seismic refraction and reflection techniques. Six of the survey sites are located in the North East of England on the Durham and Northumberland coalfields

(map 1), the sixth being in the North West of England on the Cumbrian coalfield (map 2).

The seismic data processing was carried out at Durham University using the departmental computing facilities. During the course of this project, some fieldwork and interpretation of seismic refraction data was carried out by undergraduates from within the department as described in their B.Sc. dissertations (Gilbert 1984, Wollett 1985). Other geophysical techniques were studied, such as magnetics (Goulty et al., 1984), by graduate and postgraduate students at Durham University since 1982. Magnetics has limited use in opencast exploration; it is used to precisely locate coalfield igneous dykes that are encountered in the Northumberland and Scottish Coalfields.

SURVEY SITES IN THE NORTH EAST OF ENGLAND

Durham & Northumberland coalfield

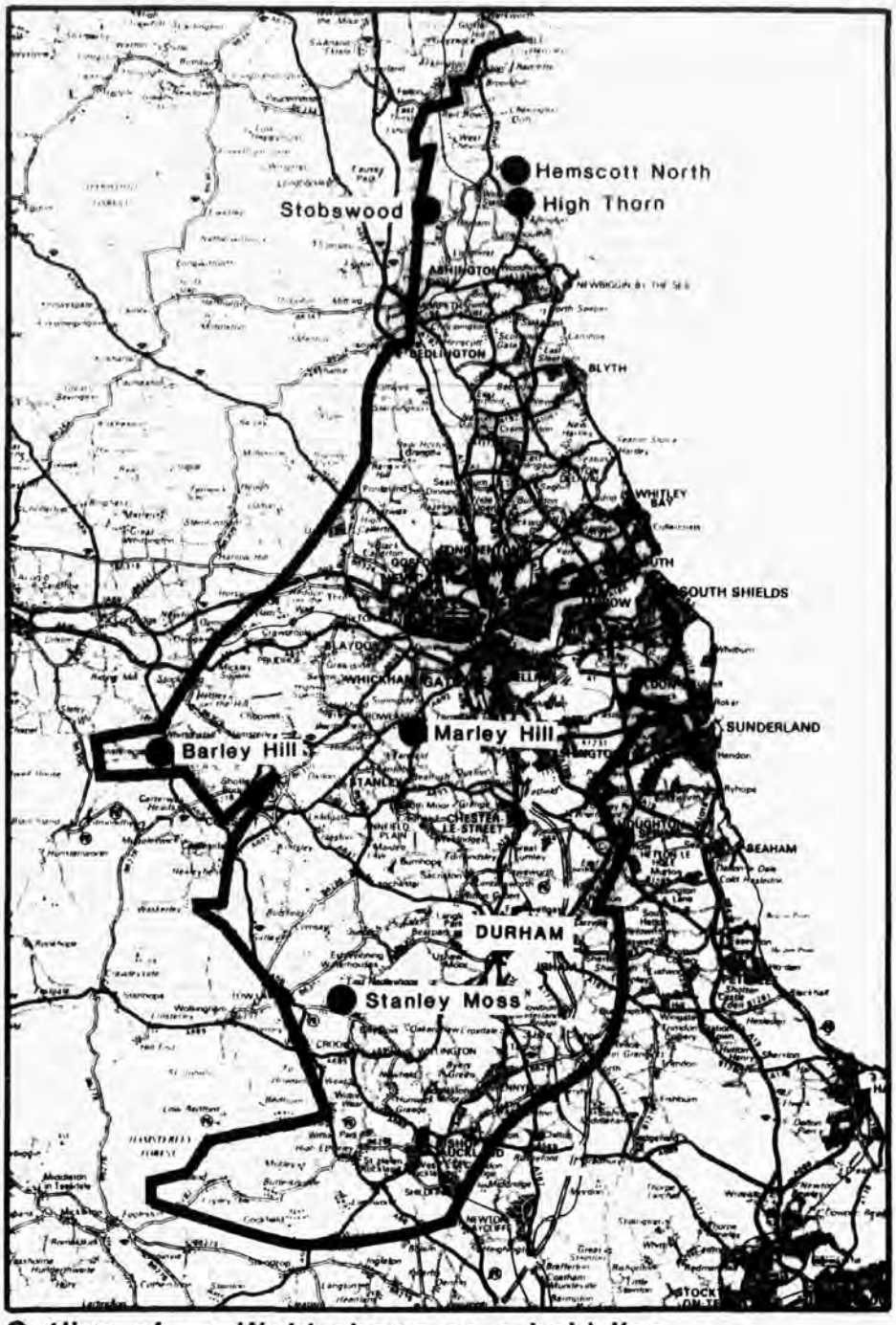

Outline of coalfield shown as a bold line

Scale 1:200000

Site Number

1. Stanley Moss
2. Barley Hill
3. Hemscott North
4. High Thorn
6. Stobswood
7. Marley Hill

MAP 1

SURVEY SITE IN THE NORTH WEST OF ENGLAND

Cumbrian coalfield

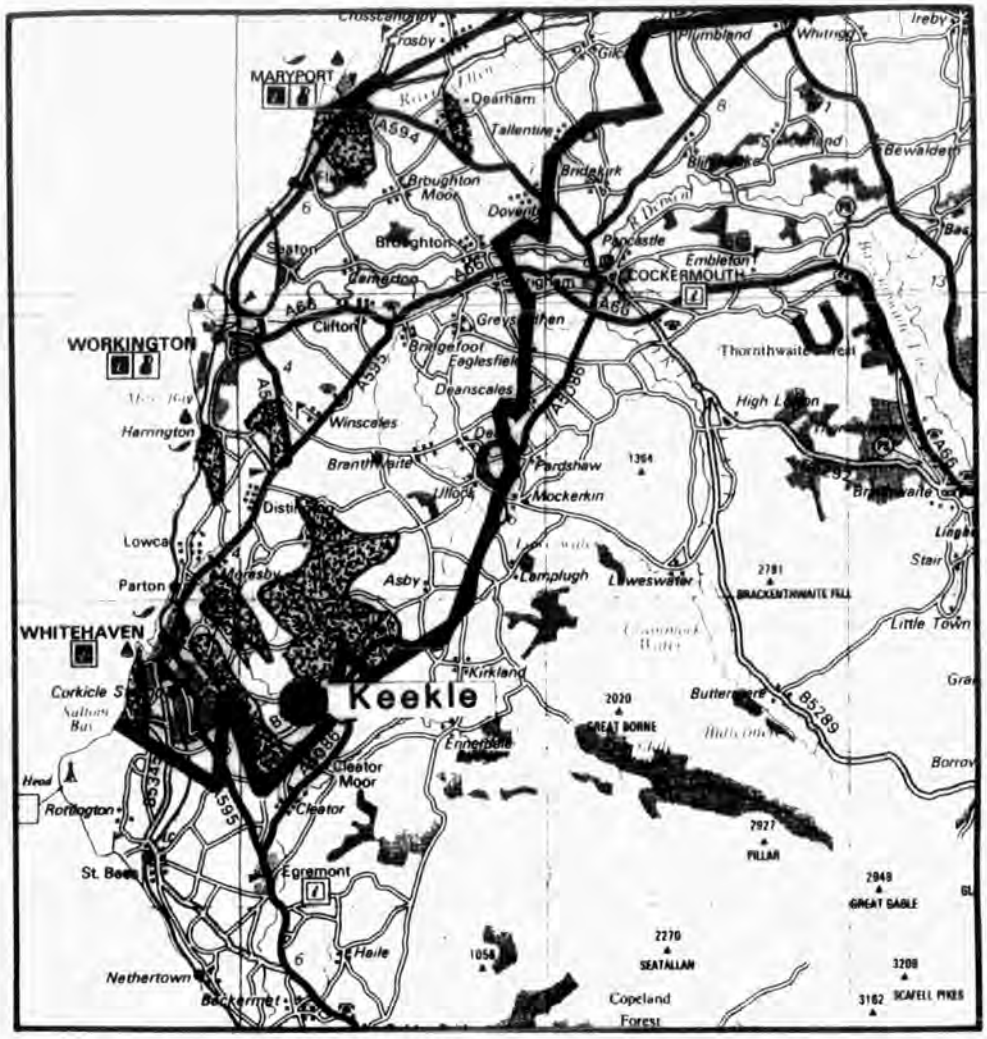

Outline of Upper Carboniferous strata shown as a bold line outcropping productive measures shown stippled

Scale 1:250000

Site Number

5. Keekle

MAP 2

CHAPTER TWO

SEISMIC THEORY

2.1 TYPES OF SEISMIC WAVES

Compressional and Shear Waves

The seismic method utilises the propagation of waves through the earth. Seismic waves are often referred to as elastic waves because they cause deformation of the material in which they propagate. Two types of elastic wave propagate through solids. The first type causes particles to move longitudinally in the direction of wave propagation and thus involves both dilation and shear. The second type causes particle motion perpendicular to the direction of propagation and thus involves only shear. The two wave types are called compressional or primary (P), and shear or secondary (S) waves.

The propagation velocities of the two wave types through a rock mass depends upon the rock's bulk modulus (K), shear modulus (μ) and the density (ρ).

The relationship between the compressional wave velocity Vp and the elastic constants is;

$$Vp = \frac{\sqrt{K + 4/3\ \mu}}{\rho} \qquad \text{Equation 1}$$

and between the shear wave propagation velocity Vs and the elastic constants is ;

$$Vs = \sqrt{\frac{\mu}{\rho}} \qquad \text{Equation 2}$$

When shear waves propagate, the motion of individual particles is perpendicular to the direction of wave propagation. If the particles all move in parallel lines the shear wave is said to be polarized. If the motion is in the vertical plane it is designated an Sv wave, if the motion is horizontal it is termed an Sh wave (figure 2.1). From equation 2 we see that Vs is dependent upon the shear modulus of the rock. As shear deformation cannot be sustained in a liquid, then shear waves will not propagate through a liquid.

If both the P and S wave velocities can be directly measured through a rock then by combining equations 1 and 2 we get;

$$\frac{Vp}{Vs} = \sqrt{\frac{K}{\mu} + \frac{4}{3}} = \frac{2(1-\sigma)}{1-2\sigma} \qquad \text{Equation 3}$$

The above equation reveals that the compressional wave velocity will always be greater than the shear wave velocity in the same medium. By re-arranging equation 3 we can directly determine Poisson's ratio (σ) for a rock by knowing the values of Vp and Vs.

$$\sigma = \frac{(Vp/Vs)^2 - 2}{2(Vp/Vs) - 2} \qquad \text{Equation 4}$$

The velocity ratio Vp/Vs for most consolidated rocks is between 1.5 and 2.0. However, in near surface unconsolidated layers, ratios between 4.0 and 8.0 have been observed (Weist & Edelmann, 1984.)

One practical feature arising from studies of wave propagation velocities is that P wave velocities are strongly influenced by the pore filling of the rock matrix. Experiments have shown that P wave velocity is increased markedly by the presence of ground water. Conversely shear wave velocities hardly change at an interface between dry and wet sand. It matters little whether the rock matrix is filled with air or water, as it is the rock matrix itself which plays the decisive role (Weist & Edelmann, 1984.).

Surface Waves

In an infinite isotropic medium only P and S waves can exist. However when the medium does not extend to infinity in all directions, but is bounded by a surface, other wave types can be generated. These waves are called surface waves since they are confined to one of the surfaces that bound the medium (Telford et al, 1976). In exploration seismology the surface waves are regarded as undesired noise and are usually referred to as "ground roll". In P wave recording the ground roll is made up of Rayleigh waves, whereas in shear wave recording we are concerned with Love waves.

Rayleigh Waves

Rayleigh waves are complex, the particle motion on the surface being retrograde elliptical. The amplitude of the wave decreases with depth below the surface. Theory shows that in a uniform half-space the velocity of the Rayleigh wave is frequency-independent and is a function of the Vp/Vs ratio of the medium (or Poisson's ratio) and the absolute value of Vs. The

Rayleigh wave velocity is just less than the shear wave velocity of the medium. For example in a medium with a Vp/Vs ratio of 1.7, the Rayleigh wave velocity is 0.92Vs, whereas for an unconsolidated medium with a Vp/Vs ratio of 4.0, the Rayleigh wave velocity is 0.95Vs (Waters, 1978).

In reality the Rayleigh wave arrivals are more complex than this. The near surface "low velocity zone" found in practice causes a disturbance to the simple conditions outlined above. For high frequencies the wave does not penetrate deeply and obtains a velocity nearly equal to that of the shear wave velocity of the near surface. Rayleigh waves of low frequency (long wavelength) penetrate into the underlying higher velocity surface layers; their velocity then approaches the shear wave velocity of the deeper higher velocity layer. This variation of velocity with frequency is called dispersion. The net effect on the seismic recording is that the wave appears as a wave train over a relatively large time interval.

Love Waves

In shear wave exploration using Sh waves, the surface waves are Love waves. Love waves are formed by energy trapped in the surface layers. They can only exist when there is a low velocity layer overlying a deeper higher velocity substratum (a condition commonly found in practice). They exist by multiple reflection between the top and bottom surfaces of the low velocity layer, the ground motion being in a horizontal plane. Love waves are also dispersive. The Love wave velocity is equal to the S wave velocity of the surface layer for short wavelengths and to the S

wave velocity of the underlying layer for long wavelengths (Waters, 1978).

Wave Generation

In land exploration seismology, elastic waves are generated by imparting a sudden stress to the earth. In practice both shear and compressional waves are generated no matter what forces are applied to the ground. The desired technique is to apply forces to the ground such that a large percentage of energy produces the wave type of interest.

For P wave land surveys, P waves can be generated by hitting a metal plate vertically with a hammer, or by dropping a weight onto the ground. By far the most efficient generator of P waves is dynamite, charges being exploded in boreholes. Dynamite is a pure generator of P waves, S waves being produced by interaction of P waves with the land surface, or other inhomogeneities in the vicinity of the source. Other modern P wave generation techniques have been used in shallow exploration projects involving the use of propane/oxygen gas guns (Mc Cann et al., 1985), vibrators (Nunn & Boztas, 1977), and mini-SOSIE tampers (Greenhalgh et al., 1986).

In contrast to P waves, shear waves are polarized. In exploration work horizontally polarized shear waves are preferred as they are autonomous, that is all transmitted, reflected and refracted secondary waves from horizontal interfaces are of Sh type only. The most common method of shear wave generation involves the use of a horizontally moving plate. Figure 2.2 displays the wave types generated by such a mechanism (Edelmann &

Elastic wave types

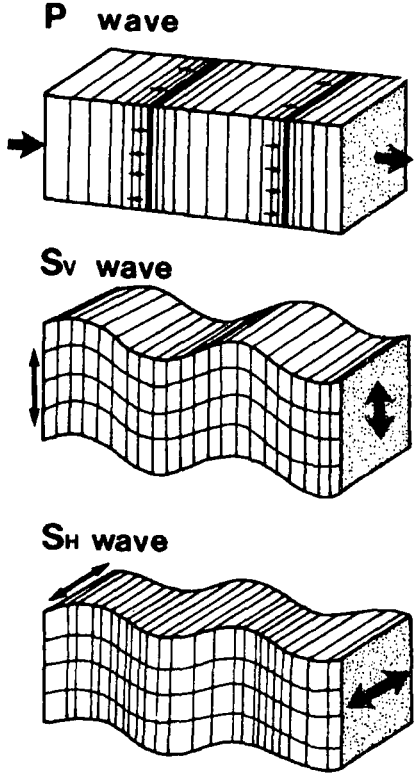

Figure 2.1

Wave types generated by shear wave stand

(Horizontal hammer technique)

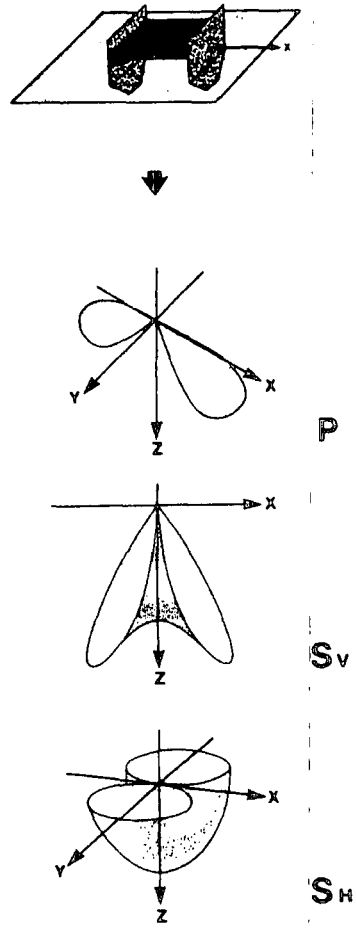

Redrawn from Edelmann and Schmoll, 1983

Figure 2.2

Schmoll, 1983a), Sh waves having a much greater amplitude than other wave types. In practice the baseplate is made up of a heavy stand which is firmly embedded into the ground. A horizontal force is then imparted to the baseplate; the force may come from a hammer, a falling weight or an accelerated mass. In the Soviet Union shear wave exploration has been carried out using explosive techniques (Edelmann & Schmoll, 1983a).

2.2 SEISMIC EXPLORATION FOR SHALLOW COAL DEPOSITS

When elastic waves are generated, the wave propagates at the compressional or shear wave velocity of that medium. The near surface layers of the earth consist of distinct layers of differing physical characteristics each one having a different P and S wave propagation velocity. When an elastic wave encounters a boundary between layers then energy may be refracted or reflected back towards the earth's surface.

The seismic refraction and reflection techniques have been developed over the past century to explore the subsurface.

It is beyond the scope of this chapter to describe both exploration techniques in great detail as many introductory texts exist for this purpose (e.g. Dobrin, 1976. Telford et al., 1976). The discussion in this chapter is restricted to those aspects which have particular relevance to exploration over shallow targets and, in particular to the exploration of shallow coal deposits.

2.3 SEISMIC REFRACTION

The seismic refraction technique works best when it is applied to geological situations where there are essentially flat lying strata, with seismic velocities which increase successively with depth.

Figure 2.3 displays the fundamental principles of the exploration method, which depends upon the seismic ray paths obeying Snell's Law. When a wave crosses from a low to high velocity medium an incident angle must exist whereby the wave is refracted along the interface between the two layers. This wave is called the critically refracted wave, and the incident angle of that wave on the boundary the critical angle.

Figure 2.3 shows a wave generated at point O and radially emanating from that point at the velocity V1 of the first layer. When the spherical wavefronts strike the boundary between layer 1 and layer 2 where the velocity suddenly increases, the energy is then refracted into layer 2 according to Snell's Law. The wavefront now radiates through layer 2 at the increased propagation velocity V2. The portion of the wavefront which travels along the interface between layer 1 and layer 2 subjects the boundary to an oscillating stress which generates new disturbances along the boundary. These disturbances in turn spread out spherically in the upper layer at velocity V1 and return to the ground surface. This is called the head wave.

The wavefront radiating downwards into layer 2 then refracts into layer 3, which produces a head wave in layer 2, subsequently

refracted back into layer 1 and so returns to the surface. Receivers can be placed on the ground surface with increasing offset from point O (shot point) to monitor the return of energy to the surface. The ray paths that produce the fastest route through the model for energy travelling from the shot to the receiver produces the "first break" on the recording system at the receiver position. If the first breaks are plotted on a time versus distance graph, the resultant traveltime graph would resemble that in figure 2.3.

It can be seen that the time-distance graph displays three distinct linear segments, the reciprocal of the gradient of each line yielding the propagation velocity of each of the geological layers. This is due to the fact that with increasing offset from the shot point, the rays that travel the longer but faster path through layer 2 overtake those travelling directly through layer 1. Therefore a point exists on the ground surface where the arrival times for the direct and refracted rays are equal. The distance from this point to the shot point is called the crossover distance. There is a second crossover distance at a greater offset where the waves that take the path through layer 3 take the same time as those critically refracted in layer 2.

The linear segments on the traveltime graph can be extrapolated back to the time axis to yield the intercept time for each layer (figure 2.3). The intercept time for each layer is a function of the propagation velocity for that layer and all the overlying layers. For a two layer model the intercept time is given by:

$$IT2 = 2z_1 . \frac{\sqrt{V_2^2 - V_1^2}}{V_2 . V_1} \qquad \text{Equation 5}$$

Refraction surveying - 3 layer case

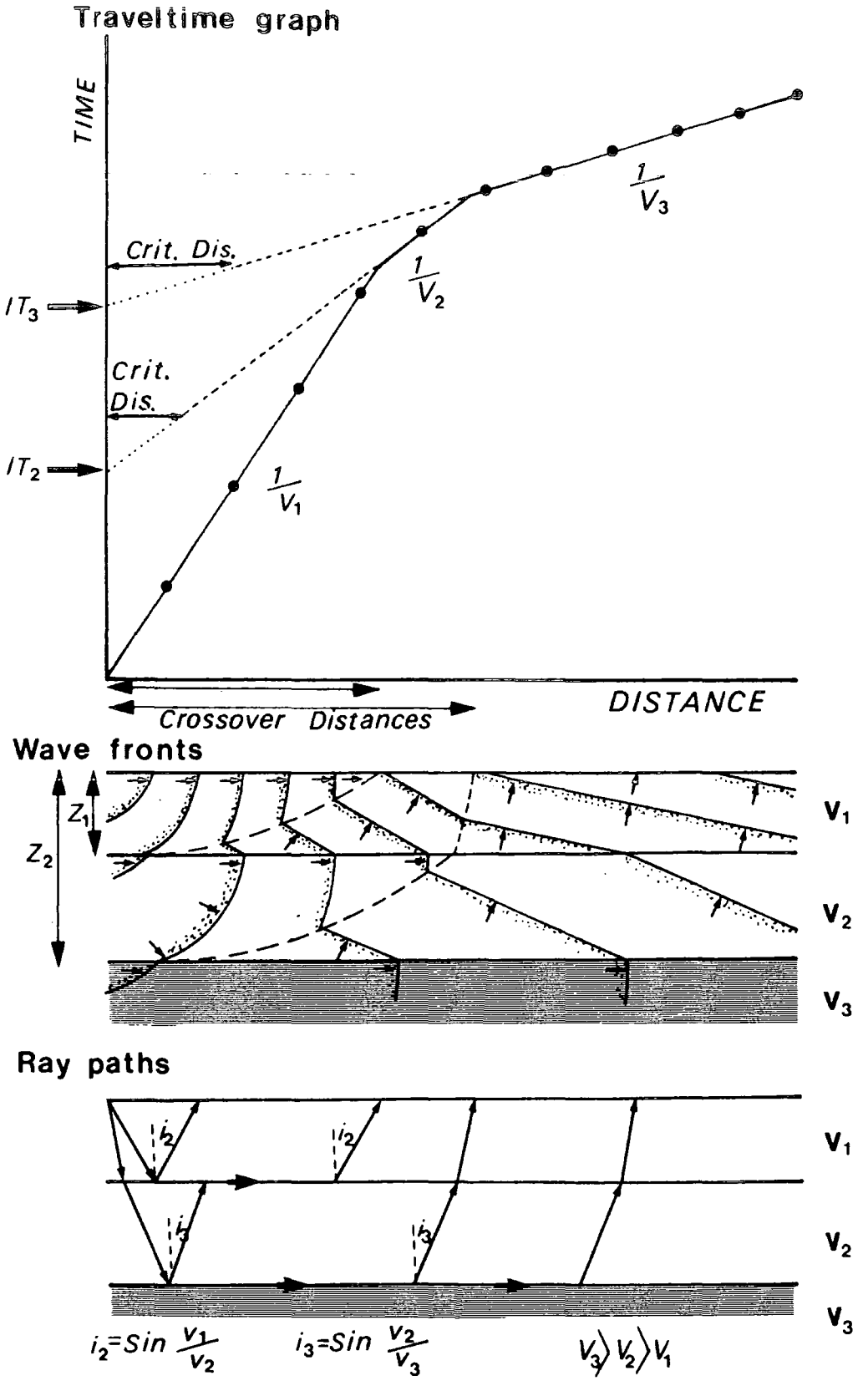

IT = Intercept Time

Figure 2.3

For n layers overlying a half space is given by:

$$ITn = 2 \sum_{i=1}^{n} Z_i \cdot \frac{\sqrt{V_{n+1}^2 - V_i^2}}{V_{n+1}\ V_i} \qquad \text{Equation 6}$$

By rearranging in terms of the layer thicknesses;

$$Z1 = \frac{IT_2}{2} \circ \frac{V_2 \cdot V_1}{\sqrt{V_2^2 - V_1^2}} \qquad \text{Equation 7}$$

The crossover distance (Cd1) can also be used to determine the layer thickness;

$$Z1 = \frac{1}{2} \cdot \sqrt{\frac{V_2 - V_1}{V_2 + V_1}} \circ Cd_1 \qquad \text{Equation 8}$$

The principle that the reciprocal of the gradients of the linear segments on the traveltime graph yield the layer velocities is only true for horizontal interfaces. If one introduces a dip to the refractor, the graph immediately becomes more complex. The dip will cause the apparent velocity of the layer to be greater or smaller than the true velocity, depending upon whether the line is shot updip or downdip. Only by shooting the line in both directions and using an averaging technique on the apparent velocities will the true velocity of the refracting layer be determined. This is called a reversed refraction line.

Various equations exist for the determination of layer velocities, depths and dips for planar layer models (Dobrin, 1978; Green, 1974). Using these simple equations an average refractor velocity and dip can be determined, but only for planar layers. If the refractor has an undulating topography or variable lateral velocity structure, the results of applying the above method will

be to produce a "best fit" planar layer solution.

In certain circumstances layers may not be detectable by the seismic refraction method. This is due to phenomenon referred to in the literature as the blind zone or hidden layer problem (Northwood, 1967 ; Sjogren, 1984). This indetectability may be due to:

1. Insufficient velocity contrast or insufficient thickness of an intermediate layer - hidden layer problem.
2. Velocity inversion, i.e. the velocity of a layer is lower than in the overlying layer - blind zone problem.

The basic assumption of the refraction method is that the seismic velocity through each successive layer will increase with depth. If this is not true then ambiguous depths will result from using the technique.

Using the refraction method over complex structures with variable velocities requires the use of more advanced interpretation techniques using reversed refraction data.

Advanced Interpretation Techniques

Advanced interpretation techniques exist, which enable complex structures with a variable lateral velocity to be explored. The techniques fall into two broad categories: those which work on wavefront reconstruction and those which use raypaths.

Graphical Construction / Wavefront Methods

Wavefront reconstruction, usually by graphical means, forms the basis of several methods; Thornburgh (1930), Gardøner (1967), Hales (1958) and Rockwell (1967). These methods rely on complete reversed coverage at every receiver location (for each refractor) on the traveltime graph. Unfortunately being graphical techniques they are very time consuming to use, especially on large data sets.

Sjogren (1984) advocates the use of Hales' method (1958) as the most convenient to use. The method considers critically refracted rays which diverge from a common point on the refractor. The technique requires two surface points which receive energy from the same point on the refractor, one in each direction of shooting. The positions of the two surface points are determined graphically. The position and radius of the circle to which the refractor must be tangential can be calculated. The method requires the prior knowledge of overburden and refractor velocities. Hales' method is particularly suitable to use when the refractor surface is very irregular.

Delay Time Methods

The delay time method was adopted for use during this project because it can be carried out easily using digital computers. This makes data processing very quick and leads to a rapid turn around in the interpretation time. The concept of delay time introduced by Gardøner (1939) is adapted by a variety of interpretation techniques. The delay time is defined as the

traveltime for any slant raypath between ground surface and a refractor minus the time required to travel the horizontal projection of the raypath along the refractor at the velocity of the refractor (Sjogren,1984). For a simple two-layer case, the total traveltime from a refracted first arrival can be considered to consist of the time taken for the wave to travel the horizontal distance between the shot and receiver at the velocity of the refractor plus the shot and receiver delay times.

Using completely reversed refraction data, interpretation techniques can separate the delay times, and determine the refractor velocity and topography. Two techniques are available, and are described in the following sections.

Common Receiver Point Method

This method was used by Hagedoorn (1959) and Hawkins (1961). It utilises the recording of a refracted arrival from the same refractor at a single geophone from two separate shot points (one each side of the geophone). Figure 2.4 shows the principle of the method. For a geophone at location G, the so-called "minus" and "plus" times can be defined. Three parameters need to be known, the traveltime from shot A to receiver G (Tag), the traveltime from shot B to receiver G (Tbg) and the traveltime from one shot point to the other via the refractor (Tab). The shot to shot traveltime is called the "reciprocal time".

By plotting a graph of minus time versus distance the lateral velocity variations in the refractor can be monitored as the gradient of the graph is equal to 1/Vr, where Vr is the velocity

of the refractor.

The plus time is a good approximation to twice the geophone delay time, and can be used to determine the depth to the refractor directly below the geophone. A depth conversion velocity (Vcon) is required to convert the plus time to depth. For a two layer case it is defined as;

$$Vcon = \frac{V_1 . Vo}{\sqrt{V_1^2 - V_0^2}} \qquad \text{Equation 11}$$

Where Vo is calculated from analysis of the direct wave and V1 is calculated from the minus graph.

$$\text{Depth to refractor} = \frac{1}{2}.\text{Plus Time} \times Vcon \qquad \text{Equation 12.}$$

Therefore by plotting the depth below each geophone location, a profile of the refractor topography along the refraction survey can be drawn.

Common Refractor Point Method

This method is essentially a more sophisticated adaptation of the common receiver point method. It is also called a curve displacement method. The technique is described by Palmer (1980;1981) and is called the Generalized Reciprocal Method (GRM). The technique has advantages over the common receiver method particularly in the increased resolution of complex refractor structure.

The method combines arrivals at two receiver locations from two shot points. The receiver locations are separated by a distance XY (figure 2.4), such that the refracted arrivals at each receiver emerge from the same point on the refractor. Two parameters are defined, the velocity analysis function and the time depth function. By plotting the velocity analysis function (at the mid point of the two receiver locations) versus distance, the refractor velocity can be mapped out, as the reciprocal of the gradient of the plot yields the refractor velocity. If the refractor is dipping at an angle i, the calculated velocity has to be multiplied by a factor cos i in order to obtain the true velocity. The time depth can be converted to depth using the same conversion velocity formula as the common receiver method (Equation 11), the value for V1 being determined from the velocity function graph.

Phantoming of Refraction Data

The delay time methods rely upon the manipulation of a complete set of first break data points from each refractor under investigation. The first stage carried out on the data set in multilayer situations is to identify from which refractor the data point originates. This may not be an easy task as inflections on the traveltime graph caused by the onset of arrivals from successively deeper horizons may not be able to be delineated from those caused by lateral geological changes. Ambiguities may only be resolved by using multiple shot points for each spread and observing the parallelism of the curves (Ackermann et al., 1986).

Common Receiver Point Method

Reciprocal method (Hawkins)
Plus-Minus method of interpretation (Hagedoorn)

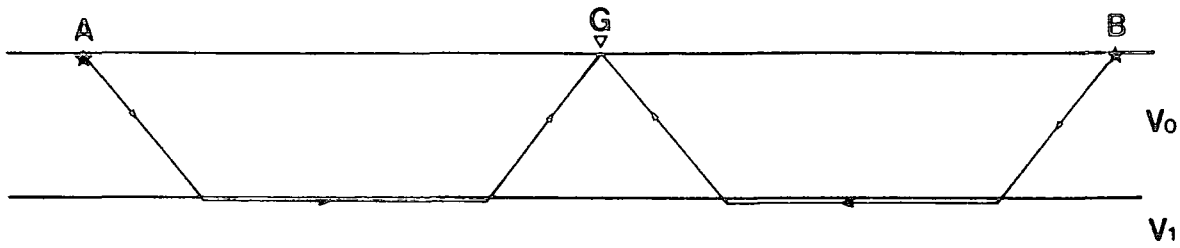

For a geophone located at G

Minus time $(T_{AG} - T_{BG})/2$ Equation 9

Plus time $T_{AG} + T_{BG} - T_{AB}$ Equation 10

Common Refractor Point Method

Generalized Reciprocal method of interpretation (Palmer)

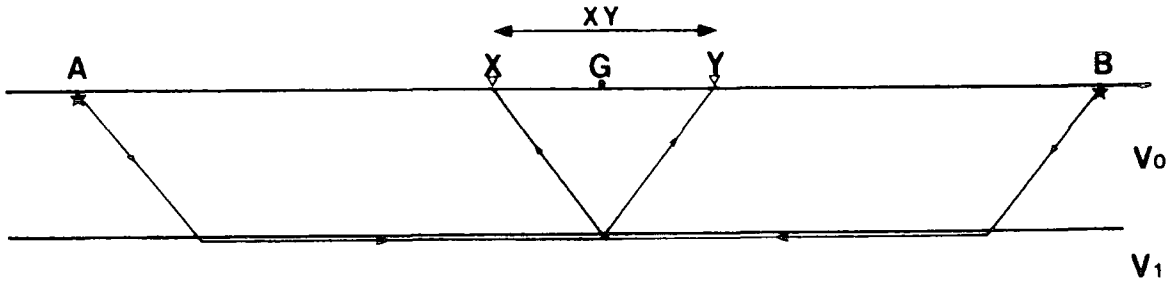

At location G

Velocity analysis function $(T_{AY} - T_{BX} + T_{AB}) / 2$ Equation 13

Time depth function $[T_{AY} + T_{BX} - (T_{AB} + XY / V_1)]$ Equation 14

Figure 2.4

When multiple coverage exists and there is no ambiguity from which refractor each data point originates, the law of parallelism of refraction data allows the tying together of data points from each refractor to yield a complete set of reversed traveltime curves for each one. This process is known as phantoming (Sjogren 1980 ; Lankston & Lankston, 1986).

The phantoming procedure allows the recording of both forward and reverse traveltime data which is identical to those that would have existed if:

1. No refracting horizon existed below the one being studied.
2. Refracted arrivals could be recorded at less than the cross-over distance.

Calculation of the Correct XY Value

The method described by Palmer (1980) for the estimation of the correct XY spacing (equation 14) is by inspection of the Velocity Function graph. Perturbations on the Velocity Function graph caused by anomalous depth variations in the refractor are removed at the optimum XY spacing. The anomalies may not be of sufficient magnitude in shallow refraction surveys for this technique to be adopted. Hatherly & Neville (1986) point out this difficulty when using a coarse geophone spacing. He states that for a depth to the refractor of less than 20m, often it is not possible to determine the correct XY spacing by this method.

The best technique to apply, is to firstly use the Plus-Minus method to calculate the refractor velocity and approximate depth

of the refractor. Then the optimum XY spacing can be determined using Snell's Law.

Calculation of Reciprocal Value

In reality the reciprocal time is rarely directly measured during the field survey, except for short refraction spreads. A practical reason for this is that it may be actually impossible to directly measure the reciprocal time in the case of a multilayer formation. The reciprocal time may be estimated in two ways. The first method is from the phantomed traveltime graph, the end times on the graph giving the reciprocal time. It is also a useful check to note that the reciprocal time in the forward and reverse directions should be equal (within error bounds). If they are not, then this indicates that an incorrect step has been carried out in the phantoming procedure, which makes the rest of the interpretation invalid The Second method for the calculation of the reciprocal time is to use a short refraction spread where the reciprocal time has been directly measured and a few plus times/time depths calculated. The "floating" plus times/time depths from the large survey line can be tied into the values calculated from the short refraction spread at the coincident geophone locations, (Lankston & Lankston, 1986).

Note that the reciprocal time does not affect the shape of the refractor topography along the line, as it is a constant value applied to the plus time/time depth calculation. The reciprocal time only affects the mean depth value.

Refractor Velocity Analysis

Figure 2.5 displays the differences between the two methods when it is used to determine the refractor velocity. As can be seen the calculation of refractor velocity using the common receiver method uses different portions of the refractor in the forward and reverse directions to arrive at the velocity calculation. Therefore an average velocity over a broad area is defined.

The common refractor point method samples the refractor between the same two points in both the forward and reverse directions to arrive at the velocity determination. It therefore seems clear that the common refractor technique has distinct advantages.

The major drawback in using the common refractor technique for velocity analysis is that two geophones with different surface locations are used in the calculation. In practice small random time delays are encountered at each geophone location due the very near surface, features such as land surface undulations, old shot holes and near surface ground variations can cause time shifts of up to 2 msecs on the data (Figure 2.6 ; Domalski, 1956). The advantage that the common receiver method has is that, because the same geophone is used in the minus time calculation, the delay due to the very near surface is removed. This results in a smooth minus graph. The common refractor technique however uses different geophones with different near surface delays. Therefore after subtraction of the two traveltimes the near surface delays do not cancel out, and some residual delay is still present. This random delay is transferred to the velocity function graph causing

Figure 2.5

Common Receiver Point Method

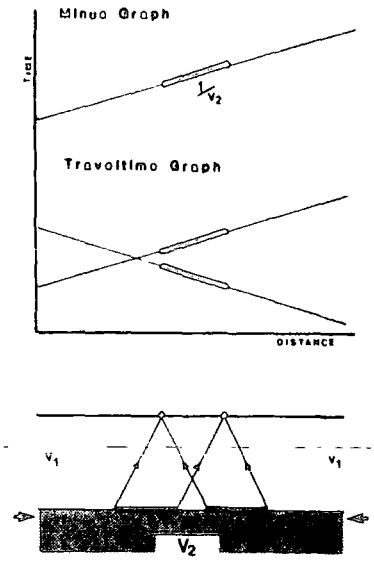

Common Refractor Point Method

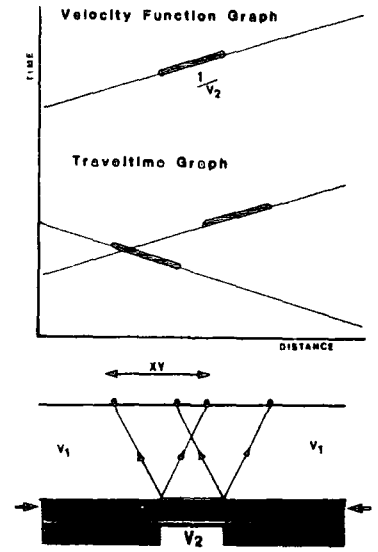

Figure 2.6

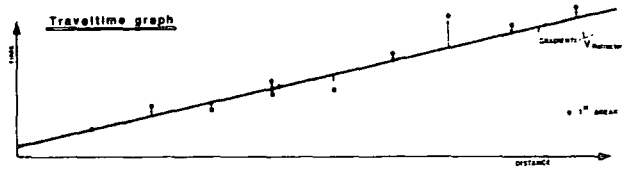

The effect of the near surface on the travel time-distance graph

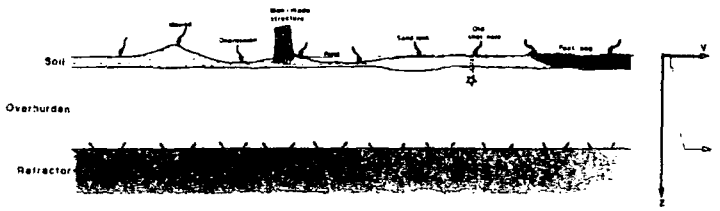

scatter of the data points.

Refraction in Multilayer Cases

In reality a simple two layer case does not exist, because even in a simple overburden/bedrock situation there is a near surface low velocity soil layer which must be taken into consideration. If this layer is not accounted for, then erroneous refractor depth estimates can result. To remove the effect of the soil layer the following technique is adopted.

Along the profile, short offset refraction spreads are used to determine the direct wave velocity and yield depth information about the soil layer. From the traveltime graph the direct wave can be extrapolated back to the time axis. Invariably the direct wave does not go through the origin, indicating that it is in fact a very shallow refraction from the base of the soil layer, the intercept time giving the depth of the soil layer. The value of the half intercept time is a good approximation of the plus time of the soil layer at the shot point. Using linear interpolation between shot points, a plus time curve can be determined along the whole refraction line. The soil plus times are subtracted from the plus times for the deeper refractor before depth calculations are carried out. For full interpretation of multilayer situations see appendix A.

2.4 REFRACTION OVER SHALLOW STRUCTURES

As stated in the introduction, the ~~structures~~ factors that affect the economic viability of a prospective opencast coal site are the overburden thickness, faulting and drift channels. Refraction surveys can help to delineate these structures, but for each structure different raypath geometries must be considered which result in dissimilar curves on the time distance graph.

Overburden Thickness

Coal seams exhibit a lower velocity than other rock units in a typical Carboniferous sequence with sandstones and shales. Typically the sandstone unit will exhibit the highest seismic velocity in the sequence. Therefore the coal seam will not act as a refractor if there are other rock types present. Consequently the depth to the coal seam cannot be measured directly using a refraction survey. The refraction technique can be used to determine the thickness of the overburden, as the overburden/rockhead boundary will act as a refractor.

The calculation of the overburden thickness can usually be carried out using either the P wave or S wave refraction technique. One disadvantage of using the P wave technique is that the P wave velocity can be affected by the presence of water in the rock pores. That is, the presence of the water table below rockhead can cause an abrupt increase in the P wave velocity, so the the top of the water table can act as a refracting horizon. This can be further complicated if rockhead exhibits severe weathering. The P wave velocity of weathered rock is

significantly lower than that of the fresh rock. The velocity can be so lowered that it does not produce a significant contrast with the overlying unconsolidated overburden. In this case the base of the weathering zone will now act as the refracting horizon. Any drift thickness estimates will be overestimated because the refracting surface is below the overburden/rockhead boundary.

Using S waves most of these problems do not seem to occur. S wave velocity is not affected by the presence of pore water (Edelmann & Schmoll, 1983a). Velocity contrasts between overburden and consolidated rock seem to be large even when the rock exhibits severe weathering.

Faulting

The accurate location of faults can be important in the assessment of the volume of coal in situ at a prospective opencast coal site, especially if the fault is a site boundary fault (figure 1.1).

For refraction surveys a fault buried below rockhead can be located in one of two ways. Firstly a fault can occur where two different rock types are brought against each other. Previous erosion may have planed the strata down prior to subsequent burial beneath a layer of glacial drift. In this case there is no refractor depth anomaly associated with the faulting. Any fault location in this case can only be carried out by monitoring the precise location where a change in refraction velocity occurs.

Figure 2.7 shows such a model, in which a buried fault is marked by a change in refractor velocity. The diagram shows the wavefronts produced by the critically refracted head waves through the model. In the forward direction, where the refractor changes from high to low velocity there is an associated change in the critical angle of the head wave. As the angle i2 is greater than i3, there exists a region where a head wave cannot occur. In this region diffracted waves which spread out spherically from the fault contact will be the first arrivals. With increasing thickness of the Vo layer the diffraction zone widens. Note that shooting in the reverse direction where the refractor velocity increases from a low to high value, there are no diffracted first arrivals.

In the forward direction, any measurement of the refracted arrivals on the land surface does not show an abrupt change in refractor velocity, but a gradual change due to the width of the diffraction zone (D). Due to the fact that the critically refracted ray returns to the ground surface at the critical angle, the point on the traveltime graph where the refractor velocity is seen to change is offset horizontally from where the fault plane intersects the refractor. The offset is a function of the overburden thickness and the velocity contrast between the overburden and the refractor.

If this case is taken one stage further and a buried fault modelled as a zone of low velocity separating two regions of comparable velocity (Figure 2.8), then the zone of diffraction occurs in both the forward and reverse directions. If the traveltime curves produced by this model are interpreted using the

The effect of a sudden change in refractor velocity

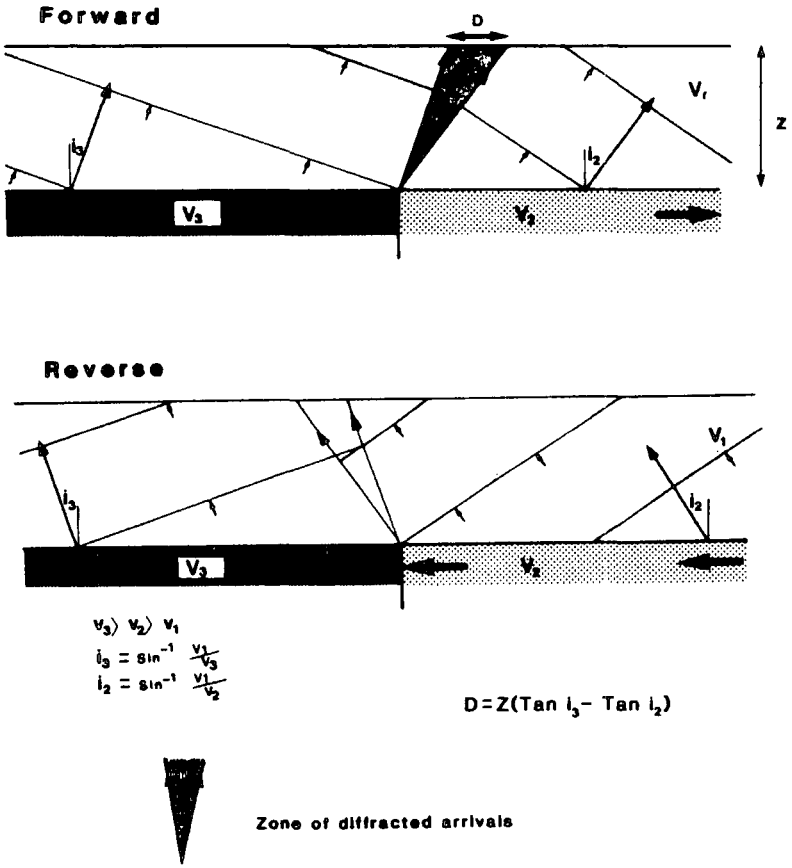

Figure 2.7

The effect of a low velocity zone

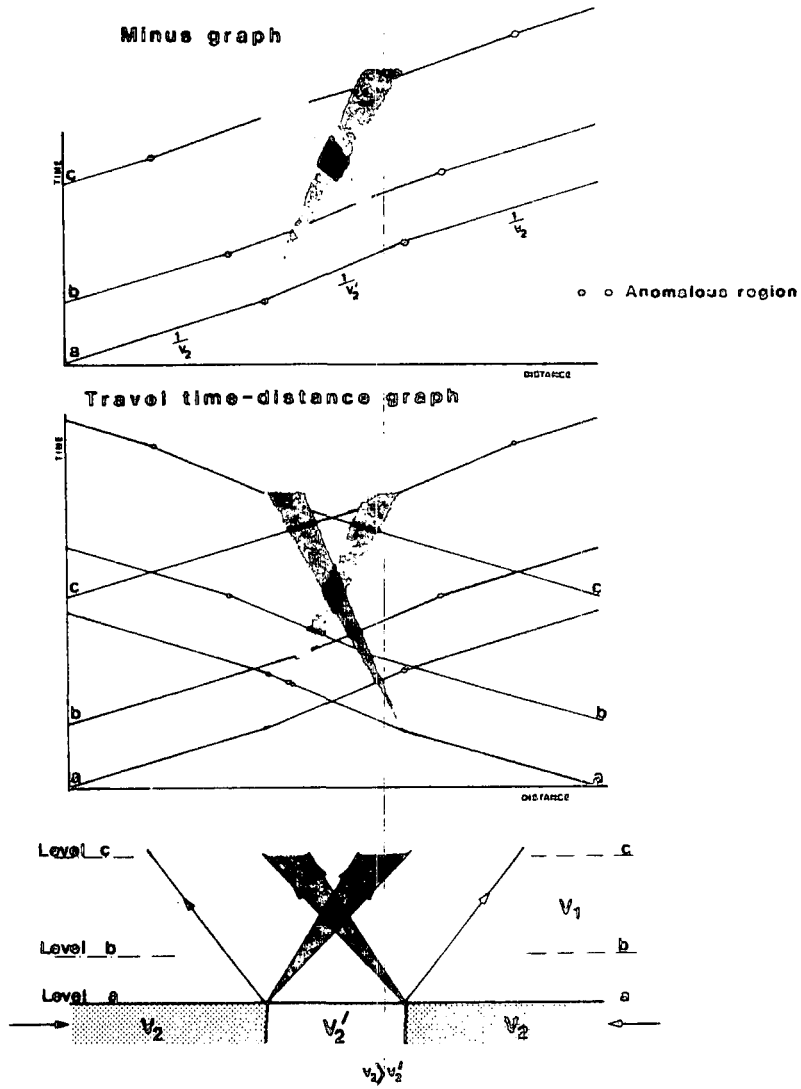

Figure 2.8

common receiver technique, the resultant minus graph displays a broad zone of low velocity much wider than the fault zone in reality. This is true except when the surface is at level a (where no overburden exists). At level c the broad zone is caused by the fact that the velocity changes monitored on the surface do not lie directly above their origin. On top of this the diffraction zones complicate the situation further. The resultant low velocity zone appears much wider than it is in reality, the apparent width being a function of overburden thickness and the velocity contrast between overburden and refractor.

The imaging of the low velocity zone can be improved by using the common refractor point interpretation technique, as this will partly compensate for the offset nature of the curves. But this technique has disadvantages when used for refractor velocity analysis (as discussed earlier).

A Fault Seen as a Step in the Refractor

A fault can also be manifested as a step in the refractor, caused by the dislocation of a high velocity layer due to faulting. The step may occur at rockhead and be buried by a layer of overburden, or there may be a planar rockhead due to previous erosion with the step occurring in a deeper high velocity refractor below rockhead.

Figure 2.9 shows the wavefronts one would expect through such a structure where the refractor velocity is constant (Sjogren, 1979). The resultant traveltime graphs are also displayed. The wavefronts are complex with diffracted and back scattered

contributions. The zones where diffracted arrivals occur as first breaks are shown with a broken line. The traveltime graphs show different forms in both the upstep and downstep directions. Figure 2.10 displays the results of carrying out both the common receiver and common refractor interpretation techniques on the traveltime graph (Sjogren, 1979).

The results of the velocity analysis using the common receiver method, show an apparent velocity anomaly on the minus graph in the vicinity of the fault step. This is due to the non cancellation of the effects of the diffracted arrivals on the traveltime graph. The common refractor method (GRM) at the optimum XY spacing effectively removes the apparent velocity anomaly due to the fault step, revealing a near constant refractor velocity. This result can be used to directly determine the optimum XY spacing to use in the time depth calculation.

The results of the depth calculation using both the common receiver and common refractor methods are also shown in figure 2.10. The depth results using the common receiver method (plus graph) show a broad zone over which the refractor depth is seen to change. This makes the fault appear as a gradual depth change, not a sharp step, making the precise location of the fault step a difficult task. Using the common refractor technique the depth anomaly is imaged much more sharply, more resembling the sharp fault step.

The model studies are for an idealised situation with a simple fault step in a constant velocity refractor, with an overburden/refractor velocity contrast of 1:2.33. The degree of

Traveltime graphs for a step in the refractor

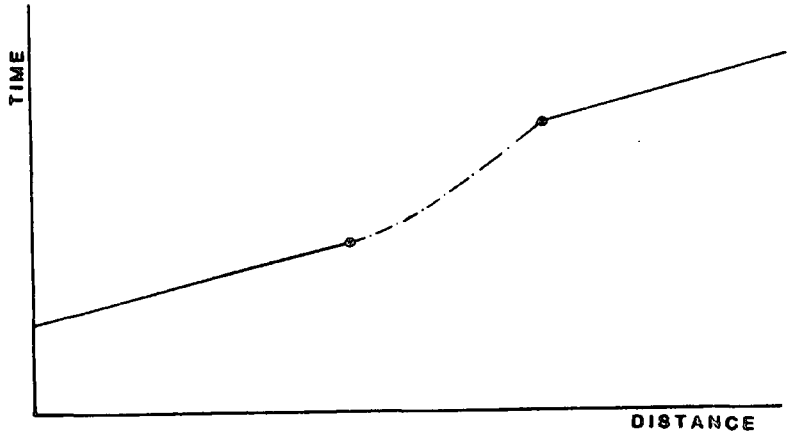

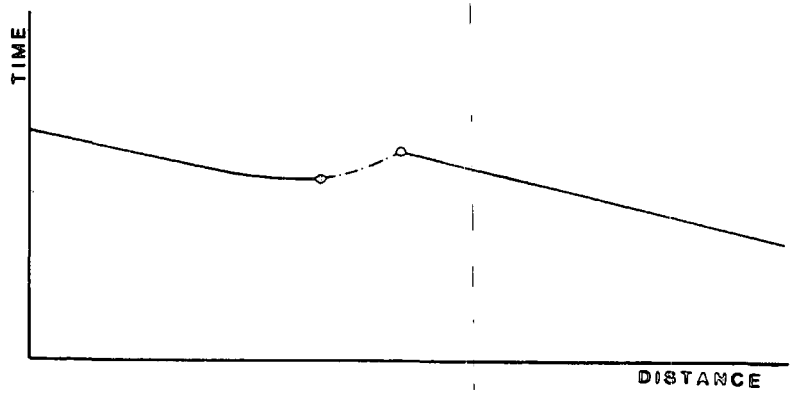

Wavefront models

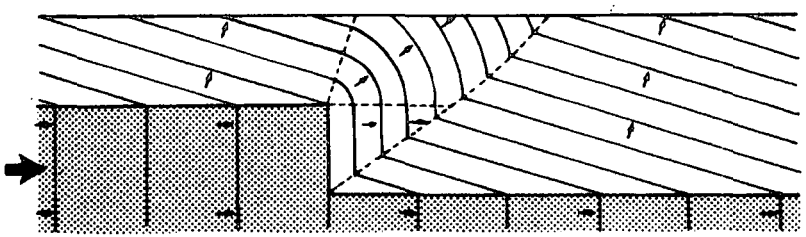

Downstep

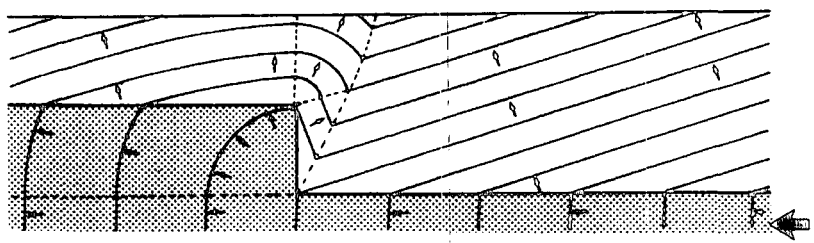

Upstep

Figure 2.9

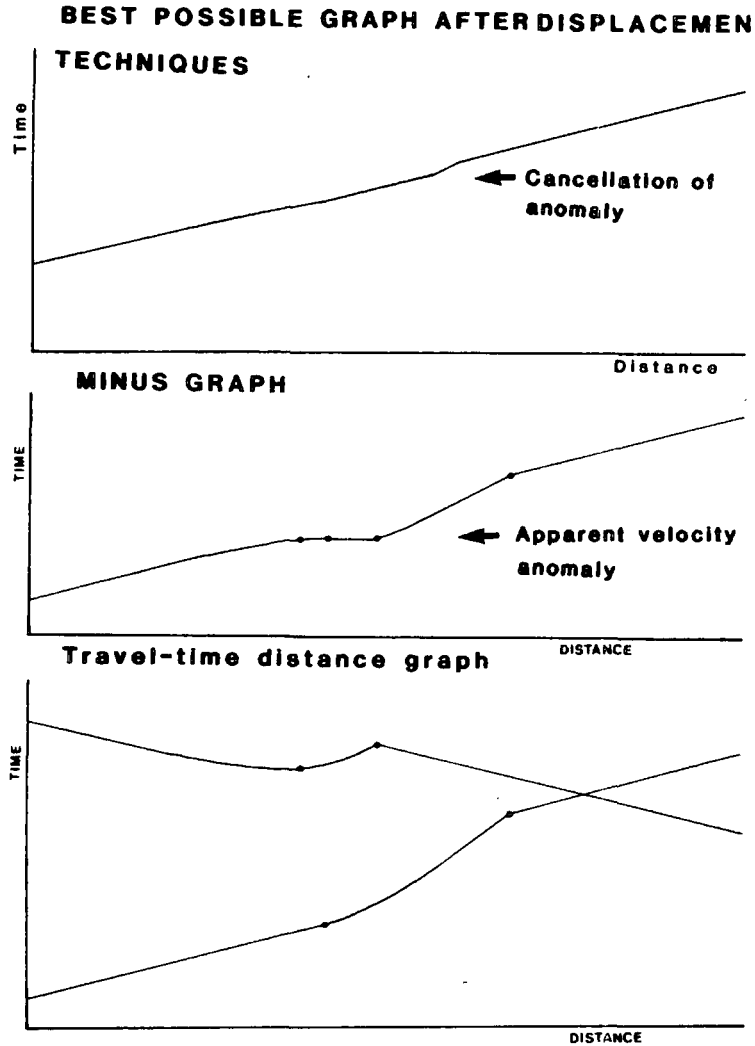

Refraction over a step in the refractor

VELOCITY

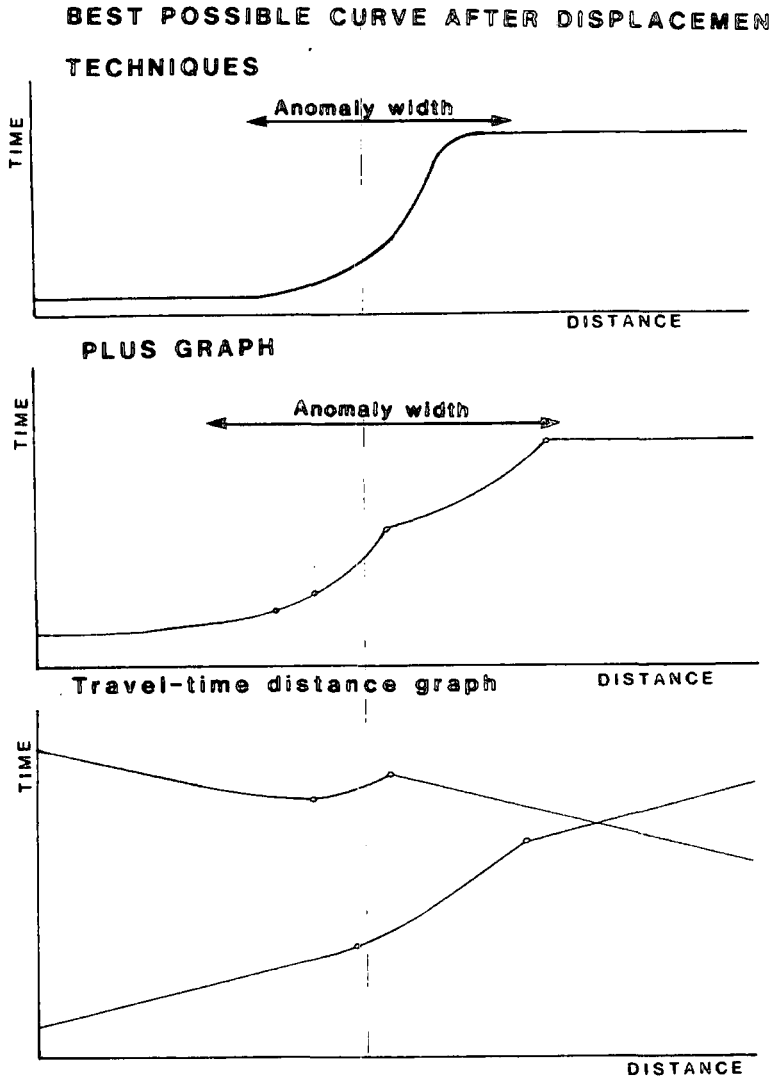

Refraction over a step in the refractor

DEPTH

Figure 2.10

resolution of the fault step is a function of the width of the diffraction zones on the traveltime graphs, which depend upon the overburden thickness and the velocity contrast between the overburden and the refractor. The velocity contrast is usually the major factor influencing the degree of resolution. S waves display a greater velocity contrast than P waves for unconsolidated overburden overlying bedrock, due to the fact that the Vp/Vs ratio in unconsolidated sediments can rise to values of 8.0. Therefore there should be a distinct improvement in the imaging of a complex structure using S waves rather than P waves.

Obviously when we are dealing with geological reality then the situation may not be as simplistic as the model studies imply. Sjogren (1984) uses more complex models in studying the reliability of the refraction technique in imaging particular complex structures. A fault may also exist as a combination of the two basic models given above; that is a step in the refractor accompanied by a change in refractor velocity each side of the fault. In this case the refraction results yield depth and velocity anomalies on which we can base our estimate of the precise fault location.

Drift Channels

A drift channel can be modelled as a U or V shaped depression in a refractor. Such a structure results in the increase in the plus time/time depth values calculated from the refraction survey over such a structure. Model studies by Sjogren (1984) show that if the depression has severe relief, the refraction results will always underestimate the depth in the central part of the

depression, and a V shaped depression will always appear to have a flat bottom. Use of the common refractor point method allows greater penetration into the structure than the common receiver method.

2.5 ERRORS IN REFRACTION INTERPRETATION

The estimation of possible or probable errors in refraction work is a very difficult task for the interpreter. Errors can be classified under three main headings (Northwood, 1967):

1. Errors caused by incorrect reading of the data.
2. Errors caused by incorrect assumptions.
3. Errors caused by incorrect geological interpretation.

The first category of errors result from interpreting data of poor quality with a low signal/noise ratio or a very low frequency content so that the first break cannot be determined with any great accuracy. This kind of error will primarily affect the final depth estimate. If the picking errors are small and random, then by fitting a least squares "best fit" (Barford, 1967) to the time versus distance data then the true velocity will be calculated, along with an error estimate.

The accurate calculation of depth relies mainly upon the accurate determination of the overburden velocity, as this is the most significant value in the calculation of the conversion velocity used in the depth conversion of the plus time[time depth]

values (Equation 11). Any depth quotations from shallow refraction surveys have a realistic error of plus or minus 10%.

The errors in depth calculations caused by making incorrect assumptions are probably greater than those due to poor data quality. The major assumption one makes is in the estimation of the velocity of the overburden. The overburden velocity may increase with depth due to compaction, although this is rarely apparent in shallow refraction interpretations (Palmer, 1983), or it may be laterally variable. These features may only be detectable by careful analysis of the direct wave arrivals. Carrying out detailed analysis of the near surface velocity structure is very time consuming, some assumptions regarding average velocities must made using the data that is available. One must also consider the possibility of a blind zone or hidden layer problem occurring. If the problem remains undetected then any depth estimates made, based on the wrong assumption, will be erroneous.

Using the delay time interpretation technique, the following two assumptions are made (Dampney & Whitely, 1980):

1. Each refractor is locally plane under the receiver.
2. All refraction paths between shotpoint and geophone are common up to the point where the refracted wave leaves the refractor.

In areas of high relief structures, these conditions are not met. Fortunately however, the earth often approximates them. Also in high relief areas the ability of the delay time method to

determine refractor velocity breaks down. An appraisal of these conditions is given by Sjogren (1979).

The result of any refraction survey can only be to define a cross-sectional velocity structure for the near surface layers. An interpretation of the significance of the velocity boundaries must be made. If borehole information exists then this process can be quite straightforward.

The most common error in P wave shallow refraction studies is in the estimation of the depth to bedrock. If rockhead is badly weathered then its seismic velocity can be so lowered that the overburden/rockhead boundary does not provide a significant velocity contrast. In this case the base of the weathered layer will be the significant refractor. Therefore any depth estimates based on the depth to this refractor will overestimate the overburden thickness. The possibility that the water table could act as refractor must also be considered in shallow refraction studies.

2.6 SEISMIC REFLECTION

The seismic reflection technique basically involves the reflection of elastic waves off geological interfaces. By measuring the traveltime of the reflection from ground surface to reflector and back to the ground surface, if the velocity of the wave through the earth is known, then the distance to the reflector can be determined.

The seismic source is located on or just below the ground surface, the reflected energy being monitored by receivers laid out on the ground. Figure 2.11 displays the simplest possible situation where a single geological interface occurs. The time taken for the reflected energy from source to individual receivers is plotted on a time-distance graph. The reflected energy takes the form of a hyperbola on the time distance graph (figure 2.11). When the source and receiver are coincident the zero offset reflection time results. The difference in traveltime between the zero offset and a finite offset receiver is called the normal moveout (NMO). The traveltime equation for a reflection is given as;

$$T = \frac{X^2}{V^2} + \frac{4H^2}{V^2} \qquad \text{Equation 15}$$

At the geological interface a percentage of energy is reflected back to the surface, whilst the rest is transmitted through the boundary to be reflected back by deeper interfaces. The relative percentages of the reflected and transmitted energy for a particular interface are governed by Zoeppritz's Equations. For a

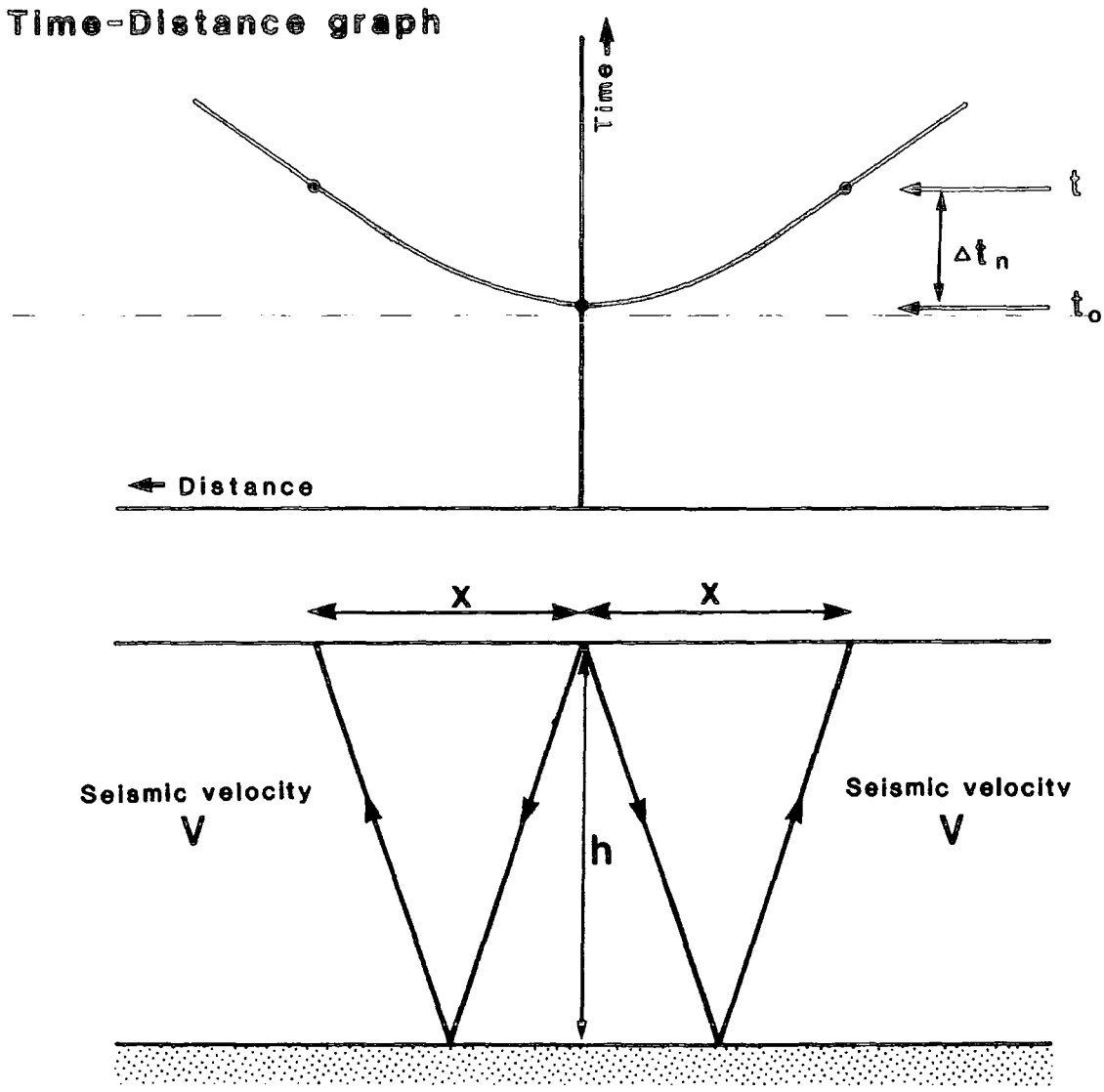

At zero offset (x=0) travel time is

$$t_o = \frac{2h}{v}$$

Travel time at finite offset is

$$t^2 = \frac{x^2}{v^2} + \frac{4h^2}{v^2} = \frac{x^2}{v^2} + t_o^2 \qquad \text{Equation 15}$$

Difference in travel time between zero offset and finite offset is called NORMAL MOVEOUT

$$\Delta t_n = \frac{x^2}{2v^2 t_o} \qquad \text{Equation 16}$$

Figure 2.11

normal incidence reflection, the relative amplitude of the reflected pressure wave is;

$$R = \frac{\rho_2 V_2 - \rho_1 V_1}{\rho_2 V_2 + \rho_1 V_1} \qquad \text{Equation 17}$$

where R is known as the reflection coefficient. For raypaths which are not normally incident, R becomes a function of incident angle, but for incident angles up to around 20 degrees, equation 17 remains a good approximation to the reflection coefficient. Coal is an unusual rock type as it has both a low seismic velocity and low density in comparison with the surrounding rocks. These properties generate a high acoustic impedance contrast across any coal/country rock interface. Reflection coefficients at normal incidence lie between 0.35 and 0.5 (Hughes & Kennett, 1983).

For shallow reflection studies the assumption that near normal incidence reflections are recorded may not hold. The maximum shot receiver distance must be small enough so that no reflections are recorded from beyond the critical angle, where large phase changes occur. A maximum reflection amplitude occurs at the critical angle.

As discussed earlier because of the presence of the ground surface, surface waves as well as elastic waves are produced by the source. The bounding velocity values of the so called ground roll have been discussed earlier. Figure 2.12 displays a schematic representation of the relationship between the ground roll and the reflection hyperbolae for both a P wave and S wave reflection survey. For P wave reflection surveys the Rayleigh wave ground roll occurs in a cone bounded by approximately 90% of

Schematic representation of P and S wave seismograms

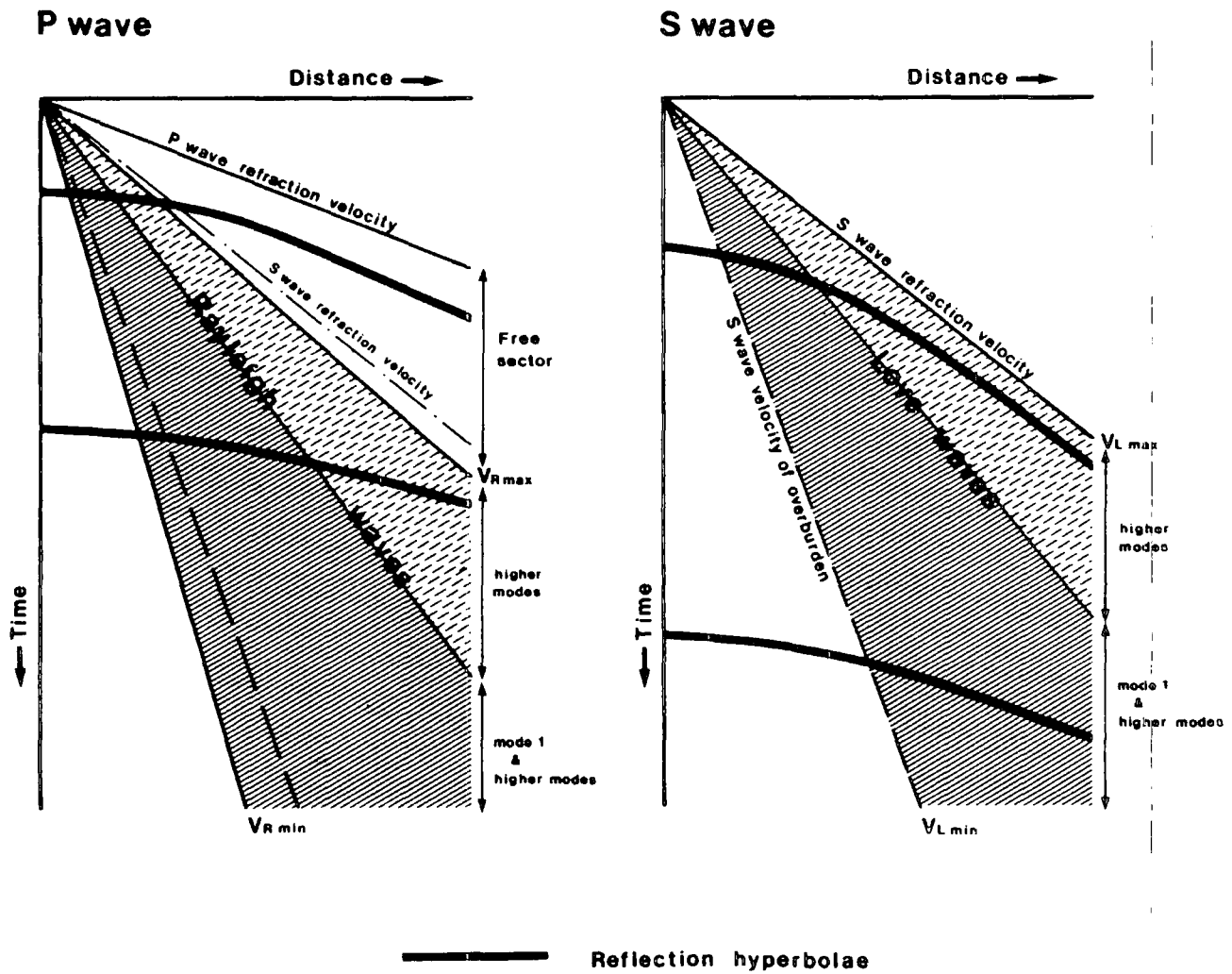

(Redrawn from Edelmann & Helbig, 1983)

Figure 2.12

the shear wave velocities of the near surface low velocity zone and the underlying refractor. For P wave surveys it is common practice to select a shot to receiver offset so that the reflection hyperbolae of interest fall into the free sector between the highest Rayleigh wave velocity and the P wave refraction arrivals. In S wave reflection surveys, the cone of ground roll due to Love waves is bounded by the shear wave velocities of the surface low velocity zone and the underlying refractor. Therefore in S wave surveys the free sector does not exist, and all reflections will occur within the Love wave cone.

Figure 2.13 displays a schematic traveltime graph for all the wave types one would record during a P wave survey. The earth model is based on typical depths and velocities one would encounter in the exploration of shallow coal deposits. The coal seams are modelled as single thin reflectors in a constant velocity country rock. The target seams are placed 50m apart. Although the modelling is simplistic it reveals that the moveout one expects on the reflections is small. Also note the complex interaction between the wave types especially for the shallow reflections. No large "window" exists for the shallow reflections.

Earth Model

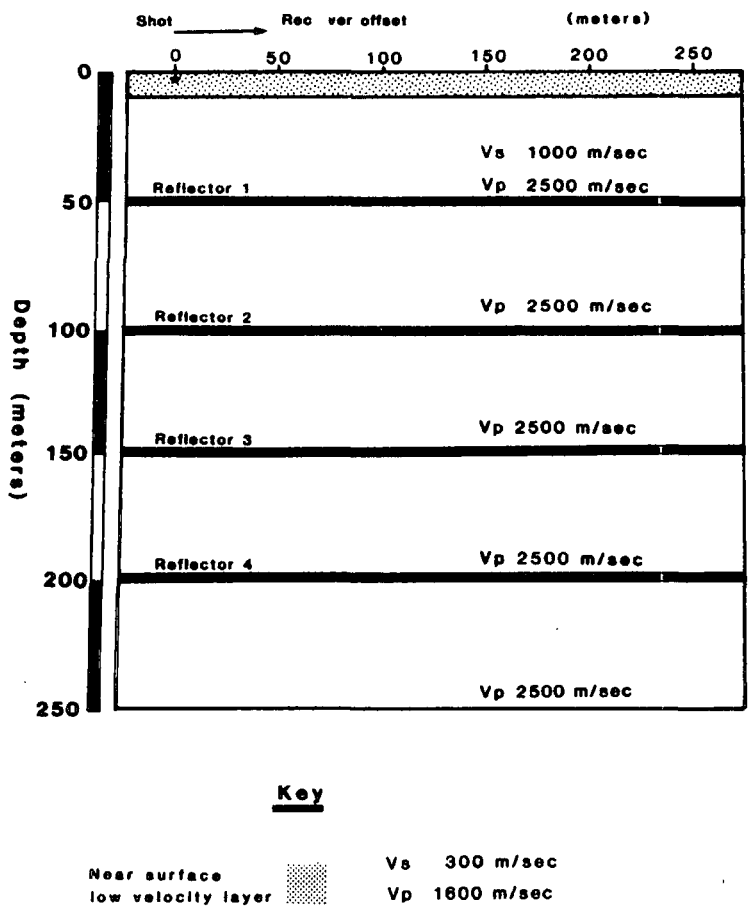

P wave
Traveltime curves derived from earth model.

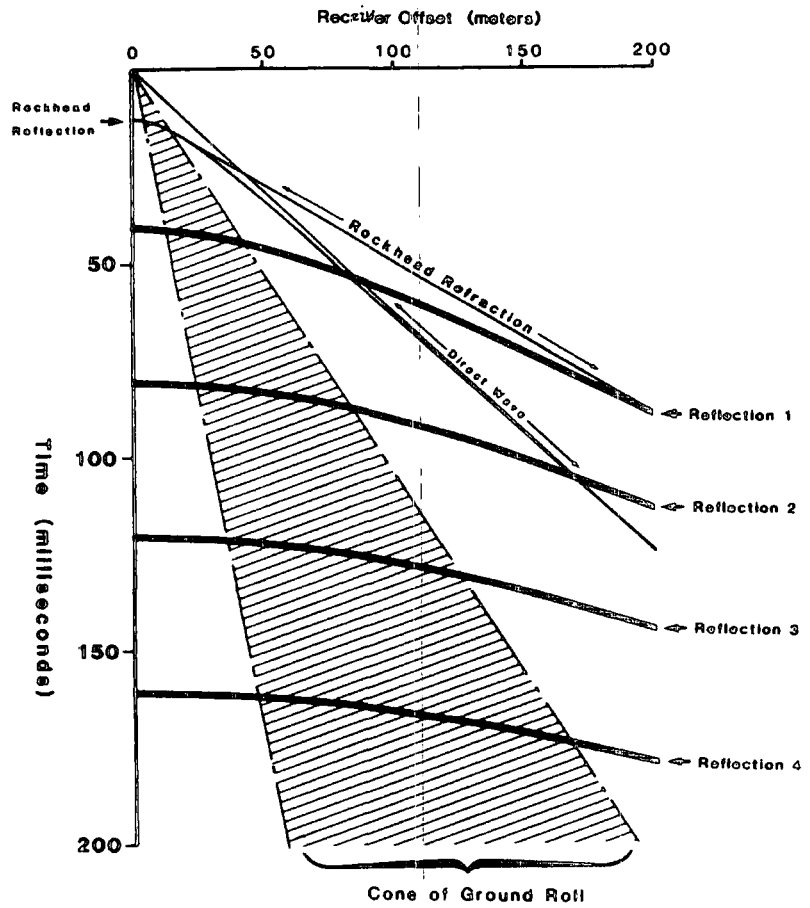

Figure 2.13

2.7 SHALLOW SEISMIC REFLECTION SURVEYS OVER COAL DEPOSITS

High resolution seismic reflection surveys for coal have been carried out in the UK by the NCB since 1973 (Ziolkowski, 1981). The target coal seams for these surveys rarely exceed 1300m (maximum depth of a modern coal mine). Opencast coal is sought after to a maximum working depth of only 200m; therefore the exploration target is much shallower. In reflection seismology it is generally more difficult to explore for very shallow targets than deeper ones, due to the interaction of the near surface reflections with refractions and ground roll events (figure 2.11).

A recent paper by Greenhalgh et al. (1986) discusses the use of the shallow reflection technique over thick Permian coals in the Sydney Basin, NSW, Australia. Their results show the difficulty in obtaining high structural resolution at depths of less than 100m.

The philosophy adopted in the data acquisition stages of this project essentially follows that proposed by Ziolkowski & Lerwill (1979) and Ziolkowski (1979), with the acquisition geometry being scaled down for the exploration of the shallower target. The above papers discuss the problems of high resolution surveys in detail. The features of relevance to this project are discussed below.

The Seismic Source

The fundamental requirement of high resolution data is that the seismic source generates frequencies over a wide spectrum typically up to 200Hz or more. It is the presence of high frequencies in the data that determines the resolution.

Dynamite is the obvious seismic source, as it produces a high energy output rich in high frequencies in the seismic bandwidth. The scaling law implies that the relationship between the charge mass (M) and the frequency content should be:

Pulse duration is proportional to $M^{\frac{1}{3}}$

Pulse amplitude is proportional to $M^{\frac{1}{3}}$

Absolute spectral bandwidth of the pulse is inversely proportional to $M^{\frac{1}{3}}$

Amplitude of the pulse spectrum is proportional to $M^{\frac{2}{3}}$

The conclusion from this is that small charges mean higher frequencies. But in an attempt to increase resolution by using smaller charges, we run into the problem that small charges also mean less energy output and therefore less amplitude on the recorded reflected events. Thus small charges should be used, but large enough to retain a sufficient signal to noise ratio of the reflected events.

The source must also be made to generate as little ground roll as possible. This can be achieved in theory by placing the shot below the surface low velocity zone. Burial of the shot also means that the seismic pulse only travels once through the highly

attenuating surface layers, thus increasing the high frequency content of the recorded signal. The medium in which the shots are exploded plays a vital part in the final data quality one obtains. Sometimes no useful seismic high resolution reflection data can be obtained when shots are placed in a particular geological horizon (Goulty, 1983 ; Greenhalgh et al., 1986).

The Receiver

For high resolution surveys, the greatest resolution on the final section is achieved with single geophones, rather than with patterns or groups favoured in oil exploration. Geophone patterns and arrays act to attenuate high frequencies, so are undesired in high resolution surveys.

P wave geophones are sensitive to vertical ground motion. Shear wave geophones used for recording the Sh arrivals are sensitive to horizontal ground motion only. The geophone must be able to reproduce high frequencies without distortion. Therefore they must have a flat response curve up to 500Hz. High frequency geophones are used which satisfy this requirement. These geophones also have an attenuating affect on the frequency range 0-30Hz which is the typical frequency range of Rayleigh waves.

As the technique relies upon a single geophone per recording point, the method depends critically on good ground coupling of the geophone. Knapp and Steeples (1986b) state that the geophone response is insensitive to geophone mass and diameter but very sensitive to soil firmness. The best recording results were achieved in their tests by using a single geophone with a long

spike on a scraped surface. A badly planted geophone has an irreparable effect on the final data quality.

The Recorder

The recording instrument must have a wide dynamic range and a fast response to changes in the incoming signal level. This is achieved by digital recording of the data. The digital sampling rate must be such that the data is not "aliased". The sampling frequency must be twice the highest frequency of interest on the data. The recording time must be long enough to record reflections from the target depth range.

Data Processing

The objective of data processing on seismic reflection data is to remove (or at best attenuate) unwanted noise from the recorded data to enhance any reflected events that may be present. Two kinds of noise of seismic origin that are present on land data are refracted arrivals and ground roll.

Removal of Refracted Events

The removal of refracted events from a seismic trace is a relatively easy task, as refractions occur as the earliest events on a seismogram prior to most of the reflected events. The refractions are removed by muting. Muting involves the zeroing of the digital samples within the window of the seismic trace which includes the refractions. The problem encountered in shallow refraction surveys is the precise point where the refraction

events end, and the reflections begin. Both the NCB and Greenhalgh et al. (1986) use velocity (f,k) filtering techniques to suppress the first breaks. This filtering technique relies on the fact that the refractions appear on the common shot gathers at a constant velocity, whereas reflections cross the CSGs at a very high apparent velocity. The two arrivals are differentiated on the basis of their velocity across the CSGs; the lower velocity refractions being preferentially suppressed. Unfortunately the software does not exist at Durham to experiment with the use of this technique on the shallow reflection data acquired during this project.

Removal of Ground Roll

In shallow reflection studies using P waves it may not be possible to record reflected events outside the cone of ground roll. In this case where the reflected events merge into the ground roll arrivals, then data processing must be carried out on the data to selectively reduce the amplitude of the ground roll with respect to the reflected arrivals. In P wave surveys, particularly in high resolution surveys where high frequencies are sought after, the frequency spectrum of the ground roll is much lower than that of the reflections and hopefully does not overlap. In this case ground roll can be suppressed by high pass frequency filtering. If their spectra overlap there will be a degradation of the reflected signal when the ground roll is suppressed in this way. In S wave surveys frequency filtering may not work due to the already limited bandwidth of the shear wave reflections (Edelmann & Helbig, 1983). More sophisticated data processing techniques may have to be adopted such as velocity and wavelength

filtering.

NMO Correction

For shallow reflections, particularly with large shot to receiver separations relative to the depth of origin of the reflection, the effect of the dynamic NMO correction will be to introduce a distortion or "stretch" to the recorded wavelet. This will degrade the resolution and continuity of events on the seismic section. Typically data with over 30% to 40% stretch applied to them should be muted (Knapp & Steeples, 1986b).

CMP Gathers

Some shallow seismic exploration projects use the optimum window (common offset) shooting technique (Hunter et al., 1984; Singh, 1986). Those referenced projects were involved with imaging the single overburden/bedrock interface, where the bed rock usually consisted of a granite or a limestone. Therefore the very large velocity and density contrast between overburden and bedrock leads to a very large reflection coefficient (equation 17), thus giving a high amplitude reflection. In this project, where we are looking at a series of reflections from a coal measures sequence, the common offset technique is not applicable and we adopted the common mid point (CMP) technique. This method was also adopted by a shallow seismic reflection survey carried out under under favourable conditions on a mud flat in the Netherlands where a multi-reflection section was obtained (Doornenbal & Helbig, 1983).

The seismic traces are acquired in a common shot gather format (CSG), and the data must be sorted into CMP gathers (Figure 2.14). The NMO correction can be applied to the traces in the CMP gather which are then summed to represent a zero offset trace acquired at the common mid point position. The number of traces in the CMP gather is termed the fold of cover. The fold of cover is determined by the number of traces in the original CSG and the shot point and geophone spacing. The advantage of this technique is that the signal to random noise ratio of the output trace can be improved as the square root of the number of traces summed.

Another advantage of CMP stacking is that due to the data redundancy, the problem of static corrections can be handled statistically, thus reducing the chance of misinterpretation of the data due to static errors.

Common Shot Gather (C.S.G)

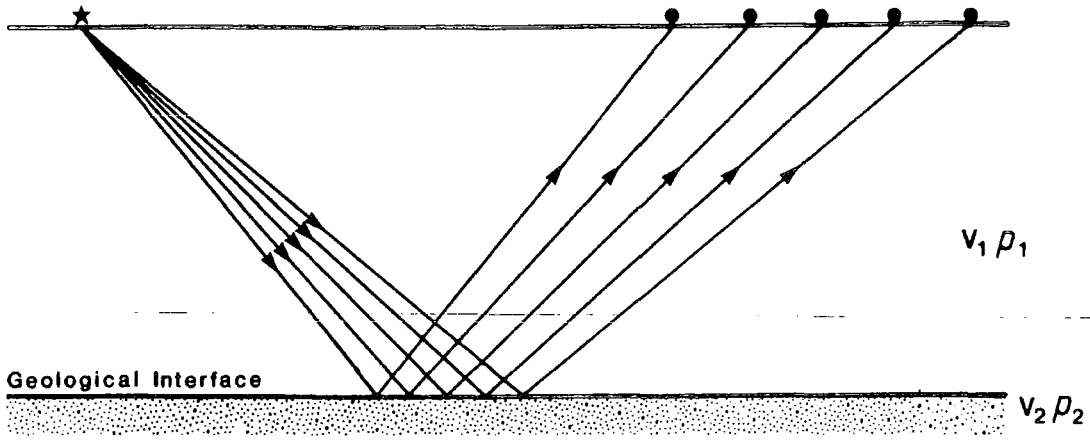

Common Mid Point Gather (C.M.P)

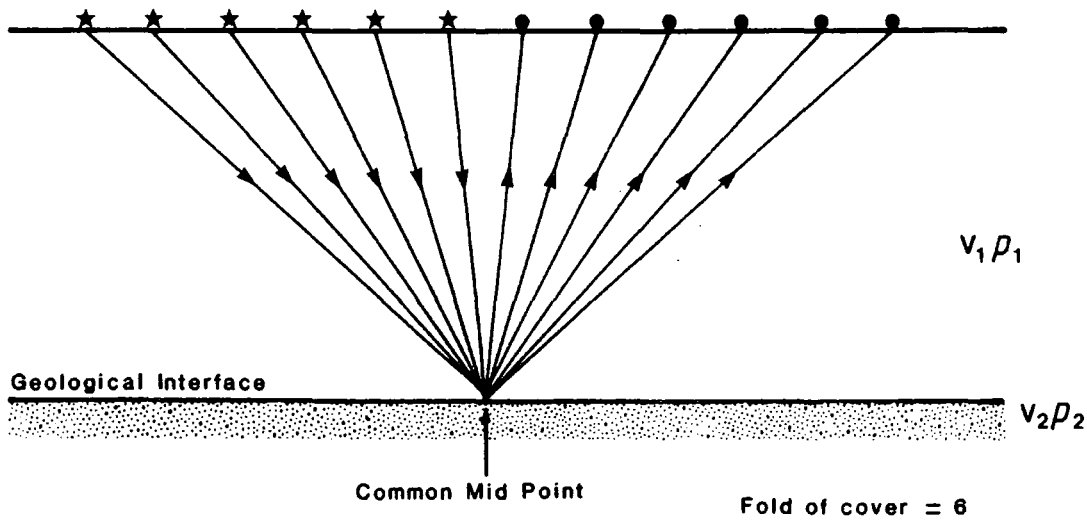

Key

★ Shot Point

● Receiver Location

V Velocity

ρ Density

Figure 2.14

2.8 STATIC CORRECTIONS

The purpose of the static corrections is to remove the effects of ground surface topography and account for variations in thickness and velocity in the near surface low velocity zone. The application of the correct static corrections to the data simulates the placing of both sources and receivers on a datum below the base of the weathering zone. The corrections are termed static shifts because the correction is assumed to be constant for each trace, and is not a function of time along the trace as with the dynamic NMO correction.

Static effects do not scale down with scaled down acquisition geometry of high resolution surveys. Static errors are more of a problem for shallow surveys than for conventional surveys. The major problem that static errors cause is that their effect on the final reflection section causes distortions which simulate the presence of apparent faulting. In fact, the threshold of identifiable faulting on the final section can be limited not by the frequency content of the data, but by the magnitude of the static errors present (Ziolkowski, 1979). It is easier to generate high frequency data with potentially high structural resolution, than it is to calculate static corrections with sufficient accuracy to allow that potential to be realised. A static error of 5msecs on a seismic trace with a predominant frequency of 100Hz results in the trace being shifted by half its period. This results in it being 180 degrees out of phase with an adjacent trace with no static error.

Waters (1979) points out that the static shift present on a single seismic trace is made up of several individual contributions:

$$T_{total} = T_{ws} + T_{wr} + T_{nmo} + T_d + T_n \qquad \text{Equation 18}$$

where;

Tws = Shift due to the weathering zone below the shot point.

Twr = Shift due to the weathering zone below the receiver.

Tnmo = Shift due to incorrect NMO correction.

Td = Shift due to structural dip differences.

Tn = Shift due to noise.

In shallow P wave high resolution work the NMO correction is typically small; therefore any errors in the correction applied are very small. When the traces are analysed in CMP gathers then the term due to structural dip (Td) disappears.

Shot Static Equalization

The shot static is unique to every shot fired in a borehole. This is due to the effects of ground deformation near the borehole from previous shots; also later shots may not be able to be re-loaded to the original depth due to borehole collapse. In small scale surveys, usually only 12 or 24 recording channels are available. A borehole may be required to be re-used so that the necessary fold of cover can be built up. In this case a single borehole static can be determined by ensuring that successive shots fired from the borehole are recorded at a common geophone location, i.e. by leaving one geophone in the ground when the

array is "moved up". Then first break times recorded at the common geophone for successive shots can be equalized, and a corresponding small static shift applied to each record. The records are equalized to the shot static of the first shot fired, as this usually has the minimum delay.

Refraction Surveys

To obtain accurate static corrections for a shallow reflection survey, the near surface velocity structure can be determined by carrying out a refraction survey. If the results of the refraction survey yield a model of the near surface velocity structure, then corrections for the shot and receiver can be calculated for each trace. Figure 2.15 shows how the corrections are calculated. Figure 2.15 just gives the magnitude of the static shift that has to be applied to each trace, as the static shifts are applied to essentially take the shot and receiver to the datum level. Conventionally the correction is taken as being negative for shot points and receivers below the datum. This implies that any reflection event on the trace is time shifted toward the zero time.

This technique will calculate any long wavelength statics due to structural or velocity variations in the near surface weathering zone. To avoid any errors due to incorrect velocities used in the calculation, the datum should be chosen as near as possible to the level of the shots.

Calculation of static corrections

Near surface velocity structure defined by refraction survey

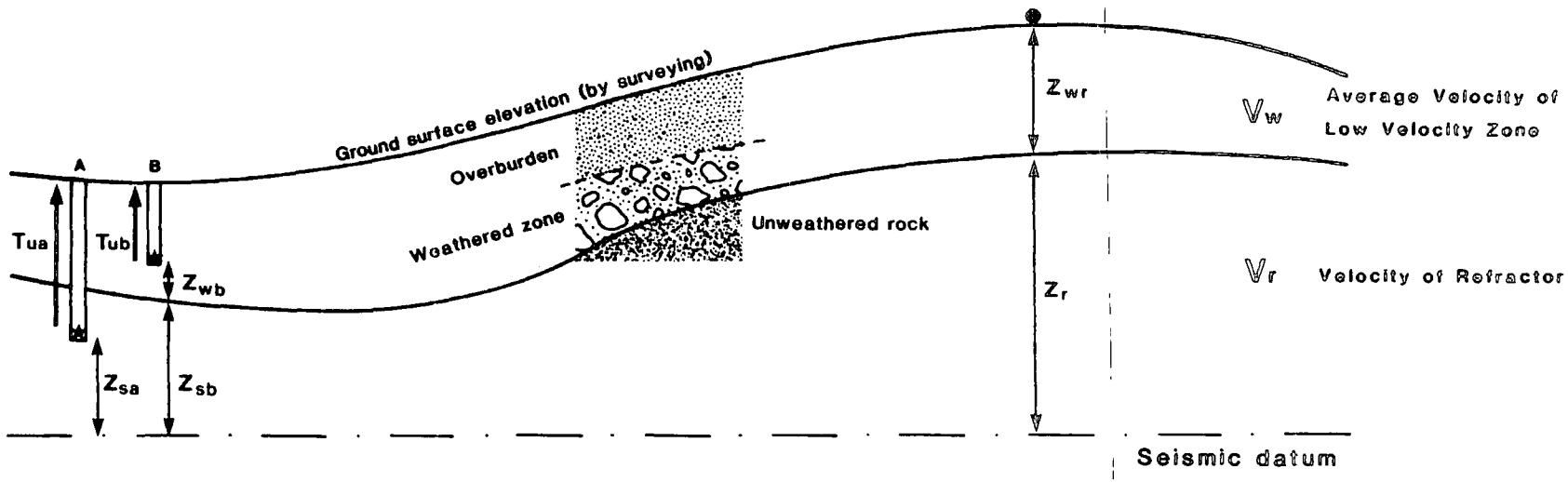

★ Shot location ● reciever location Tu - Uphole Time (measured)

Shot correction

Borehole A

shot below base of weathering $\quad \text{Static}_s = \frac{Z_{sa}}{V_r}$

Borehole B

shot in low velocity zone $\quad \text{Static}_s = \frac{Z_{sb}}{V_r} + \frac{Z_{wb}}{V_w}$

Reciever correction

$$\text{Static}_r = \frac{Z_r}{V_r} + \frac{Z_{wr}}{V_w}$$

$$\text{Total trace static} = \text{Static}_s + \text{Static}_r$$

NOTE

When receiver at a shot point

Reciever correction = Shot correction + Uphole time

Figure 2.15

First Break Plots

This method of applying static corrections was developed by the NCB and is described in Rogers (1981). A plot of the first breaks for every seismic trace recorded during the reflection survey is drawn. Then least squares best fit straight lines are the fitted to the refraction arrivals on the plot. Any time anomalies due to the very near surface anomalies at the geophone will tend to align vertically on the first break plot. The static correction is regarded as the time shift required to align all the refraction first breaks onto the best fit straight line.

This method allows for the calculation of high amplitude, high frequency static corrections. In theory as deep a refractor as possible should be used, as the raypath through the weathering zone is more nearly vertical, and nearer the path of the reflection. Care must be taken to ensure that the same refractor is used along the survey line. If the refractor fades out another of equal depth can be used. Continuity must be ensured in the overlap zone.

Residual Statics

When the above corrections have been applied to the data then any remaining static errors are termed residual statics. Automatic computer algorithims exist to remove any small amplitude residual statics. Their function is mainly a cleaning up process to remove small amplitude residual errors.

CMP Aligned Statics

When the traces are in the CMP gather format, the term in Equation 18 due to the structural dip disappears. The term due to incorrect NMO application should be insignificant in shallow reflection surveys. Therefore we are dealing with only the residual shot and receiver statics in the CMP format. The computer program used to apply CMP aligned static corrections was one initially written by Loveridge (1981), and later adapted by Hobbs (1985) to work on the Durham University processing system.

Automated statics packages make use of the cross correlation function to calculate the time shift between two traces. The cross correlation function is plotted for a window of the traces which contain reflection events with a good signal/noise ratio. The maximum value of the cross correlation function relative to zero delay, gives the optimum shift required to produce the best match between the two traces.

Before the application CMP aligned statics routines, the traces must have had some initial processing to remove refractions and ground roll, and the NMO correction must also have been applied. Figure 2.16 shows how the CMP aligned statics package works. Firstly the traces in the CMP gather are stacked to form the pilot trace (the near offset trace can also be used as the pilot trace). Each individual trace in the gather is then cross correlated with the pilot trace and time shifted to form the optimum match between the pilot and the trace. One further iteration is carried out. The traces are restacked to form a second pilot and the traces in the gather again cross correlated with the second pilot and the

CMP ALIGNED RESIDUAL STATICS PROGRAM

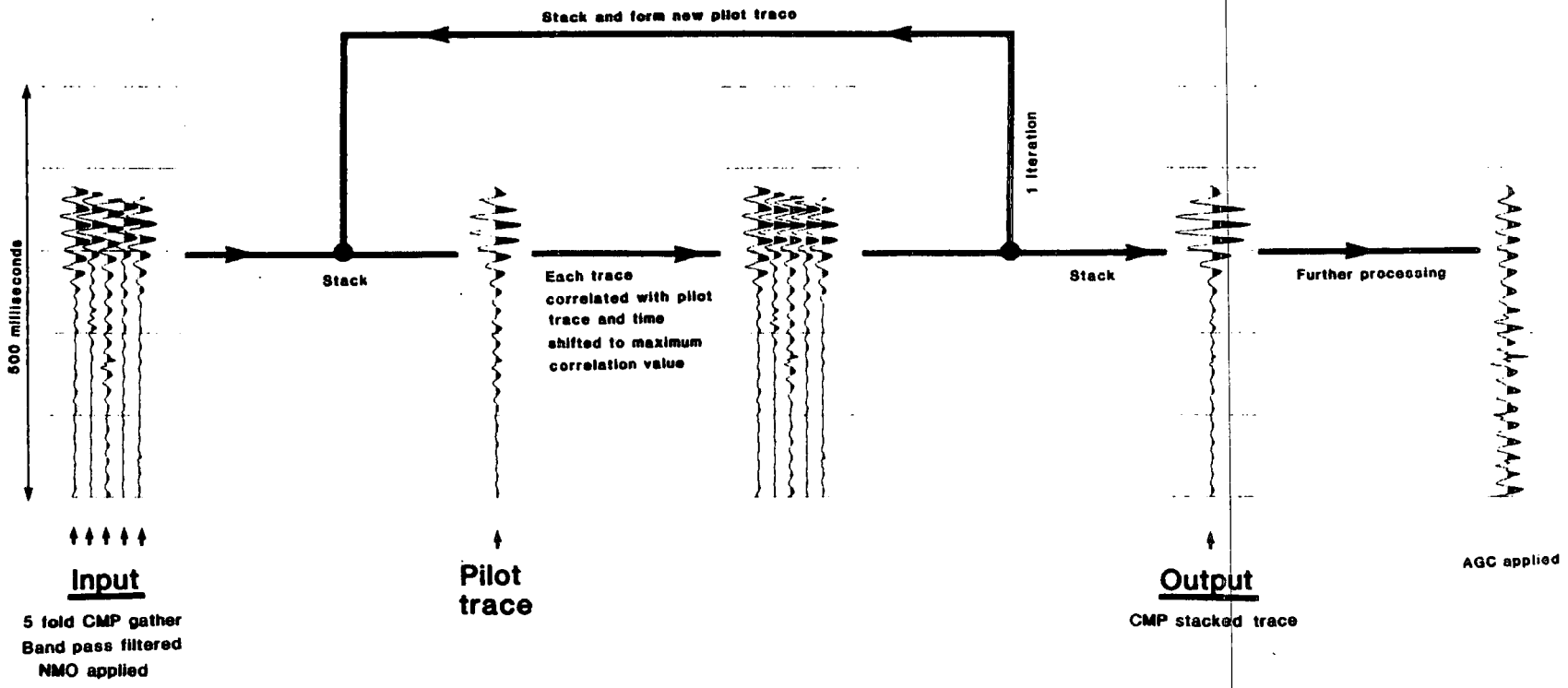

Program variables

1. Choose traces to include in the formation of the pilot trace
2. Start time & length of correlation window
3. Maximum time shift value (to avoid "cycle skipping")

Figure 2.16

optimum time shift applied.

The window used for the cross correlation function must contain pure reflections with a good signal/noise ratio. A maximum time shift that can be applied to the traces is specified as a constant. This is so that "cycle skipping" does not occur i.e. misalignment by one or more cycles of the data. For the correct application of the residual NMO correction the original field statics must be good enough so that the residual static errors are less than half a period of the dominant frequency in the seismic traces in the original CMP gather.

This process concerns itself with the best alignment of traces in the CMP gather. No attempt is made to align adjacent gathers. The basic assumption that this method makes is that the residual static shifts in the CMP gather vary in a random manner about a zero mean. If this is not true, then the initial pilot trace can have a mean time shift applied to it. The output traces in the CMP gather will show optimum alignment with each other but will all contain the time shift of the pilot trace. As there is no consistency between adjacent gathers this can lead to random small time shifts between adjacent stacked gathers causing "jiggle" on the final section.

Surface Consistent Statics

More advanced computer programs exist which apply "surface consistency" to the static shifts applied to the seismic traces. Firstly CMP aligned statics are computed but not applied to the traces. The traces are then re-sorted into the common shot

format. The static shifts computed in this format are independent of the term due to the shot static in equation 18. Likewise when the data are re-sorted into the common receiver format the term due to the receiver static in equation 18 is constant. Statistical analysis can be carried out on the three sets of static corrections and a surface consistent model resolved. A surface consistent program by Ravens (1983) existed in the department but unfortunately it was incompatible with the processing sequence required to process the shallow reflection lines acquired during this project.

2.9 RESOLUTION

In seismic exploration over coal bearing strata, resolution is a fundamental problem. Resolution can be defined as the dimension of the thinnest single bed that will have a vertical reflection signal equal in amplitude to the signal from a single interface between the two semi-infinite mediums (Ziolkowski, 1979). The ability of the final seismic section to resolve geological boundaries is dependent upon the seismic signal wavelength. As the seismic velocity of a particular geological situation is invariant, the resolution achieved on the final section is dependent upon the frequency content of the recorded signal. It is desirable to generate high frequencies at the source, and bury the source below the highly attenuating surface layer. The seismic receivers are placed on the land surface; therefore the recorded signal must at least travel once through the highly

attenuating surface layer. This must seriously impair the high frequency content of the data. Dankbaar et al. (1983) state that on agricultural land the signal spectrum is cut off at about 80Hz.

The penetration of high frequencies directly into the earth and the return of those high frequencies from the target horizons is also limited by:

1. Attenuation by solid friction.
2. Loss of energy or change in frequency by reverberations and transmission losses due to the presence of many layer boundaries.

To understand the problems of resolution of the coal measure sequences, synthetic seismogram studies have been carried out (Van Riel, 1965; Ruter & Schepers, 1978 & 1985; De Voogd & Staudt, 1982; Hughes & Kennett, 1983). The coal measure sequences are assumed to be cyclically layered, with rapidly alternating acoustic impedance contrasts, with reflection coefficients of 0.5 or greater. Even for a small number of coal seams in the model, interference effects result in complex seismograms. The major conclusions of the synthetic seismogram studies are:

1. A single seam of only one hundredth of the seismic wavelength can produce a reflection; therefore thin beds are detectable and do contribute to the seismogram.
2. Individual reflections are not visible for a sequence containing a great number of thin seams, due to constructive interference effects.
3. Only the first two or three reflections are of primary origin,

the majority of the recorded seismogram being made up of energy produced from interbed multiples.

4. A coal measures sequence acts as a high pass filter for reflections and as a low pass filter for transmitted waves. Therefore seismic data will contain low frequency primary reflections and strong high frequency multiples. Primary reflections can only be detected if low frequency signals are used, but this means poor resolution.

In theory it is difficult to correlate the reflections with individual seams. However if the seismic character remains constant over an area then there must be geological continuity.

The results of the theoretical studies seem to be very pessimistic about the ability of the so called "high resolution" techniques ability to resolve fine structures such as faults, seam splits and washouts etc.

A recent paper produced from the results of the NCB's practical experience of land reflection data (Barnett et al., 1986) seems to refute the results of the theoretical studies. Observations from real data seem to show the existence of primary energy from deep within the coal measures sequence. It is suggested that the synthetic seismogram studies fail to consider the fine detail of the coal measures, in particular how the coal seams grade into the country rock.

2.10 SEISMIC REFLECTION OVER OLD MINE WORKINGS

Waters (1979) shows an example of a P wave reflection line shot over a shallow coal seam 2m thick at 200m depth (figure 2.17). The seam had been previously mined, and in the area of the old workings (where 20 to 30m wide pillars are left behind) a large amplitude reflection occurs at the worked horizon. This is caused by the large reflection coefficient produced at the horizon due to the mined area being air filled. Therefore the mined area can be distinguished from the unmined region using the results of the reflection survey. However the individual pillars cannot be imaged using the reflection technique.

2.11 THE POTENTIAL OF SHEAR WAVES AS AN EXPLORATION TOOL

Conventional seismic exploration to date has mainly concentrated upon the generation and recording of compressional (P) waves. There is now a growing interest in the use of shear (S) waves and their use as an exploration tool. Horizontally polarized (Sh) waves are used in practice because they are less complex than vertically polarized (Sv) waves as they do not generate converted waves. The simultaneous recording of both P and S waves may be profitable because:

"The two wave types probe the earth with different stresses and strains therefore they yield different information about the substratum" (Helbig & Mesdag, 1982).

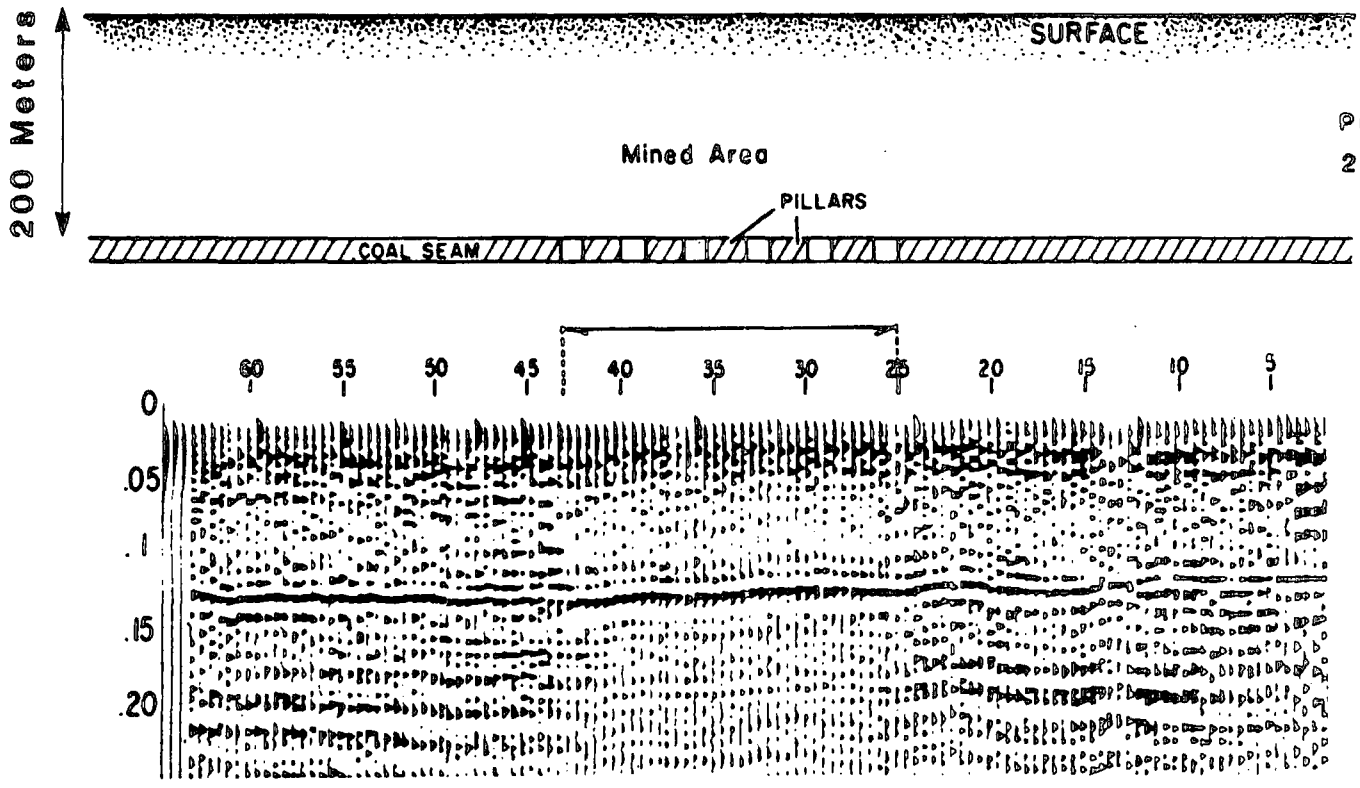

Pillar dimensions
20 to 30m

SURVEY PARAMETERS

Source Pattern :
15 positions over 20m
Reciver Pattern :
20 geophones over 20m

5 Fold stack
6.5m Trace spacing

Frequency spectrum
40 to 170Hz

High-frequency (40 to 170 Hz) seismic survey over a recently mined area of a coal mine. Mine depth is 550 ft, coal seam thickness is 7 ft, surface shot points are 40 ft apart, and the mined area is air-filled. The section was processed for equal total power in all traces, hence the large reflection over the mined area gives rise to diminished background. (Courtesy of the Continental Oil Company.)

(From WATERS 1979)

Figure 2.17

The most obvious parameter to be obtained from combined observations is the ratio of the two velocities. The Vp/Vs ratio is a sensitive parameter indicating changes in lithology. Historically it is customary to convert the Vp/Vs ratio to Poisson's ratio (Equation 4), but the velocity ratio contains the same information (Helbig & Mesdag, 1982).

What advantages does the recording of shear waves have in shallow seismic exploration ?

Shear Wave Refraction

Combined small scale P and S wave refraction studies have been used in engineering site investigation studies in order to determine the Poisson's Ratio and Young's modulus for rocks in situ. These have been carried out during the surveying and planning of major civil engineering projects; such as dams (Evison, 1956; Morris & Abbiss, 1979; Davis & Schultheiss, 1980).

The use of shear waves in shallow refraction exploration has two major advantages:

1. The velocity ratio Vp/Vs for consolidated rocks is between 1.5 and 2.0, whereas the ratio for unconsolidated rocks have even been observed up to 9.0 (Stumpel et al., 1983 ; Weist & Edelmann, 1984). Therefore this means that for an overburden/rockhead exploration target, the velocity ratio between consolidated rockhead and the unconsolidated overburden can be four times greater for shear waves than for P waves. This increased ratio has a dramatic effect on the

relative critical angles in refraction studies. In shear wave exploration the critical angles are small compared to P waves in the same situation. Small critical angles lead to higher resolution of high relief structures using delay time interpretation techniques.

2. As shear wave velocities are unaffected by water infill of the rock pores, the water table will not act as a refracting surface for shear waves and therefore complicate any lithological interpretations. Thus, they provide a better correlation between the velocity and (solid) lithology (Stumpel et al., 1984).

Shear Wave Reflection

The ability of the seismic reflection technique to resolve thin geological horizons is dependent upon the seismic wavelength. Shear wave velocities are typically 1/2 to 2/3 of the P wave velocities for consolidated rocks, so the shear wave wavelengths are smaller for S waves than P waves if the frequency content of the data is the same.

Results produced by Russian geophysicists indicate that the frequency ratio between P and S waves over an exploration target is typically 1.4 to 2.0 (Edelmann & Schmoll, 1983a) Therefore in reflection studies over consolidated sediments with small Vp/Vs ratios the wavelengths for P and S wave records are roughly the same. Only when the Vp/Vs ratio substantially exceeds 2.0 can shorter wavelengths, and consequently a greater resolution, be expected. This becomes possible, particularly in young near

surface sediments (Edelmann & Schmoll, 1983b). As the velocity ratio between unconsolidated and consolidated sediments is greater for S waves than P waves, then the reflection coefficient (equation 17) must be greater for S waves than P waves in this situation.

The disadvantage of shear wave reflection studies is that shear waves are more difficult to generate, record and process than P waves because:

1. Shear wave reflections are always contaminated by Love waves and the two wave types must be separated by data processing techniques. As their frequency spectra frequently overlap, the two wave types cannot be easily separated. Shear wave reflections may only become apparent after sophisticated data processing techniques such as velocity (f,k) filtering have been applied.
2. As a result of lower velocities relative to P waves, S wave reflections exhibit considerably larger normal moveouts, therefore requiring correspondingly larger dynamic corrections for the stacking procedure.
3. Due to the fact that the critical angle for shear waves is small for shallow reflection studies, the window of sub critical reflections is small, and beyond the critical angle 180 degree phase shifts occur and impair the stack if they are included.
4. Static corrections for S waves are much greater than for P waves, by a factor of up to 6. They require separate analysis as they often bear no resemblance to the P wave static corrections.

CHAPTER THREE

FIELD EQUIPMENT & PRACTICAL ASPECTS OF DATA PROCESSING

3.1 FIELD EQUIPMENT

The original aim of this project was to carry out seismic refraction and reflection surveys with both compressional (P) and horizontally polarized shear (Sh) waves. The only differences in the field work for reflection and refraction surveys is the acquisition geometry. The survey hardware is common to both techniques.

P Wave Source

Throughout the seismic project the P wave source used was explosive. A variety of different source types was used over the three seasons of fieldwork, from small electric detonators to charges made up with 2oz sticks of gelignite (plate 3). The gelignite sticks could be cut, or taped together to produce the required charge strength. The use of explosives may be less economic than generating P waves by hitting a metal plate for shallow surveys. Explosives, however, guarantee the recording of data with a high signal/noise ratio rich in high frequencies. The high frequencies enable the picking of the first breaks in refraction work to a high accuracy.

In refraction work the charge was buried at a depth of 1.5m below the ground surface in a shot hole. The shot holes were made by hitting a 2m steel stake into the ground using a sledgehammer.

A burial depth of 1.5m is sufficient to prevent a 2oz charge from causing a the hole to "blow out" which results in unnecessary damage to the survey field. All shots were tamped using water carried in a small bowser.

For reflection surveys a variety of shot hole depths were used throughout the project. Ziolkowski (1979) showed that for optimum data quality, it is desirable to bury the shot as deep as possible. This then limits the production of unwanted ground roll and retains high frequencies in the recorded data. Obviously for a project of limited economic budget there is a threshold to the amount and depth of drilling one can carry out. A variety of shot depths was used for the reflection surveys, ranging from standard 1.5m holes to deep 6m shot holes. The deep shot holes were drilled using the departmental Victor Products waterflush drill (see frontispiece). At one site a single reflection line was drilled using a commercial rig, which was being used in the course of conventional borehole exploration by the Opencast Executive. The rig, using a single rod, drilled twelve holes to 6m depth in only three hours, whereas using the Victor Products drill at another site it took three days to drill the same number of boreholes to the same depth.

S Wave Source

The S wave source used throughout the project was based one originally used by Hasbrouck (1982). The method of shear wave generation is termed "horizontal hammer" by Edelmann & Schmoll (1983a). The source consists of a two-legged stand which is firmly hammered into the ground. The operator then generates

Plate 3 P wave source
Seismic detonator and 2oz stick of gelignite

Plate 4 S wave source
Shear wave stand with operator

shear waves by standing on the source and swinging a sledgehammer so that the stand is hit perpendicular to the strike of the survey line (plate 4). The source is portable but has a low power output. To obtain records with a good signal/noise ratio, successive hammer blows must be summed. Trials were also carried out using a large pendulum hammer and a larger stand. Although it increased the amplitude of the recorded signal by a factor of 1.8, it was discarded due to its lack of portability.

The source is also not a pure generator of Sh waves. P waves sometimes appear on the field records as coherent noise precursors to the S wave arrivals. A field procedure can be carried out to attenuate any P wave arrivals. Edelmann & Schmoll (1983a) term the procedure the ±Y method. Firstly a number of hammer blows are given to one side of the stand and the Sh arrivals recorded using geophones orientated parallel to the direction of the hammer blows. The geophones are then rotated through 180 degrees and the stand hit with the same number of blows as previously, but this time on the opposite side of the source. The net effect of this is that the shear waves are always recorded with the same polarity, whilst the P wave arrivals are recorded with opposite polarity, thus they destructively interfere and cancel out to near zero amplitude (figure 3.1).

Receivers

The compressional and shear wave receivers used throughout the duration of the fieldwork were commercial (Sensor) wide band, digital grade miniature geophones. Vertical geophones were used to record the P wave data and horizontal geophones orientated in

S WAVES AS A SHALLOW EXPLORATION TOOL

±Y method of P wave suppression

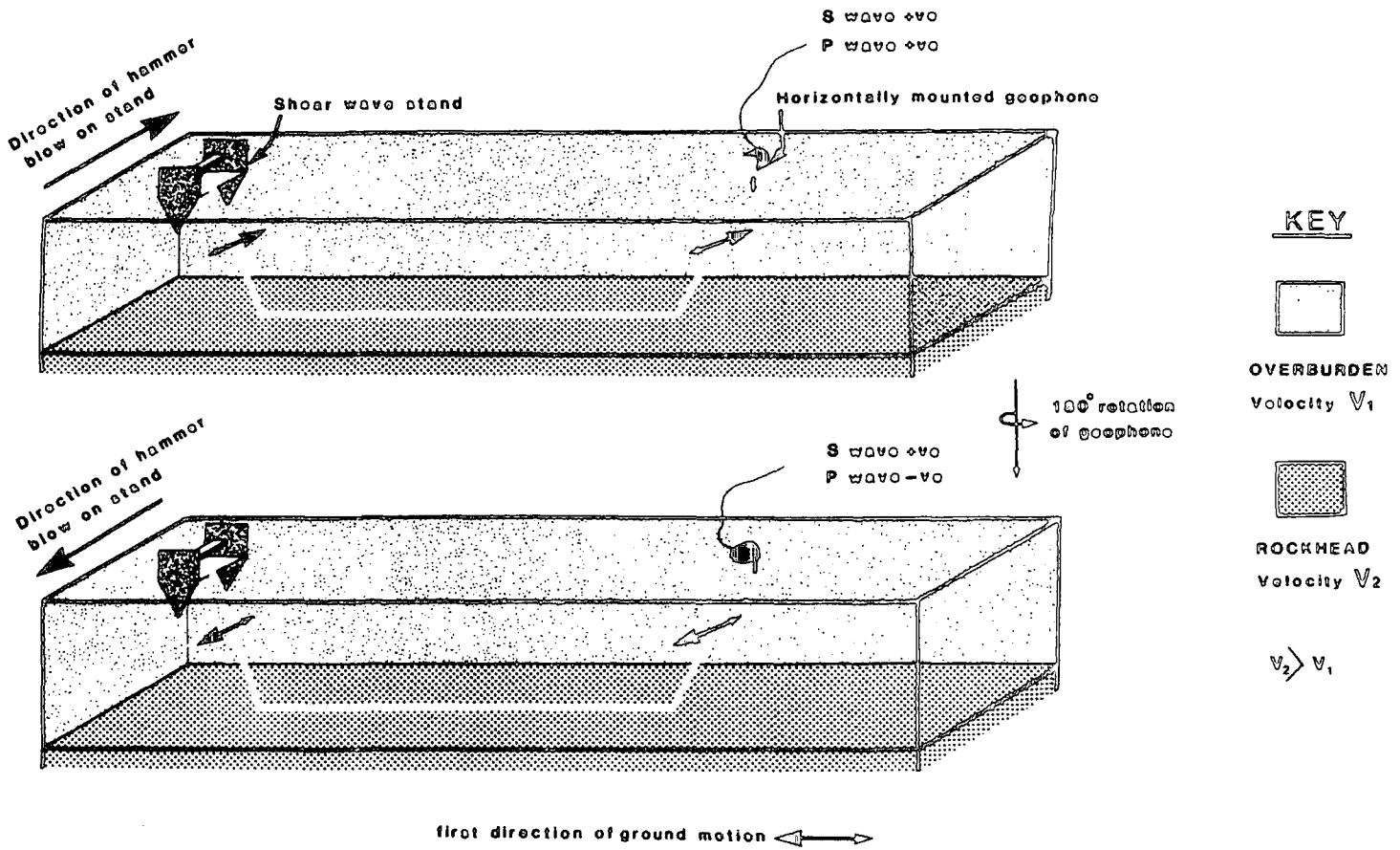

S waves recorded with same polarity — enhanced

P waves recorded with opposite polarity — suppressed

Figure 3.1

the transverse direction were used to record the horizontally polarized shear waves (plate 5). The geophones have a natural frequency of 30Hz and have an attenuating effect on frequencies below 50Hz (figure 3.2). This effect is useful in recording the P wave reflection data as it helps to attenuate the unwanted low frequency ground roll in the field recording.

During the course of our survey work it was noticed that taking care with the planting of the geophones can improve the data quality appreciably. The main source of non-seismic noise on the seismograms comes from the wind causing motion of the geophone casing. This wind-related noise is much more noticeable during shear wave recordings due to the fact that the geophones are recording horizontal motion. On windy days the data quality can be improved by digging small pits for the geophones and using the extracted divots to weight down the geophone leads.

The geophones are linked to the recording system via a 12 channel geophone cable. The cable has connectors at each end for operational ease and the geophone take-outs are spaced at 10m intervals.

Recording System

The recording system used for the field surveys was a Nimbus ES-1210F enhancement seismograph (plate 6). The system has twelve individual recording channels each with its own gain and filter settings. The filters allow for the rejection of undesirable frequencies from the data. Figure 3.3 displays the response curve for a 100Hz high pass filter setting which was used to record some

Plate 5 Receivers
Vertically and horizontally mounted geophones

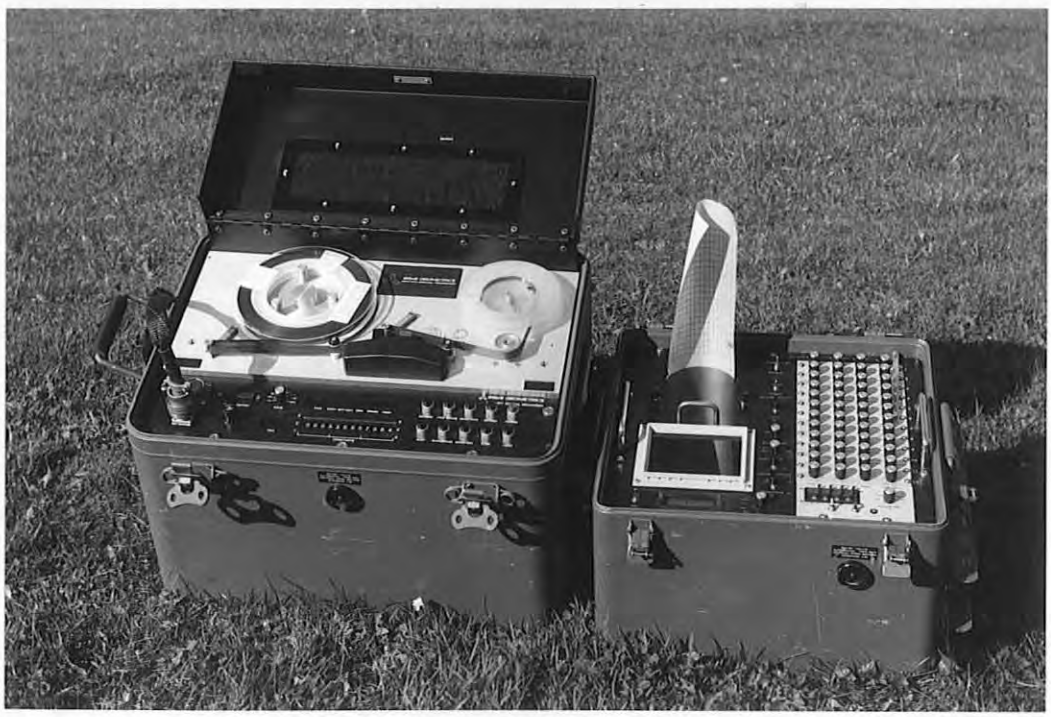

Plate 6 Recording system
Nimbus ES-1210F enhancement seismograph
with EG&G DMT-911 digital tape recorder

Figure 3.2

Geophone response curve

Type Sensor SM7
Model GT
Natural frequency 30 Hz
Shunt o.c.
Damping 65%
Coil resistance 370 ohms

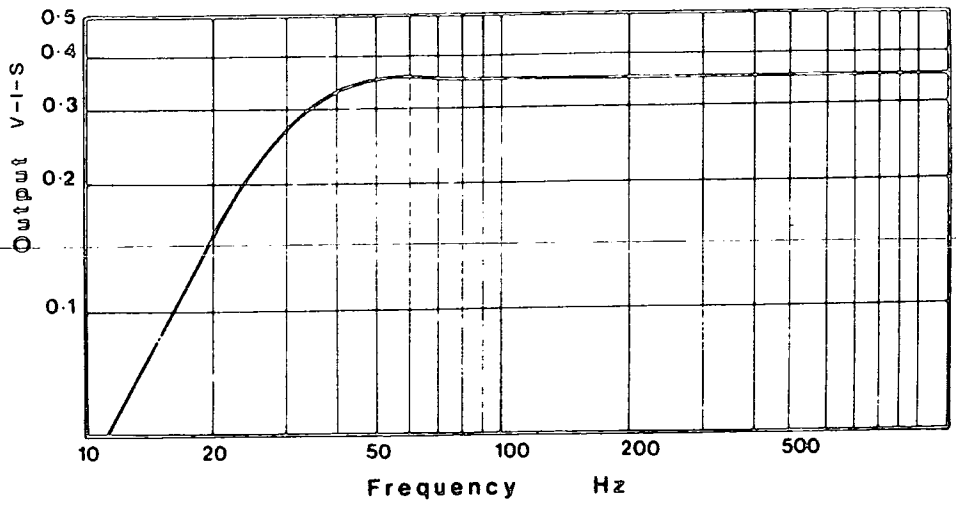

Figure 3.3

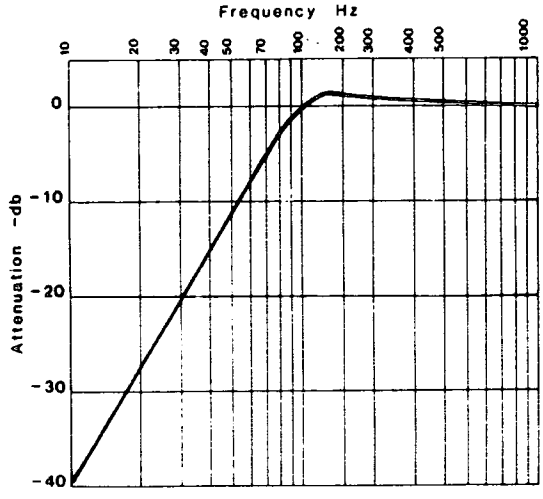

Nimbus - Filter response curve

Filter setting 100 Hz Highpass

of the reflection data during the course of the fieldwork. A 50Hz "notch" filter is also available to remove mains pickup in areas with overhead power cables. The Nimbus recorder has the facility of recording data over incremental time intervals from 50 to 2000msecs. The incoming signal is passed through an A/D converter which outputs a binary number proportional to the input voltage. The digital seismic signals are stored in the solid-state memory which has 1024 samples per trace. The amplifier gains on the Nimbus were set as high as possible to take full advantage of the dynamic range available. Care must be taken not to saturate the signal, that is, when the largest voltage is too big for the A/D converter which outputs its largest possible digital number. Saturated or clipped signals appear as square waves rather than sinusoids (Knapp & Steeples, 1986a).

The enhancement feature of the Nimbus allows successive seismic signals from a number of hammer blows to be summed in the internal digital memory. The signal stored in the memory is displayed on a built-in CRT monitor either as wiggle traces or as variable area wiggle traces. A permanent record can also be made via an ocillograph which reproduces the CRT display on electrosensitive paper. Figure 3.4 displays typical P and S wave records that were produced during the course of our fieldwork.

The Nimbus is triggered to begin recording by an electrical signal which may be produced in a variety of ways. For P wave work the firing box used to detonate the explosive also sends a voltage pulse to the Nimbus via an interconnecting wire. For S wave surveys a geophone is placed directly adjacent to the stand. On impact with the stand by the sledgehammer the geophone produces

Typical Refraction Field Records

Output from Nimbus Oscillograph

P wave

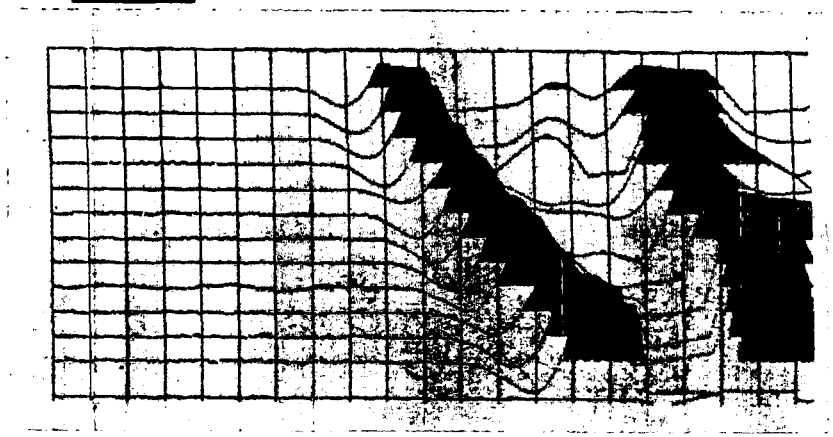

100 msec record

2oz Dynamite charge

S wave

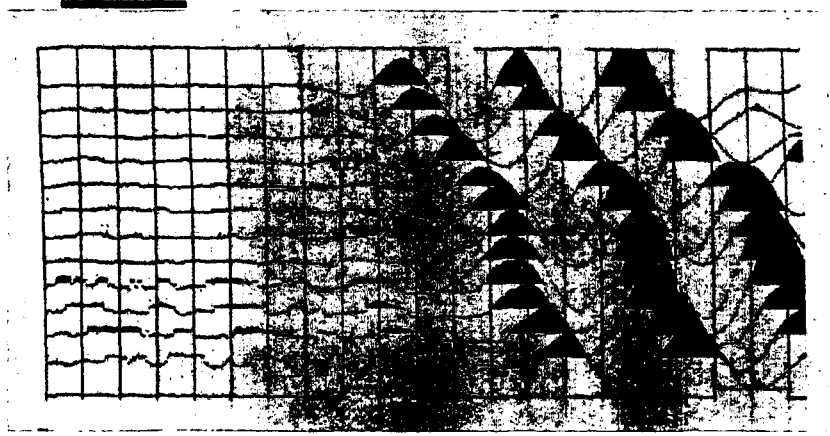

200 msec record

10 stacked hammer blows

3m Geophone spacing 12 channels

Figure 3.4

a sharp voltage pulse which triggers the Nimbus to commence recording.

For reflection surveys further computer processing of the field data is required, so a means of data transfer has to be available. A digital magnetic tape recorder support for the Nimbus was obtained for the project (EG&G Geometrics model DMT-911). This portable recorder stores each 12 channel file after each shot has been taken. The individual records are recorded in an IBM compatible SEG-D de-multiplexed format on 1600bpi, 1/2inch tape, the sample values being stored in a 2 byte quaternary exponent form (see appendix D). As the tape is IBM compatible it could be removed from the recorder and transferred directly to the tape drives of the university's NUMAC computer system for further processing.

3.2 PRACTICAL ASPECTS OF DATA PROCESSING

Refraction Computer Programs

For all the refraction lines surveyed during the course of this project (P and S wave), the data were not recorded on magnetic tape, but permanent paper records were obtained via the Nimbus ocillograph. The first break positions on each record were picked by hand and the traveltimes calculated using a rule and a pocket calculator.

Each complete data set was then transferred to a computer file on the university's NUMAC system. Plots were then made of the traveltime data using the Easyplot graphics package. The plot was then inspected and each data point was assigned to a direct arrival or a refracted event. This is a very important process, as any errors at this stage can have disastrous results. As well as using gradient changes as an indicator of refracted arrivals, the original field records were used to observe the seismic character as a means of identifying direct and refracted arrivals. After this stage had been completed a phantomed reversed traveltime graph was drawn for each refractor (Lankston & Lankston, 1986). A computer data file containing the digital values of the phantomed data was produced.

A suite of Fortran computer programs was developed by the author to process the phantomed refraction data using the Generalized Reciprocal Method (Palmer, 1980 ; see appendix B). The initial data file contains information on the peg number,

forward traveltimes, reverse traveltimes, peg spacing, reciprocal time and the range of XY spacings required. Four programs were developed to complete the processing sequence, each one being used in turn, with new information being added to the data file after the termination of each run. The programs utilise the Easyplot graphics package. The four programs are as follows;

RECIPV - This program calculates the velocity function for a range of desired XY spacings. The optimum XY spacing is chosen by inspection, or from the results of a previous Plus-Minus interpretation. The program outputs a graph of the results, as well as a data file containing the digital values.

RECIPL - After inspection of the velocity function graphs, each graph is broken down into individual linear segments. This program fits a least squares linear regression line to the data and calculates the velocity of the chosen segment, as well as giving an estimate of the error in the velocity (due to the scatter of the data points ; Barefoot, 1967).

RECIPP - This program calculates the time depth values for the optimum XY spacing. A value of the refractor velocity obtained from RECIPL has to be added to the data file prior to the running of this program. The program outputs a graph of the results as well as a data file containing the digital values.

RECIPD - This final program in the suite converts the time depth values obtained from RECIPP into depth. The values for the overburden and refractor velocities have to be added to the data file containing the time depth values. Allowance can be made for lateral variations of velocity. A graph of refractor depth is output by this program.

Reflection Computer Programs

At the beginning of this project in 1982 no facility existed to process land seismic data at Durham University. The seismic processing system at Durham had only been used to process marine seismic data up to that time. Software needed to be written to link the SEG-D format data output on magnetic tape by the Nimbus, to the seismic processing system which could only handle SEG-B format field tapes recorded in a consistent sequence or sorted SEG-Y tapes. As the departmental processing system was being heavily used at this time by an ongoing marine seismic project, the author had to develop the necessary software on the university's NUMAC system.

The processes that needed to be carried out on NUMAC were tape translation, trace sorting, trace editing, application of the field static shifts and mute. Four Fortran 77 computer programs were developed to carry out the above processes (figure 3.5).

TAPEDUMP - This program reads the field tape and removes the digital values of each seismogram from it (no information is recorded in the header blocks by the Nimbus recorder). The program translates the digital values from the 2 byte quaternary exponent form in the SEG-D format, to the IBM two's complement format required by NUMAC. The program outputs the whole data set containing the digital sample values on the field tape on to a temporary disk file as a one dimensional array. Each separate trace contains 1024 sample values, with a maximum amplitude range of +511 to -512 (10 bits).

SORTPROG - This is an interactive program which outputs a numerical data file used to sort the data into either a CSG or CMP format. The program allows for a variety of data acquisition geometries in the sort procedure. Each seismogram is indexed by its original file and record number. The value of the shot to receiver offset is automatically calculated by the program.

EDITSORT - This also is an interactive program which allows the data file produced by SORTPROG to be edited. Information can be added to include an offset-dependent mute function and individual trace static shift values. The program allows for the editing of individual traces or traces with a common offset or traces with a common original file number.

SEGDSEGYMS - This final program in the suite inputs data from both the SORT data file and the temporary disk file containing the seismogram digital values. The program makes use of the direct access command available with Fortran 77 (Munro, 1982). This command allows the program to jump immediately to the desired record on the disk file, instead of having to count the records from the beginning of the file. This makes a dramatic improvement to the time required to carry out the sort process.

Subroutines within the program carry out the mute function application and the muting of the digital samples containing the direct and refracted arrivals. The sorted tape is finally output in SEG-Y format on digital tape.

Land Reflection Data Processing Sequence

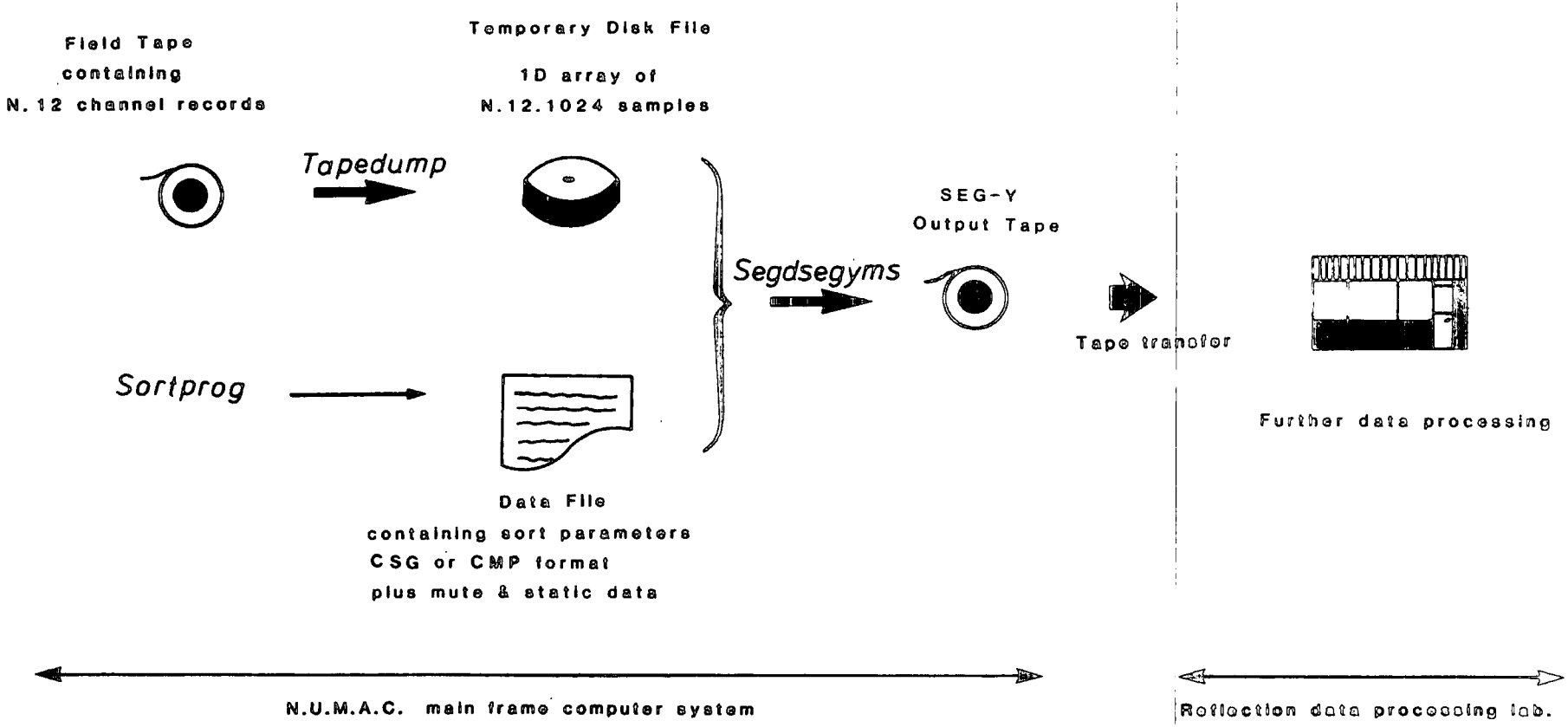

Figure 3.5

The SEG-Y tape is manually transferred between the two computer systems. As the NUMAC machine is an IBM and the departmental PDP-11/34 is a DEC machine, the two being incompatible, the first process to be carried out on the tape is one of "byte swapping" so that the tape can be read by the DEC machine. A program developed by Hobbs (1985) was used. After this process has been carried out the tape is ready for further data processing using the software available on the seismic processing system.

Reflection Processing Sequence

The time series analysis options that were used to process the shallow reflection data acquired during the course of this project are as follows;

1. Trace editing
2. Mute application
3. Band pass frequency filtering
4. Trace equalization
5. NMO correction
6. CMP aligned statics
7. Stack
8. Time ramps
9. Automatic gain control

Processes 1 and 2 are carried out on NUMAC, whilst processes 3 to 9 are carried out on the Durham University seismic processing system. A full description of the available software is given in Hobbs (1985). The relevance of these processes to shallow land seismic data is given below:

Trace Editing

Very noisy seismic traces or dead channels are edited out of the data set as the very first process which is carried out. The unwanted traces are identified on a playout of the complete data set. As the fold of cover of shallow land data is low (typically 4 to 6), the inclusion of noisy traces in the stack can significantly impair the data quality.

Mute Application

As stated previously, the mute function is applied to zero out any direct or refracted events at the beginning of each seismic trace. Normally the mute is applied down to a time specified as a function of trace offset, and this function follows the refracted arrivals. The mute function has a half cosine taper at the end to avoid introducing spurious high frequencies into the traces.

A feature seen on shallow land seismic data recorded during this project is the inconsistency between shots. Some records display trains of events following the first break arrivals at the same velocity. These have been called reverberant refractions (figure 3.6). The two CSGs displayed are from the same seismic

line, the shot points being a matter of meters apart. CSG(A) displays a clean refraction first break, followed by reflection events obeying the hyperbolic moveout one would expect. CSG(B) displays a train of events of up to 7 cycles following after the first break at the same velocity as the refraction. Clearly these are not reflections. The occurrence of the reverberant refractions appears to be related to the ground conditions immediately surrounding the shot point. The mute function has to be adjusted for each CSG to remove such events.

Band Pass Filtering

The band pass filter available on the Durham University processing system is a zero phase filter with half cosine taper ends as shown in figure 3.7. The filter is described by the four frequency values f1,f2,f3 and f4. The filter is designed and applied to the seismic traces in the frequency domain. Care was taken not to design too narrow a pass band or too short a taper, because this causes instabilities in the filter and results in "ringing" on the output seismic trace.

The band pass filter is used to attenuate ground roll on the seismic traces. The optimum filter is one which effectively removes the low frequency ground roll, whilst not impairing the reflection events. A value for the peak frequency content of the events can be determined by carrying out spectral analysis on individual traces. Separate traces containing primarily ground roll or reflections are analysed. Each trace is converted to the frequency domain and a plot of the amplitude spectrum is made. To obtain the optimum filter coefficients is a matter of trial and

Figure 3.6

The problem of reverberant refracted arrivals

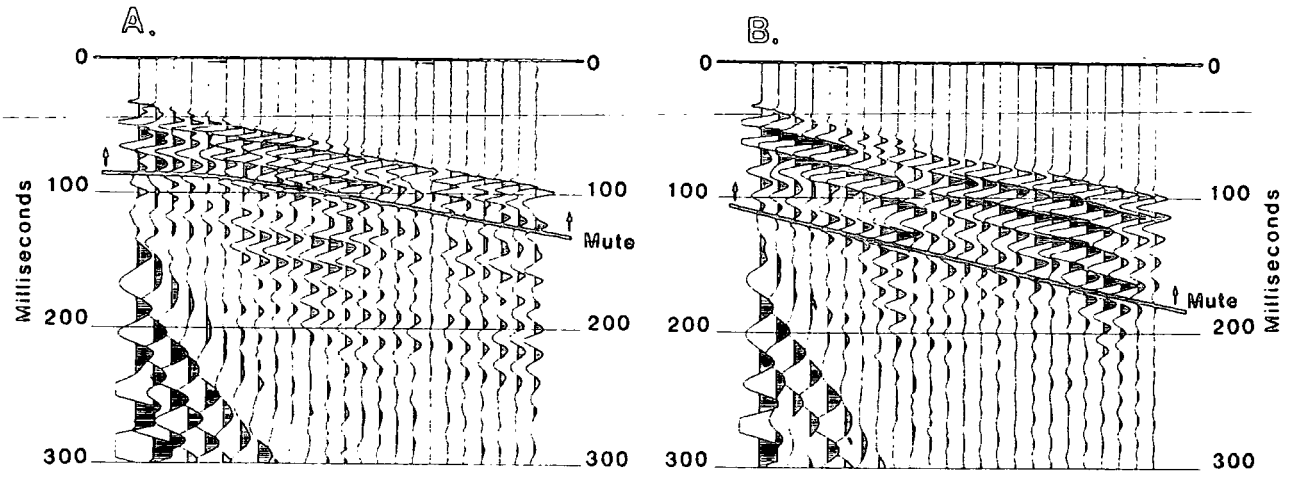

Figure 3.7

Bandpass filter design

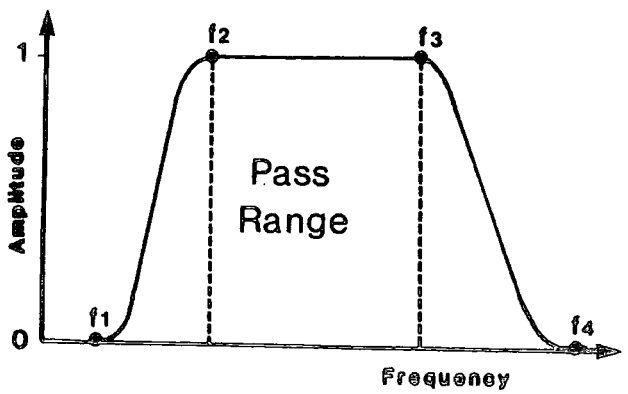

error. Tests are carried out using a variety of filters on CSGs (figure 3.8). Note that if the high amplitude ground roll is clipped on the raw field data, this introduces spurious high frequencies into the ground roll which cannot be distinguished from reflections by band pass filtering. Such traces have to be removed by editing.

A time variant band pass filter is also available. This is used to highlight near surface high frequency components, whilst allowing lower frequencies into the data with time to compensate for absorption effects.

Trace Equalization

This process is used to balance the energy or amplitude between traces in each CMP gather, mainly to account for amplitude variations due to shot point inconsistencies. The traces are normalized so that their maximum amplitude is unity or to a unit RMS energy. The process can also be applied as a cosmetic process prior to plotting. This process is not carried out if relative amplitude studies are required.

NMO Correction

The NMO correction is applied to account for the effect of hyperbolic moveout of the reflection events due to non-coincidence of shot and receiver (equation 12).

The stacking velocity required for the correction must be determined by a separate process. Velocity information may be

Attenuation of Ground Roll by Frequency Filtering

24 channel common shot gather records

Record length 500 milliseconds

P wave

Raw data

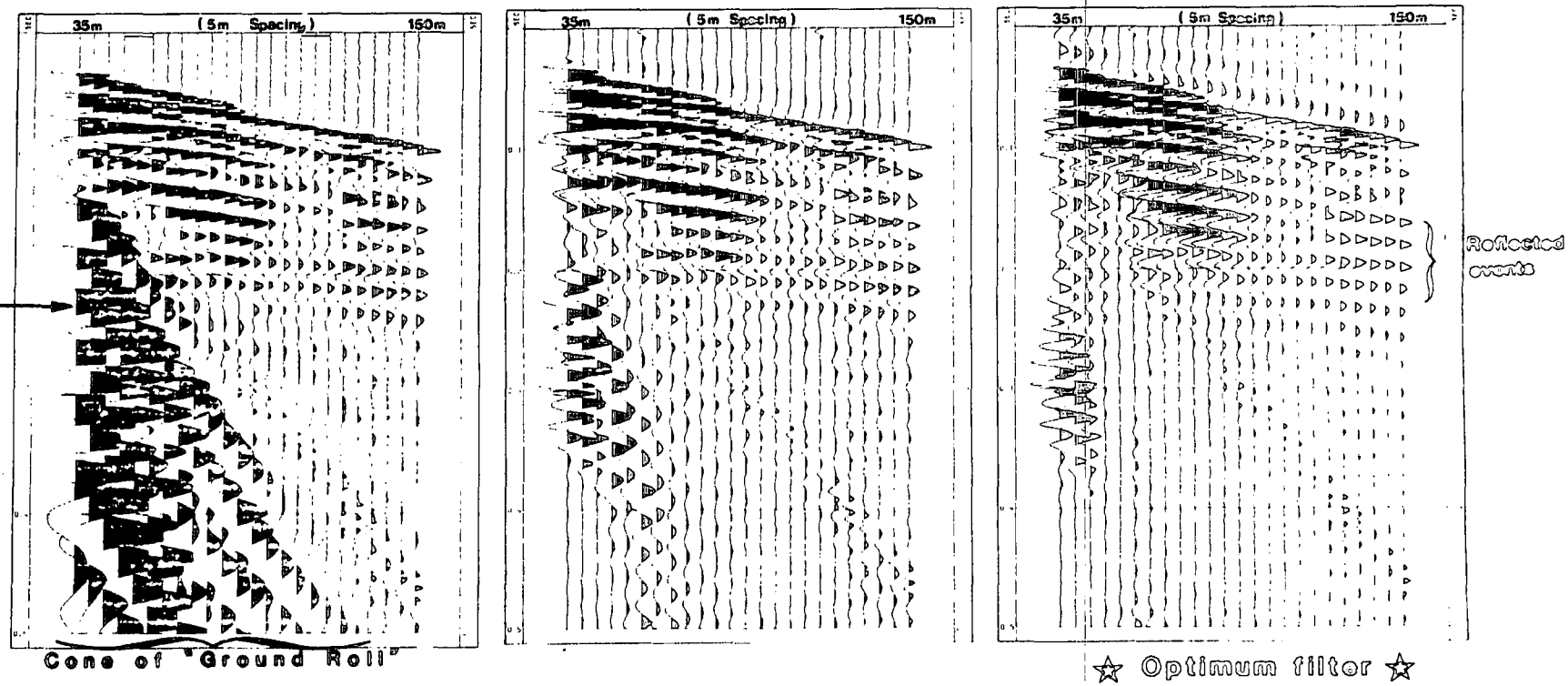

Band pass filters

NO Filter Applied

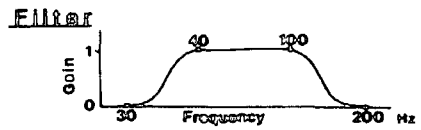

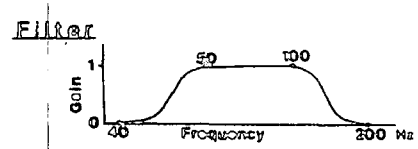

Figure 3.8

available from a refraction survey, from which values of stacking velocity may be calculated. Conventional velocity analysis techniques using semblance values are not applicable to shallow land data, due to the low fold of cover, small moveouts and residual static errors that may be present in the data. The method adopted to determine the correct stacking velocity for the final stacked section was to chose arbitrary stacking velocities and stack sections of the line known to contain good data quality. The correct stacking velocity produces the largest primary reflection amplitudes on these trial panels.

CMP Aligned Statics

The theory of the CMP aligned static technique was described in the previous chapter. The parameters required for the practical application of the process are:

1. The autocorrelation window (start time and window length) that is used to determine the static shifts. The window must only contain reflection events with a high signal/noise ratio.
2. The maximum shift value (in msecs) that is to be applied to the traces so that "cycle skipping" is avoided. This is particularly important for shallow data where the seismogram appears monochromatic.

The parameters used in the routine are described as;

window start time (window length) +/- maximum shift value (msecs)

Stacking

The stacking process sums the traces together in each CMP gather after NMO corrections and the optional CMP aligned statics have been applied.

Time Ramps

In order to enhance signal amplitude progressively down a trace, a time varying gain function is applied to the trace. For shallow land data, a gain function proportional to the square of the traveltime is often found to be suitable for making each trace more stationary. A function based on time and stacking velocity can also be used to compensate for geometrical spreading.

Automatic Gain Control

Using the AGC, the signal amplitude along the trace is adjusted in such a way that the energy contained within a window of the trace is equalized. The window length is variable. This is essentially a cosmetic process which can be used before plotting the final seismic reflection section.

CHAPTER FOUR

STANLEY MOSS : SITE NO. 1

Stanley Moss is situated between the villages of Stanley Crook and Sunniside in County Durham. The exploration phase has been completed by the Opencast Executive at this site using data gathered from boreholes drilled on a dense 30m grid pattern. The site is a single flat large field, and the subsurface geology consists of near horizontal coal measures covered by a thin veneer of glacial drift only some 3m in thickness.

This site was first investigated using seismic techniques as part of an M.Sc. dissertation in the summer of 1982 (Chester, 1982). The target of investigation at this site is a fault which crosses the prospect with a roughly east-west trend, and has a throw of approximately 5m to the north. The fault cuts the Harvey coal seam at 20m depth. This coal seam appears to have been worked only on the south side of the fault. The Tilley coal seam, at a depth of 40m, is worked on both sides of the fault. From the borehole information it is believed that the Harvey workings have now sloughed in.

The results of Chester's work established two main conclusions. Firstly, using both the P wave and S wave techniques, no reflected arrivals could be seen on the raw field records. Therefore this ruled out using the reflection technique as a means of locating the fault. Secondly, observing the first break information, only one refractor appeared on both the P and S wave profiles, even when large shot to geophone offsets were used.

The results of the refraction profiles shot by Chester were inconclusive in locating the target fault. This was due to the fact that no attempt had been made to use the Plus-Minus technique on the reversed traveltime graphs to enhance any velocity or depth anomalies associated with the fault.

The observation of anomalies originating from the refractor on raw time distance data is very difficult in an area where the overburden consists of glacial drift material. This can be due to variations in surface topography, the thickness of the near surface soil layer, or the inhomogeneous nature of the drift which may exhibit a variable seismic velocity. These features can result in the application of random small time shifts to the first break data points, which tend to mask any anomaly that may also be present due to a faulted refractor.

Survey Results

In November 1982 some initial reconnaissance work was carried out at the site. Shots were fired into a single 12 channel geophone spread straddling the proposed fault location, using a geophone spacing of 5m. Small explosive shots were fired into the geophone spread from both ends using a variety of shot to first geophone offsets. Figure 4.1 displays some of the results of these trials.

The results of this survey again show that the refracted arrivals display distinct parallelism, even using a shot to geophone offset of 200m. This result affirms that there is only one refractor which can be profiled for both P and S wave methods

Stanley Moss Reconnaissance Survey
Line 2

Only a two layer case present

arrivals display parallelism

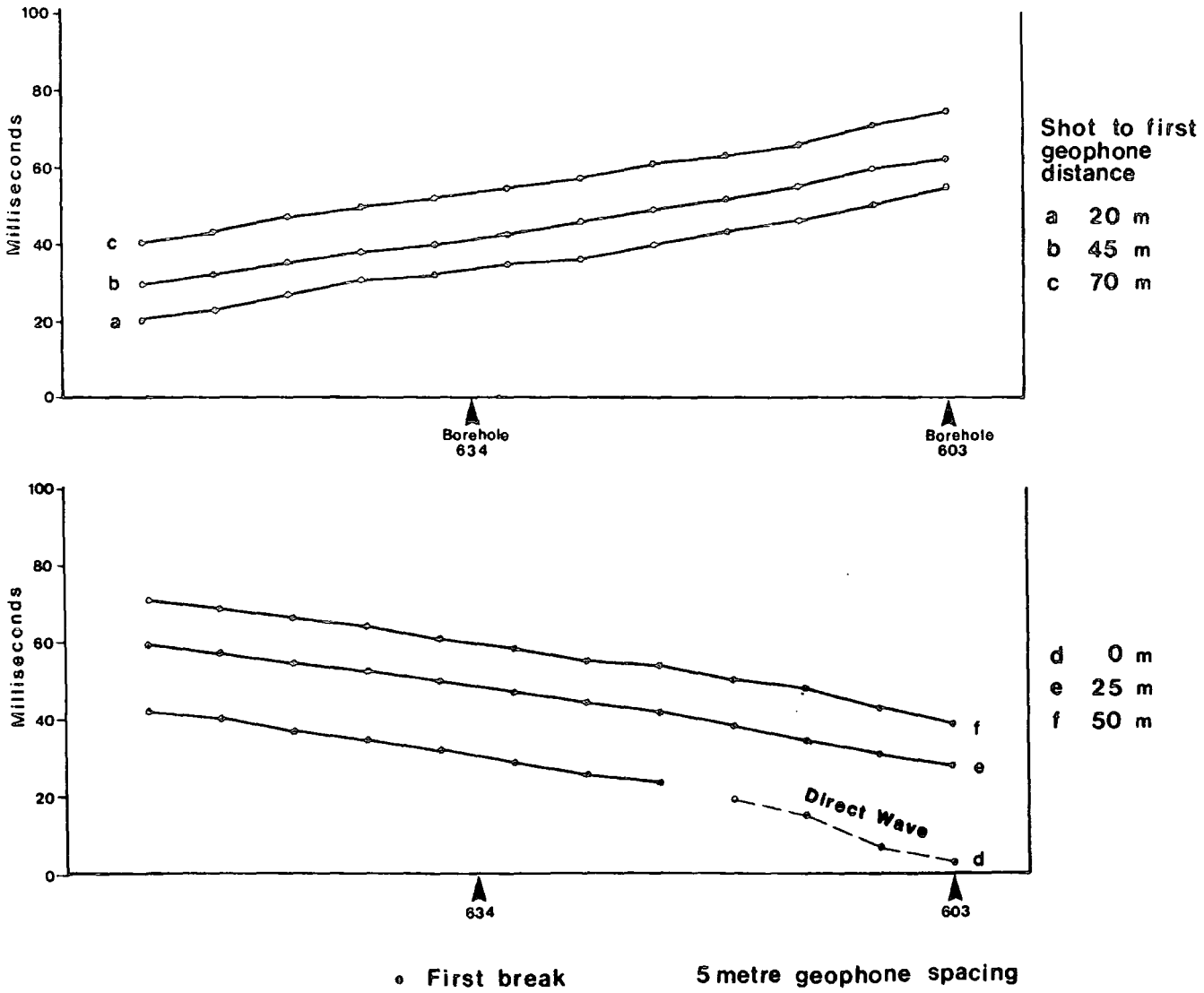

Figure 4.1

at this site. Analysis of the results using the Plus-Minus technique reveal a change in refractor velocity as the fault location is crossed. No major anomaly was apparent in the refractor depth. It was then thought that this result warranted further investigation. In the spring of 1983 further work was carried out at the site. A series of six P wave lines were recorded, three S wave lines were recorded and three further S wave lines were also compiled by re-analysis of Chester's (1982) data.

Figure 4.2 shows the location of the seismic lines with regard to relevant borehole locations. The lines were shot from north to south and are centrally located on the proposed fault positions. From previous work we knew that only one refracted arrival could be recorded at this site. Therefore a minimum offset of the shot to first geophone could be calculated such that no direct waves appeared as first breaks, while allowing the refracted first arrivals to be recorded with high signal/noise ratio. The lines were profiled using the optimum offsets of 30m and 45m for S and P waves respectively, with a 3m peg spacing, moving up ten geophones at a time, leaving a two geophone overlap between adjacent spreads. This means that any effects due to shot statics could be accounted for. A phantomed traveltime graph was built up in both the forward and reverse directions. Figure 4.3 displays the resultant graph for line 1 with both P and S waves. From these graphs it is clearly difficult to pick any anomalies originating from the faulted bedrock.

When the Plus-Minus analysis technique was employed on the reversed refraction lines, it became apparent that there was a

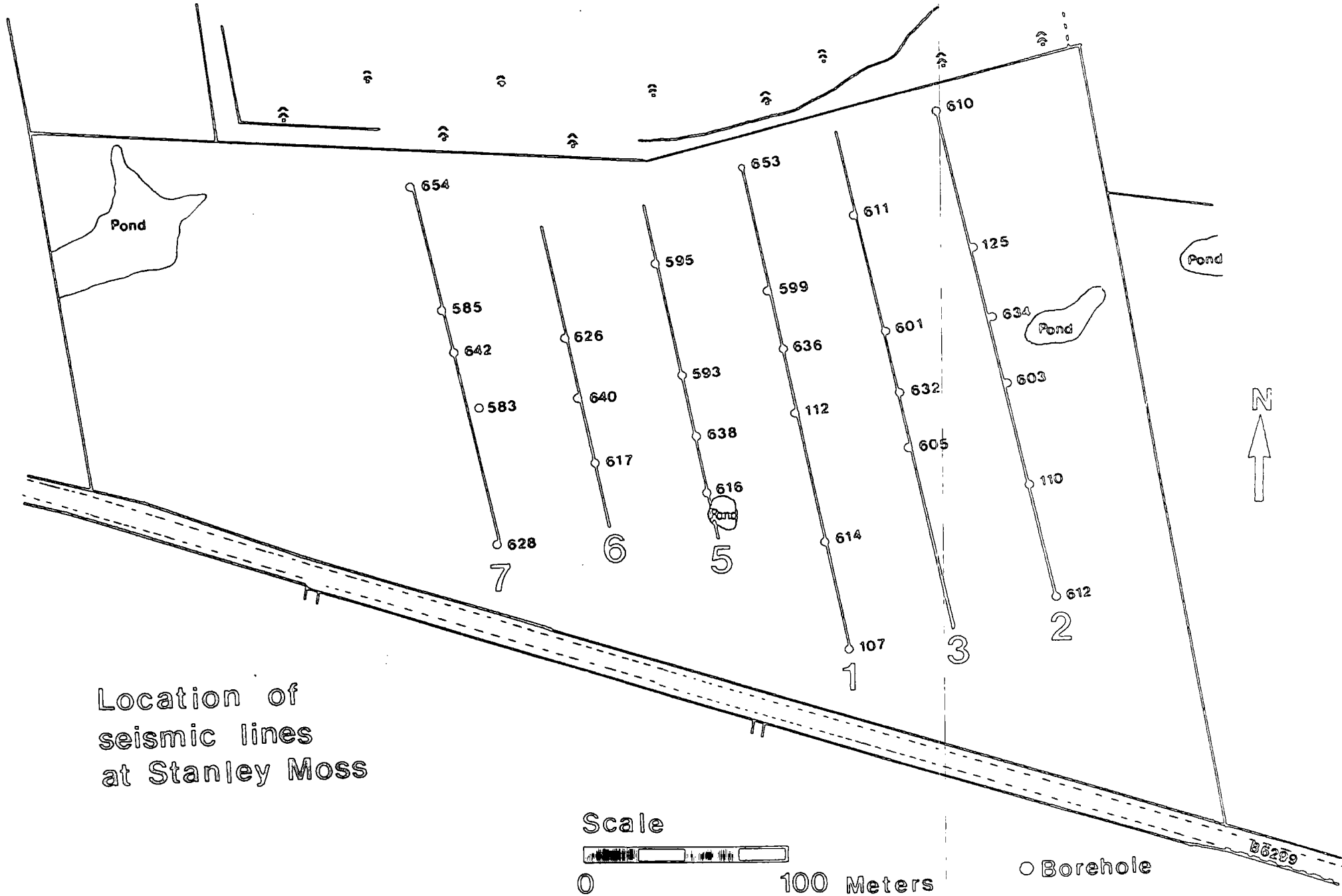
Pond
654
585
642
583
628
7
626
640
617
6
595
593
638
616
5
653
599
636
112
614
1
611
601
632
605
107
3
610
125
634
603
110
612
2
Pond
Pond
N
Location of
seismic lines
at Stanley Moss
Scale
0
100 Meters
Borehole
B6259

Figure 4.2

Phantomed Time Distance graph

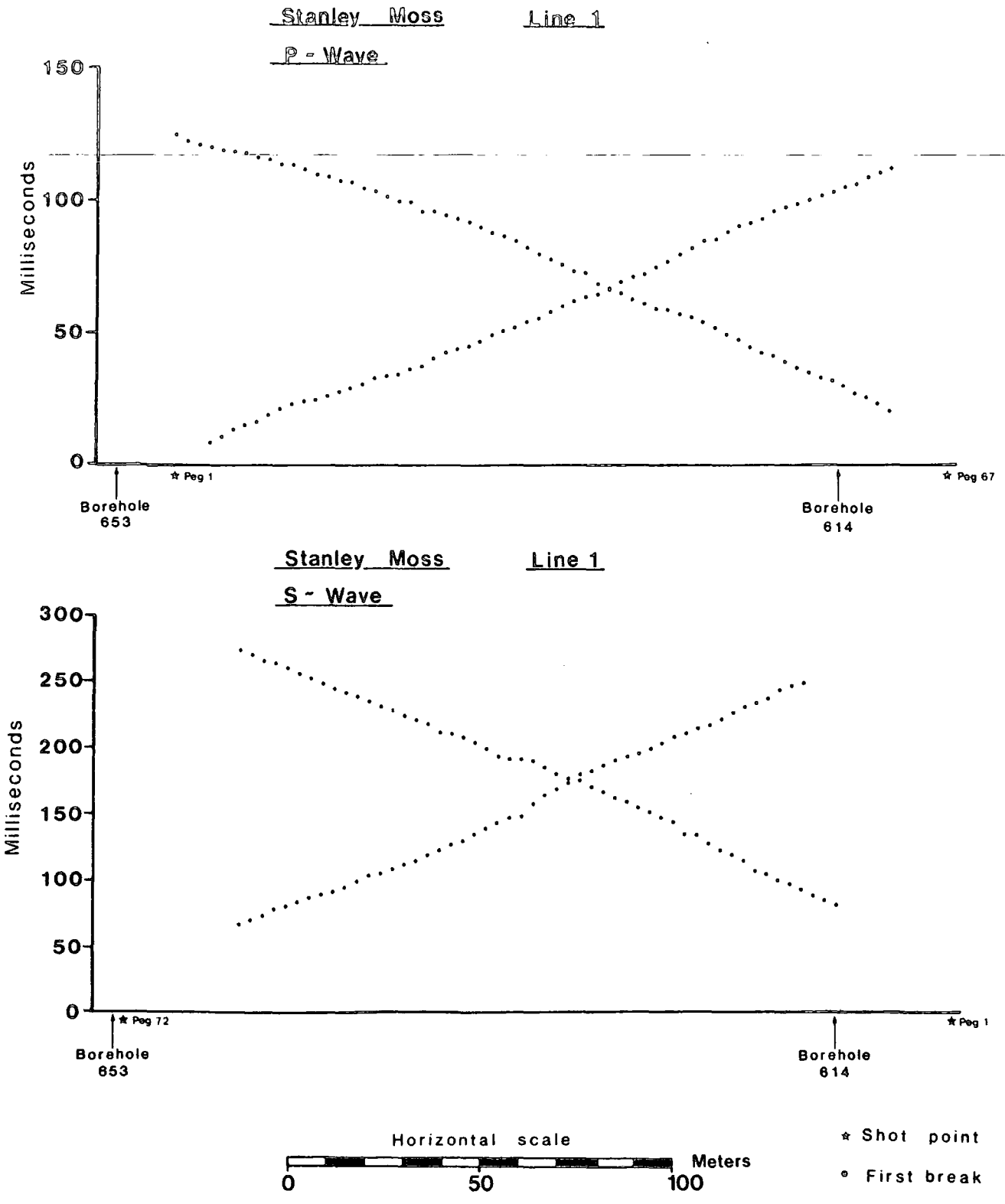

Figure 4.3

change in velocity visible on the minus graphs, indicating that there is a refractor of differing seismic velocity on each side of the fault. Figure 4.4 displays the velocity analysis techniques applied to the data acquired from line 1 P wave. The minus graph shows a velocity of 2109m/sec to the north of the line and a velocity of 1565m/sec to the southern end of the line. To further enhance this velocity contrast, a reduced minus graph was plotted by subtracting a gradient of 1/2000m/sec from the minus graph. The abrupt velocity change now becomes magnified. Further analysis was then carried out on the velocity information by producing a graph of interval velocity along the profile using a rolling least squares fit to eight data points on the minus graph. These types of analysis were carried out on all the seismic lines for both P and S waves.

Using the plus time data and a value for the overburden velocity calculated from data collected using short refraction spreads, the depths to the respective P and S wave refractors were calculated. The depth to the refractor calculated from the S wave surveys varies about a value of 3m. This depth corresponds to the drift/rockhead interface observed from the borehole data. The P wave refractor appeared to come from a depth of 6m. It is postulated that this depth corresponds to the base of weathering of the Coal Measures below rockhead. The distinction between these two refracting horizons is confirmed by the fact that the P and S wave plus time graphs show different forms along the same profiles.

Using a value for the S wave velocity of the overburden of 160m/sec and the calculated plus times, profiles of the drift

STANLEY MOSS Line 1 P-wave

Minus Graph / Velocity Analysis Function

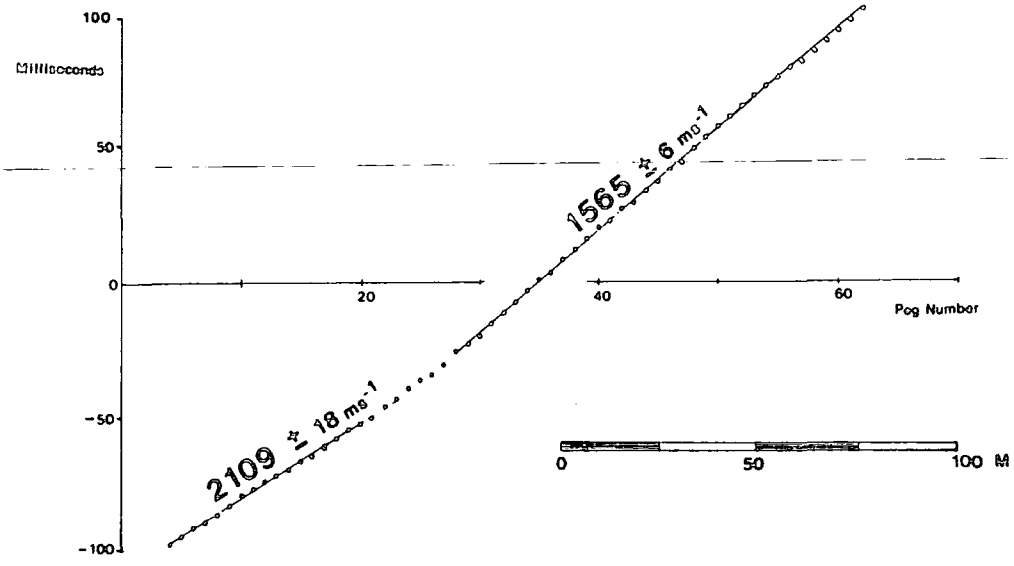

Reduced Minus Graph / Velocity Analysis Function

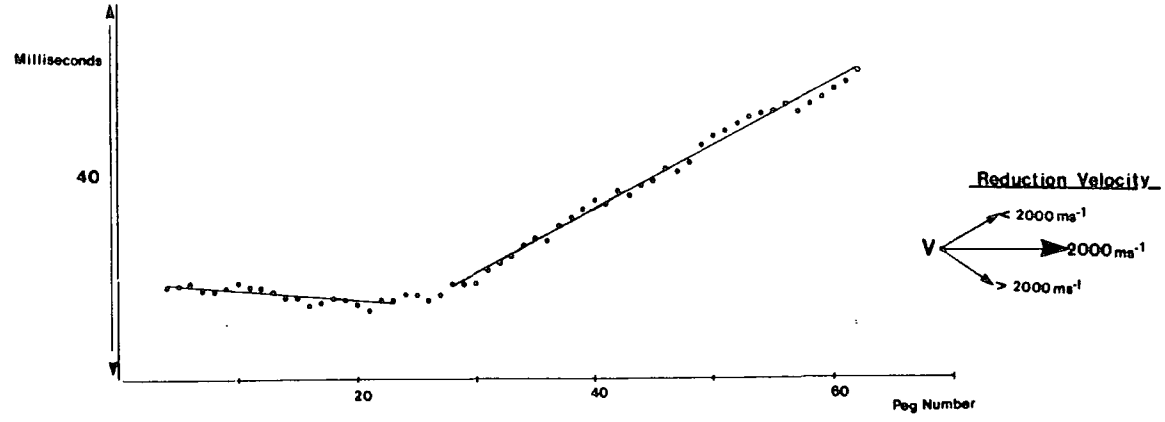

Interval Velocity (n=8)

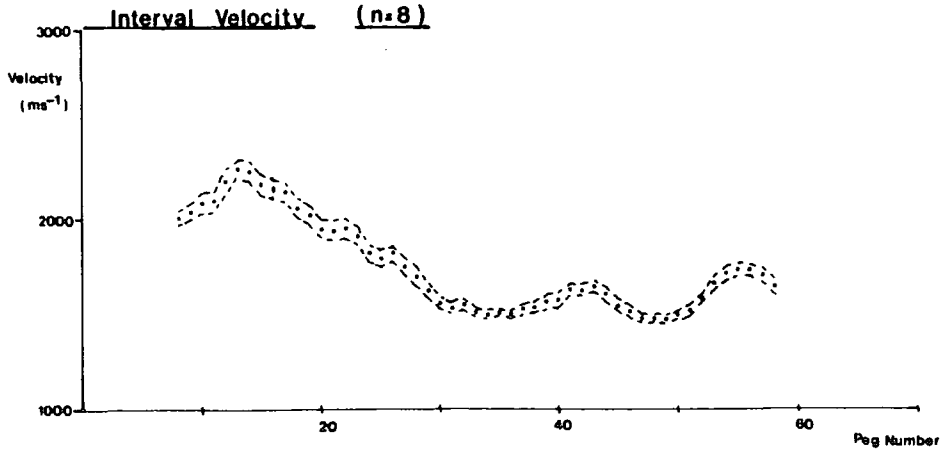

Line location

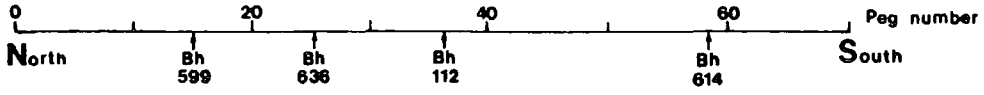

Figure 4.4

cover thickness were calculated along seismic lines 1, 2 and 7 (figure 4.5). The results show good agreement with the drift thickness values obtained from the borehole information.

Figures 4.6 to 4.11 display the final results from the Plus-Minus analysis of each of the six seismic lines along with the respective geological cross sections which include the proposed fault position for each line as located using only the borehole information in each case. Distinctive features in the plus and minus graphs from each line are noted below:

Line 1 Figure 4.6

P wave minus graph - A distinct change in velocity can be seen from 2109m/sec in the north to 1565m/sec in the south, the location of the velocity change is 10m north of the proposed fault position.

S wave minus graph - A well defined change in velocity can be seen from 895m/sec in the north to 750m/sec in the south, the location of the velocity change is 11m north of the proposed fault position.

Plus graphs - The S wave plus graph shows a step in refractor depth in the vicinity of the proposed fault location.

Line 2 Figure 4.7

P wave minus graph - The results are more complex than line 1, the reduced minus graph displays three velocity segments 2353,1833 and 1657m/sec (north to south). The transition from 1833 to 1657m/sec takes place over a low velocity zone 9m wide 2m to the north of the proposed fault location.

S wave minus graph - Three velocity segments are again seen 953,

854 and 752 m/sec along the line. A 9m wide low velocity zone is again apparent approximately 4m north of the proposed fault location.

Plus graphs - No clear anomalies are present.

Line 3 Figure 4.8

P wave minus graph - Three velocity segments are apparent on the reduced minus graphs 2282, 1468 and 1762 m/sec from north to south. There is a 10m wide anomalous zone in the reduced minus graph 8m to the north of the proposed fault location.

S wave minus graph - A clear velocity contrast from 920 to 726m/sec is located at the proposed fault.

Plus graphs - The P wave plus graph shows a region of refractor deepening coinciding with the velocity anomaly. The S wave plus graph displays a step in the vicinity of the fault.

Line 5 Figure 4.9

P wave minus graph - Three velocity segments are apparent on the reduced minus graphs, 2151,1787 and 1485m/sec. The transition from 1787 to 1485m/sec is located 3m to the south of the proposed fault location.

S wave minus graph - The graph reveals a change in velocity from 920 to 593m/sec on each side of the fault, separated by a zone 25m wide of fluctuating velocity value.

Plus graphs - No clear plus time anomalies are present.

Line 6 Figure 4.10

P wave minus graph - A refractor velocity in the north of 2072m/sec is separated from a value of 1722m/sec by a broad region of fluctuating lower velocity. The transition from the 2072m/sec

to the low velocity occurs 5m to the north of the proposed fault location.

S wave minus graph - A 6m wide low velocity zone separates a velocity of 868m/sec in the north from velocity of 738m/sec in the south centred 2m to the north of the proposed fault location.

Plus graphs - The P wave plus graph displays an anomalous increase in the plus times spanning the proposed fault location.This may indicate a deepening of the zone of weathering around the area of the fault along this seismic line. There are no anomalies in S wave plus times.

Line 7 Figure 4.11

P wave plus graphs - Two velocity segments of 1826 and 1465m/sec are separated by a 12m wide zone centred at the proposed fault location. The P wave refractor velocity to the north of the fault is less than 2000m/sec, this is the only line on which this occurs.

S wave plus graphs - A refractor velocity of 957m/sec in the north is separated from a refractor velocity of 759m/sec in the south by an area of fluctuating intermediate velocity, a 10m wide low velocity zone is located at the proposed fault.

Plus graphs - Both plus graphs display fluctuations none of which occur near the fault.

Figure 4.12 displays the fault location picks calculated from the seismic results. The trend of the fault is mapped out across the prospect (with error bars). The fault positions located by the seismic results are mainly consistent with those proposed from the dense borehole grid, with the exception of line 1. Line 1

Stanley Moss

Calculation of drift thickness using S-waves

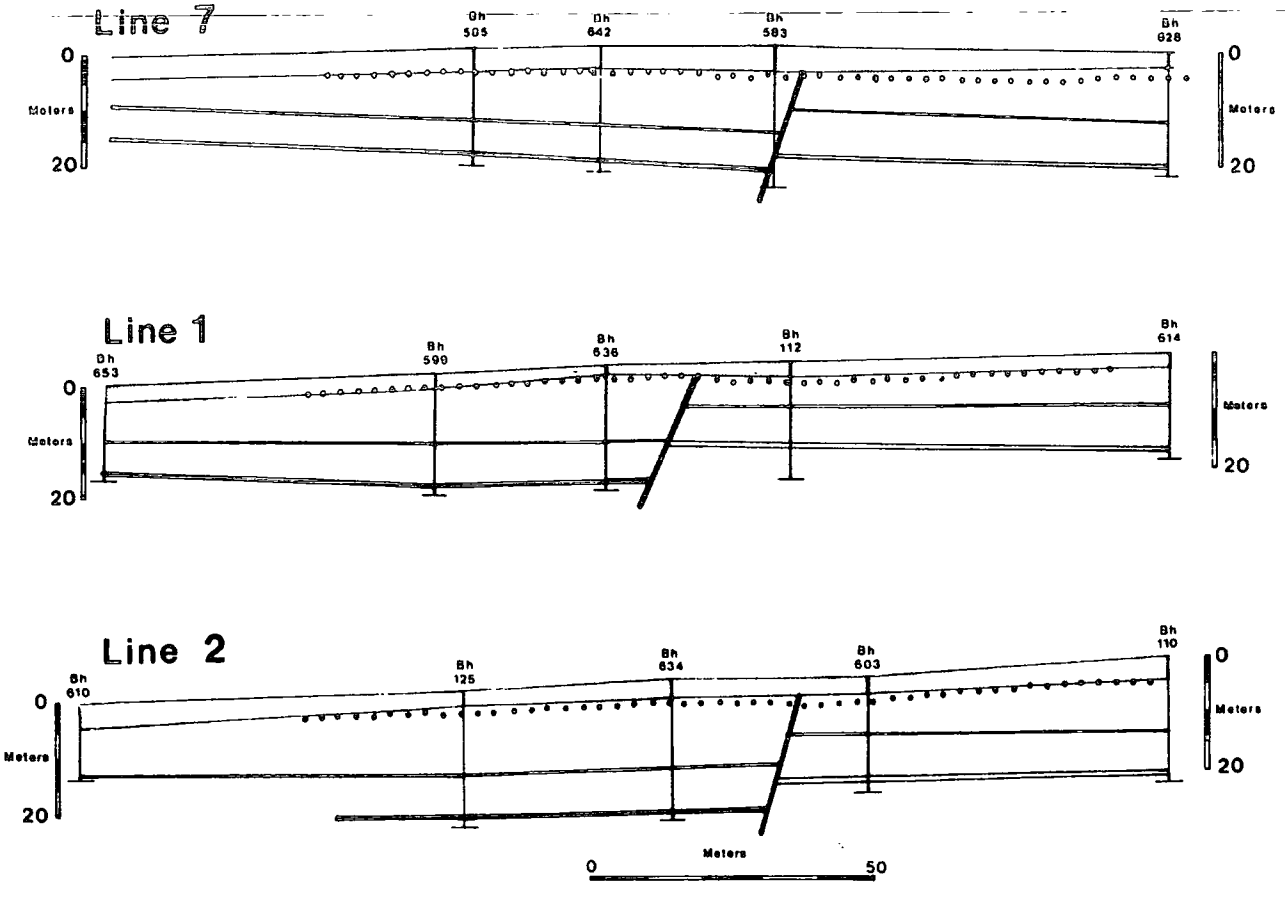

Drift thickness calculated by interpolation between boreholes

• Estimate of drift thickness from reversed S wave refraction lines

S wave velocity of drift **160** ms^{-1}

Figure 4.5

STANLEY MOSS Line 1

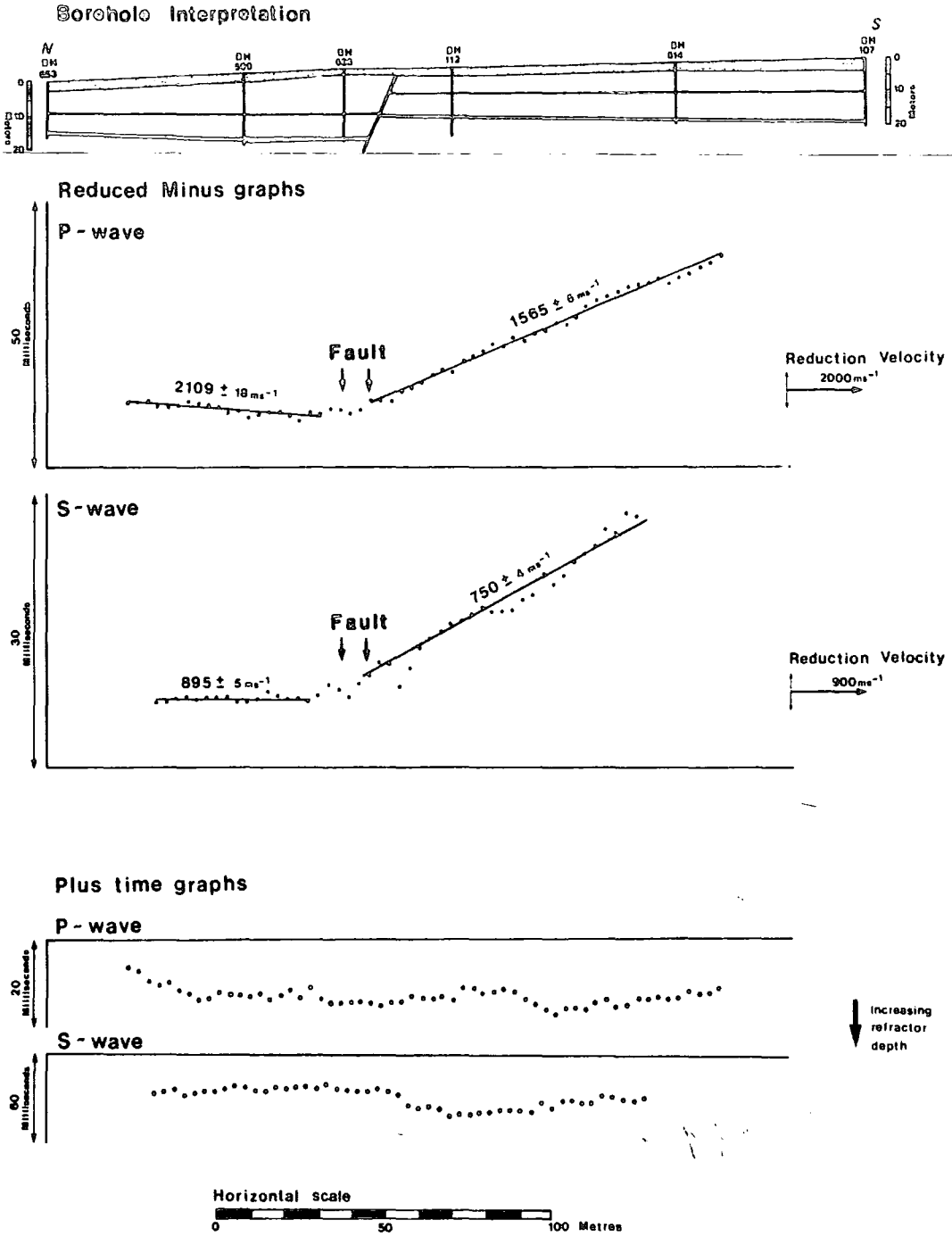

Figure 4.6

STANLEY MOSS Line 2

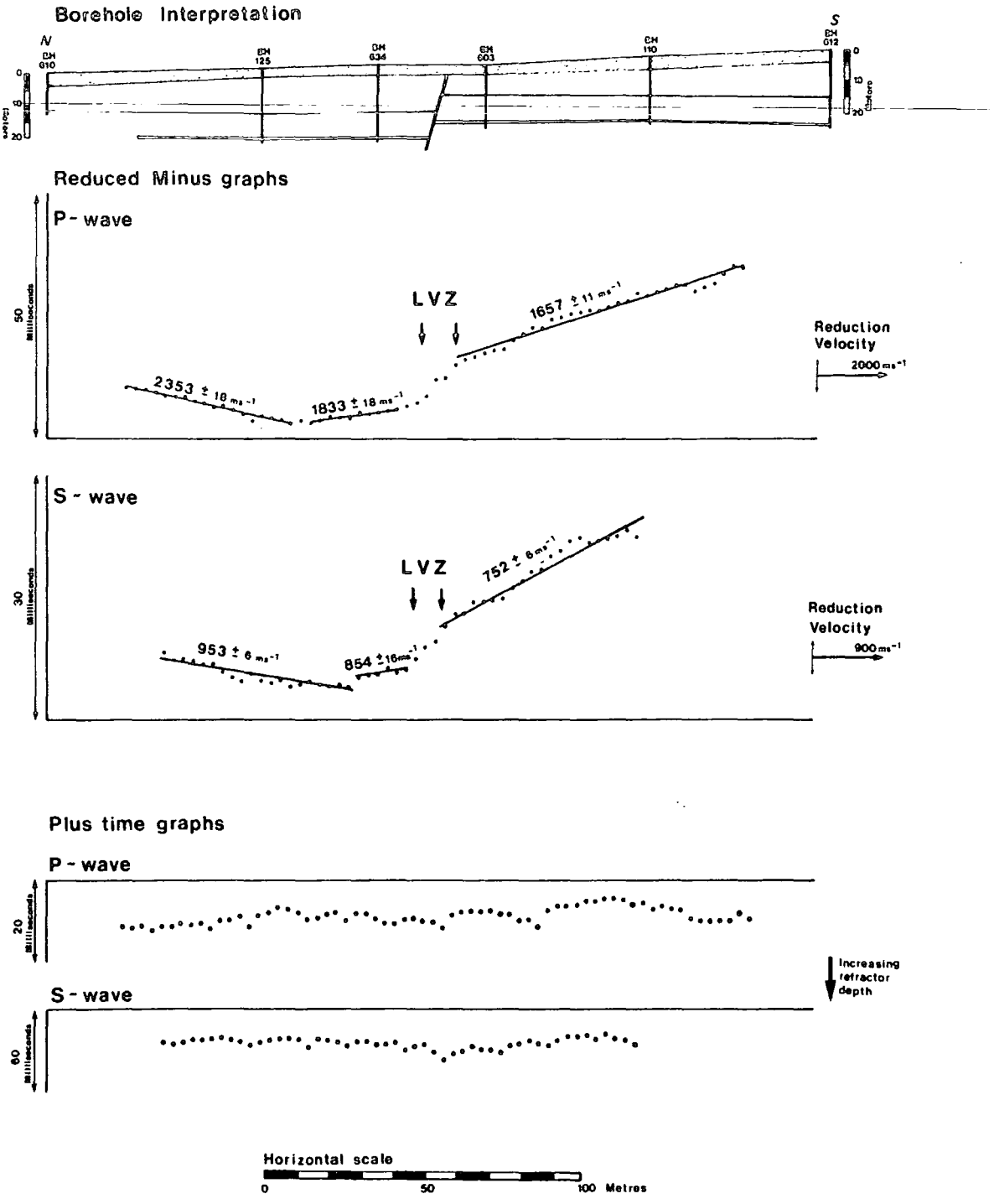

LVZ - Low velocity zone

Figure 4.7

STANLEY MOSS Line 3

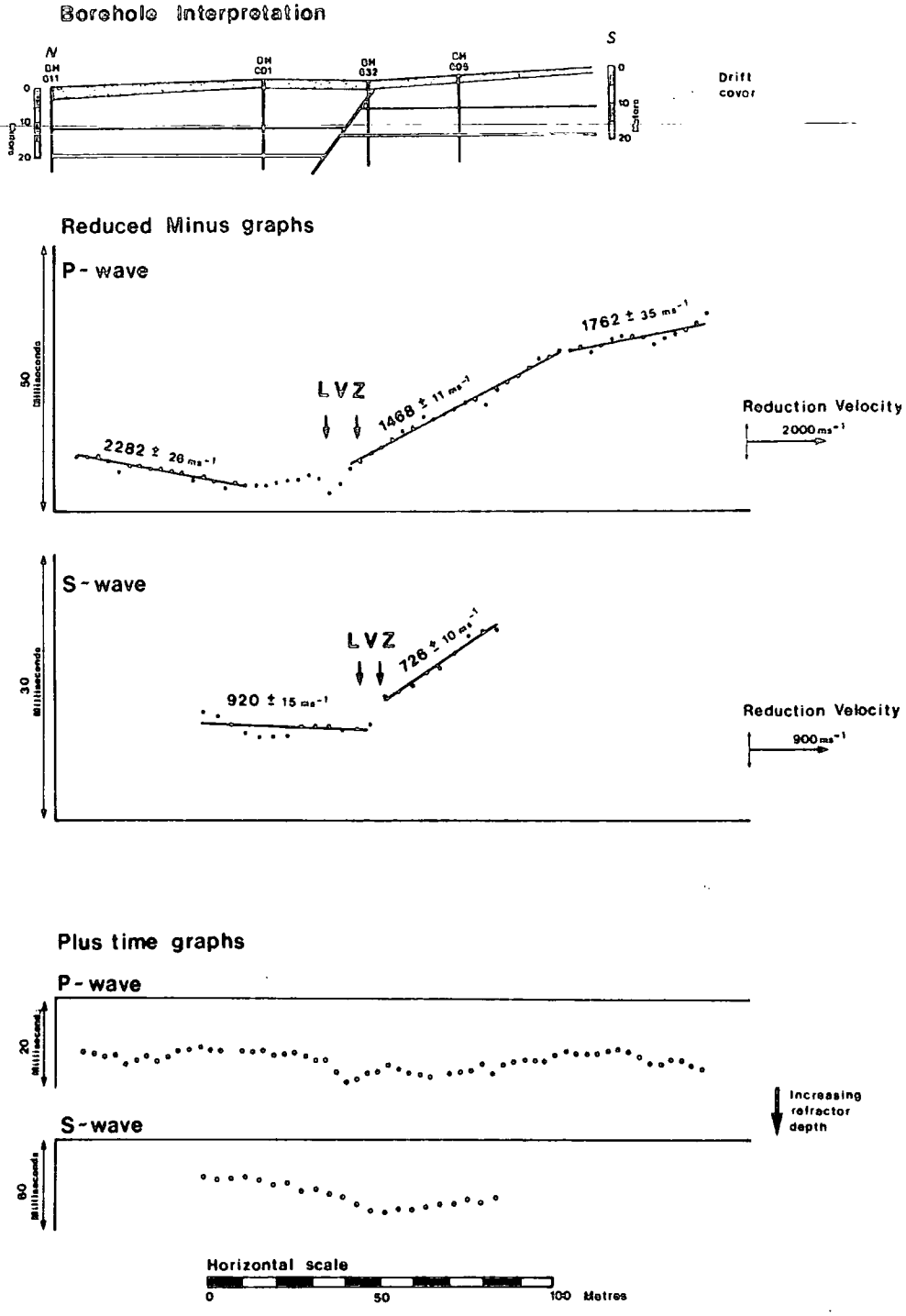

Figure 4.8

STANLEY MOSS Line 5

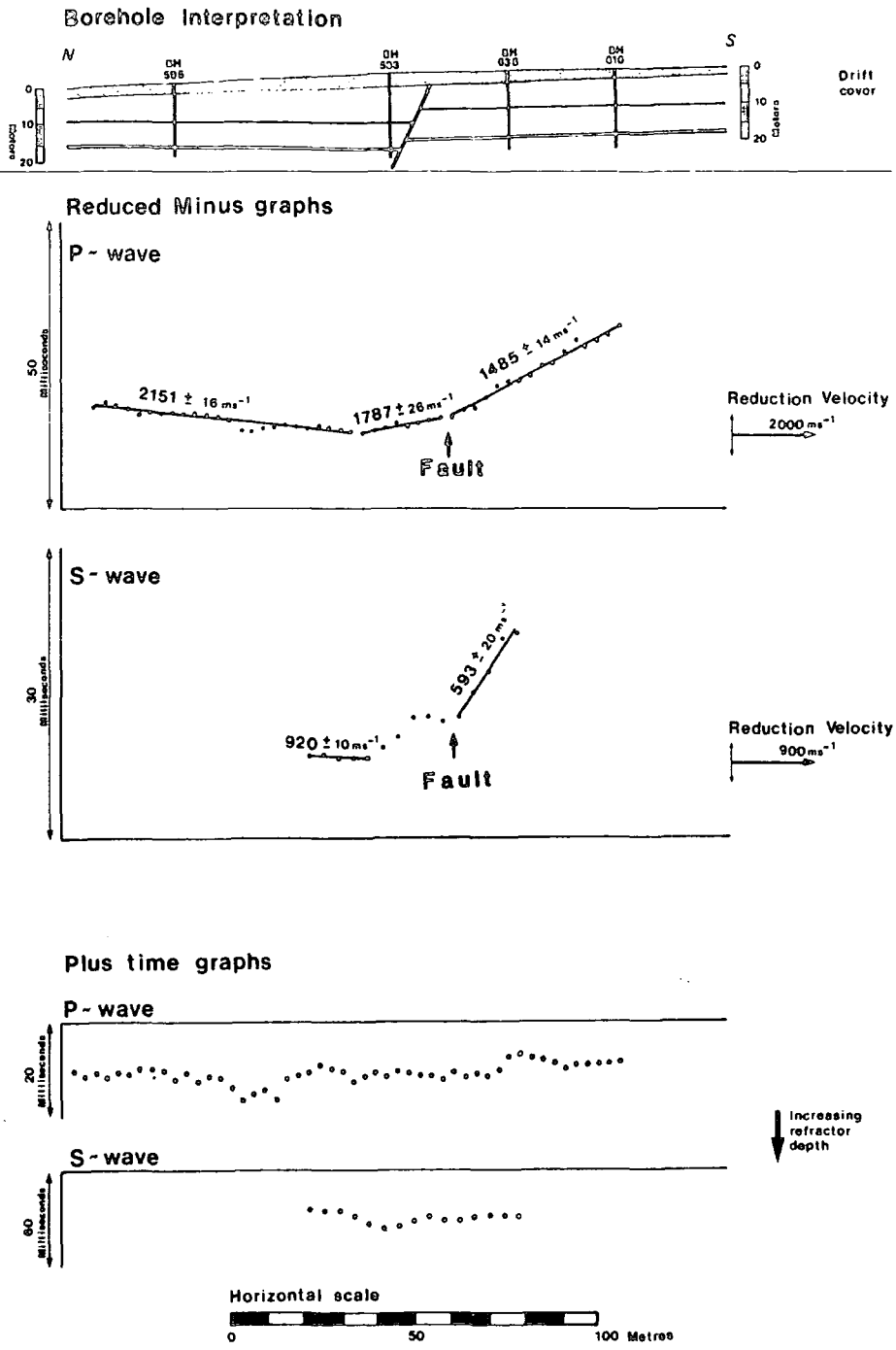

Figure 4.9

STANLEY MOSS Line 6

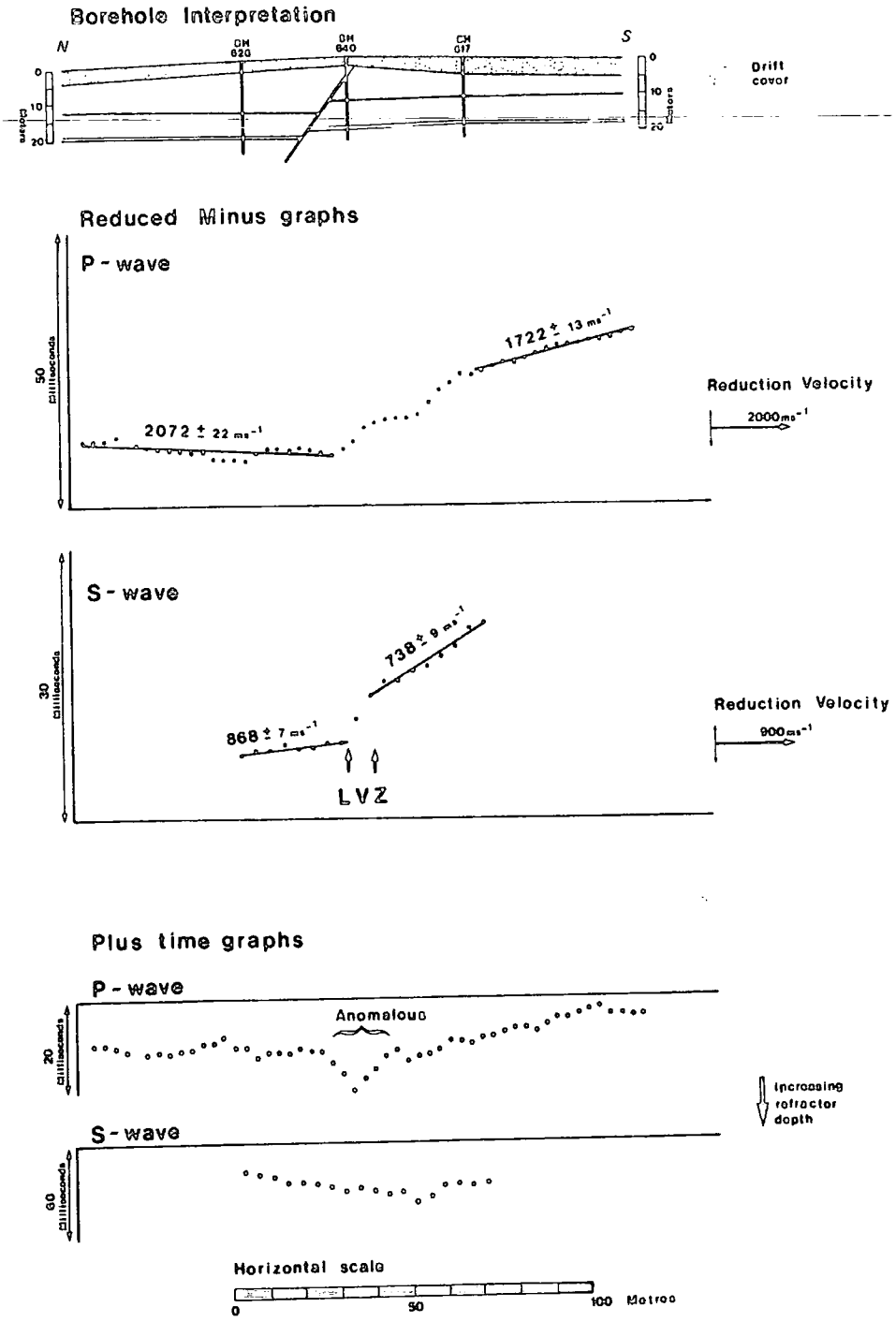

Figure 4.10

STANLEY MOSS Line 7

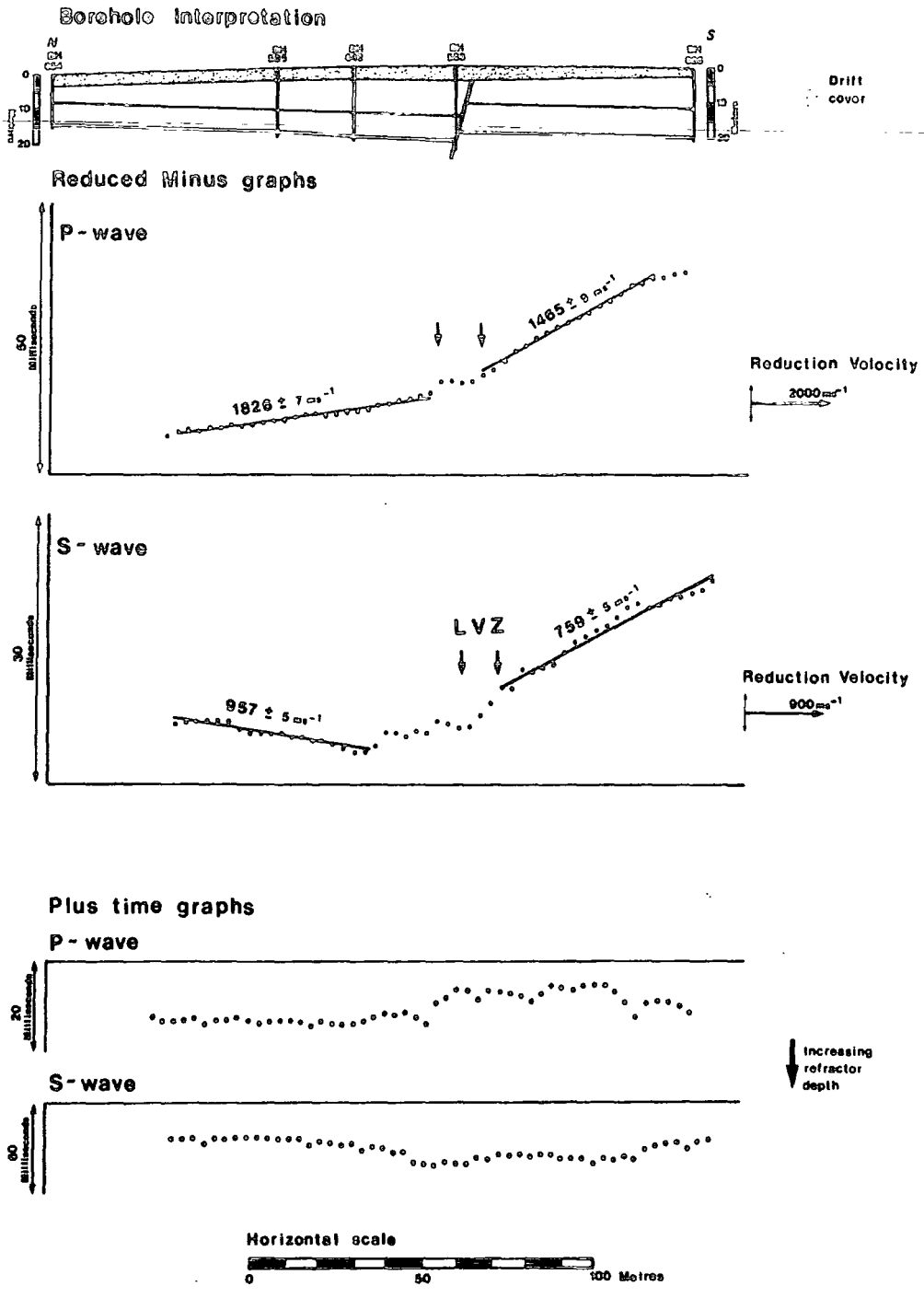

Figure 4.11

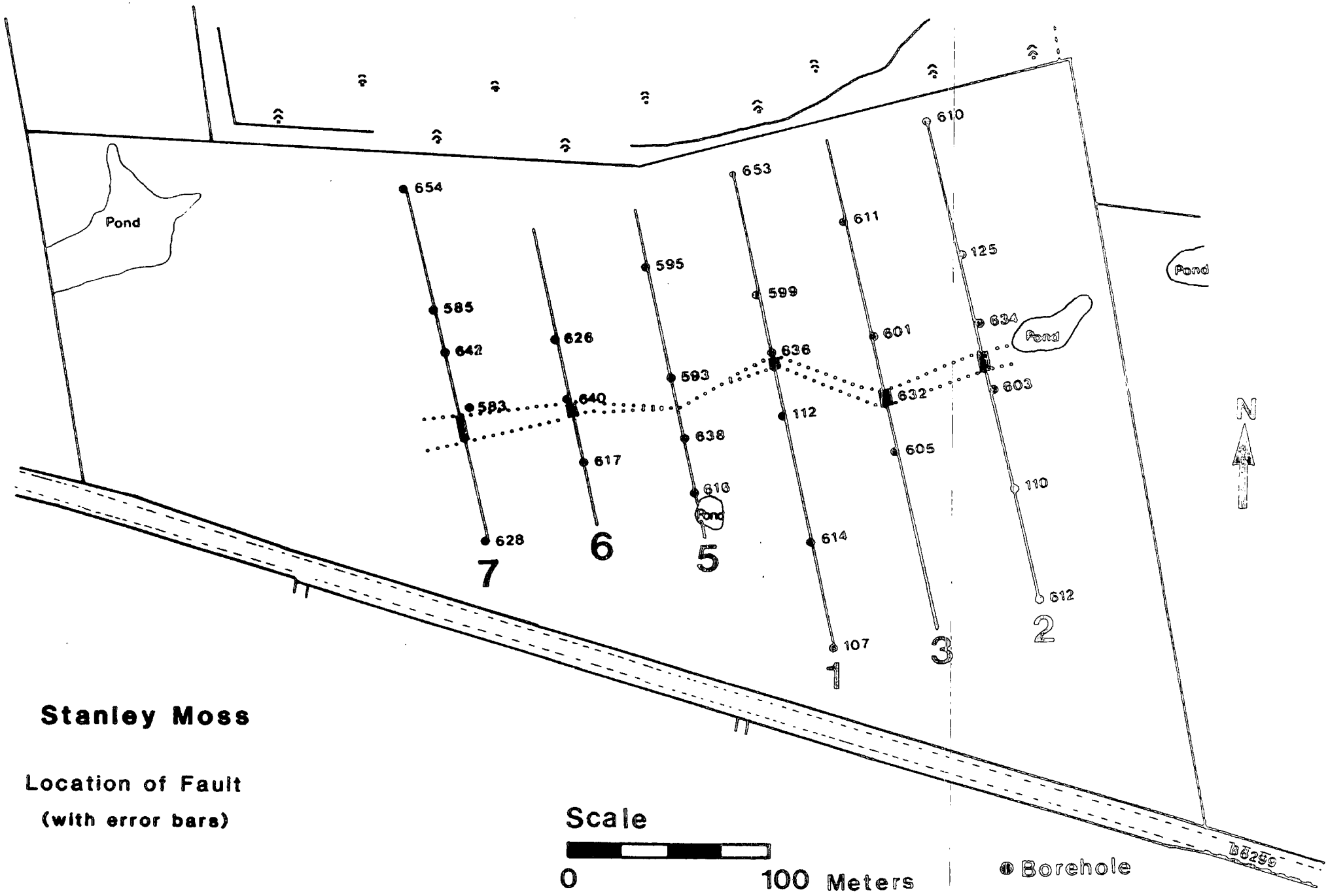
Pond
654
585
642
583
628
7
626
640
617
6
595
593
638
616
Pond
5
653
599
636
112
614
107
1
611
601
632
605
3
610
125
634
603
110
612
2
Pond
Pond
N
Stanley Moss
Location of Fault
(with error bars)
Scale
0
100 Meters
Borehole
B6259

Figure 4.12

gives clear velocity anomalies on both the P and S wave graphs at the same position, so the fault location is made with a high degree of confidence.

By analysing the interval velocity curves produced by least squares analysis of the minus graphs (figure 4.4), a contour plot of the refractor velocity for both P and S waves has been produced (figures 4.13 & 4.14). Both figures display the decrease in the refractor velocity from north to south across the site as the fault is crossed. There is also a decrease in the P wave refractor velocity north of the fault on seismic line 7 toward the west.

The velocity contrast on both sides of the fault could be due to a difference in the lithology at rockhead on both sides. There is evidence for this, in that sandstone bands only appear at rockhead to the north of the fault along lines 2 and 3 due to the fault throwing down to the north, but the bands do not occur north of the fault along the western seismic lines.

A second explanation for the velocity contrast at this site may be due to the old workings in the Harvey seam at 20m depth to the south of the fault. The subsequent sloughing in of the old workings may have caused fracturing of the overlying strata upwards, towards rockhead. This may have resulted in a lowering of the seismic velocity of the strata at rockhead, therefore providing a contrast in velocity with the unfractured rockhead north of the fault. However the Tilley seam at 40m depth is worked on both sides of the fault, therefore giving subsidence effects over the whole area.

STANLEY MOSS

Interval velocity contour diagram

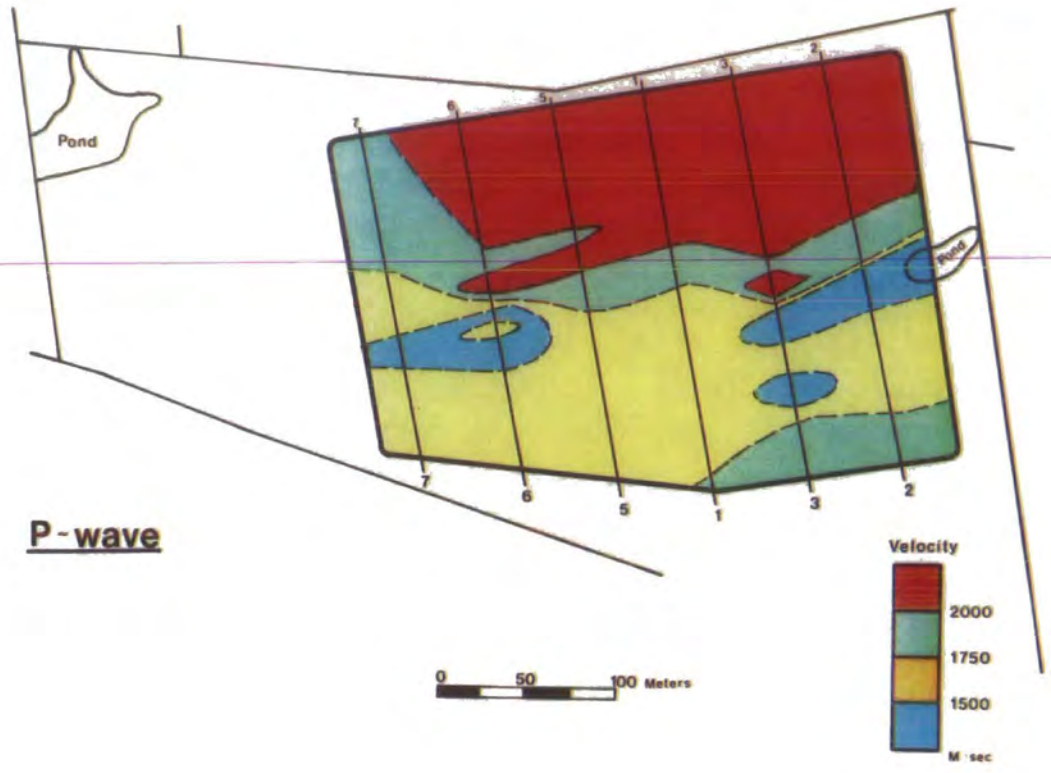

Figure 4.13

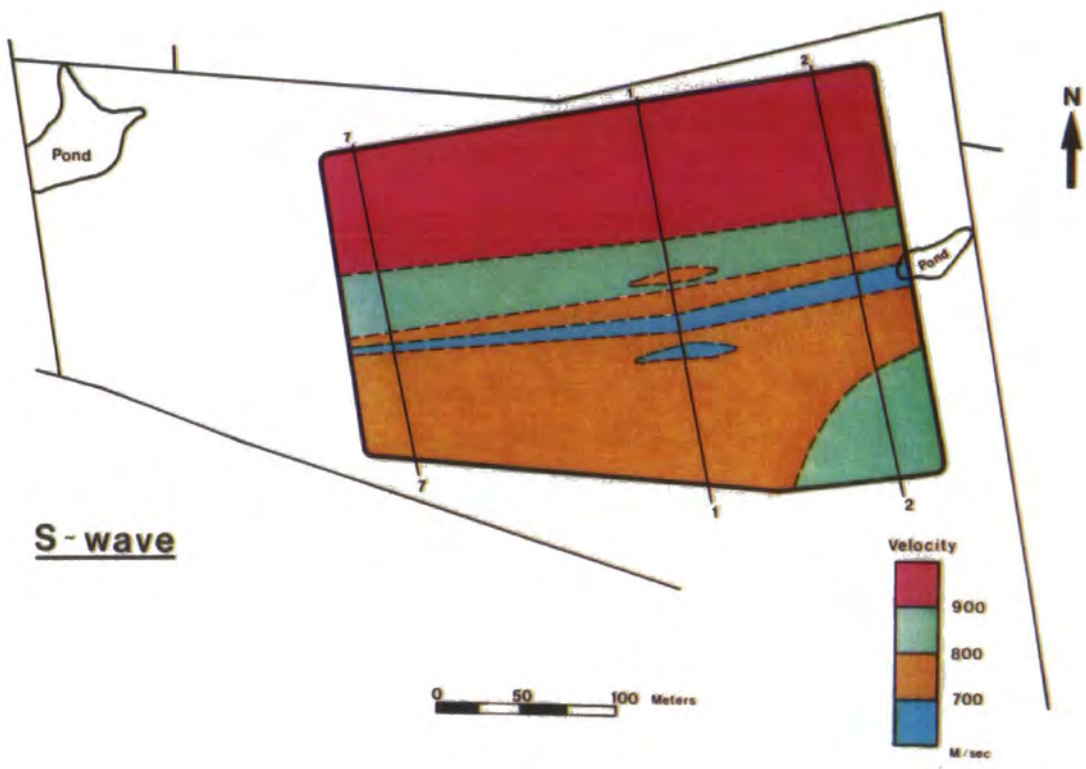

Figure 4.14

Some conclusions may be drawn from experience gained at this site. The refraction technique has been used to locate a faulted rockhead, due to a contrast in the refractor velocity on both sides of the fault. Along some of the seismic lines there has been an associated step in the refractor depth.

One problem is that the velocity contrast is not as abrupt as it might be, so the fault may only be seen as a zone of low velocity of a finite width. A second problem is that more than one anomaly may be present along a seismic line, a second anomaly may be caused by geological subcrops at rockhead. Therefore the technique can only be used to locate the fault position at this site in conjunction with borehole information.

It is difficult to compete with the accurate location of faults when the borehole spacing is only 30m. Any fault location carried out using the seismic refraction technique has to be within three or four data points (with a 3m peg spacing), to achieve an appreciable increase in resolution of fault location.

CHAPTER FIVE

BARLEY HILL : SITE NO.2

Barley Hill lies 10km to the north west of the town of Consett, just within the southern boundary of the County of Northumberland. The Barley Hill site is a prospective opencast site and was in the very early stages of exploration in June 1983 when the site was first visited by our seismic survey team.

The coal seam sequence at this site includes the Ganister Clay to the Threequarter seam. These are the very lowest workable coal seams in the Lower Coal Measures series in the NW Durham coalfield. This basal coal seam sequence is underlain by the thick (300m) Millstone Grit series which consists predominantly of sandstone with some shale horizons and overlies the major limestones of the Lower Carboniferous.

From the early borehole results obtained at this site, it appeared that the strata were cut by a north-south trending fault with a downthrow of some 20m to the east. In the north east corner of the site, due to the fault geometry, an area exists where the fault acts as a boundary to the coaling area, separating workable coal areas to the east from an area west of the fault where no coal seams are present (figure 5.1). For this reason the accurate location of the fault becomes important, because it has a direct bearing on the estimate of the amount of coal reserves present.

BARLEY HILL

Simplified geological site plan

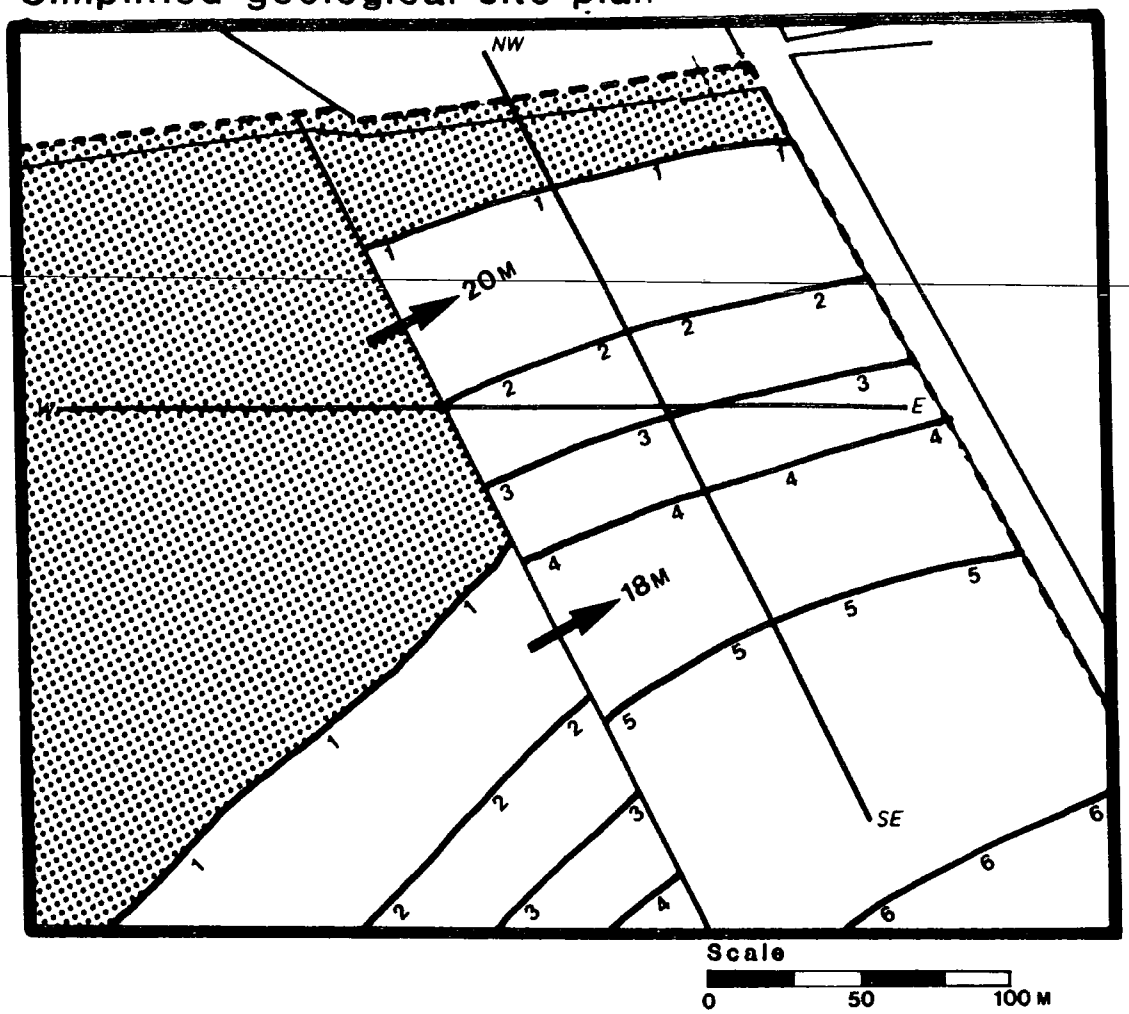

Scale
0 50 100 M

Simplified cross sections

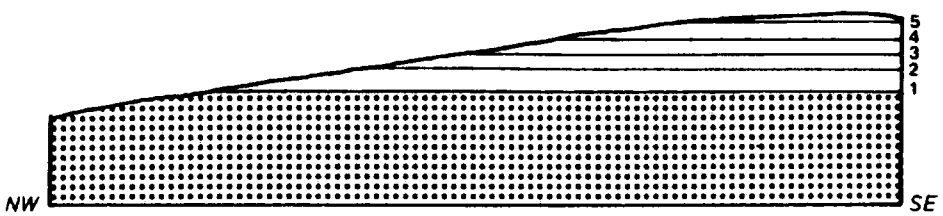

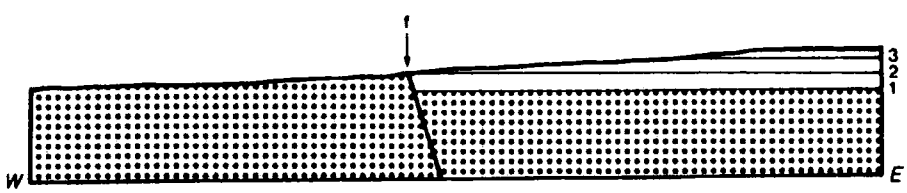

Fault position is not constrained

Generalized Vertical section

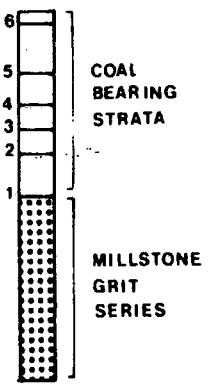

Figure 5.1

5.1 BARLEY HILL REFRACTION LINES

A series of six P and S wave seismic refraction lines was shot between June and October 1983. After some initial reconnaissance surveys had been carried out using a 5m peg spacing, subsequent lines were shot using a 3m peg spacing. The lines were laid so as to straddle the proposed fault locations (figure 5.2).

The field work was carried out in much the same way as with Stanley Moss, using small explosive charges buried at 1m depth for the P wave surveys. Short reversed refraction spreads were shot and used to measure overburden velocities and help to tie in phantomed traveltime data (Lankston & Lankston, 1986). Initially the Plus-Minus interpretation method (Hagedoorn, 1959) was employed on the results, but it soon became apparent that the fault was going to be located by sudden changes in the depth to a refractor and not by changes in refractor velocities as as was the case at Stanley Moss. The glacial drift cover at this site varied from 2 to 7m, deeper and less consistent than Stanley Moss. This caused a blurring of the abrupt changes (or steps) in refractor depth. In an attempt to increase the resolution of fault location, the Generalized Reciprocal Method of refraction data interpretation (Palmer, 1980) was used.

The decision to use the GRM was soon vindicated as it radically sharpened anomalies due to rapid changes in refractor depth resulting from faulting. The only problem that was encountered using the GRM was in the determination of the correct XY spacing to use in the time depth calculation. In theory, one should be able to determine the correct value from the inspection of the

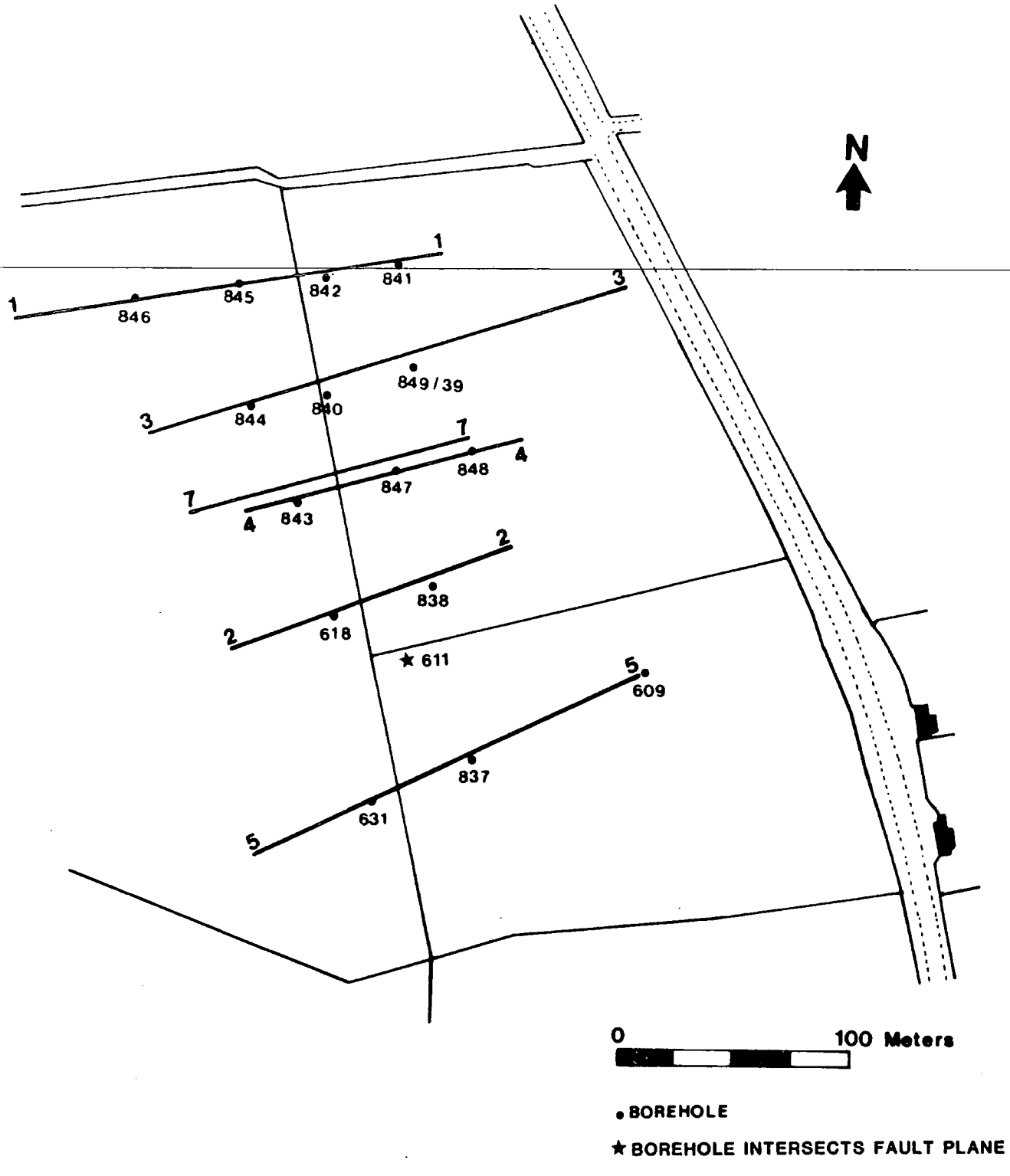

BARLEY HILL

Location of seismic refraction lines

Figure 5.2

velocity function graphs, but on some of the lines, particularly the P wave lines, the amplitude of the anomalies on the velocity function graphs were not significant enough to determine any cancellation when the correct XY spacing was used. The non-cancellation of small random time delays due to inhomogeneities in the very near surface when different geophones are used in the velocity calculation, cause fluctuations in the velocity function graph when an XY spacing greater than zero is used. This tends to mask the effect you are trying to observe. For this reason any velocity calculation is carried out when the XY spacing is zero.

The solution to this problem is to use the velocities and depths calculated from a Plus-Minus interpretation and calculate the correct XY spacing using Snell's Law.

The distinctive features seen on the velocity function and time depth graphs, along with depth converted cross-sections and their relationship to the subsurface geology (figure 5.9 gives the key to the geological logs) is summarised below :

LINE 1 Figures 5.3 & 5.10

P wave : After an initial reconnaissance survey carried out using a 5m peg spacing, the line was re-shot using a 3m peg spacing for increased resolution. Firstly, short refraction spreads were shot to determine an accurate value for the overburden velocity, and also to determine the cross over distance of the direct and refracted events. The short refraction spreads show a simple two layer case with an overburden velocity of 910m/sec. The line was then profiled using a shot to first geophone offset of 90m, and

from the results a phantomed traveltime graph produced.

The velocity function graph shows two distinct velocity segments of refractor velocity, 2277m/sec in the east and 2640m/sec in the west. An optimum XY spacing of 3m was calculated using an overburden velocity of 910m/sec, and a refractor depth of 3 to 6m calculated from a Plus-Minus interpretation. The time depth graph displays a distinct step in the refractor deepening toward the west. The step in the time depth graph converts to a depth step of 3m occurring over a region some 15m wide (figure 5.10).

S wave : This line is the original reconnaissance survey shot with a 5m peg spacing. The line was never re-shot. It was shot with a profiling offset of 30m from which a phantomed traveltime graph was built up. Short refraction spreads display a two-layer case with an overburden velocity of 400m/sec. The depth to the refractor was found to be about 8m. From the Plus-Minus interpretation it was also clear that a simple two-layer model could be used in the interpretation.

As with the P wave results the velocity function graphs show an increase in refractor velocity from east to west, 954 to 1041m/sec, but this velocity change is only just significant due to the error bars on the velocity determination resulting from the 5m peg spacing. An XY spacing of 5m was used for the calculation of the time depth values. The resultant time depth graph displays two clear anomalies, one of which is a 15m wide step which occurs in the same place as the P wave anomaly, but in the opposite sense.

The borehole information along this line marks a clear zone of weathering at rockhead on all four boreholes. Below the weathering zone a sandstone occurs in the west and a shale in the east.

It would appear that both the P and S wave profiles are sampling a badly weathered rockhead, even though the P wave refractor depth is shallow. This is probably due to inaccuracy in the calculation of the drift velocity critical in the depth conversion. It is significant that on both the P and S wave lines, the refractor velocities are greater in the west than in the east. This is consistent with the fact that the seismic velocity through an unweathered Carboniferous Sandstone is invariably greater than that through a shale.

On line 1 the fault is located by a 15m wide step in the refractor depth which occurs on both the P and S wave lines in the same location. This zone separates two distinct refractor velocities.

Line 2 Figures 5.4 & 5.11

P wave : A short refraction spread was shot along the western end of line 2. The results show a simple two-layer case of an overburden with an average seismic velocity 910m/sec overlying a refractor of seismic velocity 2500m/sec. From the short refraction spread, four time depth determinations were made, which were then used to tie in the time depth values obtained by analysis of the phantomed traveltime graph.

The velocity function graph displays a clear break in refractor velocity from 2668m/sec in the east to 2836m/sec in the west. The time depth graph was calculated using an XY value of 5m. The resultant graph displays a sharp step between boreholes 838 and 618. On depth conversion the step has an amplitude of 3m.

S wave : A phantomed traveltime graph was obtained using a 3m peg spacing and a shot to first geophone offset of 90m. Short refraction spreads display a two-layer model of a first layer velocity of 300m/sec overlying a refractor of seismic velocity 527 to 762m/sec. The refractor velocities obtained from the analysis of the velocity function graphs are 1200m/sec in the east and 1056m/sec in the west. The calculated refractor time depths are much greater than those calculated using the short refraction spreads. One can therefore conclude that on line 2 S wave we are dealing with a three-layer case.

The XY spacing used in the determination of the time depth values for the deepest refractor was calculated by inspection of the velocity function graphs using incremental XY values. An XY spacing of 9m appears to give the simplest form to the velocity function graph.

The effect that the first layer of velocity 300m/sec has on the time depth values for layer 3 was calculated and subtracted, so that an accurate determination for the thickness of layer 2 could be made.

The S wave depth converted results show a 12m wide anomalous area of refractor deepening between boreholes 838 and 618, which are the only two boreholes found on this line. As this occurs in

the same position as the step in the refractor depth found on the P wave line, it is taken as further evidence for the fault position.

LINE 3 Figures 5.5 & 5.12

P wave : Line 3 was profiled using a 3m peg spacing, and a shot to first geophone offset of 60m. Short offset refraction spreads were obtained at both ends of the line. The results show a velocity structure of 910m/sec overlying a refractor of 1835m/sec in the east and 2179m/sec in the west, at a depth of 3 to 4.5m.

The velocity function graphs produced from the phantomed traveltime graphs display refractor velocities of 2666, 2986 and 2656m/sec from east to west. These refractor velocity values are greater than those determined from the short offset spreads; the time depth values are also greater. This indicates the presence of a three-layer structure.

A depth section produced for this three-layer case is complex, with no clear fault indicator present. We would appear to imaged a complex overburden/rockhead/weathering situation using P waves.

S wave : In complete contrast to the complex P wave line, the S wave results display the simplest possible results that you would hope to obtain for a faulted refractor: a step with time depths corresponding to the top of the sandstone, which is at rockhead on the west side of the fault.

No short refraction spreads were shot along this line, but a value for the apparent velocity of the overburden was obtained from the adjacent line 7, where detailed analysis of the

overburden velocities was carried out. The results give an apparent layer 1 velocity of 490m/sec in the east, and 395m/sec in the west.

The velocity function graph displays a refractor velocity of 1147m/sec in the east and a velocity of 1128m/sec in the west, separated by an anomalous zone of fluctuating velocity produced as an artefact of a sharp step in the refractor depth.

Taking the simplest velocity function graph, using an XY spacing of 9m, the time depth graph was calculated. The resultant graph displays a dramatic step in the refractor, deepening toward the east, of amplitude 20msecs. When the data is depth converted this corresponds to a step in the refractor of some 18m. The resolution of the fault is better than 9m.

When one compares the result with the borehole information obtained along this line, it can clearly be seen that the S waves only see the sandstone horizon on both sides of the fault as a refractor. This is an excellent result and is a dramatic fault location indicator.

LINE4 Figures 5.6 & 5.13

P wave : Line 4 P wave was profiled using the same acquisition parameters as line 3 P wave, but gave remarkably different final results.

The velocity function graph displays a refractor velocity of 2899m/sec in the east and 2973m/sec in the west. The velocity function graph did not indicate correct XY spacing to use. An

estimation of the correct XY spacing of 12m was made from the velocity structure derived from the original Plus-Minus interpretation.

The resultant time depth graph displays a significant fault indicator by a sudden change in time depth from 3msecs to 7msecs over 3 pegs. On depth conversion this results in a step of amplitude 13m.

The borehole information reveals a similar geology to that found along line 3, with a sandstone at rockhead in the west, and a shale in the east, underlain by a sandstone at 17m depth.

Why are the results from this line dramatically different to those found along line 3? The answer must lie in the fact that the sandstone horizon east of the fault is some 4m deeper on line 3 than the corresponding sandstone on line 4, causing the cross over distance to be greater for the sandstone refractor on line 3. If the seismic velocity of the shale is greater on line 3 than line 4 it would further increase the offset required from shot to receiver before one was able to detect the deep sandstone horizon in the east on line 3.

LINE 7 Figures 5.7 & 5.15

An S wave survey was shot 10m north of line 4, lying exactly along the Barley Hill reflection line. It was envisaged that the near surface geological structure would be defined using this refraction line. S waves were used because they gave the best fault resolution. The P wave velocity values from line 4 were substituted into the structural model and used in the field static

calculations for the reflection data.

Some detailed near surface short refraction spreads were shot along this line, and from the results it was possible to distinguish a velocity sub-division within the strata overlying the deep faulted refractor seen on lines 3 and 4.

A velocity of 300m/sec was determined for the drift. The drift is underlain by a refractor of velocity 654m/sec in the east which corresponds to the velocity of the shale at rockhead. In the west the drift is underlain by a refractor of velocity 534m/sec, this is probably the weathered top of the sandstone indicated by borehole 843. The velocity function graph gives a refractor velocity of 1206m/sec in the east and a value of 1017m/sec in the west. The time depth graph again displays the characteristic step in the refractor seen on lines 3 and 4 S wave. The fault can be located within a zone 6m wide.

LINE 5 Figures 5.8 & 5.14

Line 5 is the southernmost refraction line recorded at this site. It is thought that the fault may splay and its throw decrease, because the borehole data in this area cannot be reconciled by a single large fault.

P wave : The P wave line was shot with a 3m peg spacing and a shot to first geophone offset of 60m. The velocity function graph produced from the phantomed traveltime graph displays a complex lateral velocity structure, with velocities ranging from 2516 to 3478m/sec being recorded.

The time depth graph shows a highly irregular refractor topography, with sharp steps at the eastern and western ends of the line. These may be fault indicators, but we are obviously dealing with a complex geological cross section here.

S wave : The velocity function graph produced from the data acquired along this line again displays a complex S wave refractor velocity structure.

Unlike the P wave time depth graph, the S wave graph shows a relatively smooth refractor topography, dipping toward the west. The only anomalous feature being a depression in the vicinity of borehole 837, where a 5m thick weathering layer is recorded on the borehole log.

Line 5 shows no consistency between P wave, S wave and borehole results. The P wave graph looks the most convincing as a fault indicator (figure 5.8), but the fault cannot be located as a single anomaly along this line. This may be due to a complex geological cross-section in this area, too complex to be imaged by the refraction technique. No fault prediction can be made along this line.

Figure 5.16 displays the final results of the refraction surveys shot at Barley Hill, showing the fault trend through the site with error bars on the resolution.

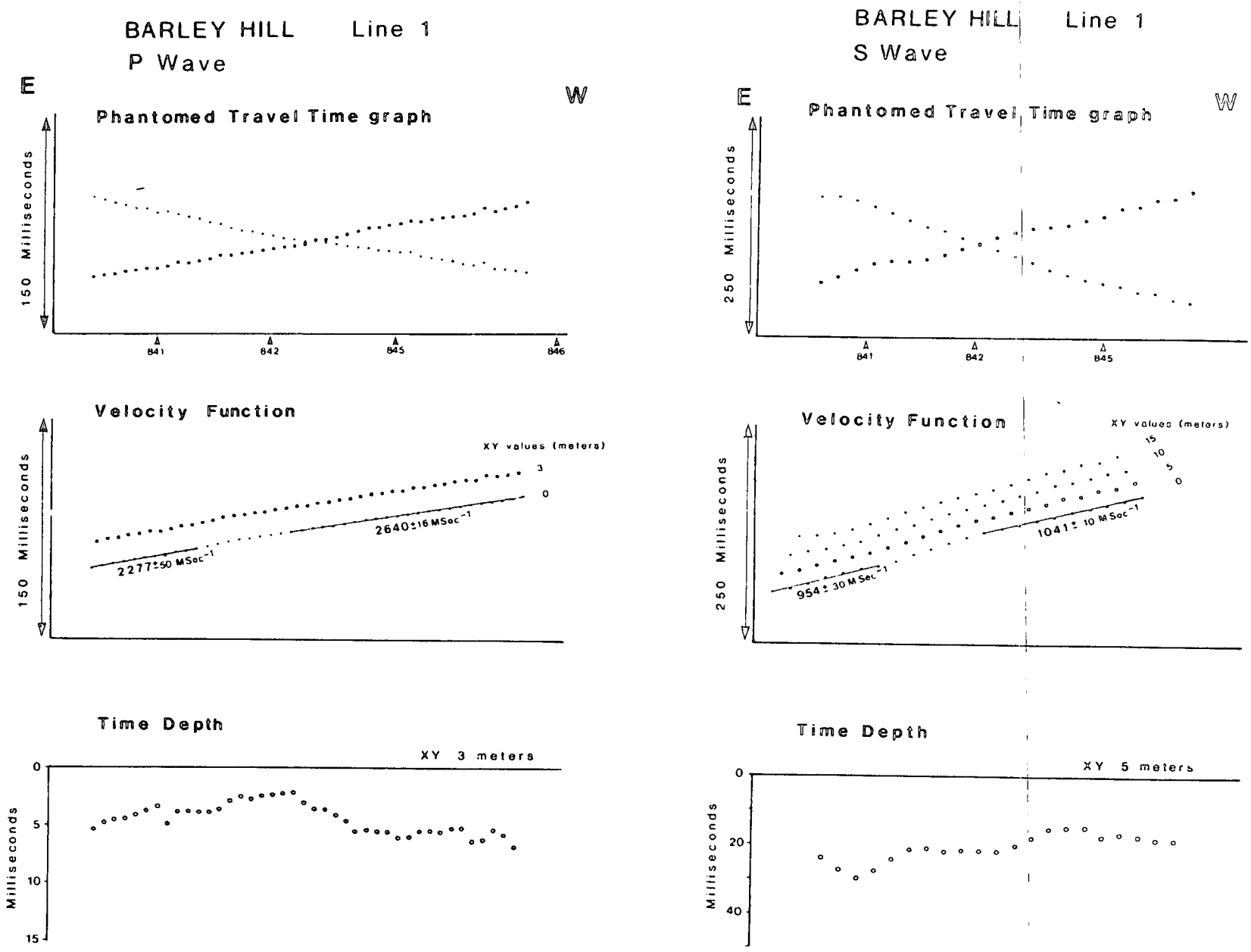
BARLEY HILL Line 1
P Wave
E
W
Phantomed Travel Time graph
150 Milliseconds
841
842
845
846
Velocity Function
XY values (meters)
3
0
2640±16 MSec⁻¹
2277±60 MSec⁻¹
150 Milliseconds
Time Depth
XY 3 meters
0
5
10
15
Milliseconds
BARLEY HILL Line 1
S Wave
E
W
Phantomed Travel Time graph
250 Milliseconds
841
842
845
Velocity Function
XY values (meters)
15
10
5
0
1041 ± 10 MSec⁻¹
954 ± 30 MSec⁻¹
250 Milliseconds
Time Depth
XY 5 meters
0
20
40
Milliseconds

Figure 5.3

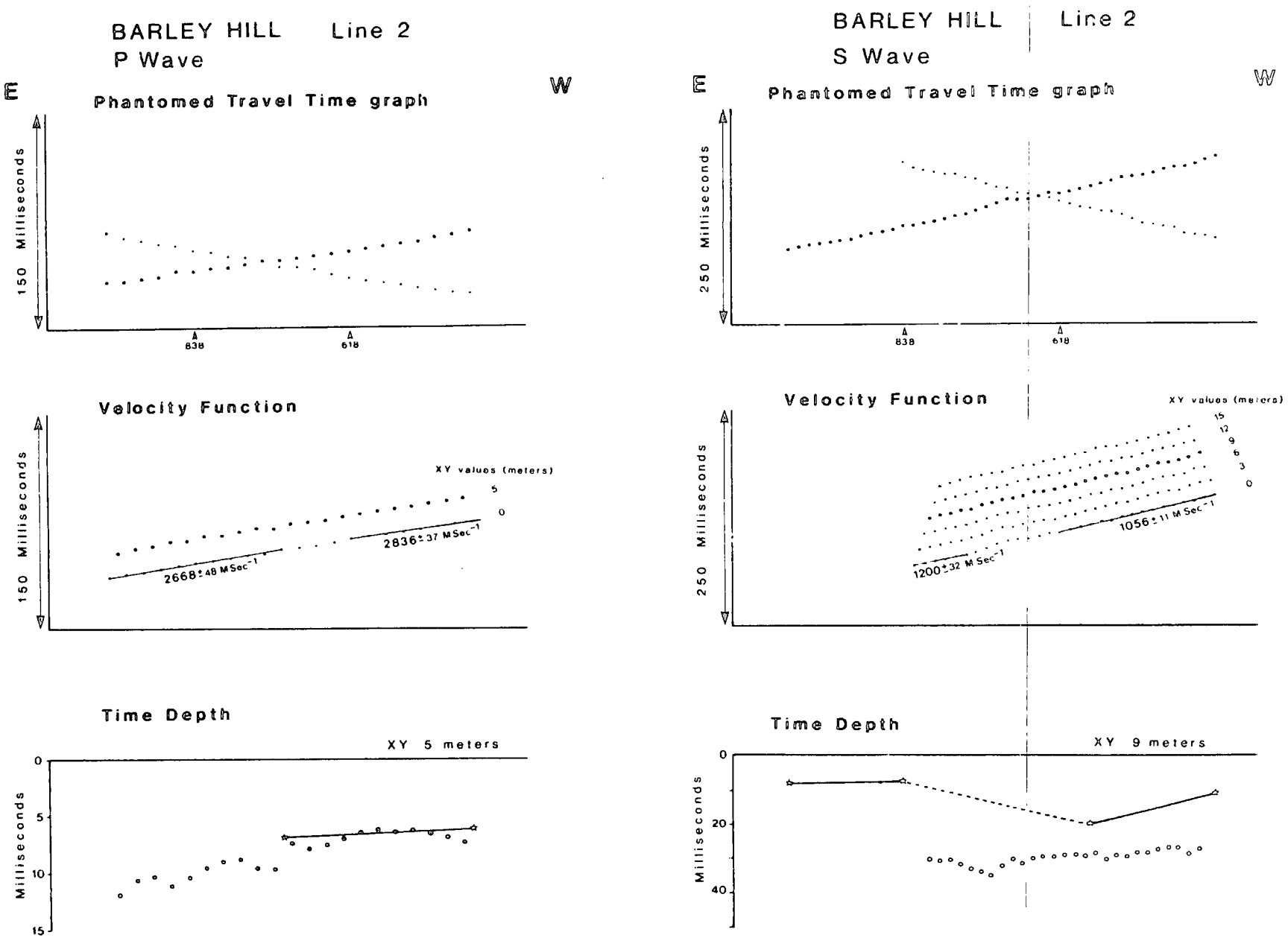
BARLEY HILL Line 2
P Wave
E
W
Phantomed Travel Time graph
150 Milliseconds
838
618
Velocity Function
150 Milliseconds
XY values (meters)
5
0
2668±48 MSec⁻¹
2836±37 MSec⁻¹
Time Depth
XY 5 meters
0
5
10
15
Milliseconds
BARLEY HILL Line 2
S Wave
E
W
Phantomed Travel Time graph
250 Milliseconds
838
618
Velocity Function
XY values (meters)
15
12
9
6
3
0
250 Milliseconds
1200±32 MSec⁻¹
1056±11 MSec⁻¹
Time Depth
XY 9 meters
0
20
40
Milliseconds

Figure 5.4

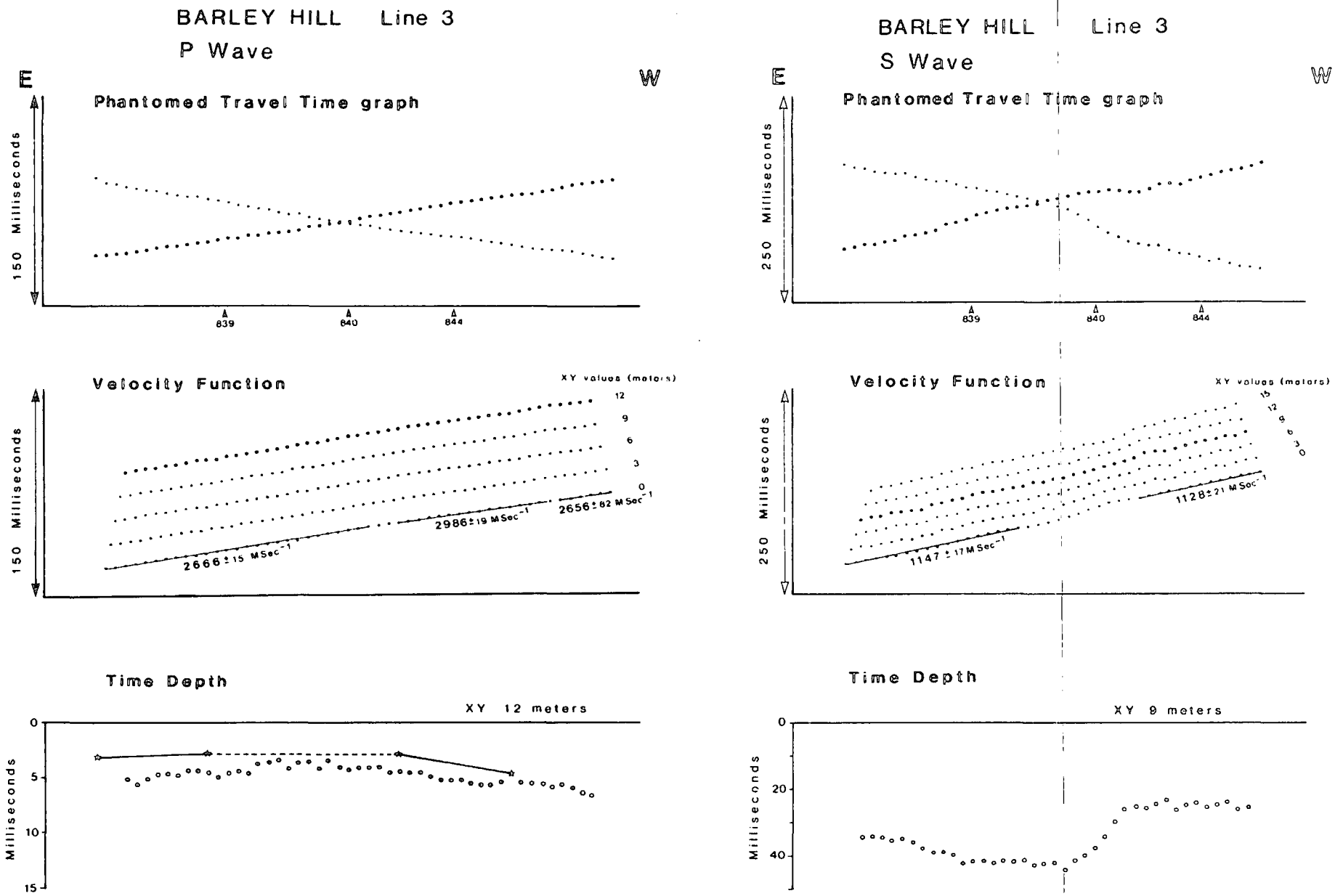
BARLEY HILL Line 3
P Wave
E
W
Phantomed Travel Time graph
150 Milliseconds
839
840
844
Velocity Function
XY values (meters)
12
9
6
3
0
2666 ± 15 MSec⁻¹
2986 ± 19 MSec⁻¹
2656 ± 82 MSec⁻¹
Time Depth
XY 12 meters
Milliseconds
0
5
10
15
BARLEY HILL Line 3
S Wave
E
W
Phantomed Travel Time graph
250 Milliseconds
839
840
844
Velocity Function
XY values (meters)
15
12
9
6
3
0
1147 ± 17 MSec⁻¹
1128 ± 21 MSec⁻¹
Time Depth
XY 9 meters
Milliseconds
0
20
40

Figure 5.5

BARLEY HILL Line 4
P Wave

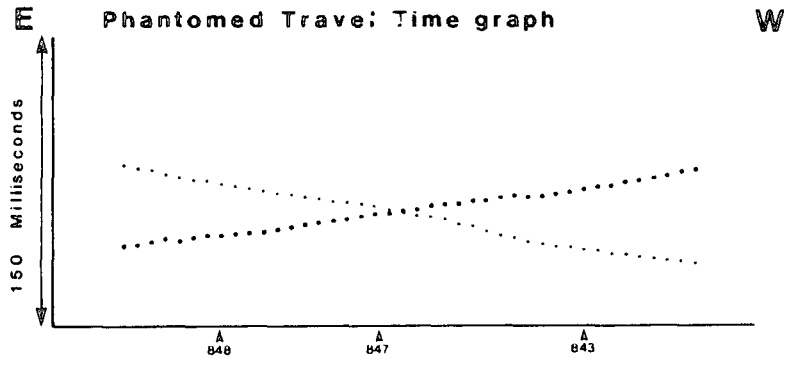

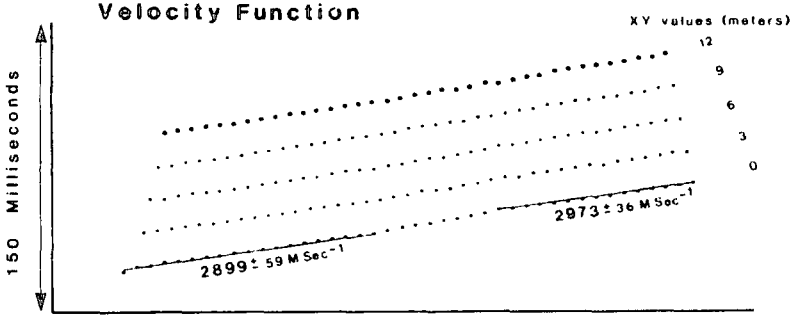

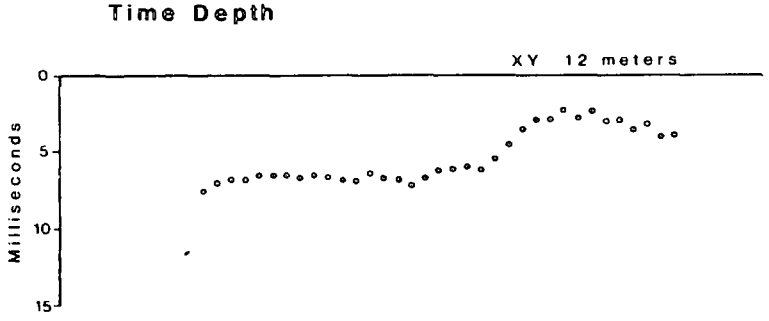

BARLEY HILL Line 4
S Wave

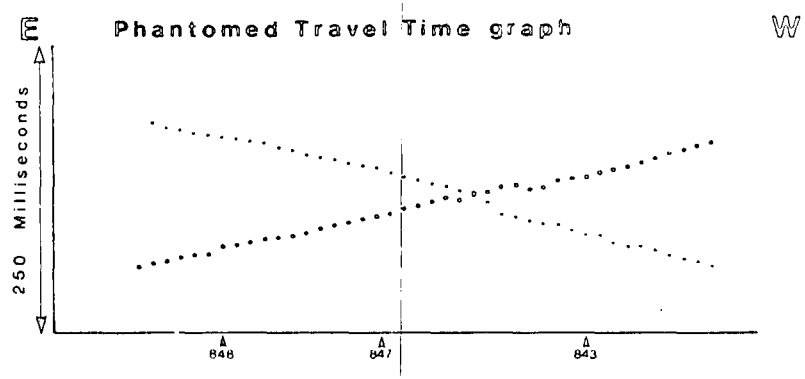

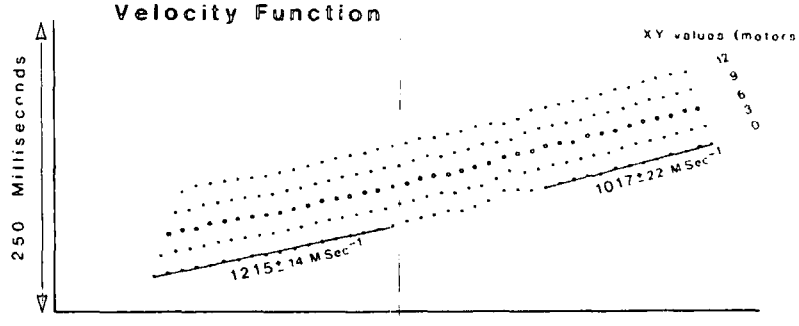

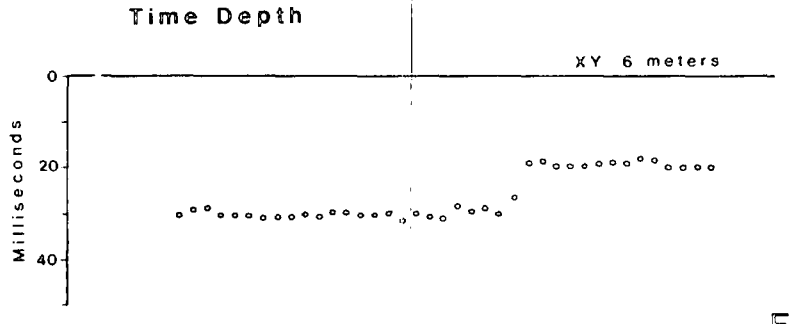

Figure 5.6

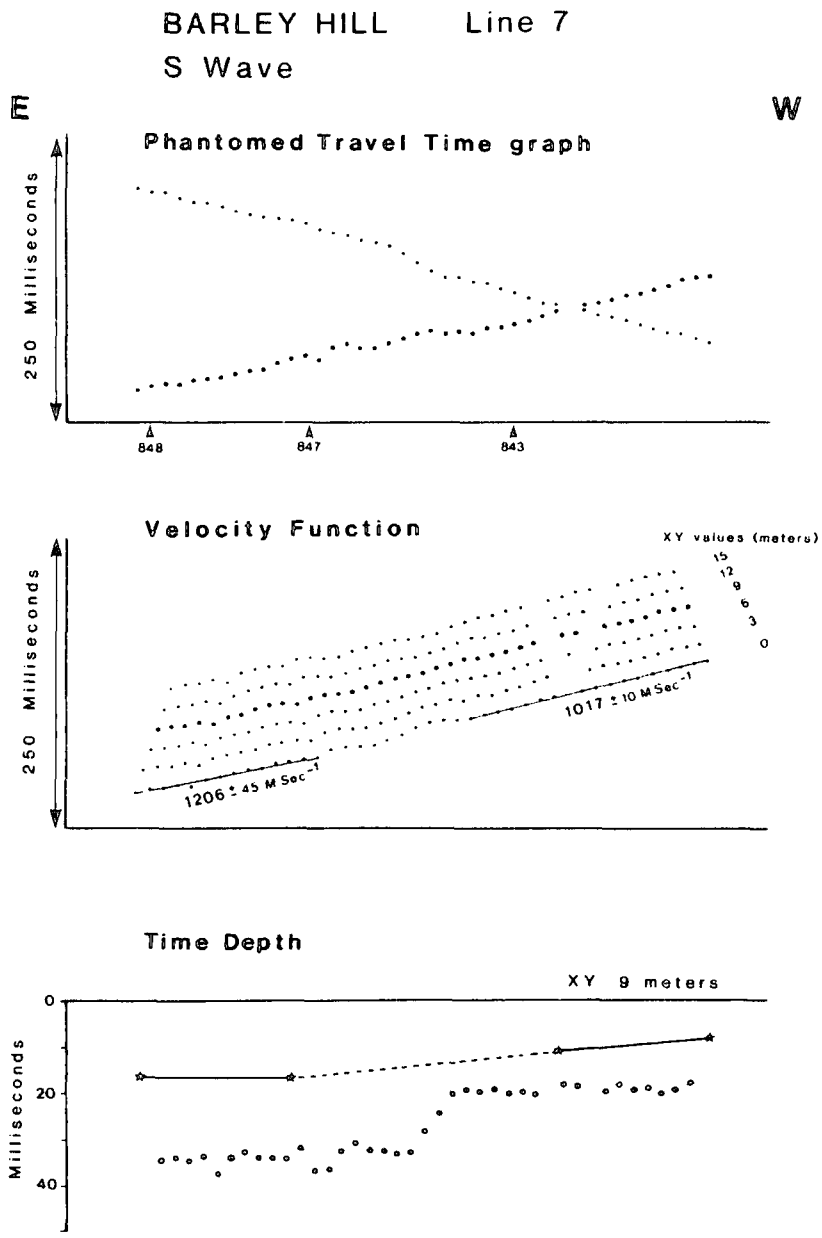

Figure 5.7

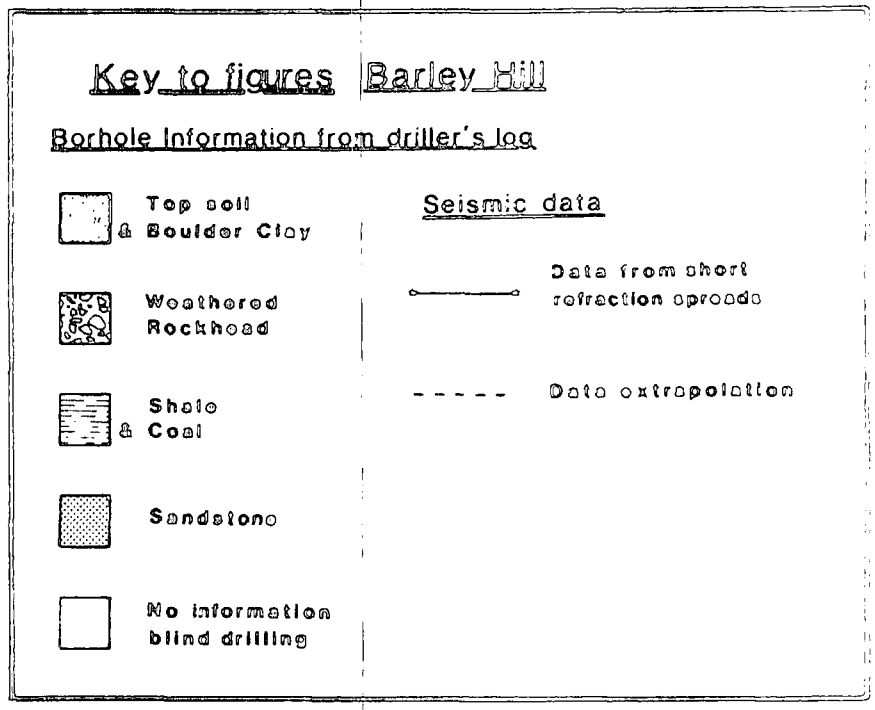

Figure 5.9

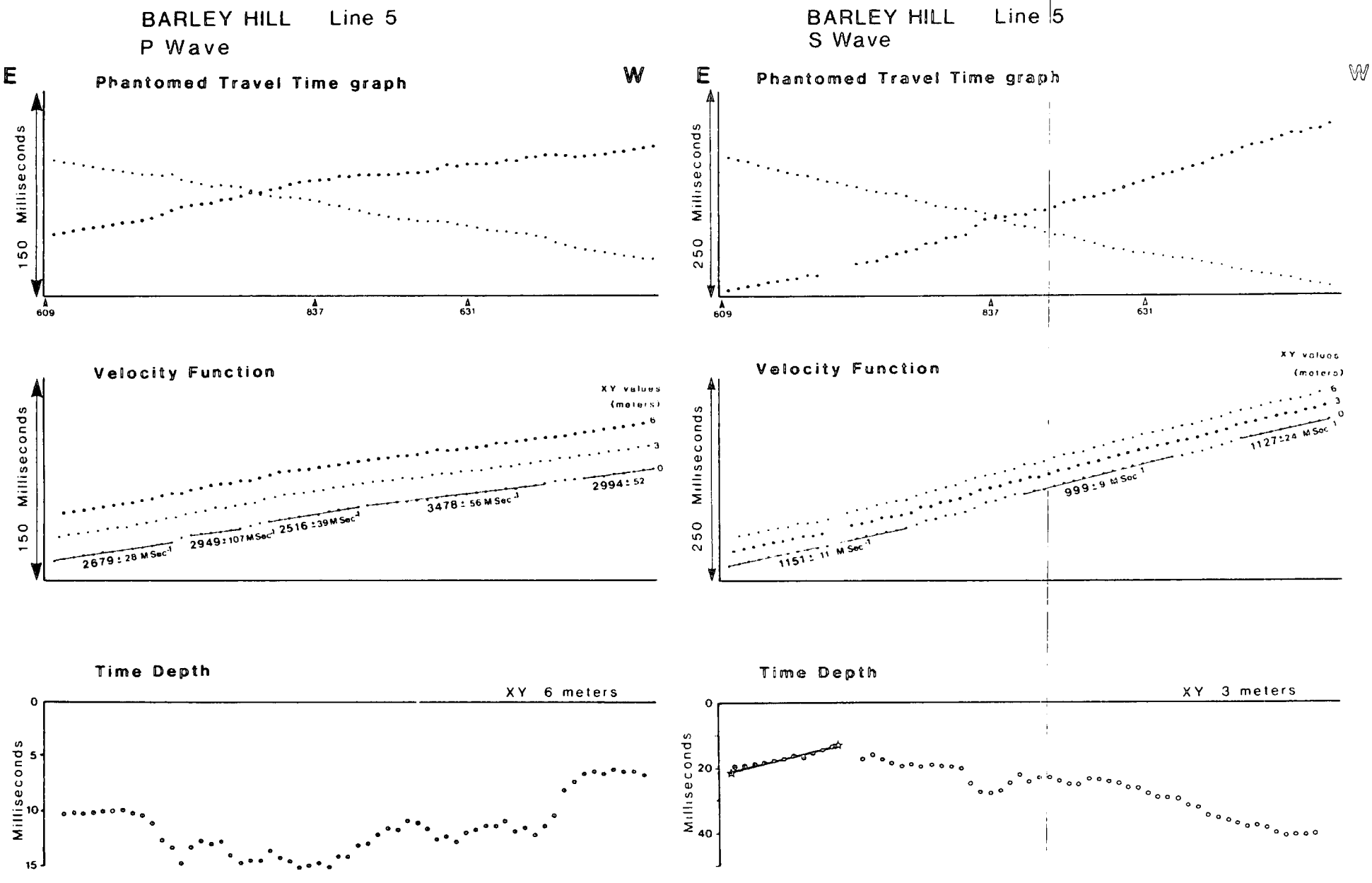
BARLEY HILL Line 5
P Wave
E
W
Phantomed Travel Time graph
150 Milliseconds
609
837
631
Velocity Function
XY values
(meters)
6
3
0
2679 ± 28 M Sec-1
2949 ± 107 M Sec-1
2516 ± 39 M Sec-1
3478 ± 56 M Sec-1
2994 ± 52
Time Depth
XY 6 meters
Milliseconds
0
5
10
15
BARLEY HILL Line 5
S Wave
E
W
Phantomed Travel Time graph
250 Milliseconds
609
837
631
Velocity Function
XY values
(meters)
6
3
0
1151 ± 11 M Sec-1
999 ± 9 M Sec-1
1127 ± 24 M Sec-1
Time Depth
XY 3 meters
Milliseconds
0
20
40

Figure 5.8

BARLEY HILL Line 1
Interpretations

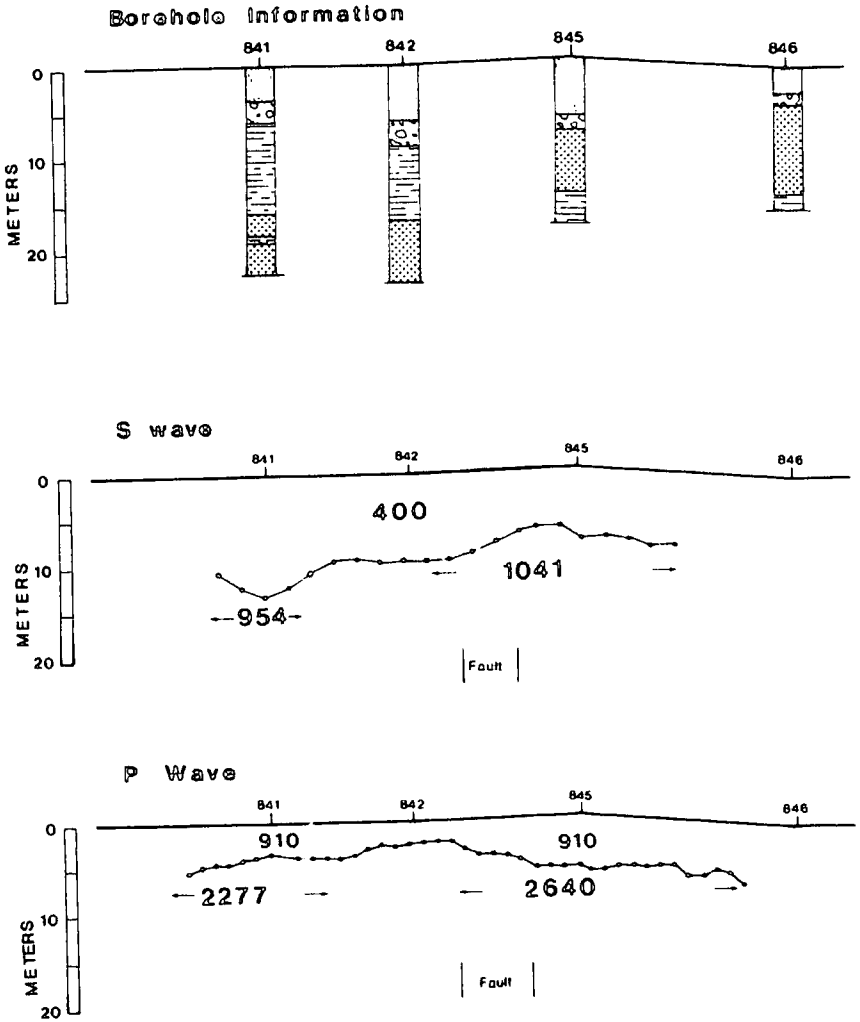

Figure 5.10

BARLEY HILL Line 2
Interpretations

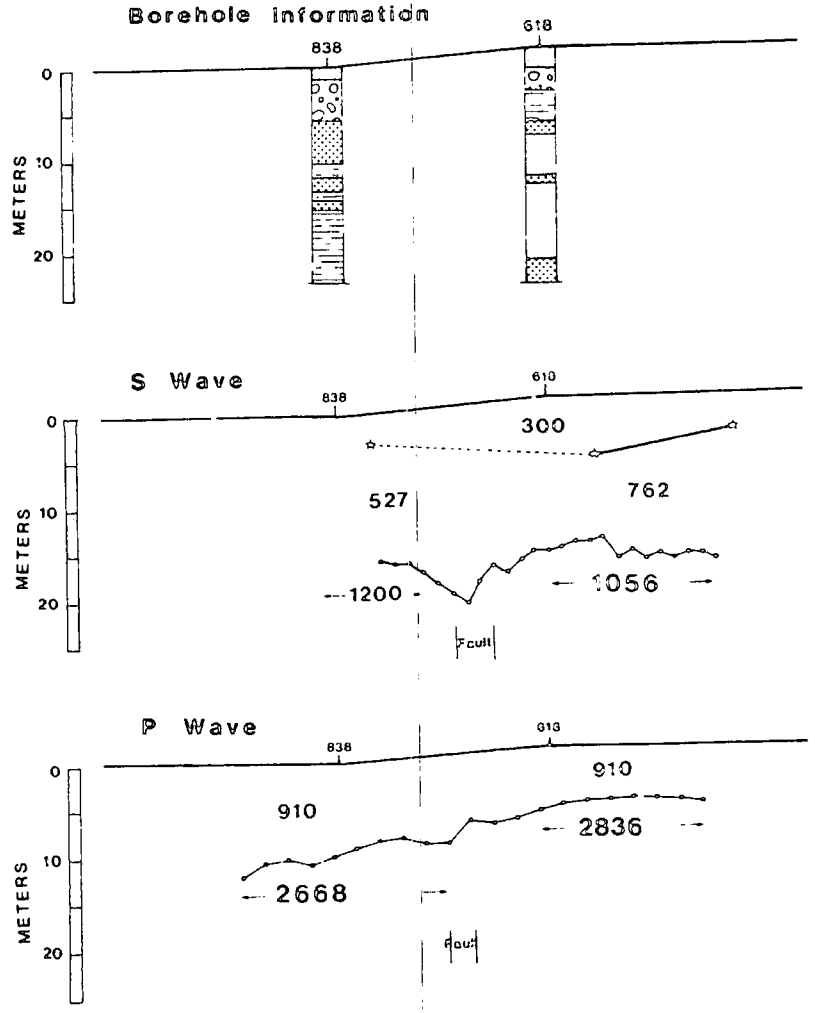

Figure 5.11

2x Vertical Exaggeration

BARLEY HILL Line 3
Interpretations

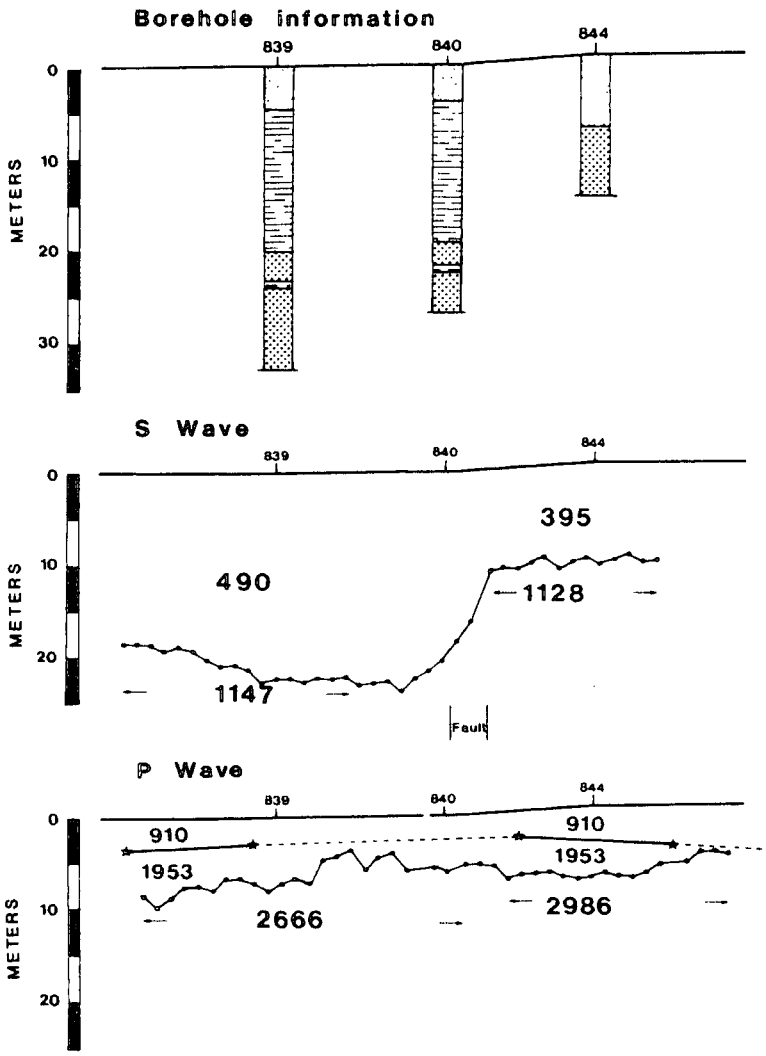

Figure 5.12

BARLEY HILL Line 4
Interpretations

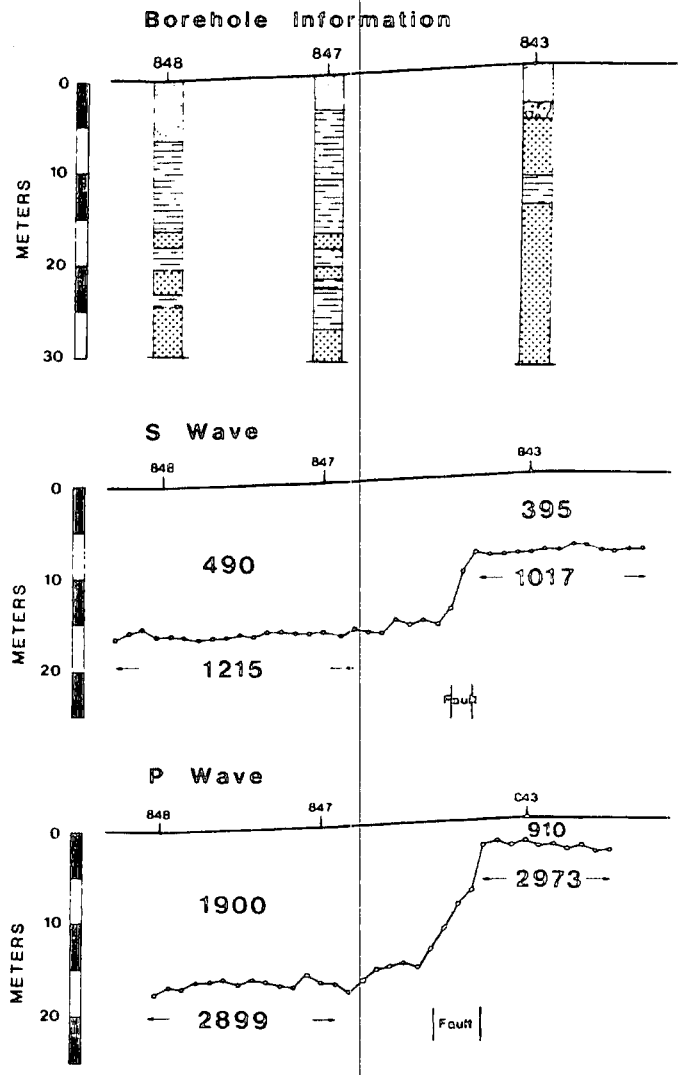

Figure 5.13

2x Vertical Exaggeration

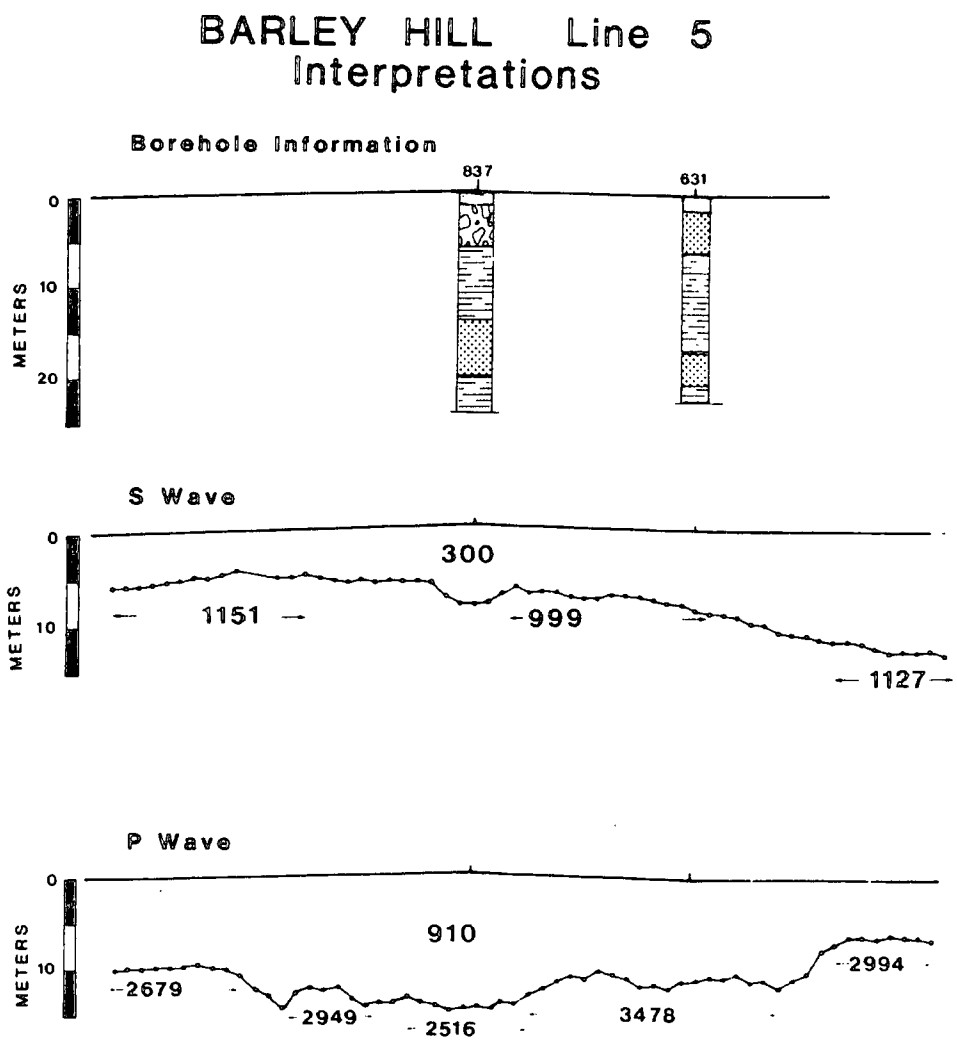

Figure 5.14

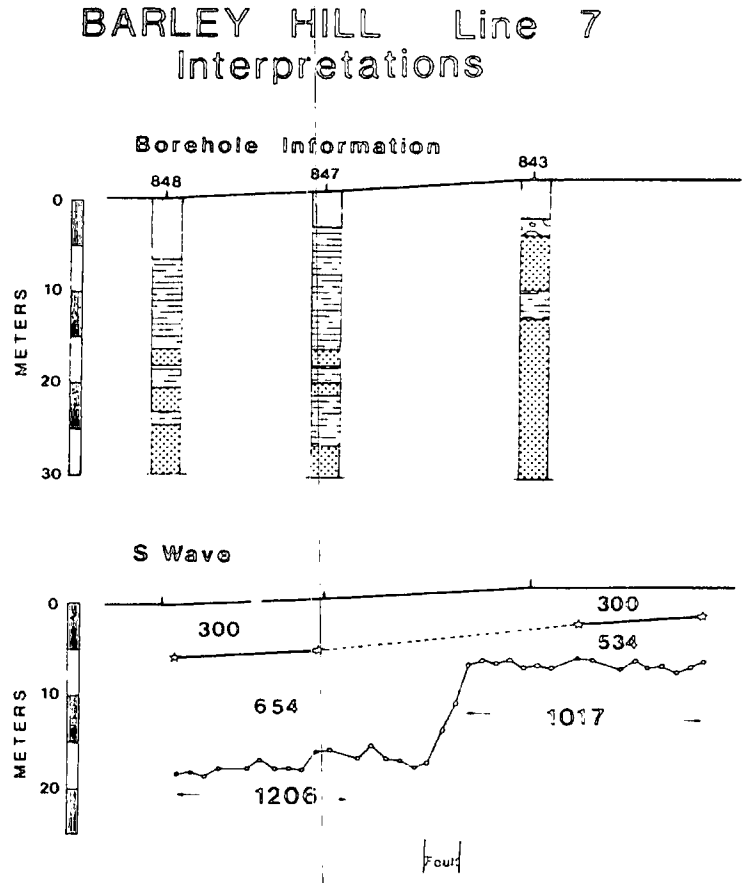

2x Vertical Exaggeration

Figure 5.15

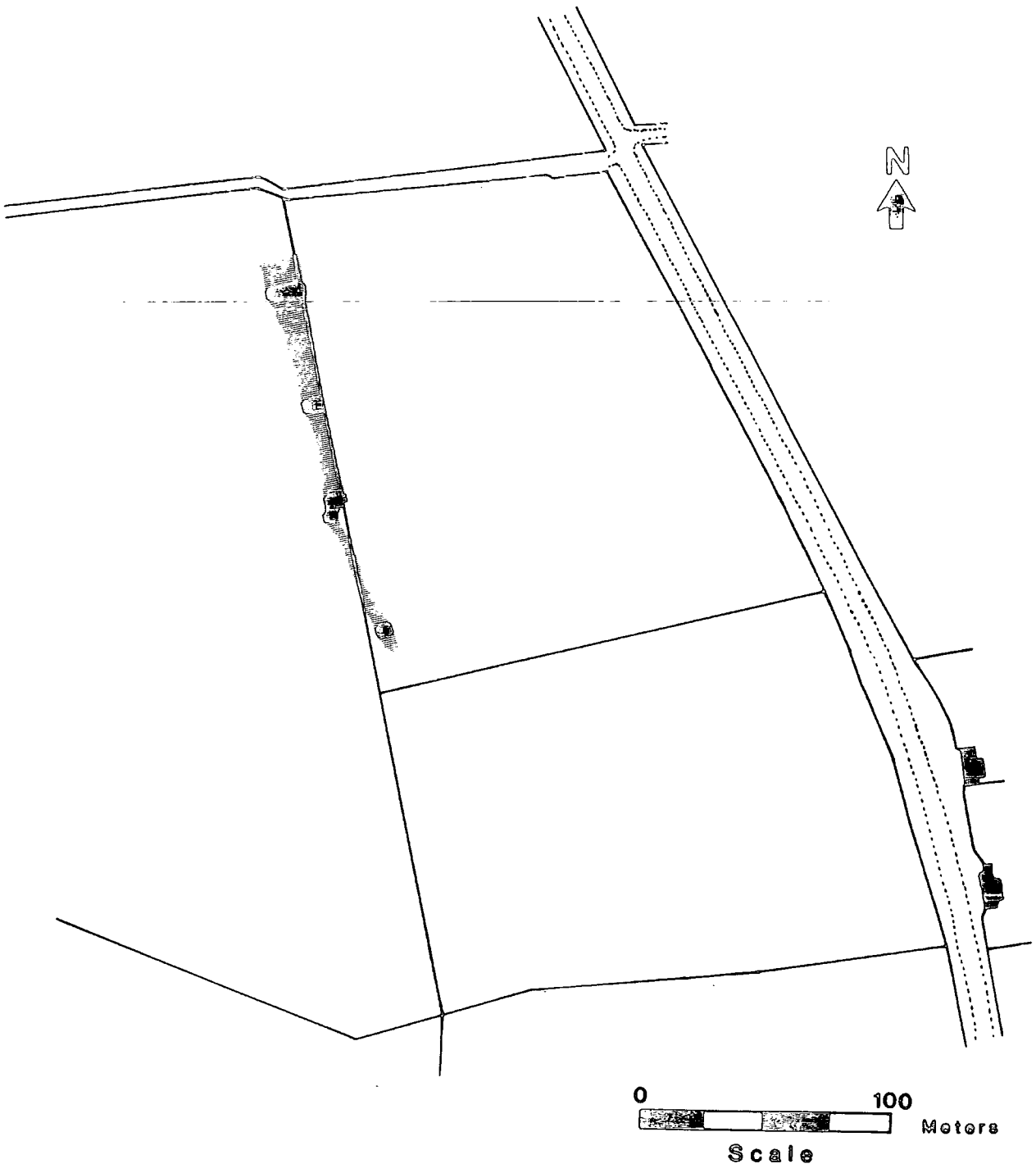

Barley Hill

Fault position and trend with error bars as located from seismic lines.

Figure 5.16

5.2 BARLEY HILL REFLECTION LINE

In August 1983 a seismic reflection line was shot at Barley Hill, along the same profile as seismic refraction line 7 (figure 5.17).

The first requirement in the acquisition of high quality shallow seismic reflection data at this site, was to drill shot-holes into rockhead or preferably below the weathering layer, so as to minimise the production of unwanted ground roll waves and to retain high frequencies. At this period the Department of Geological Sciences at Durham University had just acquired a Victor Products drill which would in theory be able to carry out the task of drilling into rockhead. In reality this proved difficult, due to teething problems encountered with the drill, and the bouldery nature of the glacial drift at this site. After many problems ten shot holes were finally drilled to a depth of 20 feet (6m).

The source used for the survey was a single seismic detonator. The seismic data were acquired using single 30Hz geophones, using a straddle spread with a 5m peg spacing and a maximum offset of 155m. The data were recorded for just over 500msecs (1024 samples at 0.5msec sampling rate). No frequency filters were used on recording.

Figure 5.18 displays the result of one of the better quality common shot gathers recorded at this site. It is clearly apparent from the raw data that severe ground roll problems were

BARLEY HILL

Location of reflection line

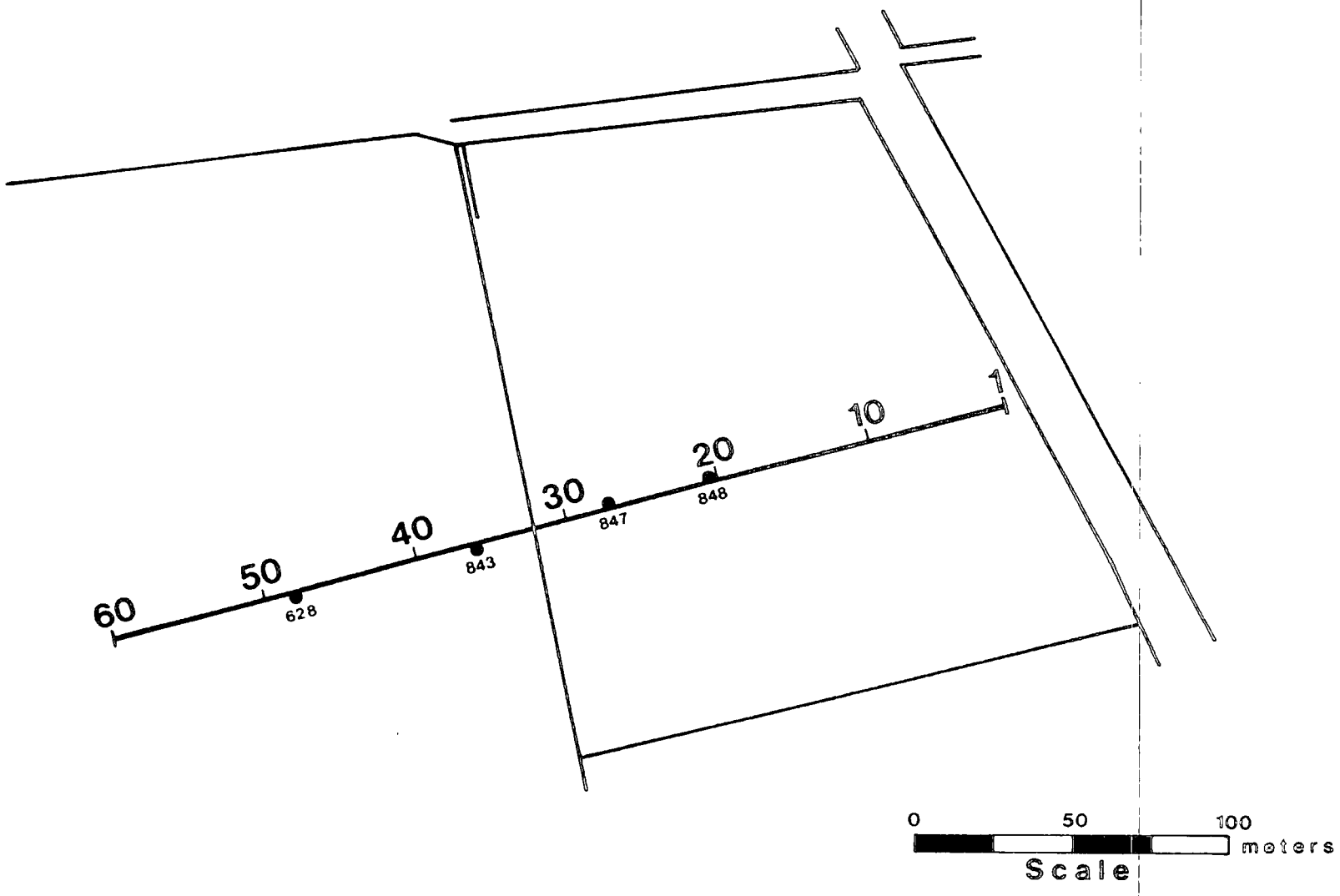

Figure 5.17

encountered, with ground roll velocities of up to 700m/sec seen on the record. Another problem is that due to the large amplitude of the ground roll on the near offset traces, the A/D converter of the Nimbus has become saturated resulting in severe clipping of the traces. These traces are of no use in further processing and have to be discarded. The only clear reflection events seen on the raw data are on the far right of the diagram at 140msecs, just outside the cone of the ground roll.

Figure 5.18 also displays the common shot gather after various pre-stack processing operations had been carried out, including band pass frequency filtering and trace editing. The optimum band pass filter was decided by carrying out frequency spectra tests on the data. The results show a typical frequency range of 20 to 60Hz for the ground roll and reflection frequencies around 120Hz. A typical amplitude spectrum is displayed in figure 5.19. A mute has been applied to remove the refraction events recorded as first breaks. The result is that the ground roll has been removed due to its low frequency compared to the reflected arrivals, and the reflections on the right of the diagram have been enhanced. Little or no reflected energy was seen on the common shot gathers below 300msecs, so it was decided to concentrate on the first 300msecs (figure 5.20).

The results of refraction line 7 were used to delineate the near surface geological structure found along the reflection line down to a depth of 25m (figure 5.21). The ground surface elevation was measured by levelling. From this both shot and geophone statics were calculated for each trace by removing the effect of the near-surface geology down to a datum of 220m above

sea level. The traces were then sorted into common mid point gathers and stacked, with a fold of cover of 9 traces. Figure 5.22 shows the results of stacking velocity tests carried out on a panel from pegs 45 to 52, where the best data occur. The tests reveal that the variation of the stacking velocity makes very little effect on the final section due to small move-outs encountered on the traces. This is due to the small offsets used in data acquisition relative to the depths under investigation. The stacking velocities used, were based on the P wave refraction velocities calculated along this line.

Figure 5.23 is the best final stacked section produced for the Barley Hill line. A CMP aligned autostatics routine with a maximum trace shift of +/-1 msec was applied to account for any residual statics left over after the field statics had been applied. The final section is of very poor quality, the only reflections present being at the far western end of the profile. The fault should be approximately at peg 30 on the section, but no structure can be interpreted from this reflection section.

The geology along this reflection line is that below the lowest coal seam (Gannister Clay), of the Coal Measures in Northumberland. The strata consist of thick sequences of coarse sandstones (or "grits") separated by relatively thin argillaceous measures which include marine shales. This therefore may have been a very poor location to try to obtain shallow reflection data due to the fact that there are no large reflection coefficients present in the sequence. A particular problem at Barley Hill is the high velocity of the ground roll which is up to 500m/sec. With hindsight, during the data acquisition larger offsets should

BARLEY HILL

Common shot gather

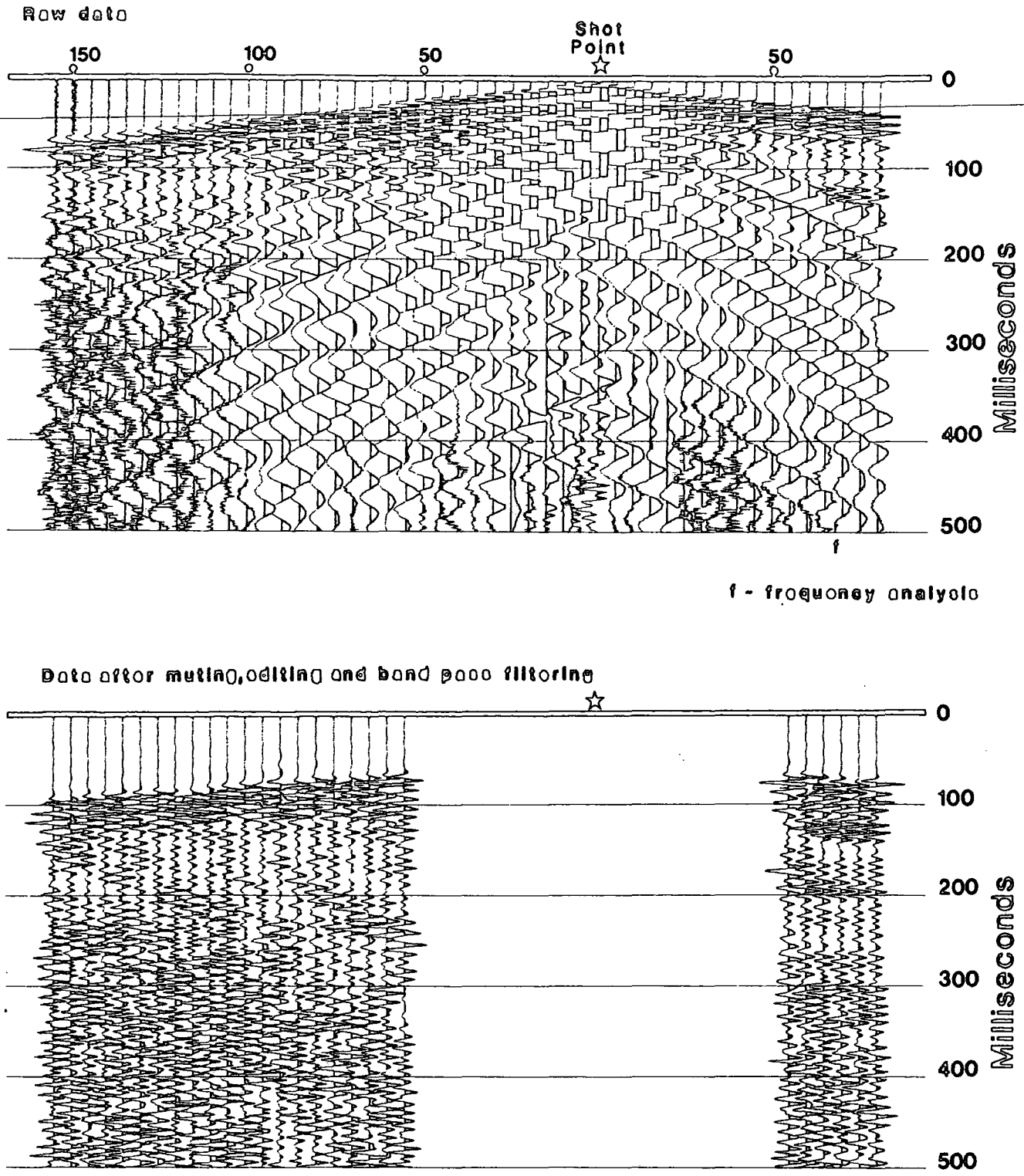

Figure 5.18

Amplitude Spectrum

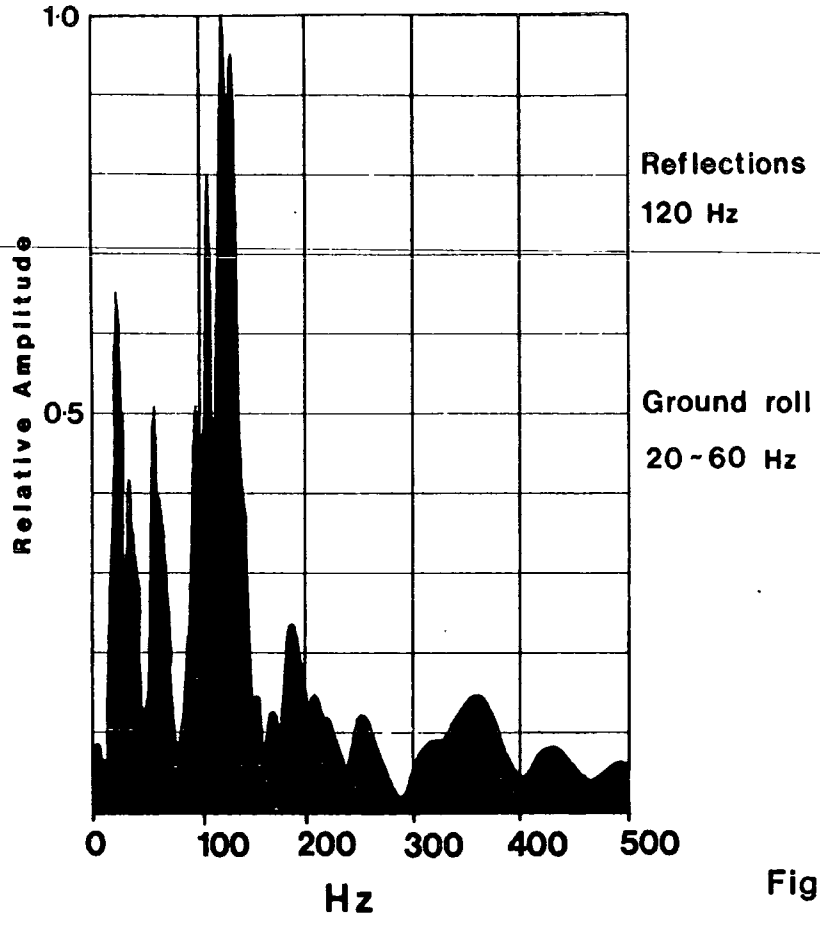

Figure 5.19

Barley Hill

Near surface model for the calculation of statics

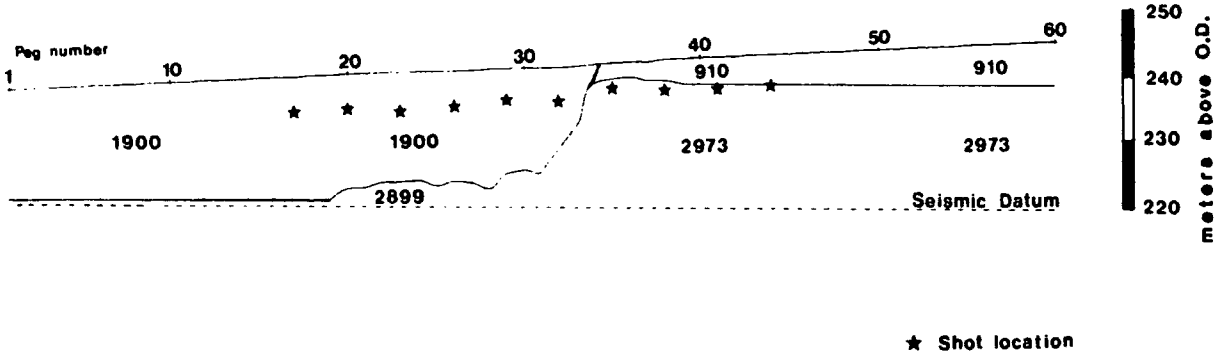

Figure 5.21

BARLEY HILL

Common shot gather

Data after muting, editing and band pass filtering

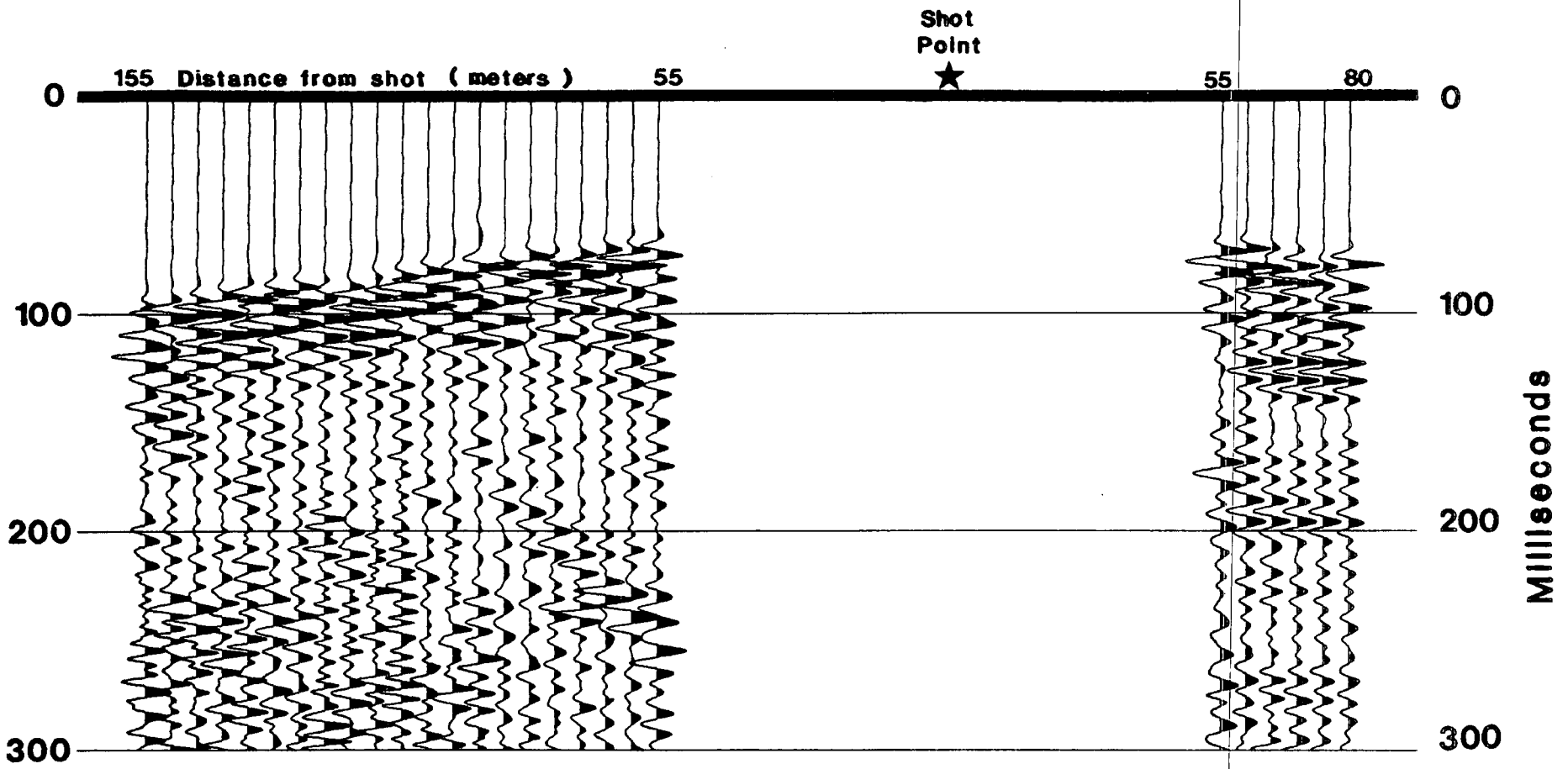

Band pass 45/65/200/300
120 msec A.G.C.

Figure 5.20

BARLEY HILL Reflection Line

Velocity Panels

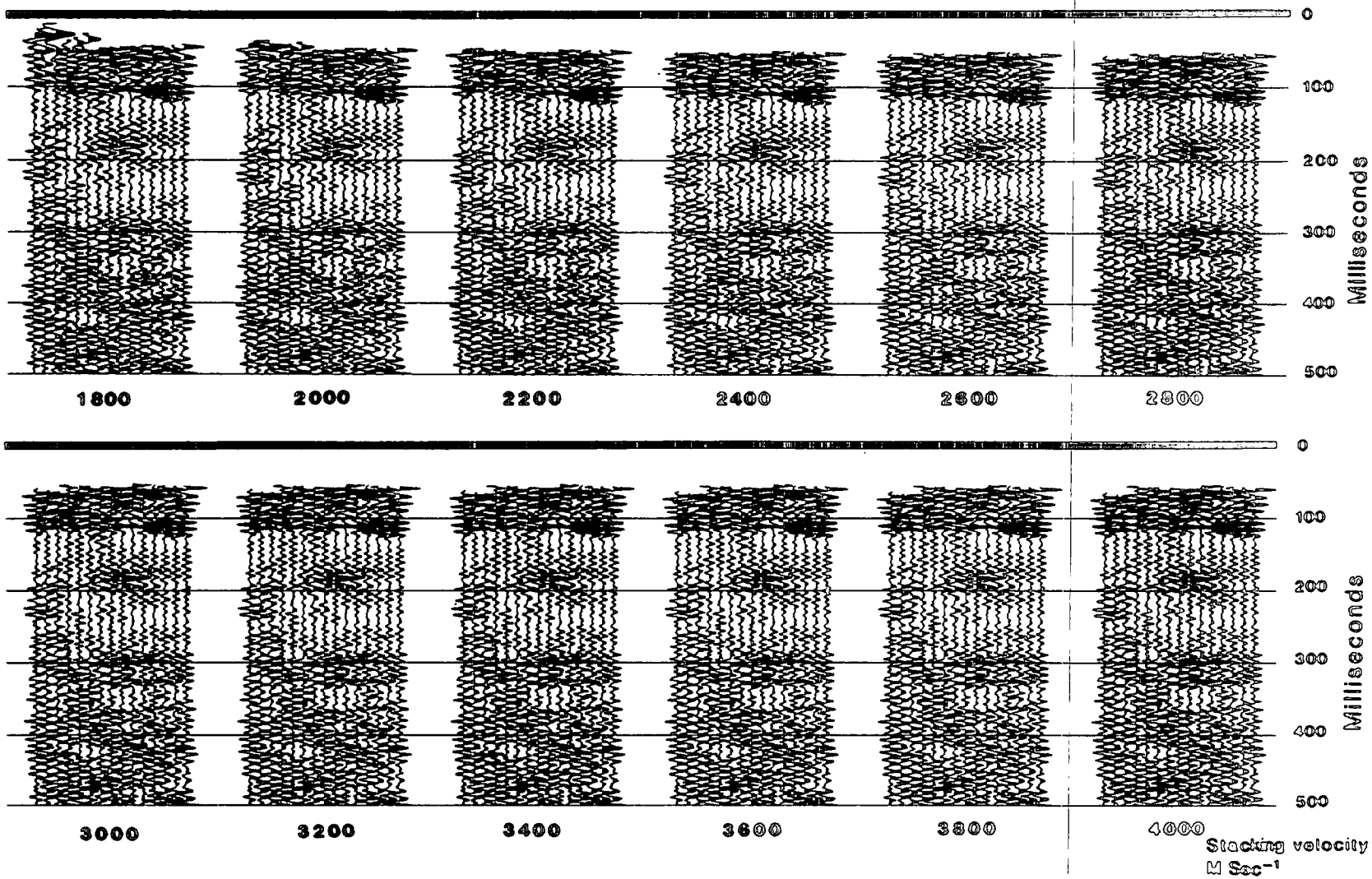

Figure 5.22

Barley Hill Reflection Line

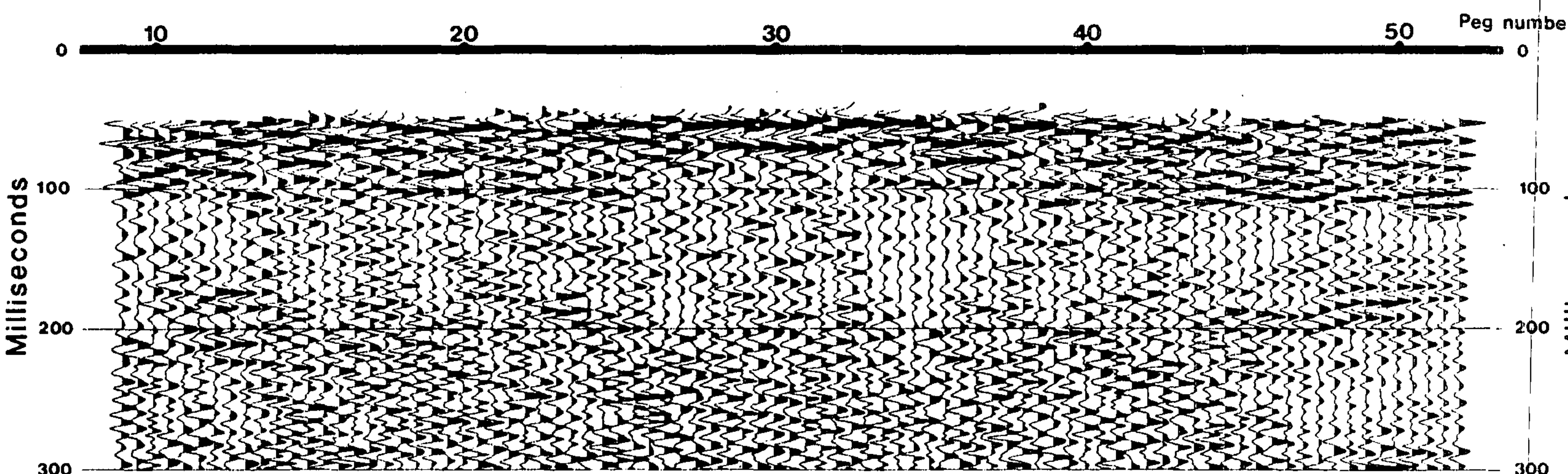

5 m Peg spacing

2.5m CMP spacing

Processing Sequence

Band pass	45/65/250
Time varying band pass	200 msec 65
	400 msec 65
Trace equalization	
Time varying gain function	
Normal moveout correction	
Autostatics routine	
Stack	
Automatic gain control	150 msec

Velocity

Figure 5.23

have been used to obtain more data outside the cone of the ground roll.

5.3 BARLEY HILL OLD WORKINGS PROBLEM

In the western corner of the Barley Hill site there is an area of 500 square meters which had been previously worked in 1953 to extract the Brockwell coal seam. The Brockwell coal seam lies stratigraphically above the coal seams found in the north of the site. In the area of the old workings the Brockwell seam is at a depth of 8m, overlain by 7m of sandstone and sandy-shale bands, plus 1m of drift. In modern times, due to advances in excavation equipment, it now becomes economic to mine the coal seams below the area of the previous old workings.

An old site plan shows the area of the previous old workings (Figure 5.24), but old plans are sometimes unreliable. Therefore the problem under investigation was to detect the edge of the previous old workings. A P wave survey was chosen because of the necessary depth penetration required and the attenuation effects of backfill material on our low energy S wave source.

A seismic line was orientated so that it lay perpendicular to the strike of the edge of the old workings (figure 5.24). A 3m peg spacing was chosen as this would give the necessary resolution. Due to the quite severe topography encountered along the seismic line, it seemed advisable to level the line so that

the topographic effects could be accounted for.

The first stage of the survey was to shoot two short refraction spreads, one on the known worked area, the other on the virgin geology. The results can be seen in figure 5.25. The short refraction spread located on the virgin area displays a simple two-layer case with an overburden of velocity of 865m/sec overlying a refractor of velocity 1594m/sec at a depth of 2m. The refraction spread located on the backfill material also displays a two-layer velocity structure of 686m/sec overlying a refractor of 2005m/sec at a depth of 6m. These depth estimates show good agreement with available borehole information.

Both the calculated overburden velocities seen at this site display a low P wave velocity even for unconsolidated glacial drift material, compared with previous experience at different sites. This may indicate the presence of backfill material used for ground restoration after the coal was extracted. The refractor velocity of 1594m/sec found at the virgin end is probably the weathered rockhead. The refractor of velocity 2005m/sec found at the worked area is likely to be the floor of the previous old workings.

A phantomed traveltime graph was compiled along the whole profile by analysing refraction data produced at 60 and 90m offsets (figure 5.26). Problems with data quality were encountered when the shots were fired on the area of backfill material, due to high attenuation effects in the unconsolidated material.

The data was analysed using the Plus-Minus technique. The resultant minus graph displays two distinct velocity segments of refractor velocity 2112m/sec in the east and 2208m/sec in the west. The plus graph shows a dramatic step when the edge of the old workings is crossed, with an increase in the depth to the refractor over the worked area.

Figure 5.27 displays an interpreted cross-section along this seismic line. The thickness of the weathering layer in the unmined area cannot be estimated with any degree of accuracy, but the important parameter required is the boundary of the mined area. The edge of the old workings was located to within an estimated accuracy of 3m, and coincided with the edge displayed on the old site plan (figure 5.24).

BARLEY HILL (Old workings problem)

Site plan of previous opencast working

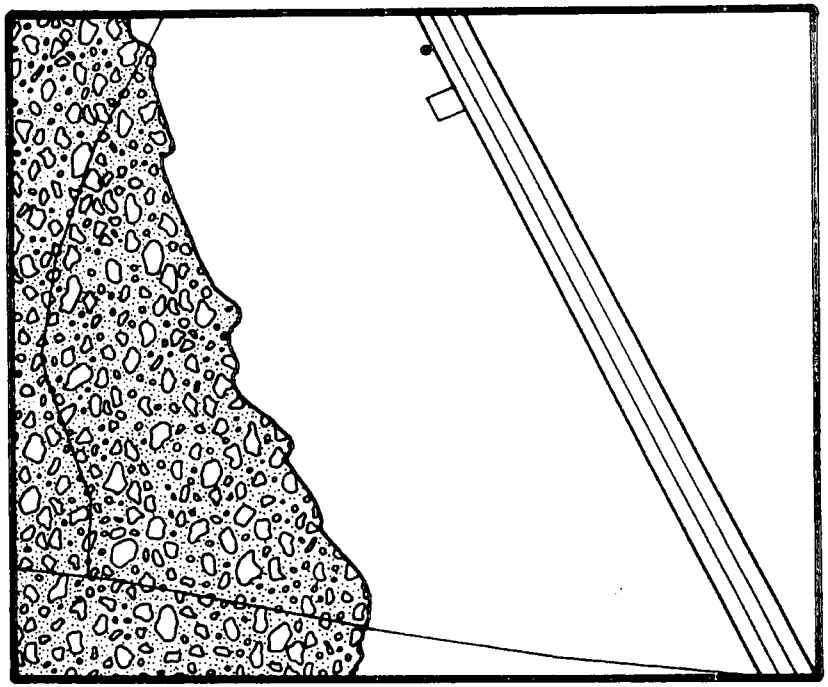

Location of seismic line

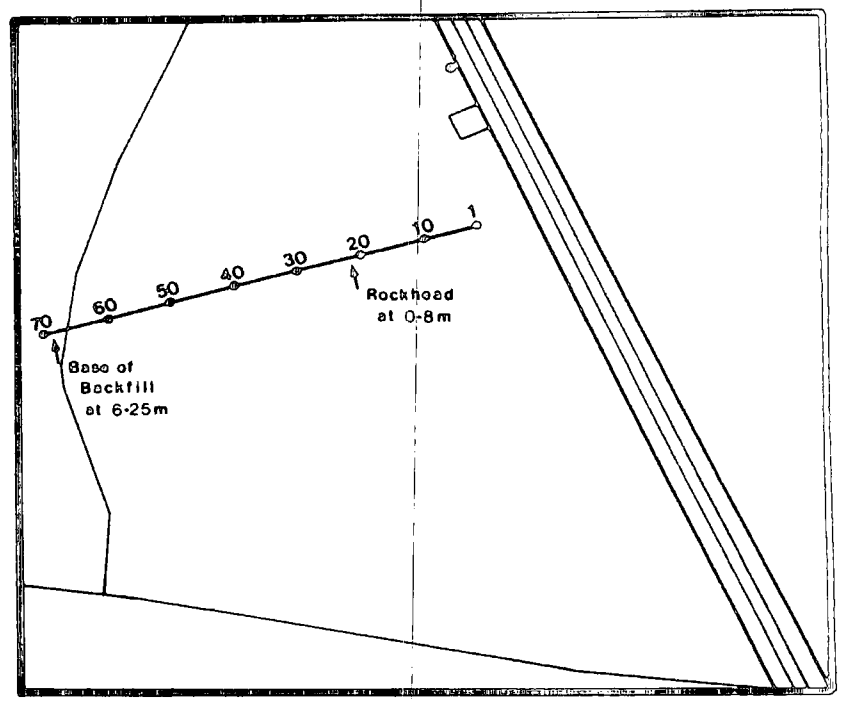

Key

Area of previous opencasting

Scale

0 50 100 Meters

Borehole information

Figure 5.24

BARLEY HILL

Interpretation of short reversed refraction spreads

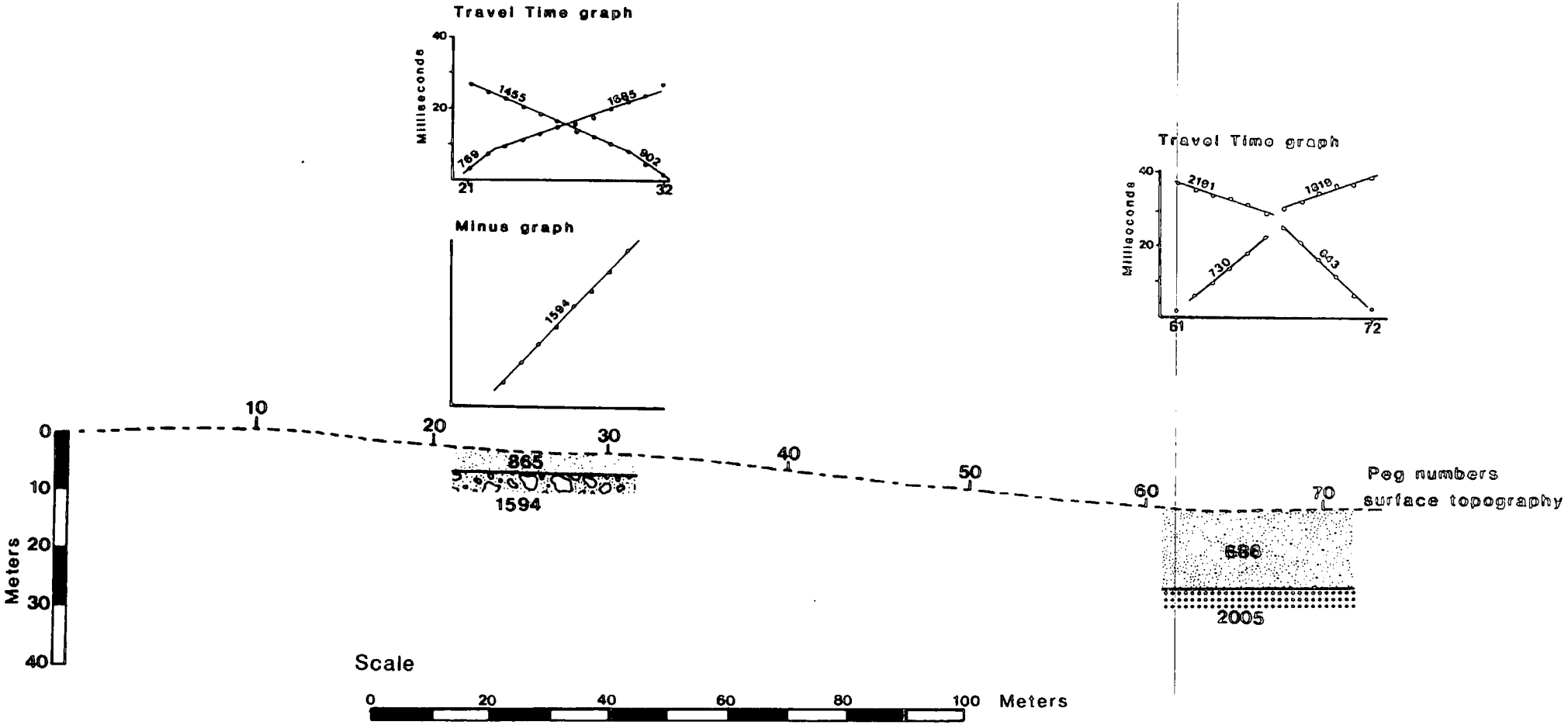

Figure 5.25

BARLEY HILL (Old workings problem)

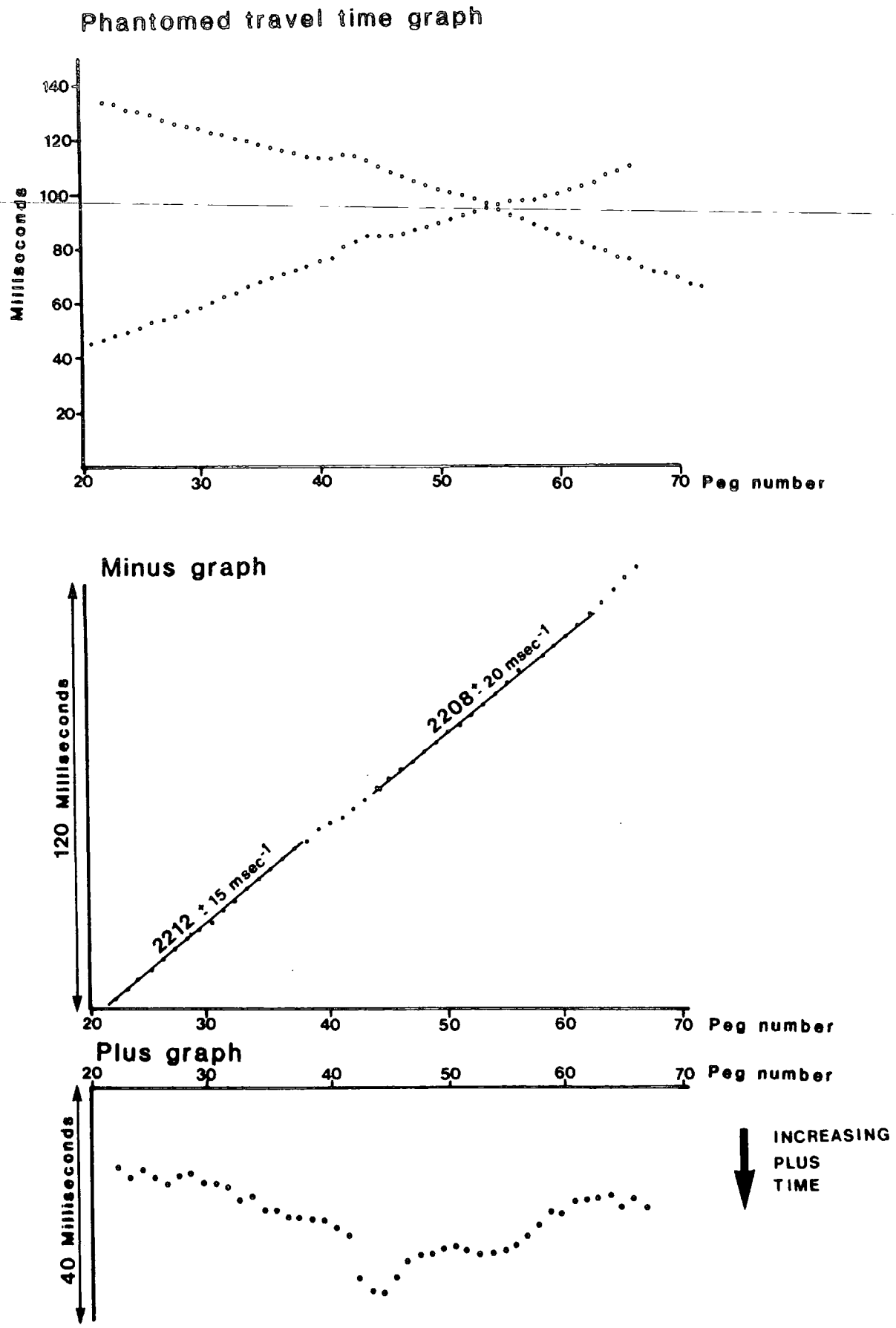

Figure 5.26

BARLEY HILL (old workings) Interpretation

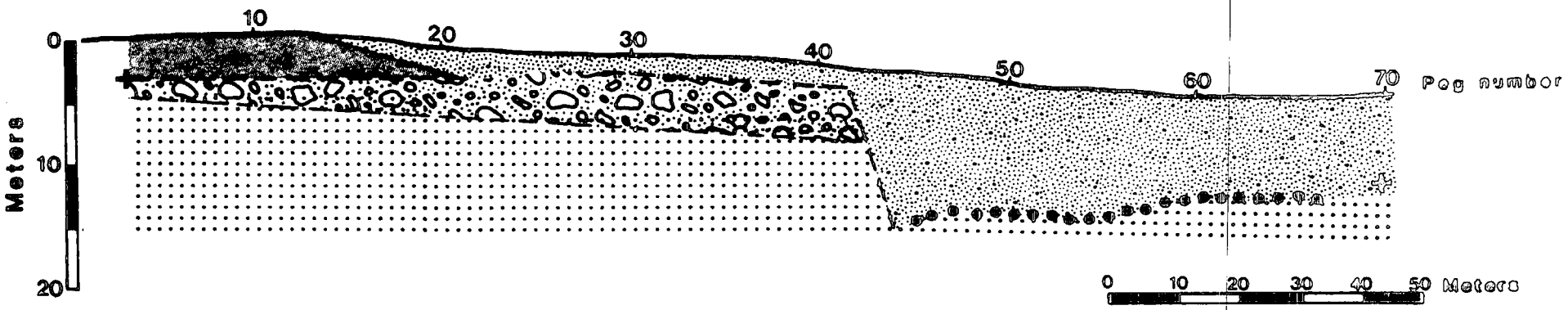

Key

- Backfill material 680 ms^{-1}
- Glacial drift 1140 ms^{-1}
- Weathered Sandstone 1594 ms^{-1}
- Sandstone 2210 ms^{-1}

Symbols

- ⊕ Depth plot from Plus Minus interpretation
- + Depth plot from single ended profile
- ---- Inferred boundary

Figure 5.27

CHAPTER SIX

HEMSCOTT NORTH : SITE NO. 3

The Hemscott North site is situated on the coastal plain, at Druridge Bay in eastern Northumberland. The target of our investigation was the Grange Moor Fault which is one of a series of ENE - WSW major normal faults which cut the Carboniferous strata in Northumberland. Coal mining has taken place in the area over the past century and from old mine plans it is known that the Grange Moor Fault downthrows the strata to the south by approximately 40m (Fowler, 1935). From the results of preliminary drilling at the time the seismic survey was carried out, the Opencast Executive believed the Grange Moor Fault to consist of a single main fracture, with splays off toward the south. Later drilling, on a fine 30m grid pattern in the area of the fault, revealed a complex zone of faulting over a region 60m wide.

Figure 6.1 outlines the geology at Hemscott North. The diagram displays a generalized sequence through the Carboniferous strata in the area. The major sandstone units are highlighted and the coal seam horizons are labelled H to U. A plan of the final interpretation of the fault geometry interpreted from borehole information from the area is also displayed. The Grange Moor Fault zone consists of two major normal faults, a northern fault (fault 1) with a throw of around 20m, and a southern fault (fault 2) with a throw of 8 to 16m. There is a complication to this model. A third fault with a throw of 13m is thought to form a link between the two main faults in the area of our survey. Using borehole information, a cross-section of the near surface

The Geology at Hemscott North

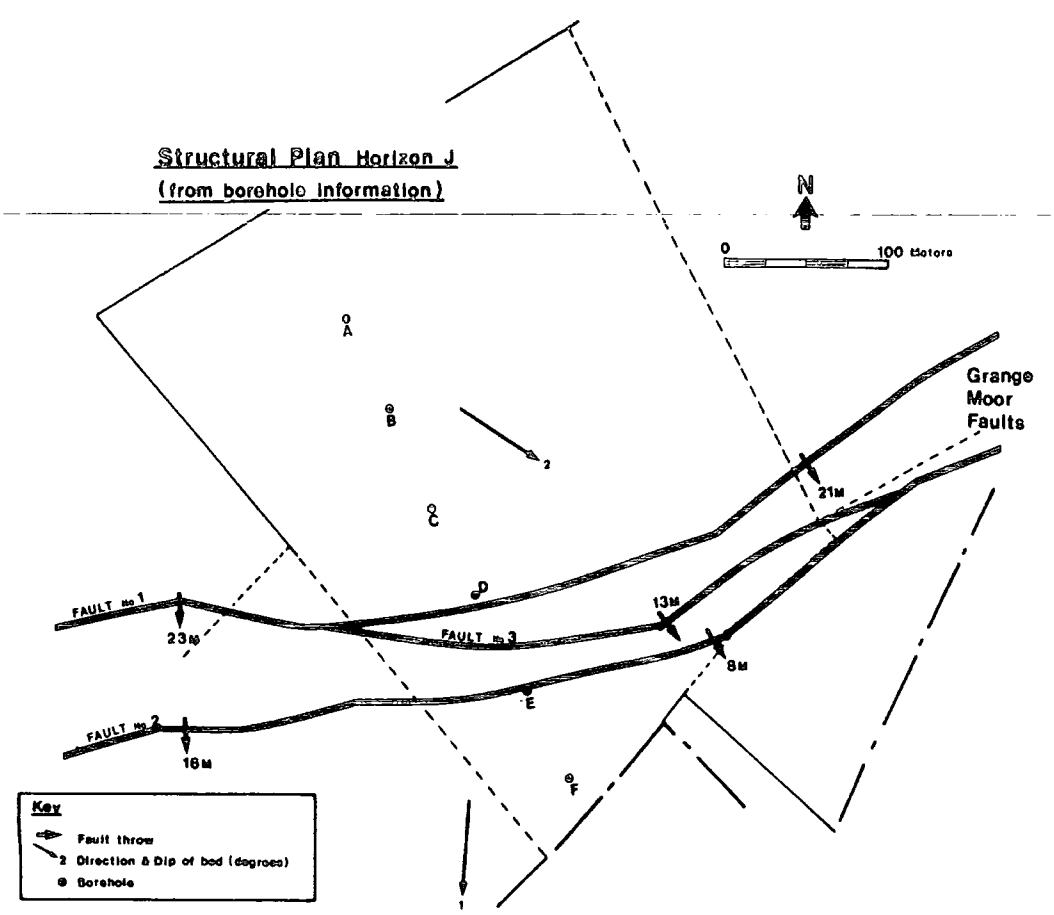

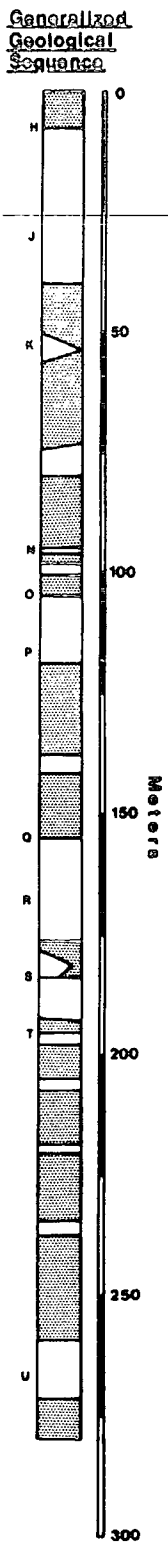

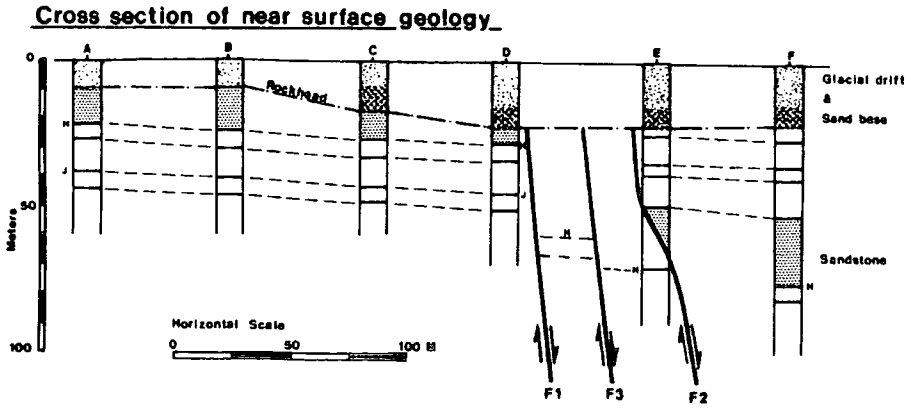

Sandsone horizons are shown stippled

Figure 6.1

perpendicular to the fault plane is drawn. The total fault throw across the area is 42m.

The landsurface topography is flat, but this masks severe rockhead topography in this area. A major pre-glacial valley, now drift filled, meanders across the area. The sandy drift cover varies in thickness from 10 to 30m (Anson & Sharp, 1960).

The site was visited between August and October 1982. A considerable amount of effort went into the collection of seismic data at this site. Originally trials were carried out using P and S wave refraction and reflection lines. No S wave reflections were apparent on the field records collected at this site, so the method was abandoned. The S wave refraction technique proved successful in another area of the site, where it was used to determine the drift thickness over the drift filled channel. The technique was successful in outlining the shape of the drift channel. The results of this survey were included in the paper by Goulty & Brabham (1984).

Figure 6.2 displays the location of the P wave refraction and reflection lines which were shot over the proposed location of the Grange Moor Fault, along with an overlay showing the drift thickness contours in the area of the survey lines.

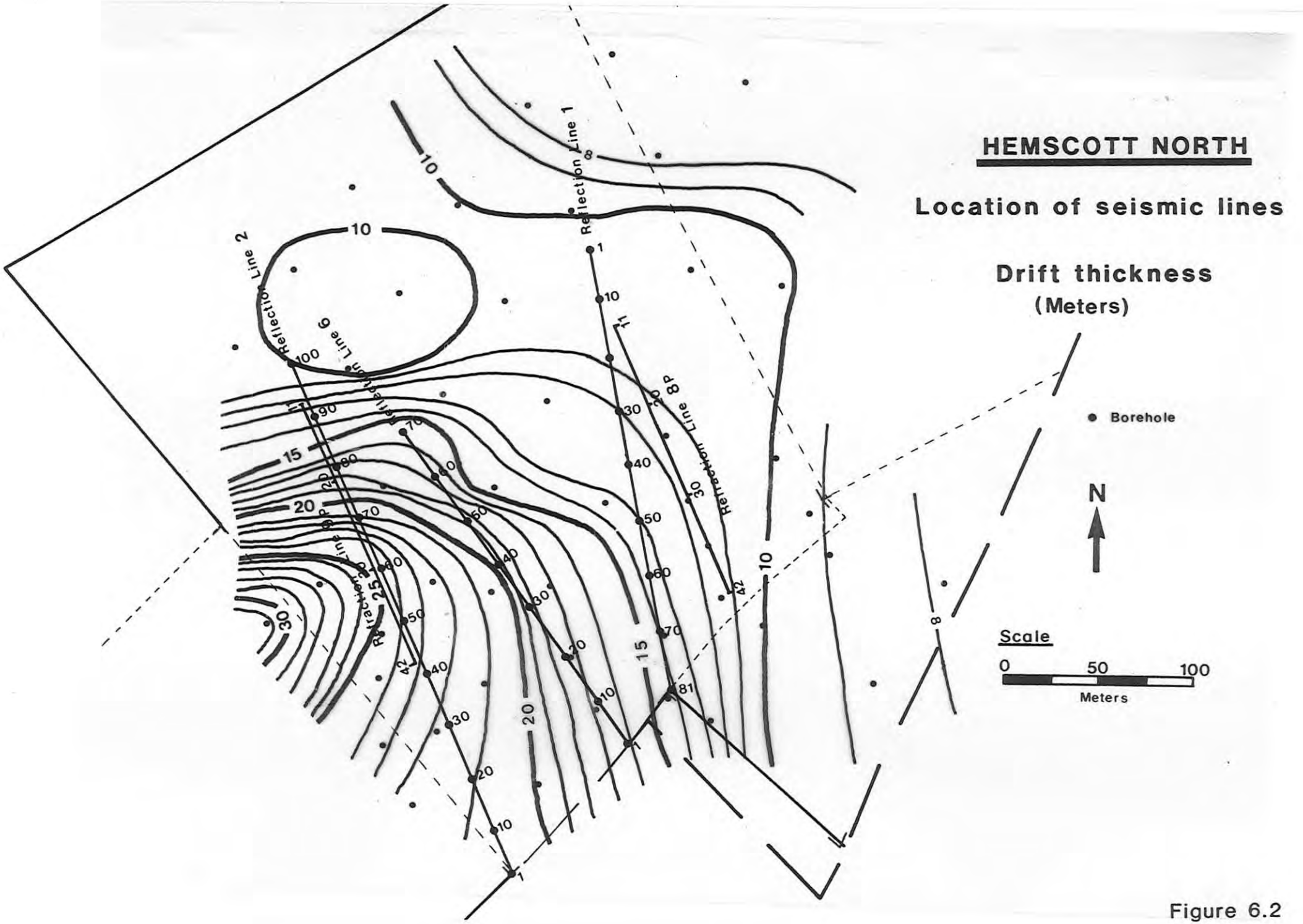
HEMSCOTT NORTH
Location of seismic lines
Drift thickness
(Meters)
Borehole
N
Scale
0
50
100
Meters
Reflection Line 1
Reflection Line 2
Refraction Line 6
Refraction Line 8P
Refraction Line 9P
Refraction Line 10P

Figure 6.2

6.1 P WAVE REFRACTION LINES

Two seismic refraction lines were shot over the Grange Moor Fault (lines 8P and 9P). Because of the large scale of the fault zone, a 5m peg spacing was used for the survey. Due to the thick drift cover, the direct wave (or a very shallow drift refractor) with a P wave velocity of 1800m/sec was recorded out to 100m. Shot to first geophone offsets of up to 180m were required to record refracted arrivals from below rockhead. Due to the deep drift at this site charge sizes of 2oz (buried at 1.5m depth) were required, to obtain refracted arrivals with sufficient signal/noise ratio.

In an attempt to account for the very near surface geology, the direct wave arrivals were recorded across the array in both directions. A time-distance graph was plotted, and straight lines were fitted to the direct arrivals by least squares. The difference between the measured arrival times and the straight line was taken to represent the near surface static corrections. These statics were then subtracted from the refracted arrivals at each geophone. The corrections proved to be less than plus or minus 1msec. This technique helped to improve the data interpretation, especially the calculation of the refractor velocities.

The data were interpreted using simple planar dipping layer models. This is due to the depth from which the refracted arrivals originate, and the problems of obtaining reversed data for each horizon with a complex fault model. Where arrivals were positively identified as coming from the same refractor in both

the forward and reverse shooting directions, minus graphs were then plotted where possible, to achieve accurate velocity determinations.

Figure 6.3 shows the final interpretations of the refraction lines 8P and 9P.

Line 8P

The drift thickness along this line is consistently around 12m, as revealed by borehole information (figure 6.2). North of the fault there is a sandstone horizon at rockhead, but seismically this is transparent, indicating that it must be weathered. The 2400m/sec refractor may be the base of weathering of the coal measures, but this depth also correlates with the water table as given by geophysical logs.

The deep refractor of seismic velocity 3124m/sec north of the fault would appear to correlate with the sandstone unit just below horizon J (figure 6.1). The fault position was estimated by calculating the position where the 3124m/sec refractor is terminated.

South of the fault the 1800/1900m/sec boundary is undoubtedly rockhead, whilst the 2248m/sec refractor may again be the water table as picked out from geophysical logs. The position of the fault as given by the seismics agrees well with position of fault 1, located by boreholes.

Line 9P

From the borehole information, the drift thickness along this line varies from 10m in the north to 25m in the south (figure 6.2). This is borne out by the refraction data, where there is an increased thickness of the 1800m/sec layer relative to Line 8. North of the fault a similar velocity structure to that of line 8 is seen. The depth and dip of the 3165m/sec refractor along this line agree well with the depth and dip of the sandstone unit below horizon J as seen from the borehole information. South of the fault the 1800/2400m/sec boundary is 7m below driller's rockhead. The origin of this refractor is not clear. The fault location is achieved by the pinpointing of the termination of the deep 3165m/sec refractor north of the fault. This position also agrees with the position of fault 1 from the borehole information.

The complexity of this faulted region does not lend itself to investigation by the refraction method, which relies upon simplistic layer models for interpretation. Nevertheless, the position of the major fault (fault 1) is accurately located by its downthrowing of a large sandstone unit at 50m depth.

Hemscott North

Interpretation of seismic refraction Lines

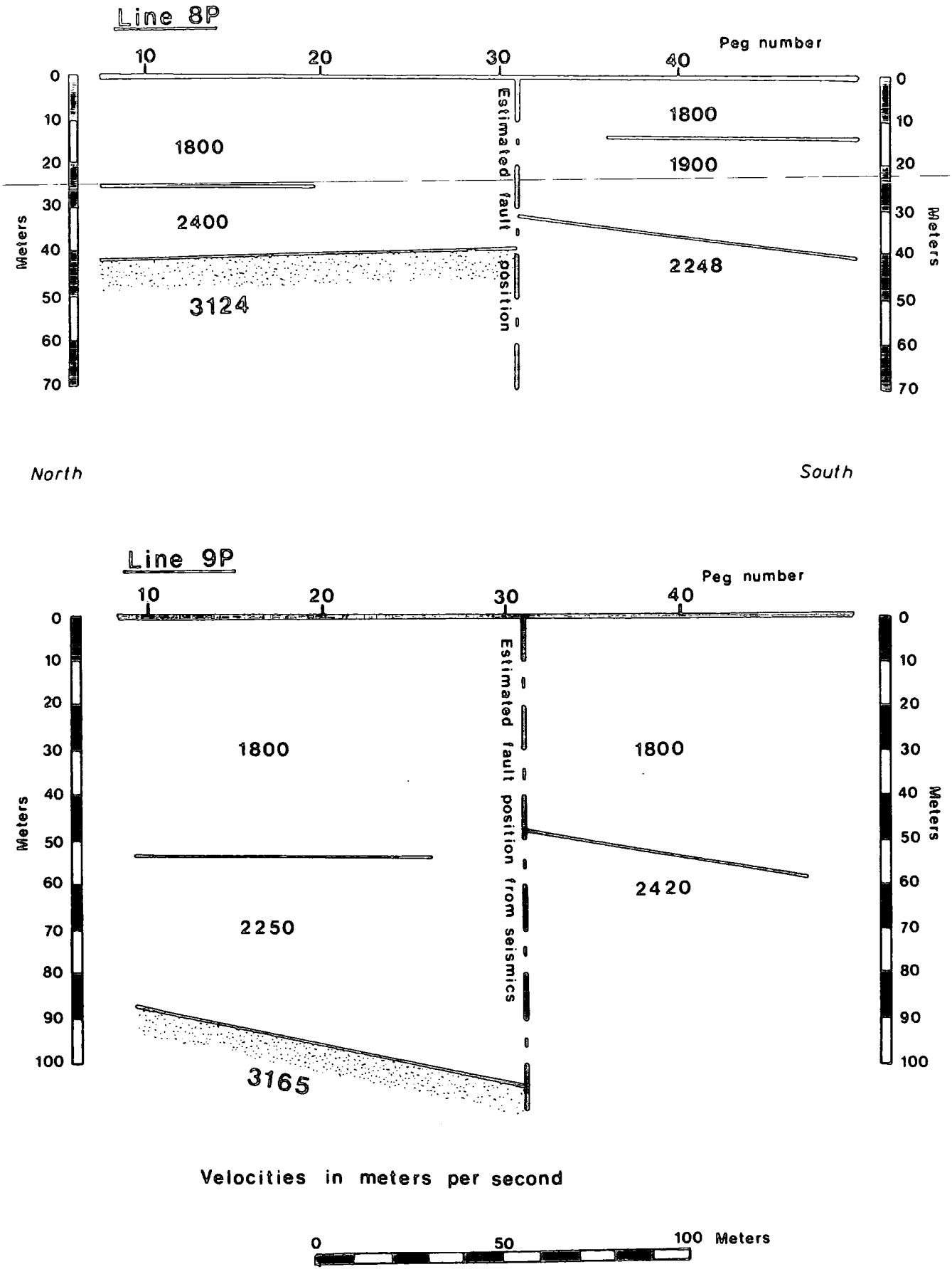

Figure 6.3

6.2 P WAVE REFLECTION SURVEYS

Three reflection lines were shot at Hemscott North over the Grange Moor Fault. Figure 6.2 displays the location of the lines. The lines are numbered 1, 2 and 6. Line 1 was shot twice with different acquisition parameters.

Data Acquisition

For each of the seismic lines shot at Hemscott North, the seismic source was a single detonator and the data were recorded for just over 200msecs on magnetic tape (1024 digital samples, at a sampling frequency of 5 samples per msec). No band pass filters were used to record the data in the field. A peg spacing of 3m was also used throughout the surveys, which gives a common mid point (CMP) spacing of 1.5m.

Line 1 (Shallow)

The seismic detonator was buried at a depth of 1.5m in the glacial drift overburden. The very first reflection records that were shot at Hemscott North, at the southern end of line 1, were very encouraging. This was because strong reflected arrivals were clearly apparent on the field monitor record between 100 and 180msecs, even without band pass filtering the data.

In all, 41 shots were fired on this line, at a shot spacing of 6 pegs (18m). The common shot data were mainly recorded using two 12 channel spreads, with six coincident geophones between spreads.

This effectively produced an 18 channel common shot gather (CSG) at each shot point. Mainly offsets of 21 to 72m were used, although some extra offsets were added.

Figure 6.4 displays the CSG recorded at shot point 81, where an effective 24 channel CSG was recorded with offsets of 3 to 72m. This figure displays the relationship between the near horizontal reflected arrivals, with the low velocity, low frequency ground roll and the refraction arrivals which appear as first breaks. Problems are also encountered with reverberant refracted events which run parallel with the first breaks. The reverberant refractions mask the very near surface reflections. Figure 6.4 also displays the same CSG after trace editing and band pass filtering, which effectively removes the ground roll from the records. The acquisition geometry results in a CMP fold of cover of four over most of the line, decreasing towards the ends. Folds of cover of less than three were not included at the ends of the final sections.

Line 1 (Deep)

In an attempt to improve upon the data quality and resolution along this line, the line was re-shot burying the detonator at a greater depth. The OE arranged the drilling of twelve 20ft (6m) deep shot holes at an 18m spacing. The borehole depth was chosen because this is the length of a single drill rod of the available rig. The twelve shot holes were drilled in 3 hours by the rig, making it a relatively economic way of carrying out a seismic survey. Although the source would still be buried in the drift, which is about 10m thick along line 1, it was hoped that by

burying the charge the amount of ground roll would be reduced and the dominant frequency of the reflections would be increased, due to less absorption of the higher frequencies by the drift. In total 45 shots were taken using a straddle spread geometry with offsets of zero to 78m (3m peg spacing). There was a two geophone overlap on adjacent 12 channel geophone spreads. This results in an effective 42 channel CSG.

Random shot statics (due to the use at that time of non-seismic detonators) of up to 5msecs were apparent on the records. These were removed by correcting the zero offset first break to equal zero time. Far offset spreads were adjusted by making the first break times between adjacent spreads (where there was geophone overlap) equal. Figure 6.5 shows a CSG recorded on this line. The data quality improved on that recorded using the shallow shots. The reflected arrivals display a slightly higher dominant frequency and the ground roll is not as severe. The ground roll velocity is 200m/sec. Figure 6.5 also displays the same CSG after trace editing and band pass filtering have been applied.

Due to the fact that we only had twelve relatively widely spaced shot holes available, the resultant fold of cover was inconsistent, alternating between 2, 3 and 4 along the line after near offset traces were edited out.

Line 2

Line 2 was again shot using a single detonator buried at a depth of 1.5m in the glacial drift. The data were recorded using a split straddle spread acquisition geometry. Two 12 channel

geophone spreads were used per shot point, with minimum and maximum offsets of 39 and 72m. The result of this geometry is that virtually all the traces are recording outside the cone of ground roll, so no traces were edited out before sorting. Figure 6.6 displays a typical CSG from this line. The data quality is poor and any reflections that are present are of low amplitude.

To account for the random time delays introduced by the detonator, the first break times at the nearest (39m) geophone were equalized for all the CSGs in the profile. The refraction data showed that nowhere did refracted arrivals from rockhead become first breaks until offsets greater than 100m were reached. Therefore all the first breaks on the reflection data originate from the direct arrivals. By making the 39m offset first break the same time as on line 1(shallow), then inter-line compatibility is achieved. Any residual statics would later be removed by applying the CMP aligned statics routine to the data set.

Line 6

Line 6 was again shot using a single detonator buried at a depth of 1.5m. In total, 31 shot points were used at a 2 peg (6m) spacing. A straddle spread acquisition geometry was used, with geophone offsets of zero to 63m. Figure 6.7 displays a single CSG recorded along this line, combining three separate 12 channel records. The random time delays introduced by the detonator were corrected for by making the zero offset first break times equal to time zero. Then the first break of the first trace in each far offset spread was adjusted to equal the first break of the last geophone in the near spread (as they have an equal offset).

Hemscott North Line 1 (shallow)

Common shot gather

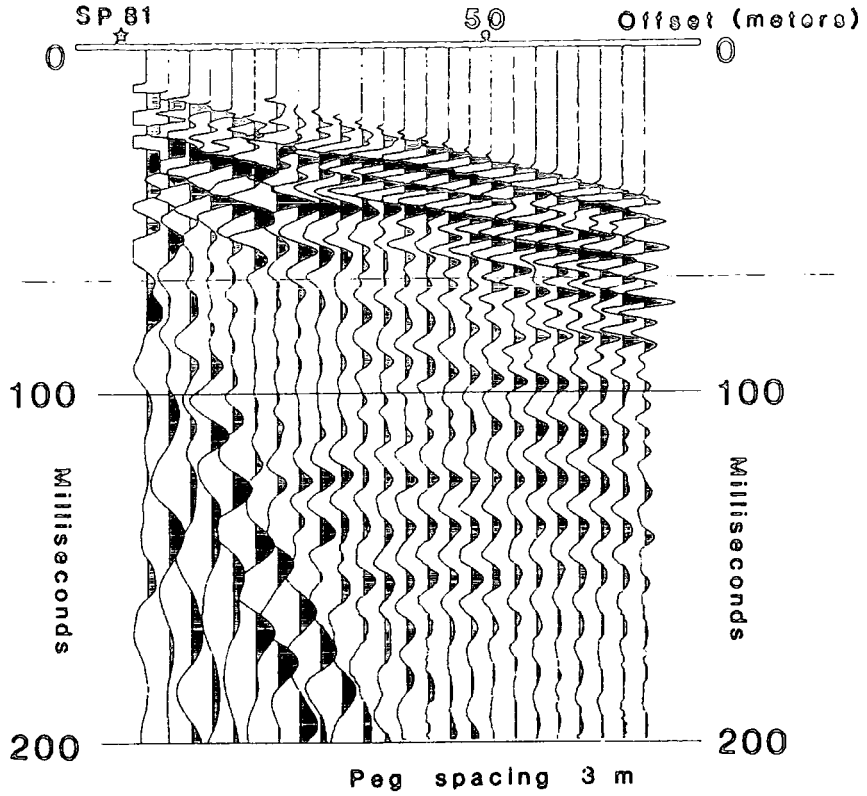

Editing & Band pass filtering

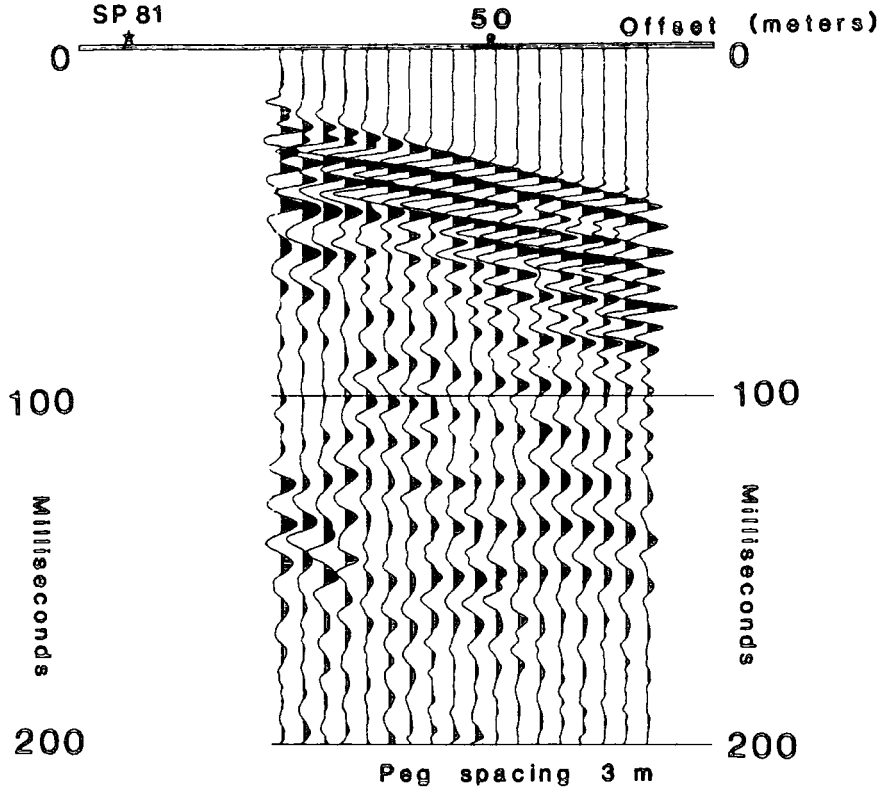

Band pass 55/85/300/400

Figure 6.4

Hemscott North Line 1 (deep)

Common shot gather

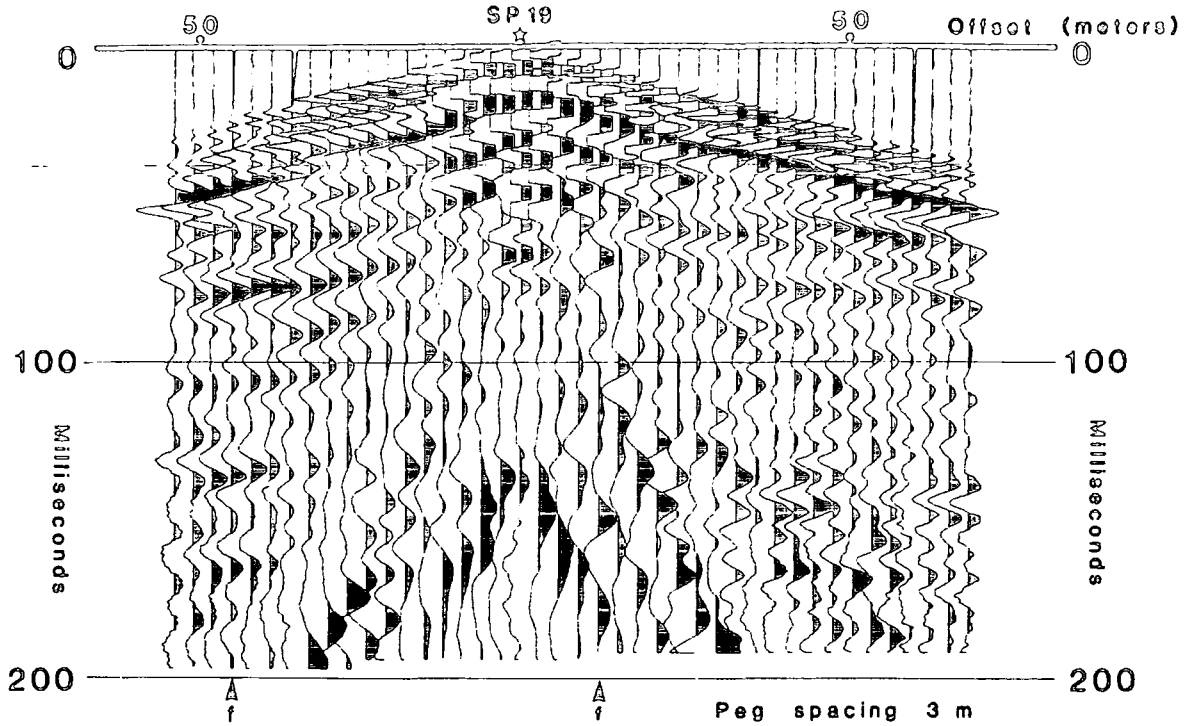

f - Frequency analysis

Editing & Band pass filtering

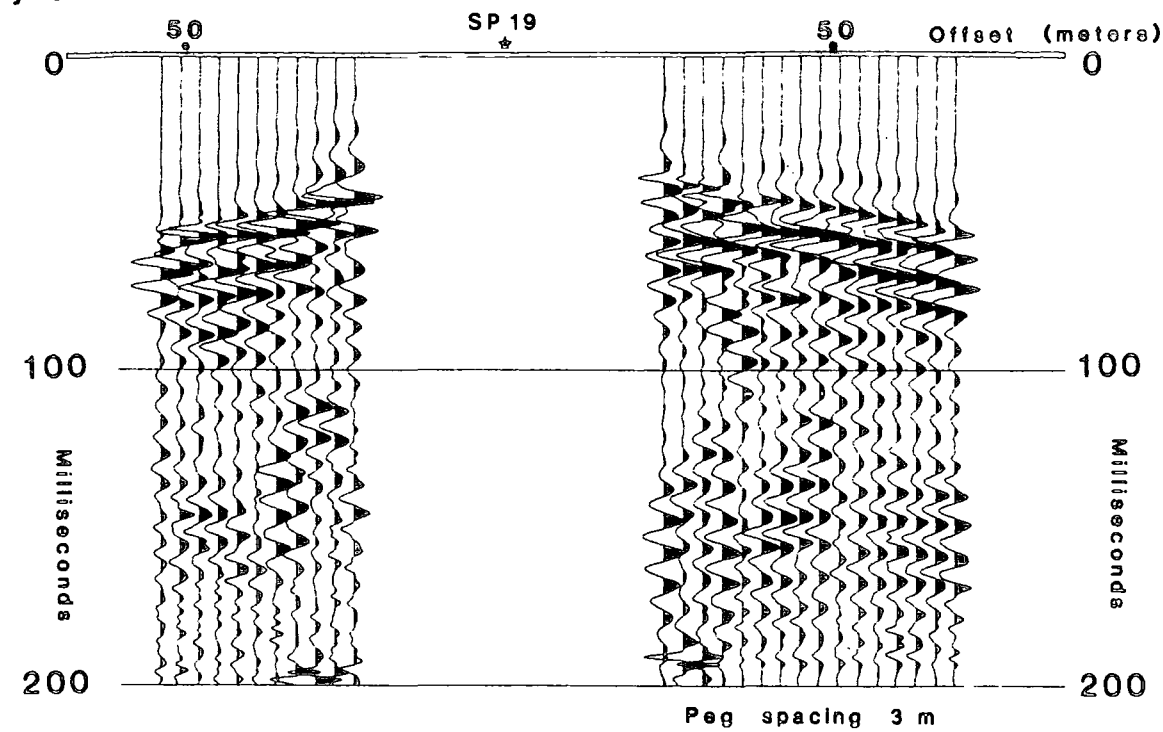

Band pass 70/100/300/400

Figure 6.5

Hemscott North Line 2

Common shot gather

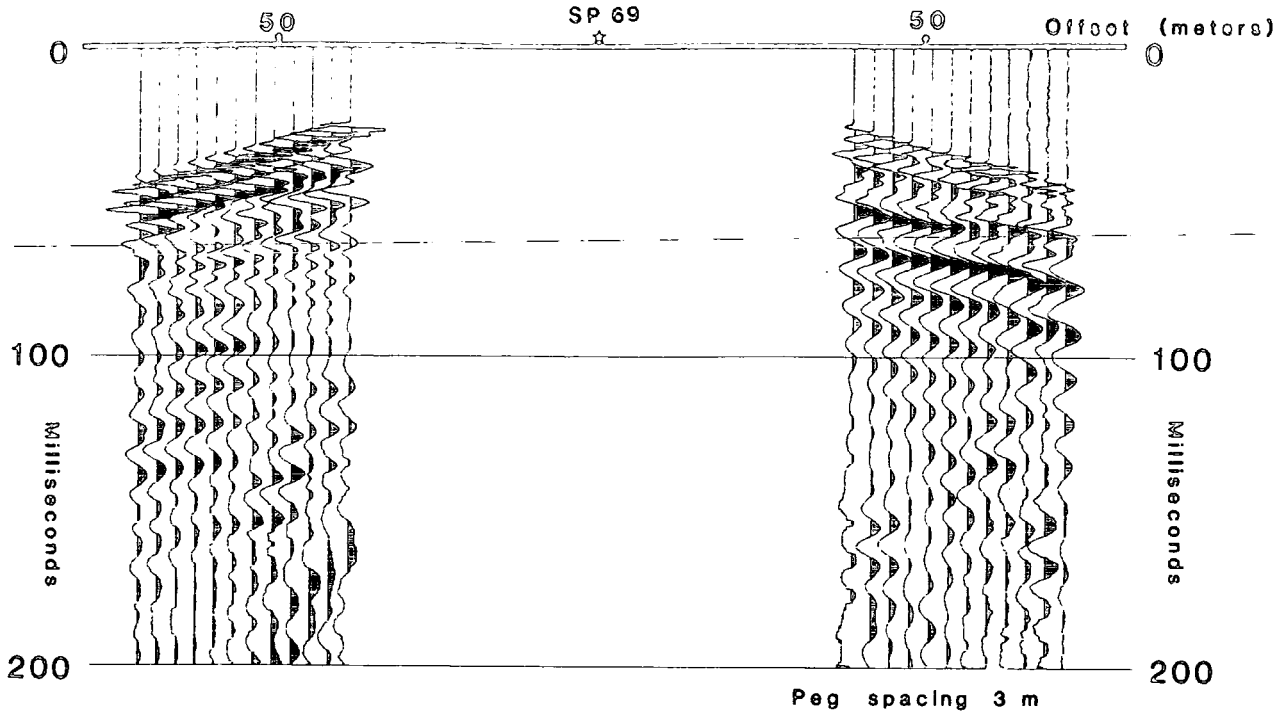

Editing & Band pass filtering

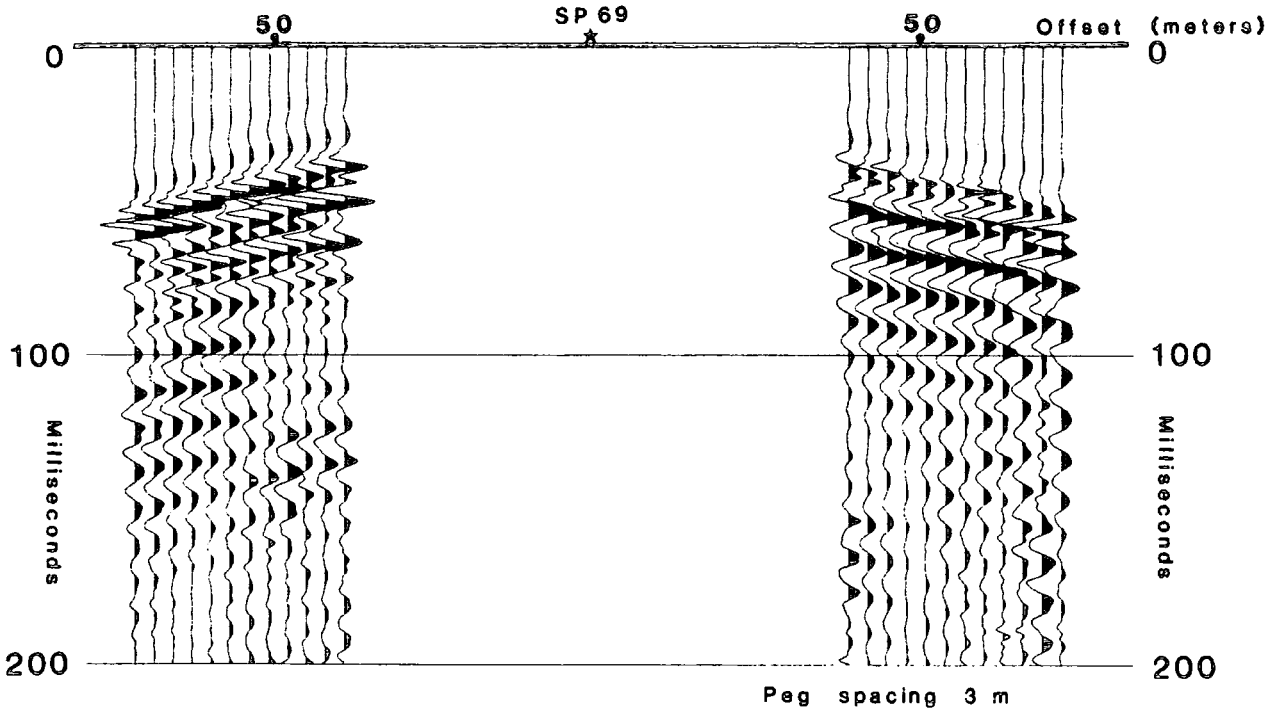

Band pass 55/85/300/400

Figure 6.6

Hemscott North Line 6

Common shot gather

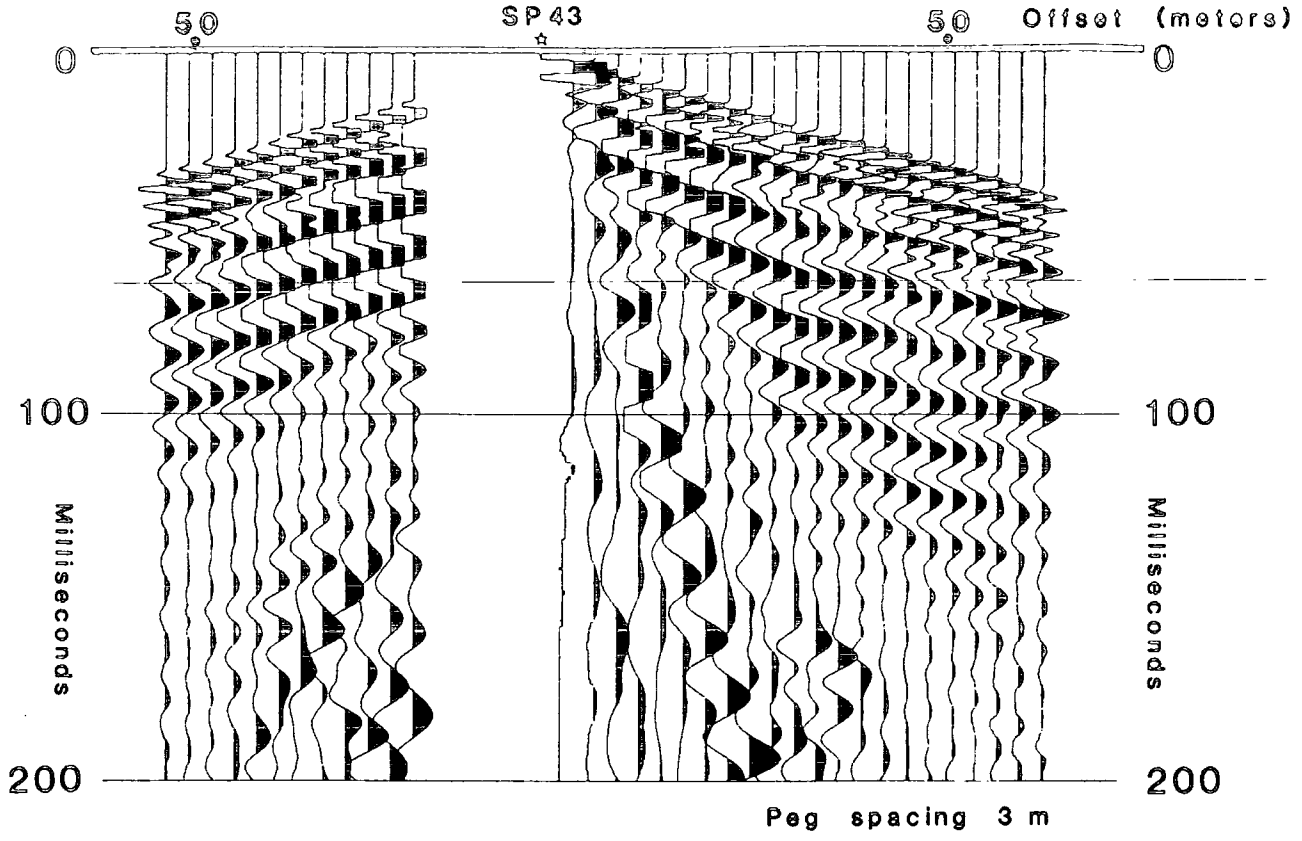

Editing & Band pass filtering

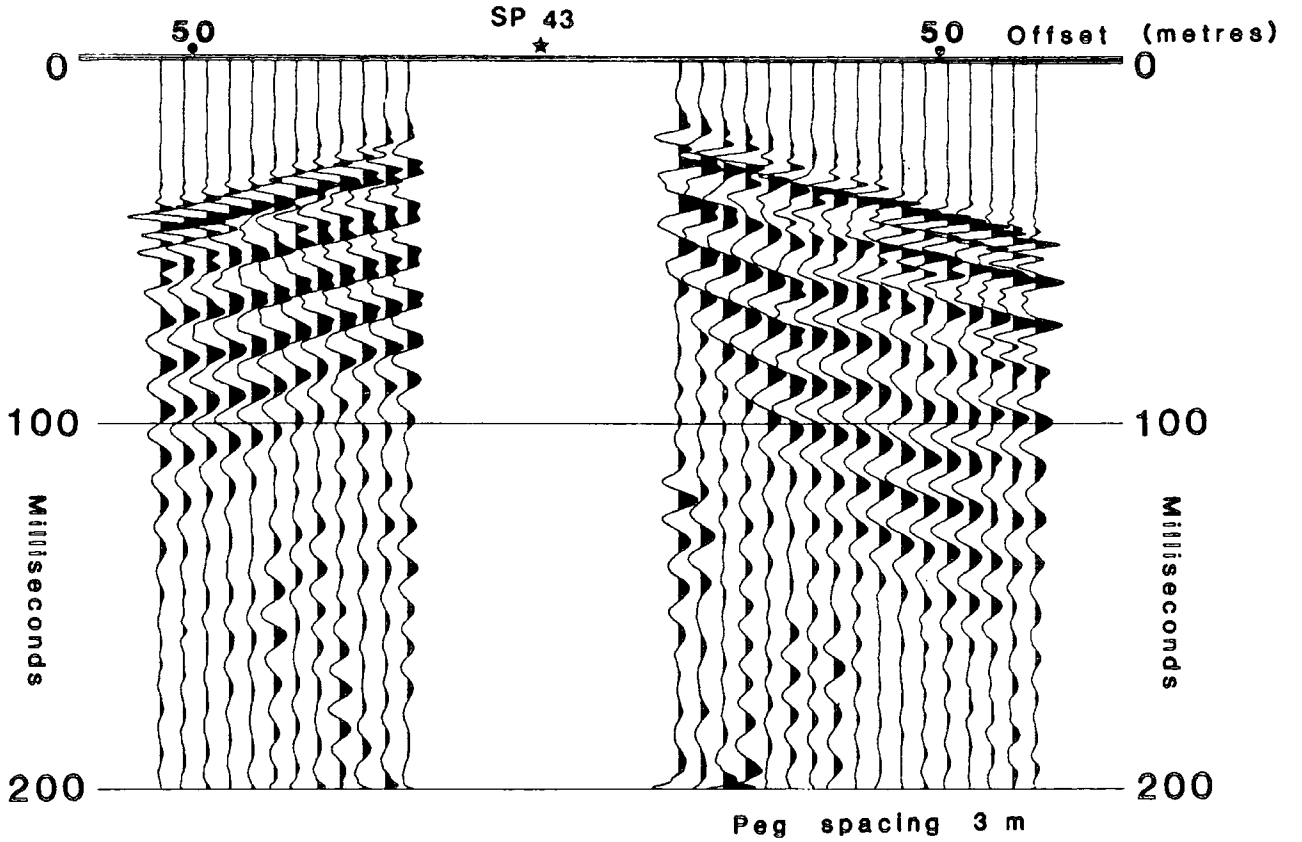

Band Pass 55/85/300/400

Figure 6.7

Traces with offsets of zero to 12m were edited out before sorting due to trace clipping. Figure 6.7 also displays the CSG after editing and band pass filtering. The acquisition geometry results in a CMP fold of cover alternating between 4 and 5 along the seismic line.

Data Processing

There was a long delay between the acquisition of the field data in 1982, and the data processing at Durham, due to the fact that the software required to process the seismic reflection data at Durham had not yet been written at that time. Initial brute stacks of line 1 were processed by Digicon on contract to NCB (deep mines). The sections that were produced are shown in figure 6.8. From these initial sections it is clear that there is a marked improvement in the quality for the deep shot holes. Although the data quality of both lines is not good, the fault zone can be clearly identified.

The first stages of data processing carried out on these data sets at Durham were trace editing, the application of the field static corrections and the muting of refraction events. The static corrections have previously been outlined for individual seismic lines. The data were then sorted into CMP gathers, the fold of cover of each line being a function of the acquisition geometry. By far the most crucial factor in the processing sequence of this shallow land reflection data is the application of a band pass frequency filter. The application of the optimum filter can effectively remove unwanted ground roll and high frequency noise. Three techniques are employed to determine the

HEMSCOTT NORTH LINE 1 (N.C.B. Processing)

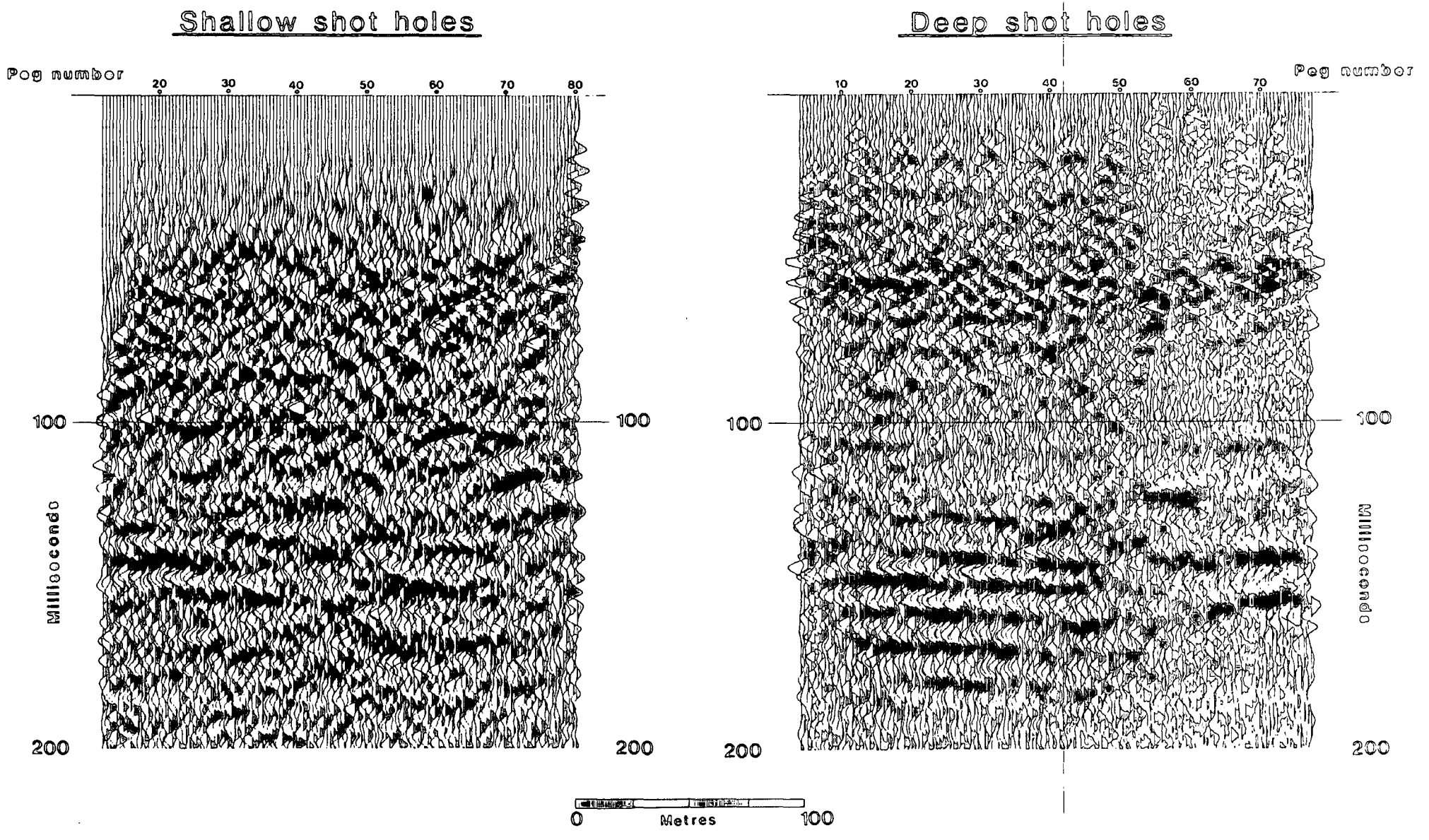

Figure 6.8

correct filter coefficients for each individual line.

Traces are analysed using Fourier analysis to determine the peak frequencies of the ground roll and reflected events. Figure 6.9 displays the results of this technique as applied to traces from line 1 (deep). Peak frequencies of 30 and 70Hz are calculated for the ground roll and reflected events.

A variety of filters coefficients were applied to CSGs and the optimum filter was chosen by inspection of the results. Figure 6.4 displays how the application of an optimum filter enhances reflections on a CSG.

A variety of filter coefficients were also applied to the whole data set pre-stack, the data were then stacked. One is able to observe directly how specific filters affect the final section. Figure 6.10 displays the results of this technique on line 1 (deep). This method is a very time consuming technique and is only feasible when small data sets are involved.

The optimum band pass filter coefficients for lines 2 and 6 are 55/85/300/400Hz. Line 1 (shallow) filter coefficients are 40/70/300/400Hz. For line 1 (deep), because the source was deeply buried compared to other lines, there is a slight increase in the frequency content of the reflections. The optimum filter coefficients for this line accounted for this, being 70/100/300/400Hz.

The stacking velocities used for these data sets were based on velocities calculated from the refraction lines. The velocity

Hemscott North Line 1 (deep)

Amplitude spectra

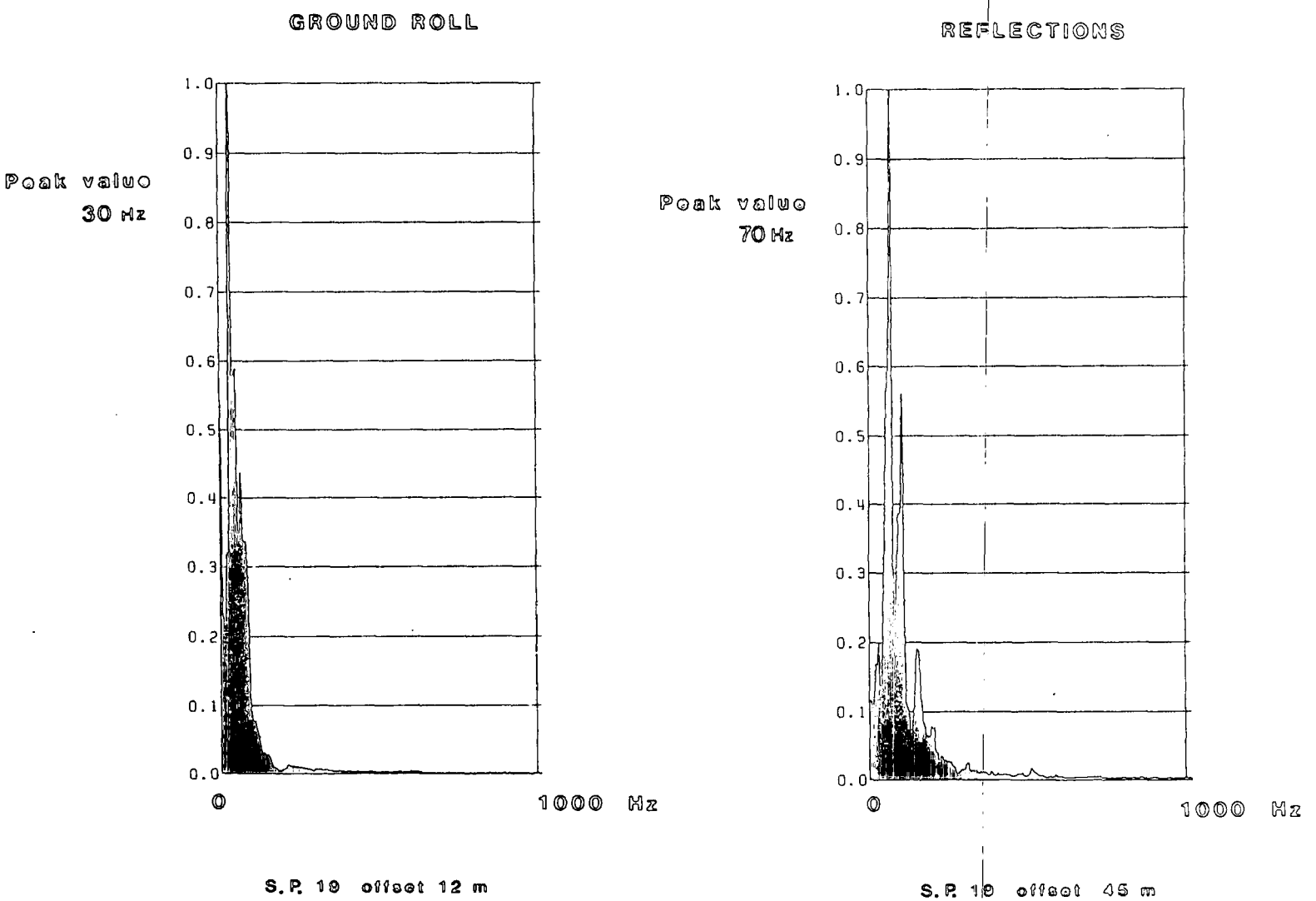

Figure 6.9

HEMSCOTT NORTH LINE 1 (DEEP SHOTS)

BAND PASS FILTER TRIALS

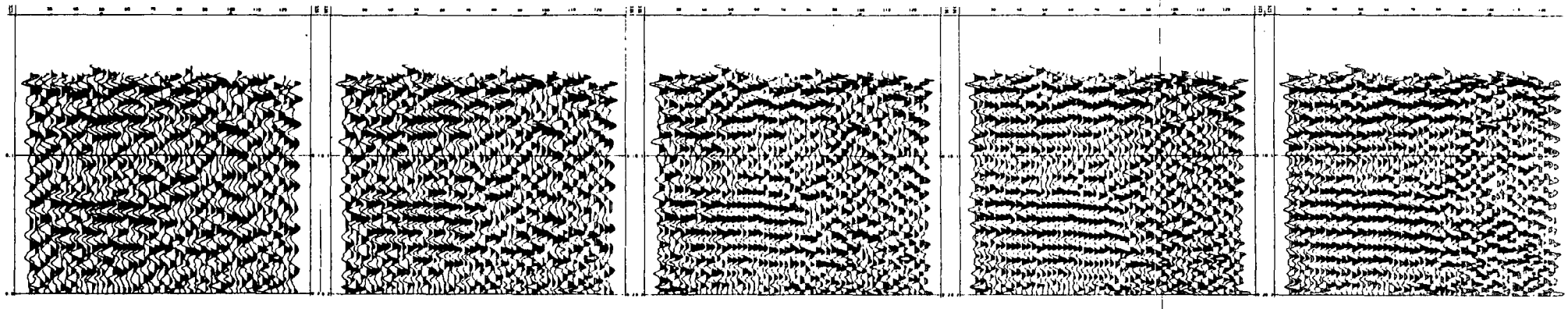

Figure 6.10

profile used was 1600m/sec (0-60msec), 1800 m/sec (60-200msecs) and 2800 m/sec (200msecs onwards).

A CMP aligned statics routine was applied to the data after the NMO correction had been applied before stacking. The static shifts that were applied to individual traces were constrained to a maximum shift of plus or minus 4msecs to avoid "cycle skipping". The routine worked by optimising the correlation of reflection events between 120 and 200msecs, where the strongest reflections occur. This accounted for any residual statics and small errors resulting from the NMO correction and any small geophone statics (less than 1msec). The data were then stacked and a 50msec AGC was applied to the traces before plotting. The final sections are reproduced as figures 6.11, 6.12, 6.13 and 6.14.

After the processing stage had been completed on all three lines, it was decided that the data quality of lines 2 and 6 were so poor that any interpretation of the final section would be questionable. The reason for the deterioration in data quality from line 1 (shallow) to lines 2 and 6 can be put down to effects at the source. The figure shows the drift thickness contours in the area of the survey lines. There is a significant increase in the drift thickness from line 1 (10 to 15m) to lines 6 (16 to 20m) and line 2 (15 to 25m). Therefore there is a direct correlation between the drift thickness and the deterioration in data quality. Although the seismic detonator is adequate for the penetration of a drift cover of 15m, the greater drift cover of lines 2 and 6 causes the greater attenuation of the seismic pulse. Thus the signal to noise ratio of the reflection events is significantly reduced. The attenuating nature of the drift is further increased

Hemscott North Line 1 (shallow)

Figure 6.11

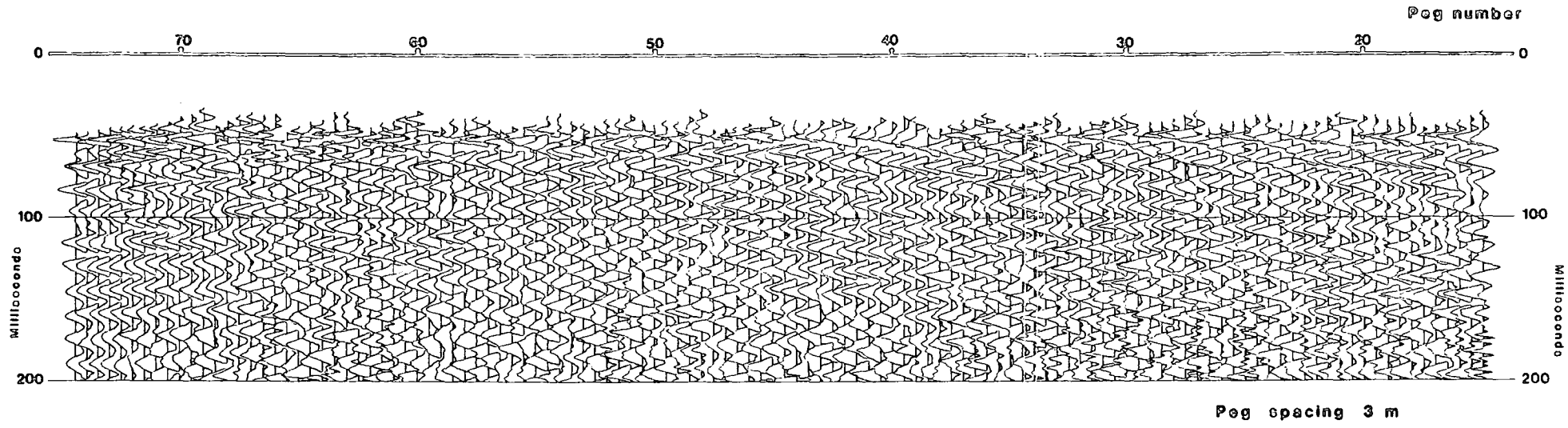

Hemscott North Line 1 (deep)

Figure 6.12

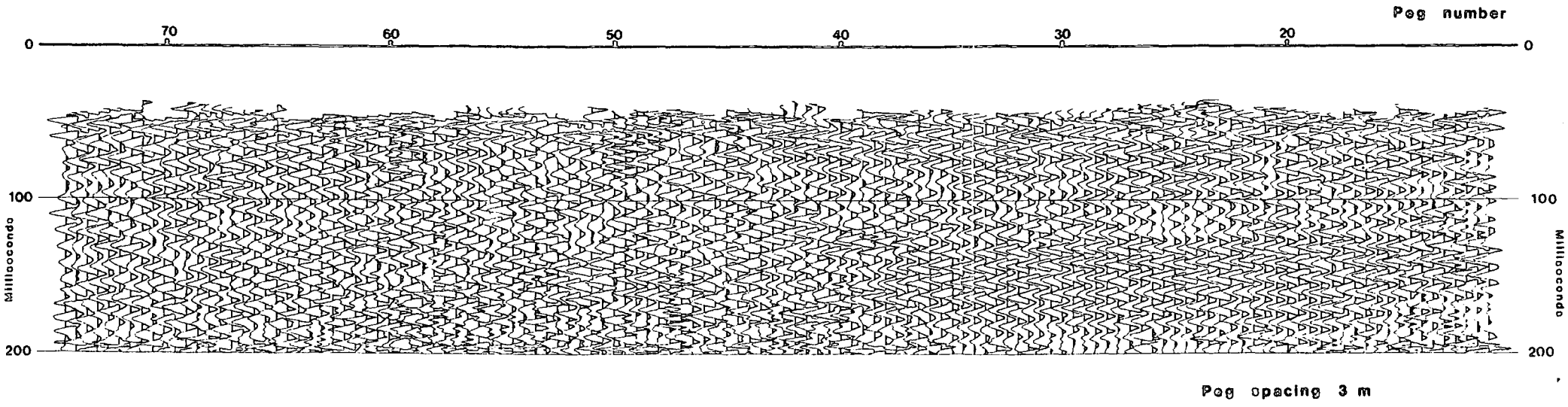

Figure 6.13

Hemscott North Line 2

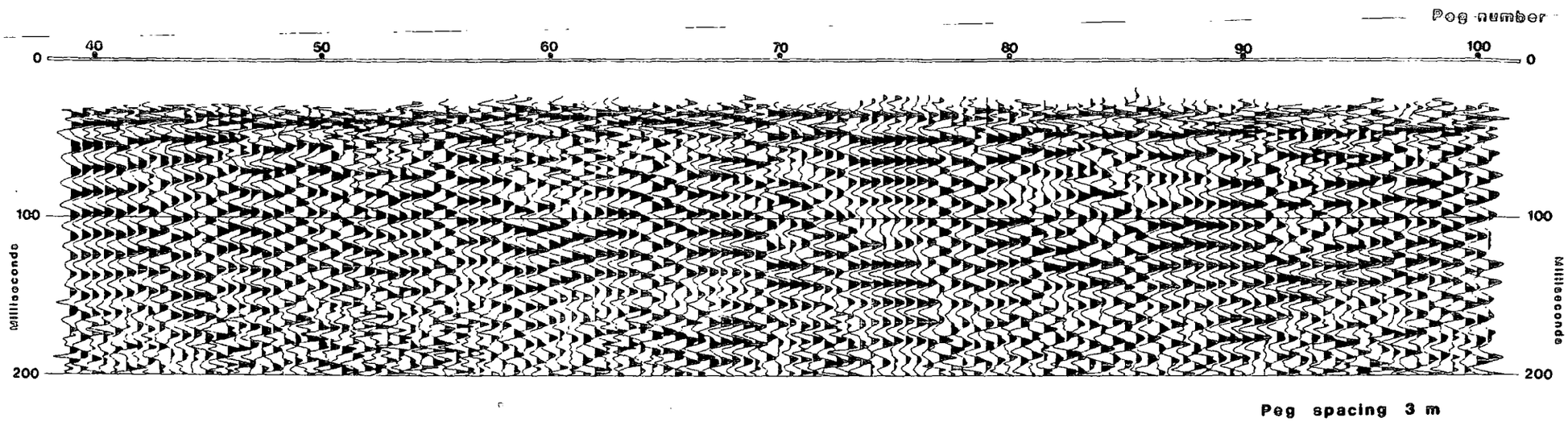

Figure 6.14

Hemscott North Line 6

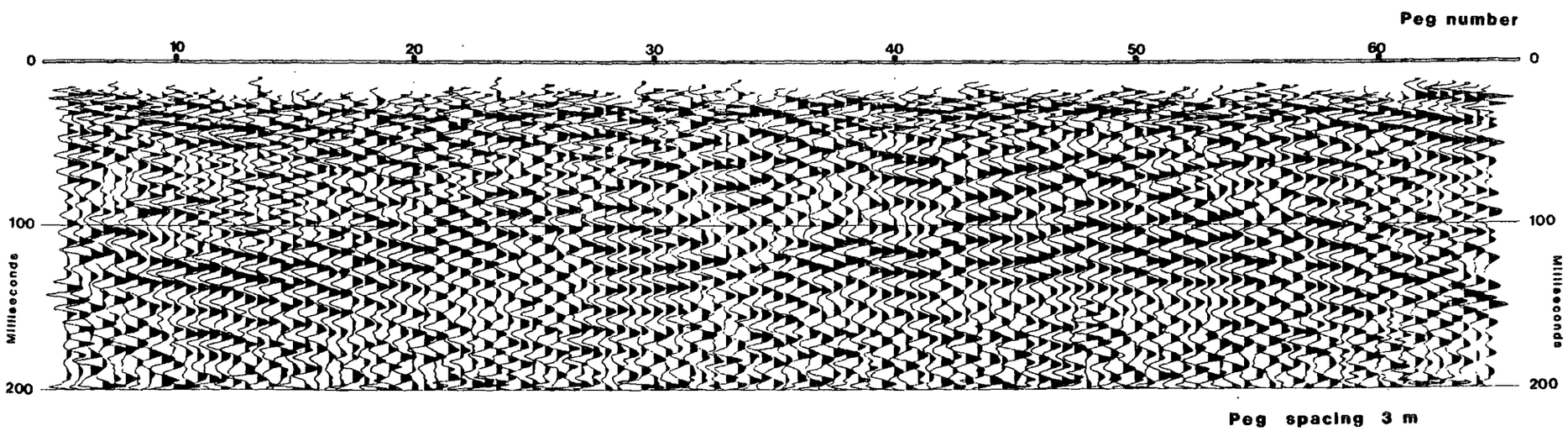

by the fact that the deeper drift has a sand base which is a highly attenuating medium. The philosophy of using a single detonator was that it produces a higher frequency seismic signature to a dynamite charge. It is unfortunate that line 1 was shot first, because the shooting parameters were set on the basis of this line.

Interpretation of the Reflection Data

The interpretation of the reflection data concentrates on line 1 due to the poor data quality of lines 2 and 6. The final seismic reflection sections suffer from the fact that the reflections show little character. This makes it impossible to correlate horizons each side of the fault zone. Where there is a consistent band of reflection events down the section, the ground is regarded as being unfaulted. A fault appears on the seismic section as a region of non-reflection separating areas of differing seismic character.

The line drawing of line 1 (figure 6.15) was produced by combining the results of both the deep and shallow data. Although the deep data is higher quality, the shallow data displays a more consistent band of reflectors at the southern end of the line. The interpretation of the NCB processed data is given in figure 6.16. Two separate faults are interpreted from the reflection data at pegs 48 and 64, with a possible third also present. The southern fault at peg 64 occurs 6m north of the postulated position of fault 3 interpreted from the borehole data. The northern fault coincides with the postulated position of fault 1. When the seismic lines were originally shot, the target was

thought to be a single fault. Only after subsequent drilling has the three fault model arisen. Unfortunately, therefore, the seismic line has not extended far enough southwards to completely cross fault 2 (figure 6.1). There is some evidence for the identification of fault 2 on the extreme southerly end of the shallow data in figure 6.16.

The major reflection events occur between 150 and 200msecs. Using a conversion velocity of 2600m/sec these times depth convert to between 180 and 240m. Comparing these depths with the generalized section of figure 6.1, the reflection horizons would appear to originate from the sandstone cycles between geological horizons T and U.

Considering the marked improvement in data quality found on line 1 using the deep shot holes, one could reasonably assume that had we exploded the detonator in rockhead or, better still below the weathering zone, further improvements in the reflection data quality could be achieved. But at Hemscott North where the drift cover varies from 10 to 25m, this would not have been economically viable for this survey. One could also have improved the data quality by increasing the power of the P wave source using gelignite on lines 2 and 6 in the areas of thick drift. As this was the first reflection data we ever shot, we had no previous experience of the data quality required on the field records to produce a quality final section.

HEMSCOTT NORTH

Interpretation of seismic line 1

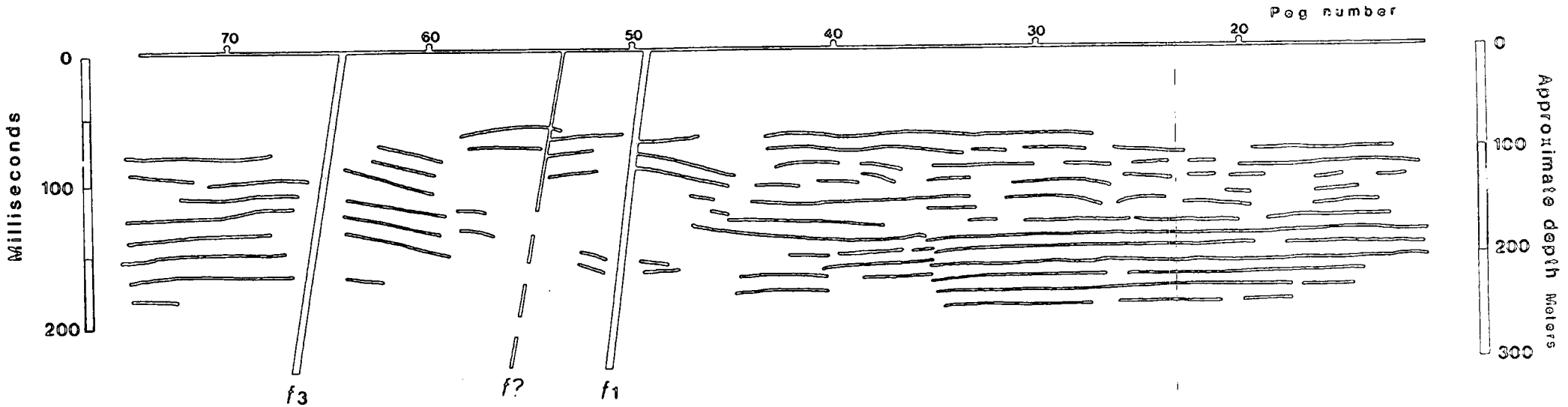

Figure 6.15

HEMSCOTT NORTH LINE 1 (N.C.B. Processing)

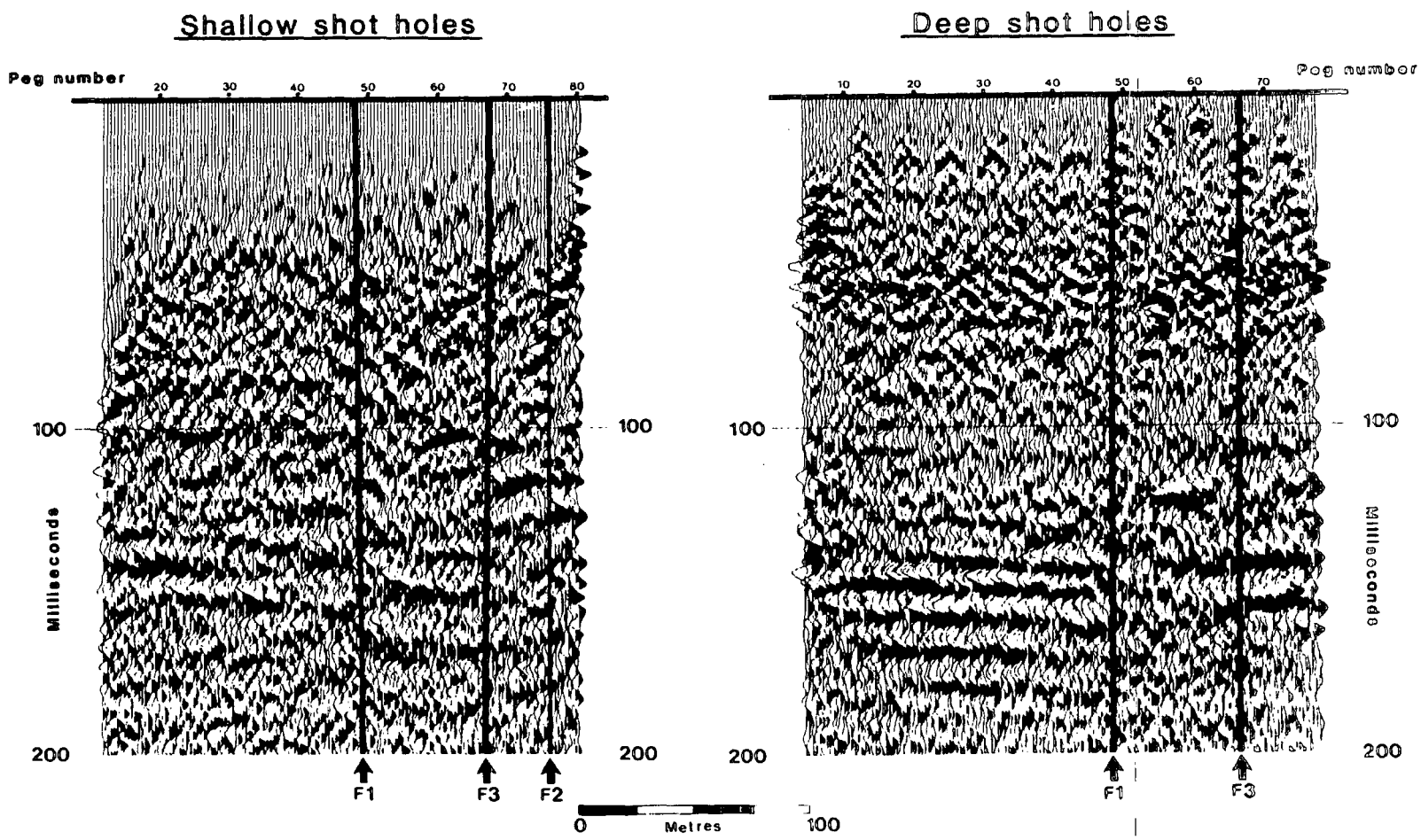

Figure 6.16

CHAPTER SEVEN

HIGH THORN : SITE NO. 4

High Thorn is situated on the coastal plain at Druridge Bay in eastern Northumberland. The site is 1.5km south west of the Hemscott North survey area, which was visited in the autumn of 1982, and is south of the Grange Moor Fault. The purpose of the seismic surveys at High Thorn was to use the P wave reflection technique over an area of old mine workings, to observe what effect the presence of the workings has on the reflection section. The intention was to see whether the technique can be useful in the determination of the position of the boundaries of old mine workings. An example of seismic reflection section recorded over an area of old mine workings by is displayed in Chapter 2 (Waters, 1979).

The High Thorn site is ideal for investigating the possibility of using the P wave reflection technique for this purpose. This is because at High Thorn, only one coal seam has been worked in the Carboniferous sequence. Therefore this makes interpretation of the results less difficult than if two or more seams have been worked vertically above each other. The Yard seam has been worked in a 2km square area at High Thorn (at a depth of approximately 55m below land surface) over the past century, firstly by the Ferney Beds Colliery (abandoned 1924), in the early 20th century, and secondly in the late 1960s by Ellington Colliery. The Ferney Beds Colliery used pillar and stall mining including where the pillars had also been removed by retreat mining (goaf). Ellington colliery on the other hand used the modern longwall panel mining

method. This situation is ideal for the purpose of our exercise, as a variety of ground conditions related to old mine workings can be investigated at this site.

When coal is extracted from an area by underground mining, the overlying strata naturally subside to fill the void created (plate 2). The effects of this subsidence may extend all the way to the surface if the workings are shallow. The area of subsidence extends upward from the edge of a mined area typically at an angle of 35 degrees with the vertical: this is known as the "angle of draw" (NCB, 1975 ; Ward, 1984). The collapse of the roof of the coal seam causes a zone of broken rock above the workings. The ability of the reflection technique to detect areas of mine workings, must be based on the fact that the zone of broken rock will exhibit a significantly lower and more variable seismic velocity than adjacent unworked areas. This effect will manifest itself on the final section by an increase in the reflection time to a particular horizon. Other effects such as static errors and areas of poor data quality due to the areas of broken rock may occur. If the workings are still intact and are air or water filled, then a large reflection coefficient will occur at this horizon, so the old workings will appear as a bright spot on the reflection section.

From information gathered from old and modern mine plans, and from exploration drilling by the Opencast Executive, a site plan showing the P wave reflection lines and the areas of old workings has been compiled with help from the site geologist (figure 7.1). The map represents all the information known about the underground layout. One cannot totally rely on old mine plans, especially

Plan of mine workings

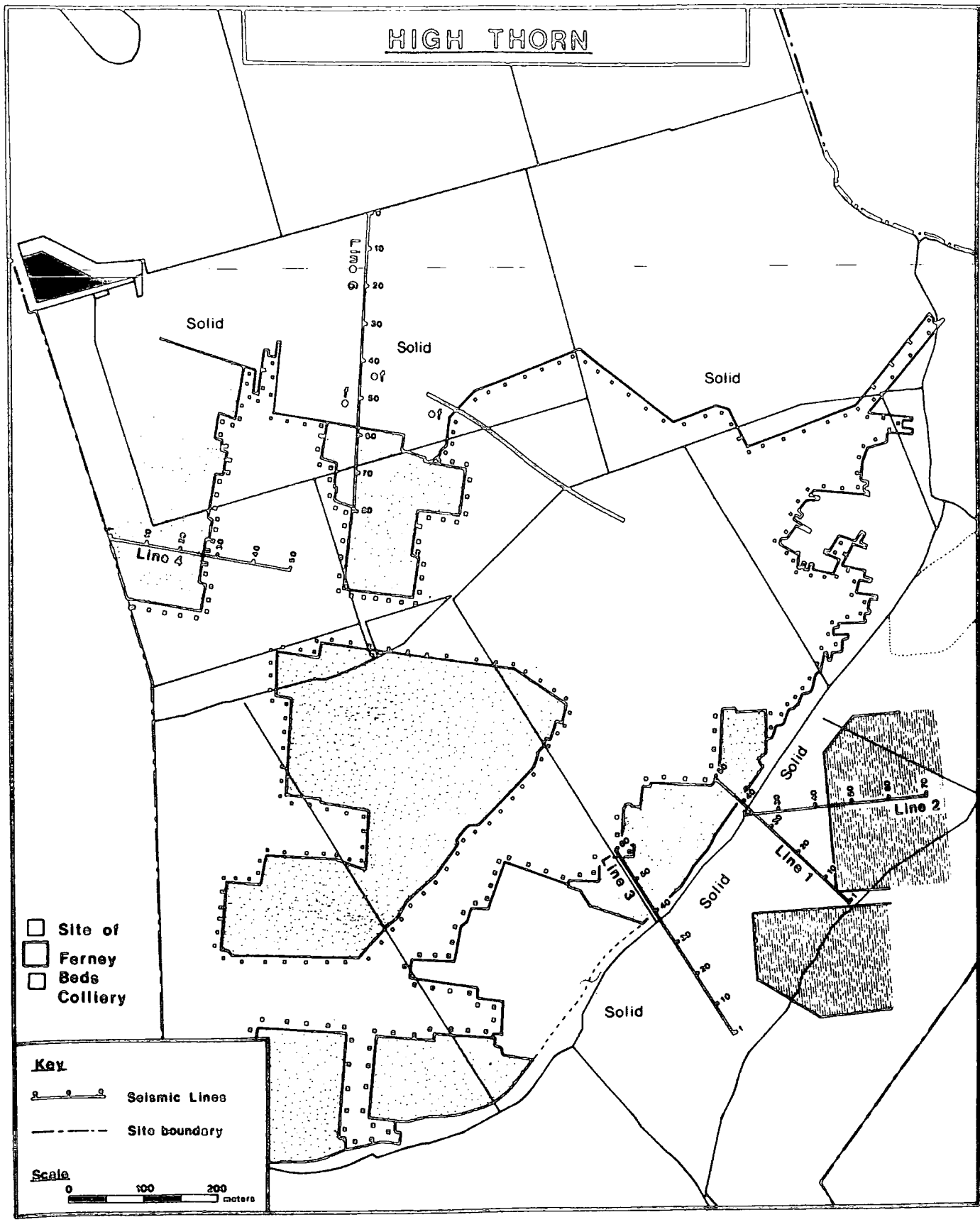

Fault on old mine plans

of - evidence of faulting

Mine Workings

Goaf

Pillars

Longwall Panel

Figure 7.1

where mining was supposed to terminate at a royalty boundary. The plan can be unreliable because it is not uncommon to find that the mining trespassed over the boundary. Also another factor in the exact positioning of the underground workings is the accuracy of the surveying techniques used at the time. Therefore the map must be used with some scepticism.

Data Acquisition

High Thorn was first visited in August 1984 in our last field season, when lines 1 to 4 were shot. Line 6 was the last profile to be shot by the seismic crew, at the end of September 1984. Five seismic lines were shot at High Thorn. Four of the lines were designed to cross over the proposed boundary between unworked and worked strata. Line 4 traversed a proposed boundary between an area of pillar and stall working and goaf (figure 7.1).

After the experience of using ordinary electrical detonators at Hemscott North, and the problems that were caused by the random time delays that they exhibited, seismic detonators were used throughout the surveys at High Thorn in conjunction with 1oz or 2oz gelignite charges, depending upon data quality tests employed on each line. The source was buried at a depth of 1.5m in the glacial drift overburden for all the surveys. A 5m peg spacing was used throughout the surveys.

Due to the effects of clipping of the near offset traces seen at Keekle, no frequency filters were used on recording throughout the surveys carried out at High Thorn. The reflection data was recorded for 500msecs (1024 samples at 0.5msec sampling interval)

on each of the lines.

Line 1

Line 1 is located in the south east of the survey area with the intention of crossing the boundary of the solid ground and an area of goaf (figure 7.1).

Line 1 was shot using a 5m peg spacing. In total 23 shots were taken between pegs 1 and 33, at a shot point interval of 10m. 17 shots were recorded using a 12 channels only, whilst six shot points (at the southern end of the line) had two shots taken from each of them, resulting in a pseudo 24 channel CSG. Shot to geophone offsets of 35 to 90m (12 channel CSG), and 35 to 150m (24 channel CSG) were employed. The acquisition geometry results in a maximum CMP fold of cover of six.

Line 2

Line 2 was located with the intention of crossing the boundary between the unworked ground and the longwall panel from Ellington colliery. This seismic line also intersects line 1. In total 18 shot points were used for this survey, 9 shot points having been used with a single 12 channel spread, whilst 9 shot points in the centre of the line were recorded on two 12 channel spreads (producing a 24 channel CSG). Shot to geophone offsets of 35 to 90m (12 channel CSG) and 35 to 150m (24 channel CSG) were used in this survey. The acquisition geometry results in a maximum CMP fold of cover of six.

Line 3

Line 3 is also located in the south west of the site. As with Line 1, Line 3 was located with the intention of crossing the boundary between an area of unworked ground and an area of goaf from Ferney Beds Colliery. 18 shot points were used, with a 2 peg (10m) separation between them. For 12 shot points a 24 channel CSG was acquired, whilst for the northernmost 6 shot points only a 12 channel CSG was acquired. The shot to receiver distances are the same as previous lines. The maximum CMP fold of cover is six.

Line 4

Line 4 is located in the north west of the survey area and was designed to cross the boundary between areas of goaf and pillar and stall workings from Ferney Beds Colliery. 17 shot points were used in total (at a 10m shot interval). From each shot point a single 12 channel spread was recorded. The shot to geophone offset was increased from previous surveys, using a near geophone offset of 135m to a far geophone offset of 190m. This acquisition geometry results in a maximum CMP fold of cover of three for this seismic line.

Line 6

Line 6 was the last and most ambitious P wave reflection line shot at High Thorn. The seismic line was designed to start in an area of solid ground and continue southwards to cross into an area of goaf from Ferney Beds Colliery. The boundary marked on figure 7.1 was not taken to be totally reliable, so the seismic line was

started well away from the proposed boundary in anticipation of the boundary being further northward than indicated on the plan (figure 7.1).

The seismic line was laid out with a 5m peg spacing. In total 30 shot points were used on this survey. For the first 24 shot points, two geophone spreads were used, using two separate shots at the same location. Spread offsets used were 35 to 90m (near spread) and 95 to 150m (far spread). No geophone overlap between adjacent spreads was required due to the reliability of the seismic detonators. For the last six shot points only the near geophone spread was recorded. The result of this geometry is a maximum CMP fold of cover of six.

Data Processing

The first stage of the data processing sequence carried out on the reflection data acquired at High Thorn was to sort the data into common shot gathers for each line. Band pass filter trials were then carried out on the CSGs to determine the optimum filter for each line. The process of determining the optimum band pass filter was aided by plotting amplitude spectra from particular seismic traces containing predominantly ground roll or reflections. The filter trials were carried out individually for each seismic line and optimum filter coefficients for each line determined.

The first stage in the determination of static corrections on the High Thorn data was to observe that the first breaks in adjacent 12 channel geophone spreads in each CSG show alignment.

For all the data recorded at High Thorn only one 12 channel record displayed a large time shift relative to another record in the same gather. This was probably due to a defective detonator. A static shift was applied to this record to correct for the error. As all the shots at High Thorn were buried at 1.5m below the land surface, which is near horizontal over the survey area, no static corrections were needed to account for elevation changes.

The alignment of the first breaks on each complete CSG was inspected to see if any significant systematic time shifts off a constant velocity could be observed on the first breaks. This method of geophone static calculation is hampered on the High Thorn field records, as two distinct arrivals are observed on the first breaks. But by observing the deepest refracted arrival, (which comes from a depth of 30m), no significant deviations from a straight line could be observed. Therefore no geophone statics were applied to the reflection data at High Thorn.

From the CSGs compiled for each seismic line, offset dependent mute functions were designed.

Some near offset traces contain large amplitude ground roll arrivals which have saturated the A/D converter of the Nimbus recorder. The resultant effect is to square off the traces. Later stages of processing on clipped traces will introduce unwanted noise into the final section. Therefore all traces displaying clipping were removed.

Line 1

Figure 7.2 displays a typical common shot gather from line 1 as recorded in the field, and the same CSG is shown after some initial processing has been applied. An optimum band pass filter of 35/50/90/105Hz was chosen for line 1 based on examination of amplitude spectra. Near offset traces (35m, 45m and 50m) are edited out of the data set due to clipping.

A feature of the data recorded at High Thorn is the high frequency, low velocity air wave which can be seen on each CSG. Even though the shot holes were well tamped with water to minimise the air wave, it is noticeable that even after band pass filtering has been applied to the data, the air wave is not removed. Therefore the air wave must contain frequency components which are equal to the frequency components of the reflected arrivals. Below 300msecs on the records, the air wave amplitude is significantly larger than the low amplitude reflections arriving at the same time. This causes the final reflection section between 300 and 500msecs to have a low signal/noise ratio.

Line 2

Figure 7.3 displays a common shot gather from line 3, before and after band pass filtering, muting and trace editing have been applied. An optimum band pass filter of 35/50/150/250/Hz was applied to the CSG. The mute and trace editing parameters are the same as line 1. Typical amplitude spectra from this line are shown in figure 7.4. The ground roll exhibits a typical peak frequency of 22Hz, whilst the reflected events have a peak

frequency of around 60Hz.

Line 3

Figure 7.5 displays a typical common shot gather recorded on line 3. The optimum band pass filter coefficients used on this line are 35/50/90/105Hz, whilst the mute and editing parameters are the same as previous lines.

Figure 7.6 displays amplitude spectra of records obtained on line 3. The main spectrum displays three major peaks. The first peak at 15 to 20Hz, corresponds to the low frequency window of the ground roll arrivals. The broad peak between 35 and 90Hz corresponds to the band of frequencies which contain the reflected arrivals, whilst the peak at 115Hz is the peak frequency of the air wave. Although it is impossible to completely isolate the air wave from the reflection arrivals on a seismic trace, the subsidiary amplitude spectrum is constructed from a portion of a trace where only the air wave is apparent shows that the air wave contains frequency components within the bandwidth of the reflected arrivals. Hence it is impossible to completely remove the air wave by frequency filtering without impairing the reflected arrivals.

Line 4

The acquisition parameters for line 4 are different from other lines recorded at High Thorn. The shot geophone offsets used to record the data are much greater than other lines. The reason for this was to record data outside the cone of ground roll which has

a velocity of 260m/sec as seen on previous lines. This was carried out primarily to see whether it would make any significant improvement to the final section. The problem with this method is that the raypath length of the seismic wave is increased, so more attenuation of the seismic pulse must occur. This can have a significant effect on the signal to noise ratio of the recorded reflections. Figure 7.7 displays a typical CSG from line 4, before and after initial processing had been carried out. It is apparent from the raw field data that no ground roll was recorded. Data quality is poor below 300msecs. The air wave is not noticeable until 400msecs on the field records, due to the increase in the trace offsets. A band pass filter was applied to the CSG in an attempt to remove low and high frequency unwanted noise.

Line 6

Figure 7.8 displays a typical CSG recorded on line 6. The data quality of the records from line 6 is better than previous lines at High Thorn. This is apparent from the raw field record (figure 7.8), where strong reflected events are clearly displayed between 150 and 250msecs.

An optimum band pass filter of 40/50/150/250Hz was applied to the data to remove the low frequency ground roll. Traces with offsets of 35 to 50m were removed at this stage, due to the introduction of unwanted noise by trace clipping. The result of the editing is that one trace is removed from each CMP gather, thus reducing the maximum fold of cover from six to five.

Figure 7.9 displays a typical amplitude spectrum obtained from the gather in figure 7.8. Figure 7.9 shows a ground roll peak frequency of 24Hz with the reflection events having frequency components between 35 and 65Hz.

After the initial trials had been completed on CSGs from each of the seismic lines, to determine band pass filters and mute functions, the edited data were then sorted into common mid point gathers, so that further processing could be carried out to produce a final seismic section for each line.

Before the final sections could be produced a value for the stacking velocity was required for the NMO correction. Figure 7.10 displays velocity panels from line 6. The panels are produced by applying the optimum band pass filter pre-stack and using an arbitrary stacking velocity in the NMO correction then stacking the traces. The optimum stacking velocity function was chosen on the basis of the best final stack. This process was carried out on each seismic line in regions of each line where data quality is known to be good.

It is apparent from figure 7.10, that by increasing the stacking velocity from 1600 to 2000m/sec a significant improvement can be seen in the final stack. Increasing the velocity value in the stacking velocity beyond 2200m/sec makes very little difference to the panel. This is due to the very small amount of moveout seen on the records (due to the relatively small range of offsets used). By observing the reflections around 200msecs on figure 7.8, it can be seen that the total moveout of the

High Thorn Line 1

Common Shot Gather

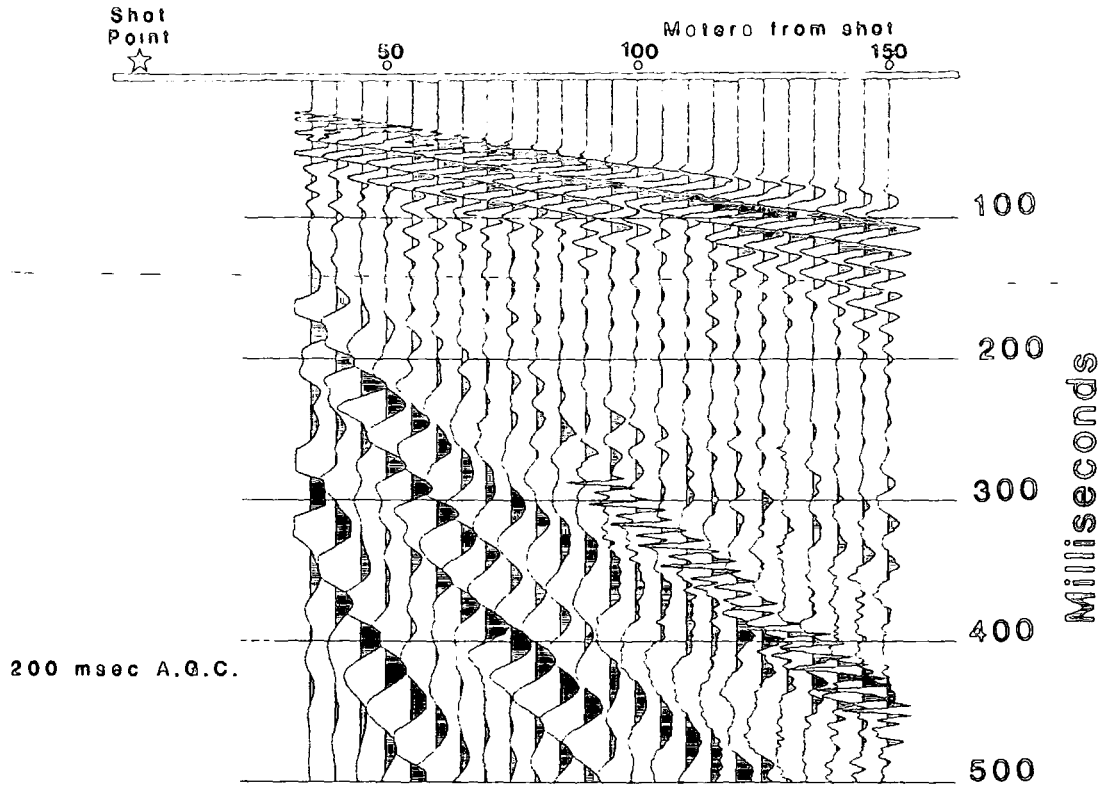

Data after editing, muting & frequency filtering

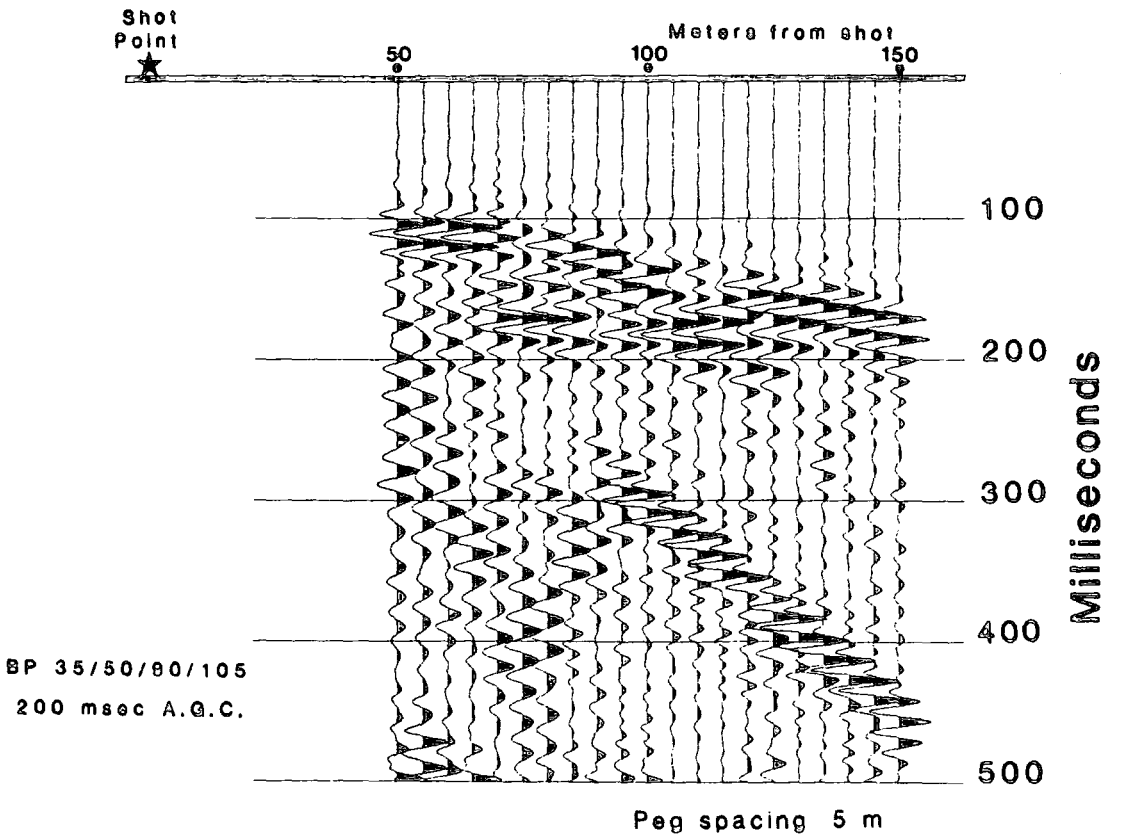

Figure 7.2

High Thorn Line 2

Common Shot Gather

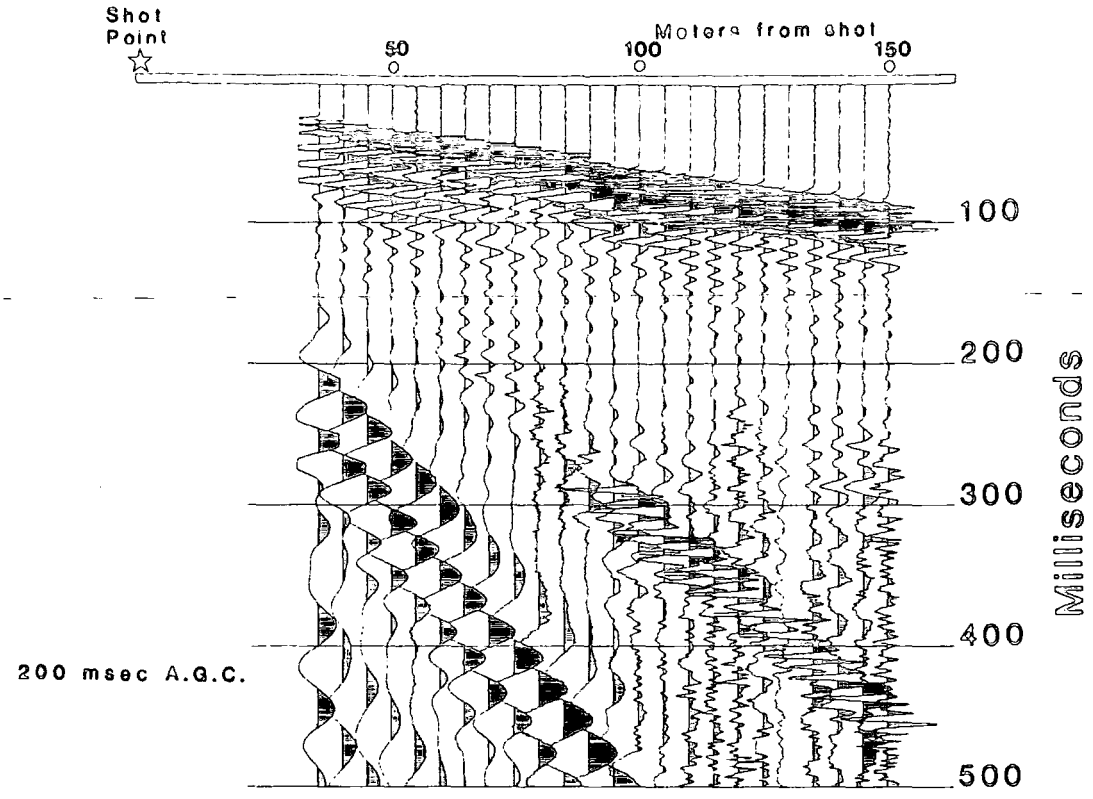

Data after editing, muting & frequency filtering

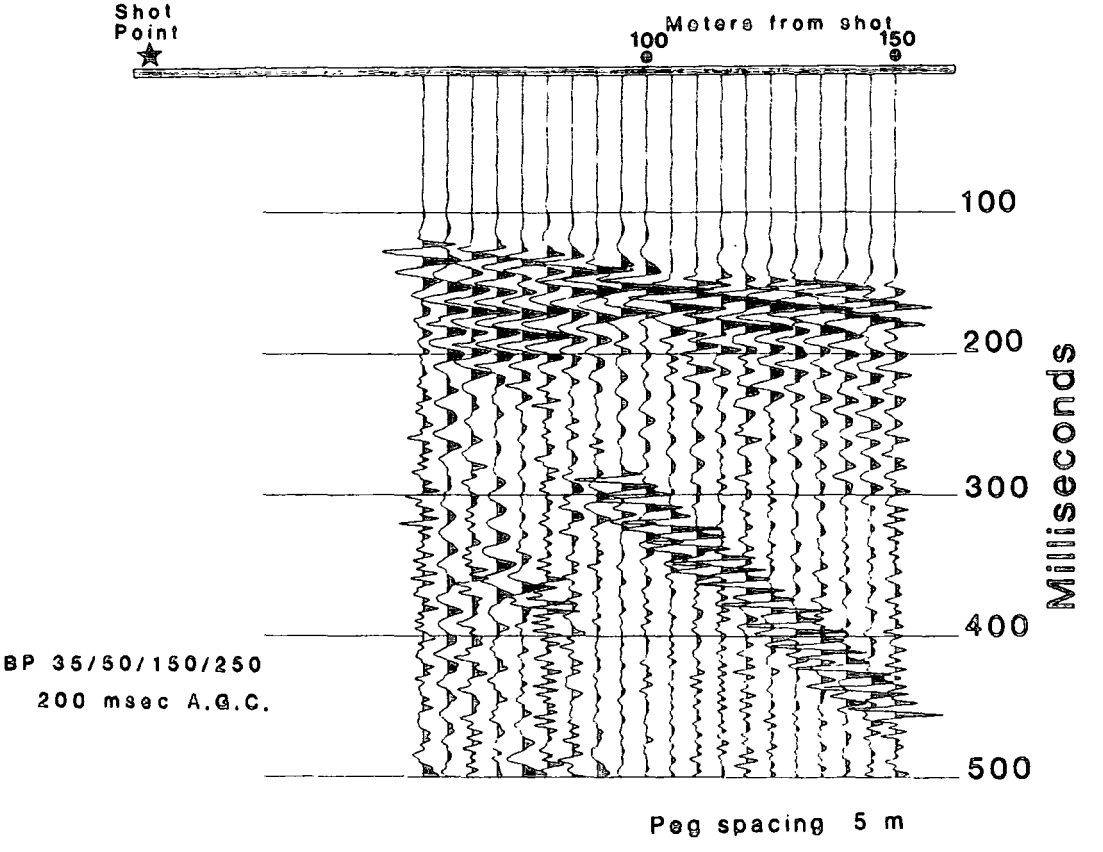

Figure 7.3

High Thorn Reflection data

Amplitude Spectra

Line 2

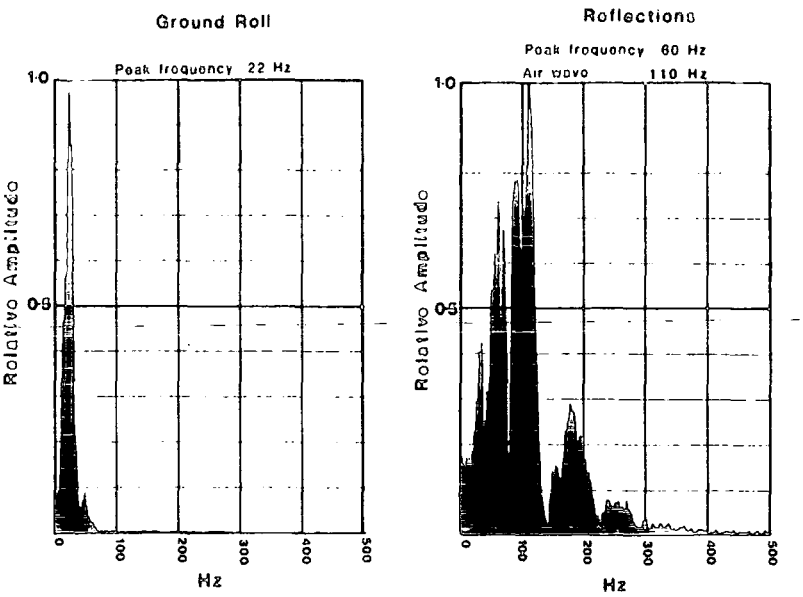

Figure 7.4

Line 3

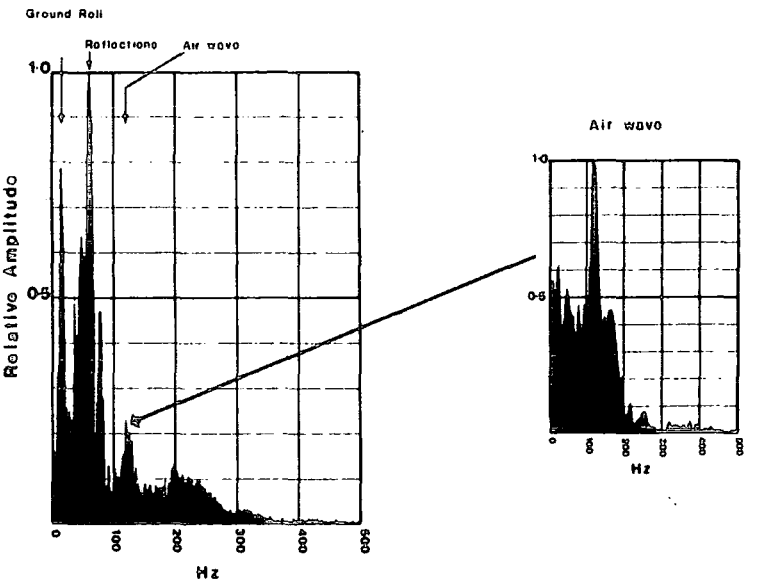

Figure 7.6

Line 6

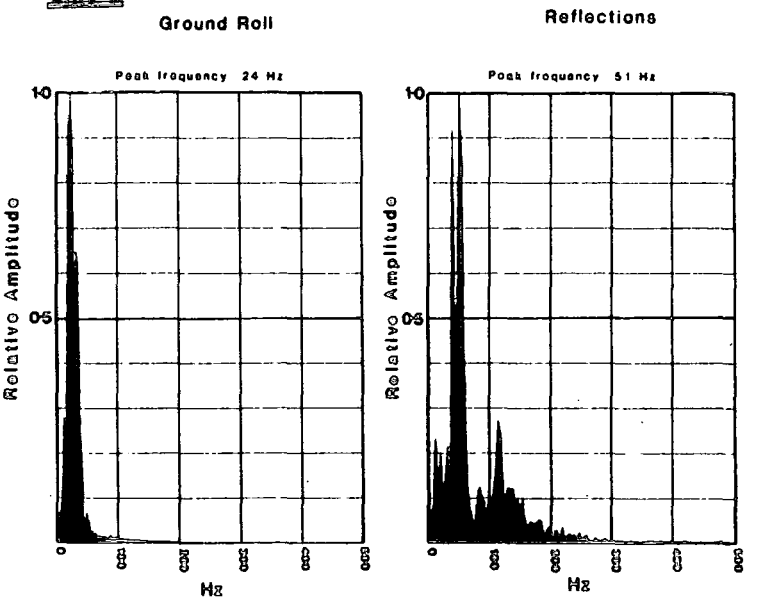

Figure 7.9

High Thorn Line 3

Common Shot Gather

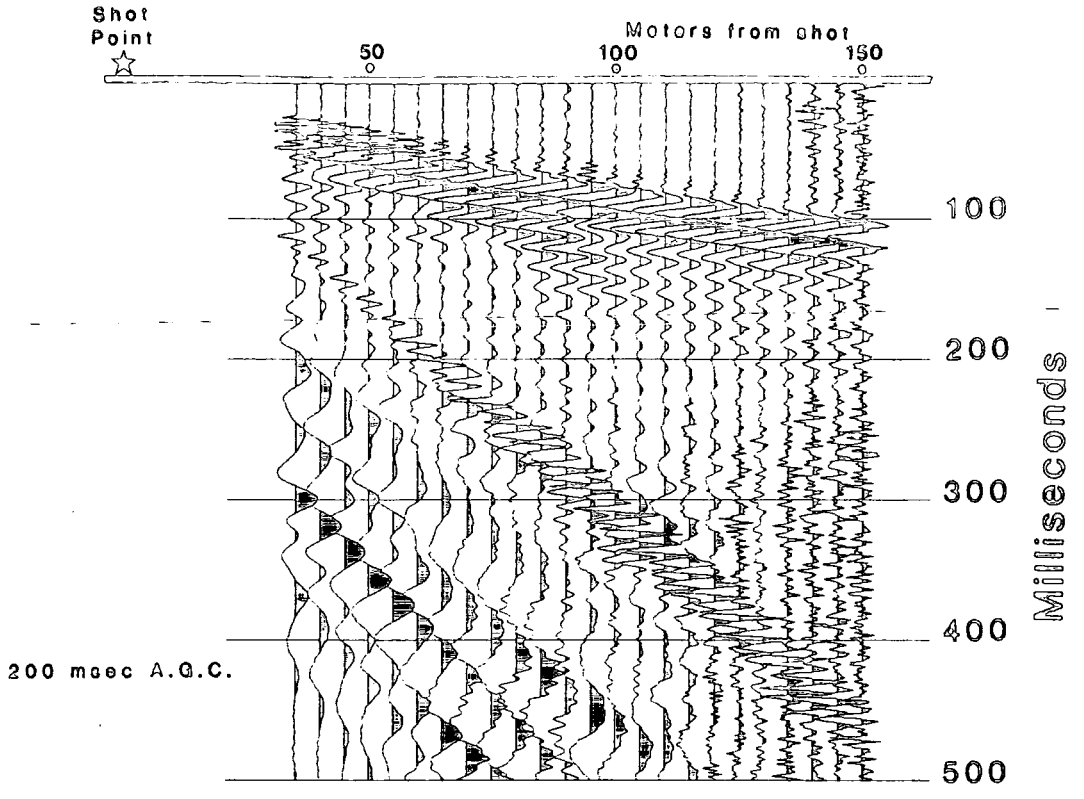

Data after editing, muting & frequency filtering

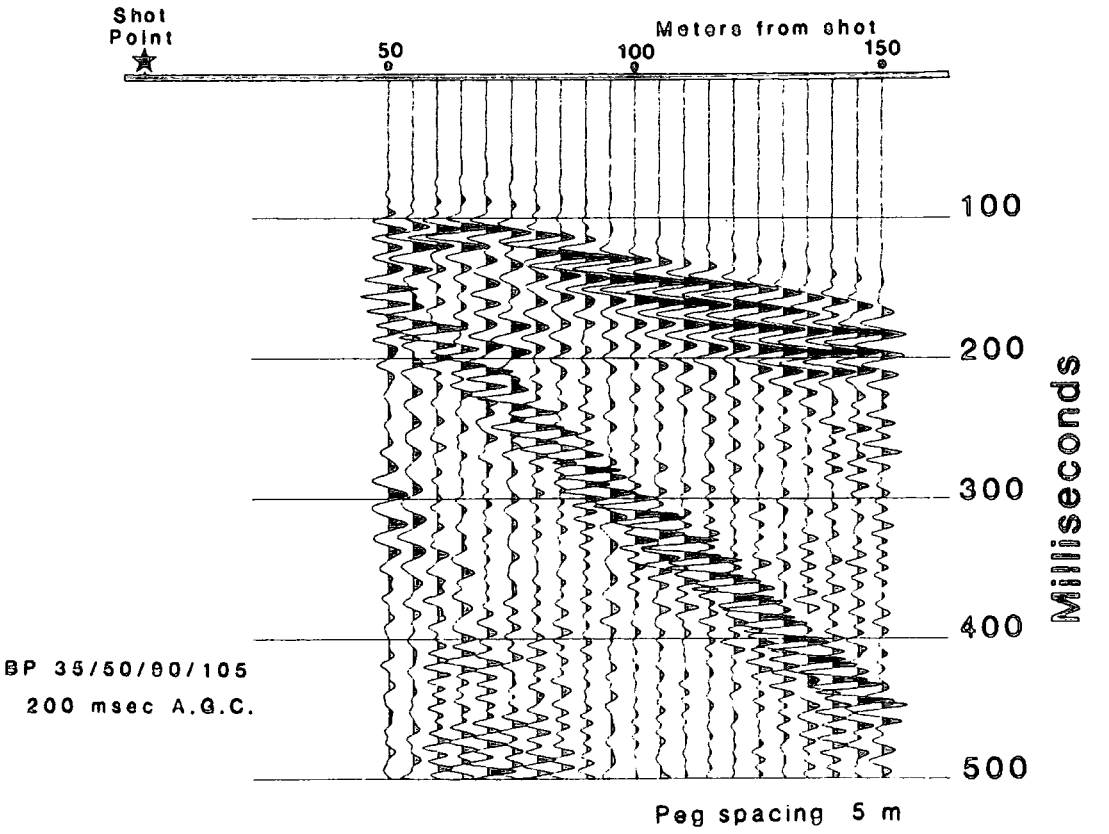

Figure 7.5

High Thorn Line 4

Common Shot Gather

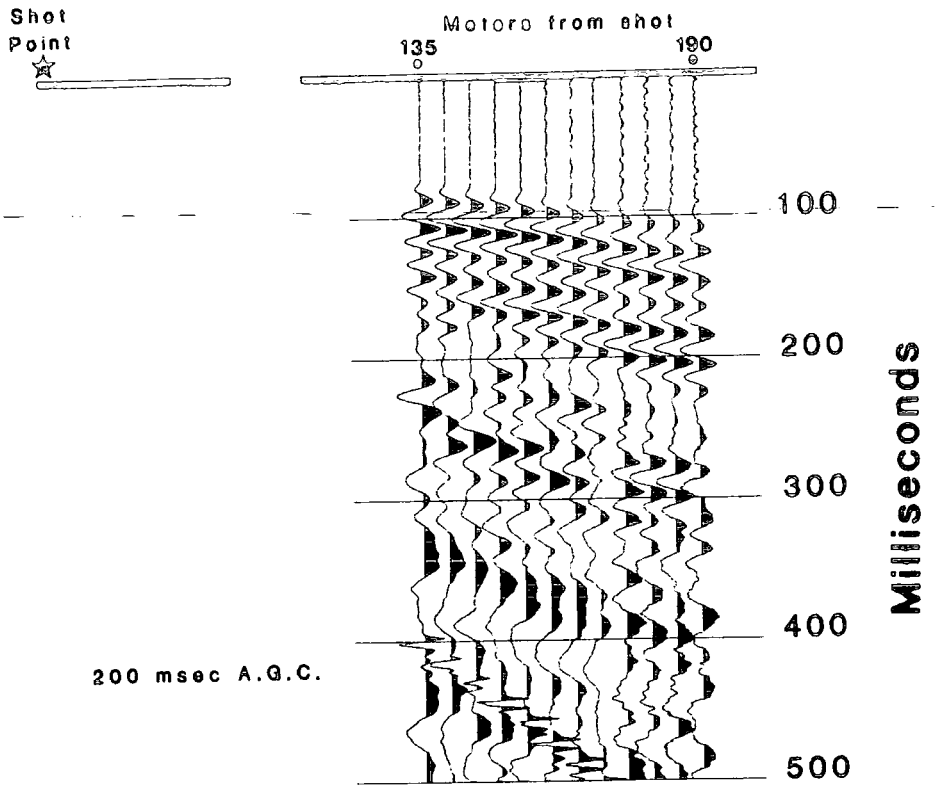

Data after editing, muting & frequency filtering

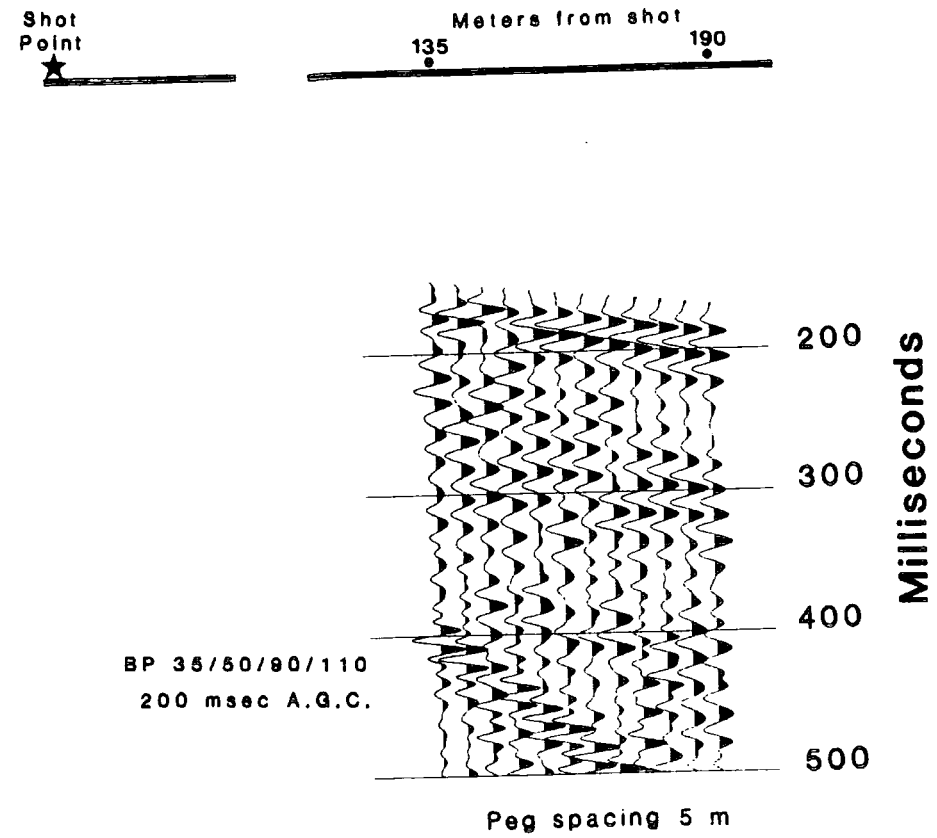

Figure 7.7

High Thorn Line 6

Shot point 9

Common Shot Gather

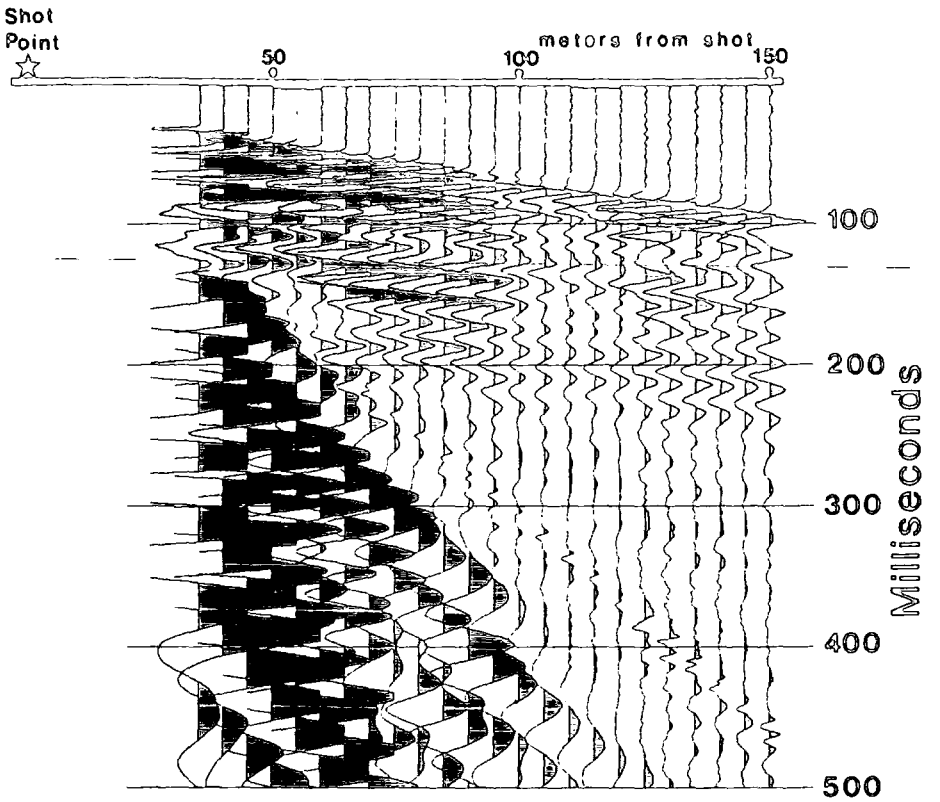

Data after editing, muting & frequency filtering

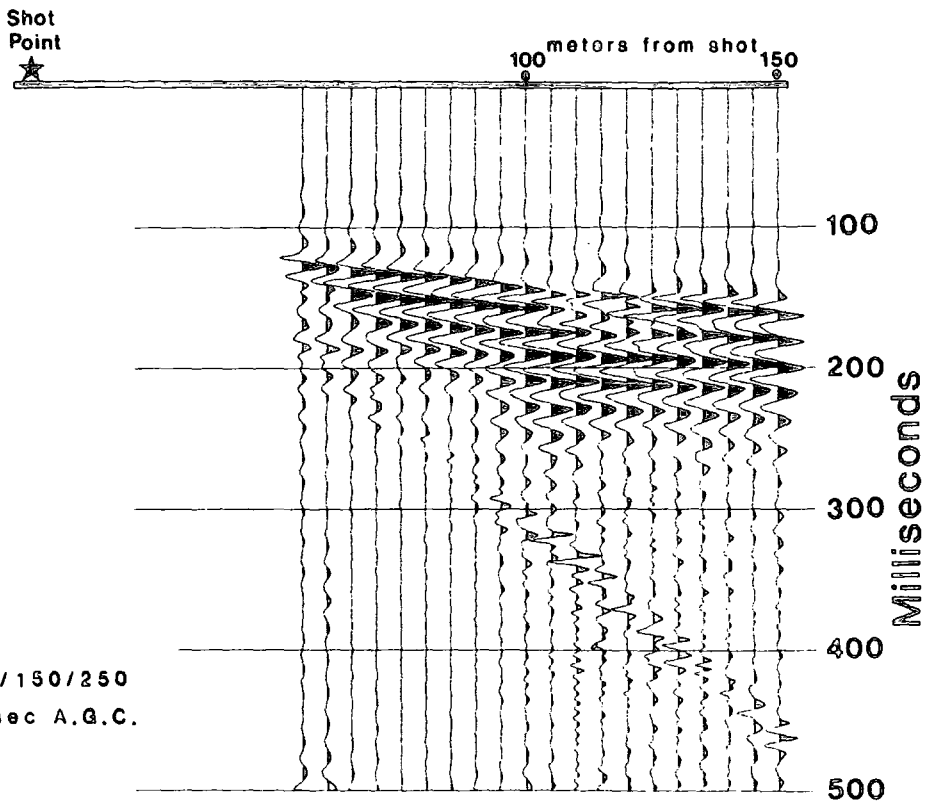

BP 40/50/150/250
200 msec A.G.C.

Peg spacing 5 m

Figure 7.8

High Thorne Line 6

Velocity panels

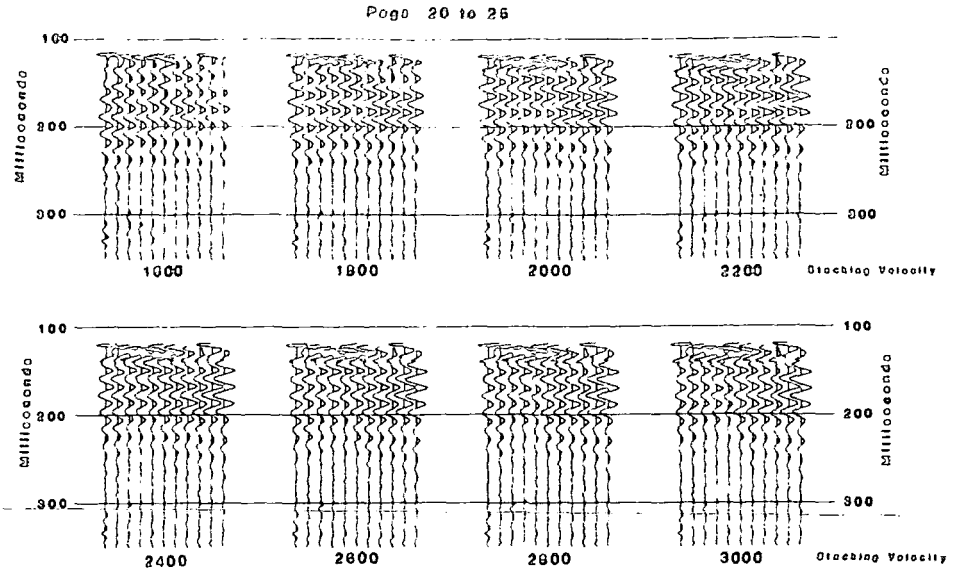

High Thorn Line 6

Velocity panels

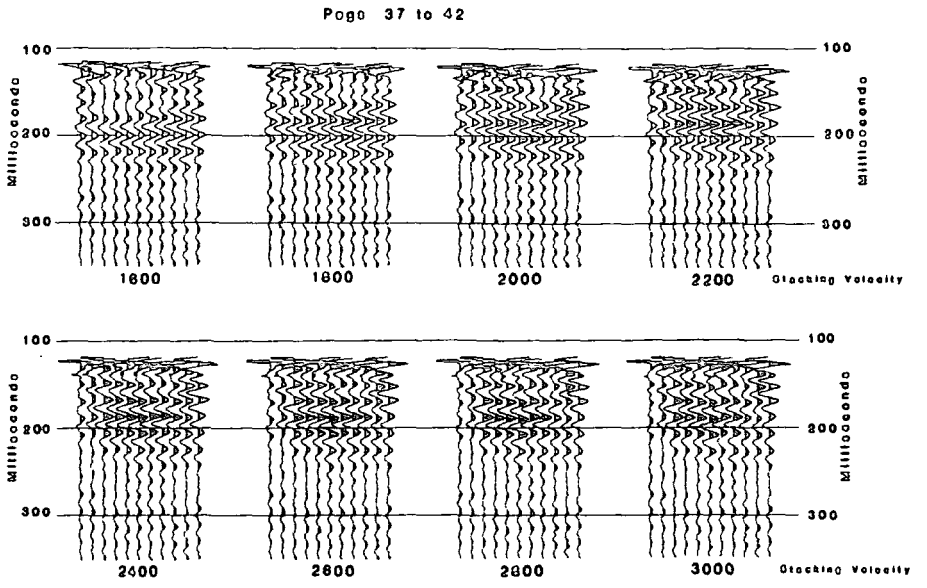

High Thorn Lin: 6

Velocity Panels

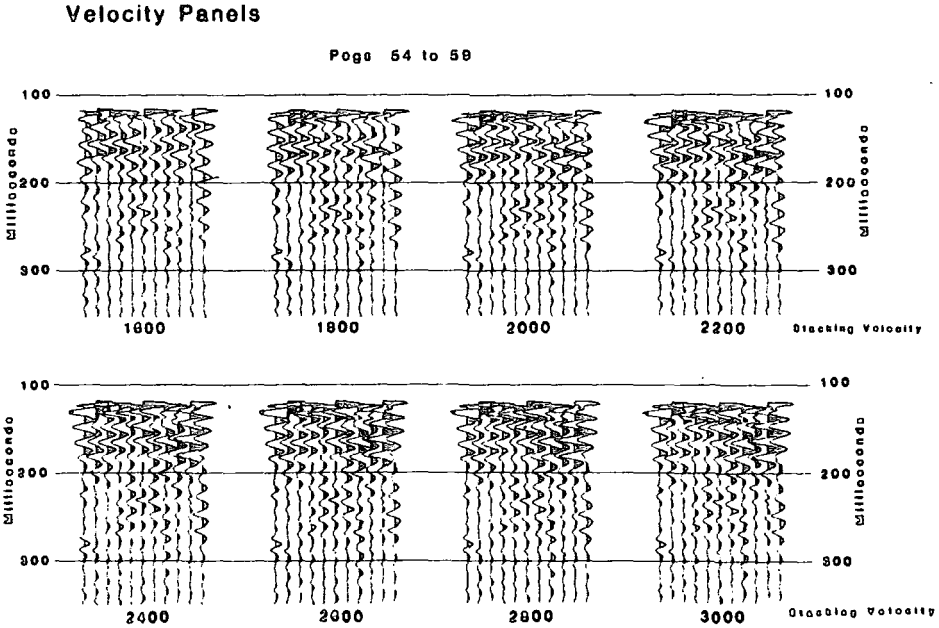

Figure 7.10

reflections is less than 10msecs over a distance of 100m.

Results

As the boundary between unworked and worked strata may be marked by an increase in static effects on the final section, for lines 1,2,3 and 6 two final stacked sections with and without the CMP aligned statics routine included in the processing sequence, are plotted. By comparing the two sections, the areas exhibiting static effects can be distinguished.

Line 1

The final stacked sections for line 1 are shown in figure 7.11. Both sections show a two leg reflection event, at a two way traveltime of between 170 and 200msecs. On section B, with the CMP aligned statics routine used, the amplitude of the reflection event relative to the background noise is improved upon. This is particularly true toward the higher peg numbers, indicating that there are some static errors present.

Between pegs 15 and 27 the reflection is almost horizontal. The traveltime of the reflection increases to a maximum value around peg 33. Beyond peg 33 the reflection event appears to be displaced toward a smaller value of traveltime. This feature is highlighted on figure 7.12 where only the largest positive amplitude peaks are plotted. The reflection event around 200msecs stands out as the single coherent event on the section.

Line 2

Figure 7.13 displays the final sections from line 2. As with line 1, which line 2 intersects, a reflection event is seen at a two way traveltime of around 180msecs. The sections from line 2 display more reflection energy than line 1, but the reflection events are laterally inconsistent.

The use of the CMP aligned statics routine in the processing sequence does improve the data quality but not by a significant amount. This result indicates that although there may be static errors present, they are of a small amplitude. The reflections are almost horizontal across the section, but are displaced in two areas around pegs 27 and 33. The data quality decreases toward the end of the line around peg 50, but this may only be due to a decrease in the fold of cover toward the end of the seismic section.

Line 3

Figure 7.14 displays the final sections produced from line 3. The data quality is poor compared to lines 1 and 2. The use of the CMP aligned statics routine does make an improvement to the data quality. The two features apparent on the sections are a reflection from around 180msecs between pegs 10 and 20, and a shallower reflection from around 125msecs between pegs 20 and 31. Between pegs 31 and 40 the data quality decreases and no coherent reflections can be seen.

Line 4

Line 4 was shot totally over an area of old workings, with a different field acquisition geometry to the other lines. Both sections displayed in figure 7.15 have the CMP aligned statics routine included in the processing sequence. Because all the reflection data were recorded outside the cone of ground roll, this allows the use of a wider frequency bandwidth into the lower frequencies than can be used on all other lines. Section B has the lower frequency content, which improves the data quality of the deeper reflections from around 300msecs.

The most significant event seen on line 4 is the band of reflections between 120 and 200msecs. These strong events appear horizontal between pegs 57 and 47, but increase in traveltime from peg 47 to peg 33. Beyond peg 33 they appear to die out.

Line 6

As figure 7.16 shows, line 6 displays the best data quality of all the seismic reflection lines recorded at High Thorn. Strong reflection events between 140 and 220msecs occur across the whole section.

Section A, without the CMP aligned statics routine included in the processing sequence, has patches of poor data quality notably around pegs 27,33 and 54. Section B with the CMP aligned statics routine included displays lateral consistency of the reflections. The areas of poor data seen on section A are now infilled. This indicates that these patches of poor data quality are due to

static effects impairing the stack of the CMP gathers at these locations.

Interpretations

Although all the sections recorded at High Thorn display clear reflections, except for line 6 the reflections show no lateral consistency. For the interpretation of the results from each line, a line drawing of the section is displayed vertically above a proposed geological cross-section constructed from available borehole information.

Line 1

Figure 7.17 shows the relationship of the seismic section to the proposed geology. The reflection events on line 1 originate from approximately 200 to 250m below the surface. This depth is well below the depth of the mine workings, being only 50m below ground level. No direct reflections off the worked seam can be imaged.

The band of near horizontal reflections between pegs 20 and 28 occur over an area of unworked ground. The increase in traveltime of the reflections between pegs 28 and 33 is consistent with a lowering of the seismic velocity of the near surface strata due to the cone of subsidence. The decrease in data quality beyond peg 34 may mark the area of pillar and stall working.

Line 2

Figure 7.18 displays the relationship of the seismic section of line 2 and the proposed cross-sectional geology. The section displays patches of reflections which are difficult to relate to the proposed geological cross-section. The decrease in the data quality beyond peg 48 may be a result of the longwall panel.

Line 3

As figure 7.19 shows, Line 3 exhibits a band of reflections between pegs 10 and 30 over the unworked strata. The reflections suddenly die out beyond peg 30, this point coinciding with the transition from unworked strata to goaf.

Line 4

Figure 7.20 shows a strong band of reflections from 100 to 200msecs, between pegs 57 and 33. These reflections depth convert to around 150 to 200m, well below the mining horizon at 50m depth. The reflections exhibit an apparent dip toward the lower peg numbers, and suddenly die out at peg 31. There is no evidence for a structural dip from the borehole information. The apparent dip must therefore be a velocity pull down feature related to the lowering of the seismic velocity of the near surface strata, due to mining induced subsidence. The point at which the reflections die out at peg 33 may mark the boundary between pillar and stall mining and goaf.

High Thorn Line 1

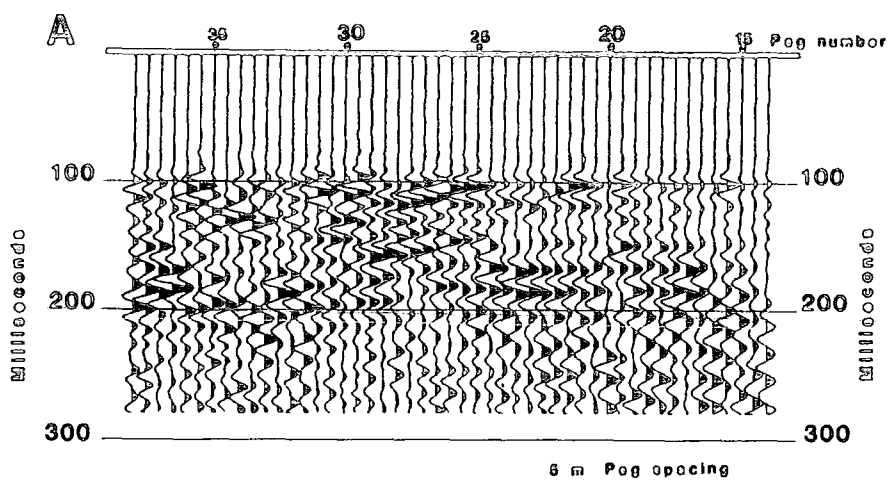

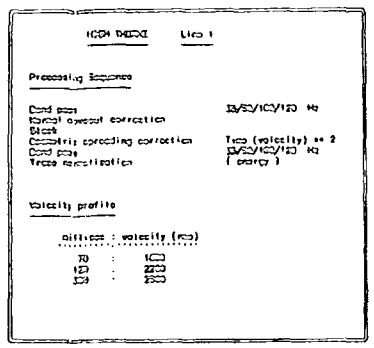

High Thorn Line 1

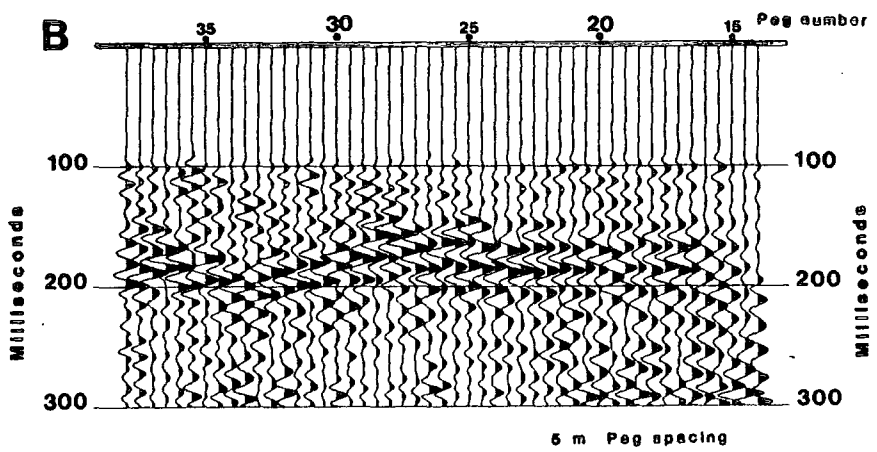

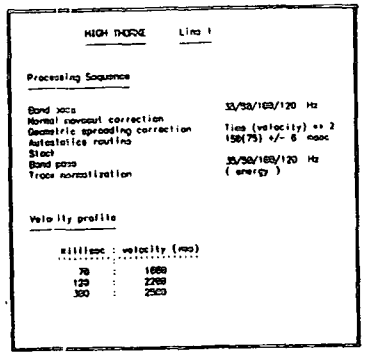

Figure 7.11

High Thorne Line 1

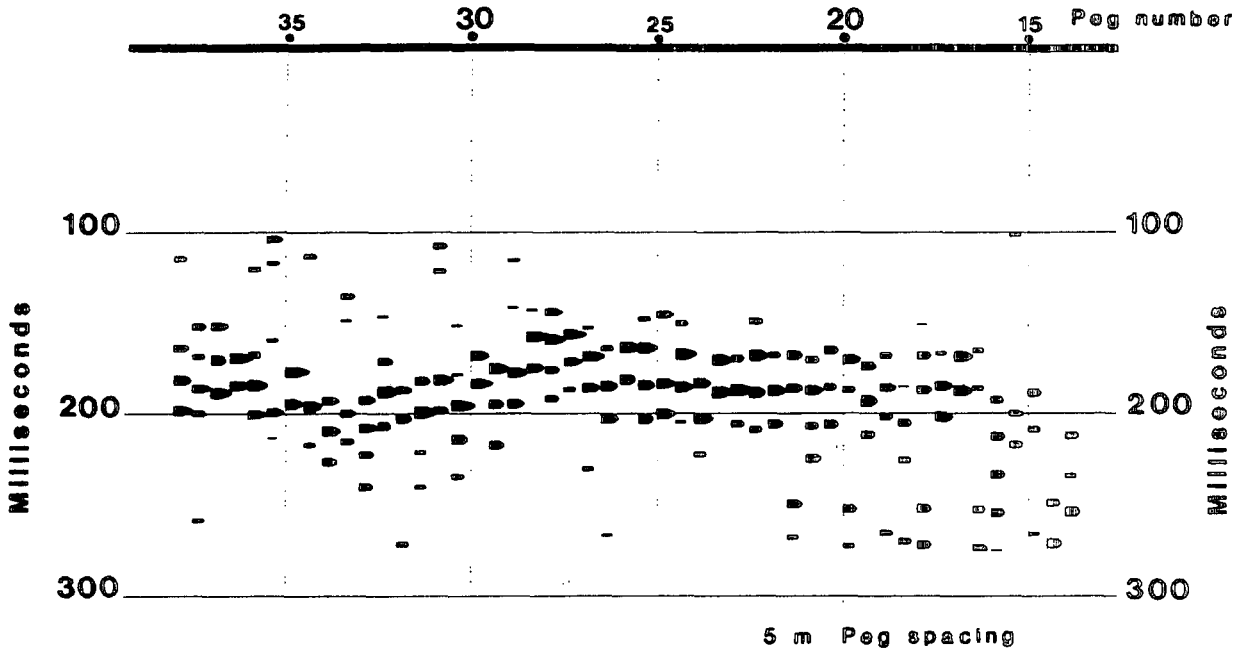

HIGH THORNE Line 1

Processing Sequence

Band pass	35/50/160/120 Hz
Normal moveout correction	
Geometric spreading correction	Time (velocity) ** 2
Autostatics routine	150(75) +/- 6 msec
Stack	
Band pass	35/50/100/120 Hz
Trace normalization	(energy)

Velocity profile

pilipac	velocity (mps)
70	1600
120	2200
320	2500

Figure 7.12

High Thorn Line 2

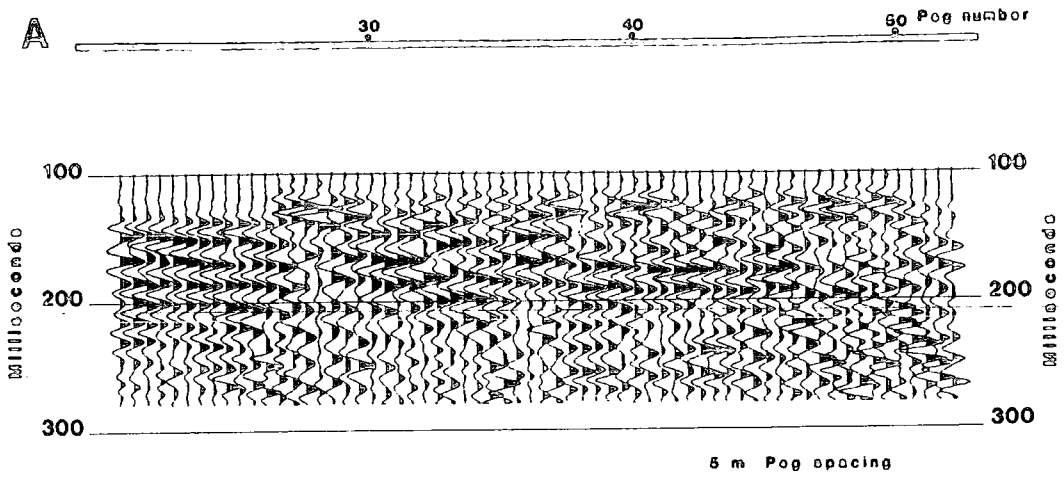

HIGH THORNE Line 2

Processing Sequence

Band pass	35/50/100/120 Hz
Normal moveout correction	
Stack	
Geometric spreading correction	Time (velocity) ** 2
Band pass	35/50/100/120 Hz
Trace normalization	(energy)

Velocity profile

millisec	velocity (rms)
70	1750
120	2200
300	2500

High Thorn Line 2

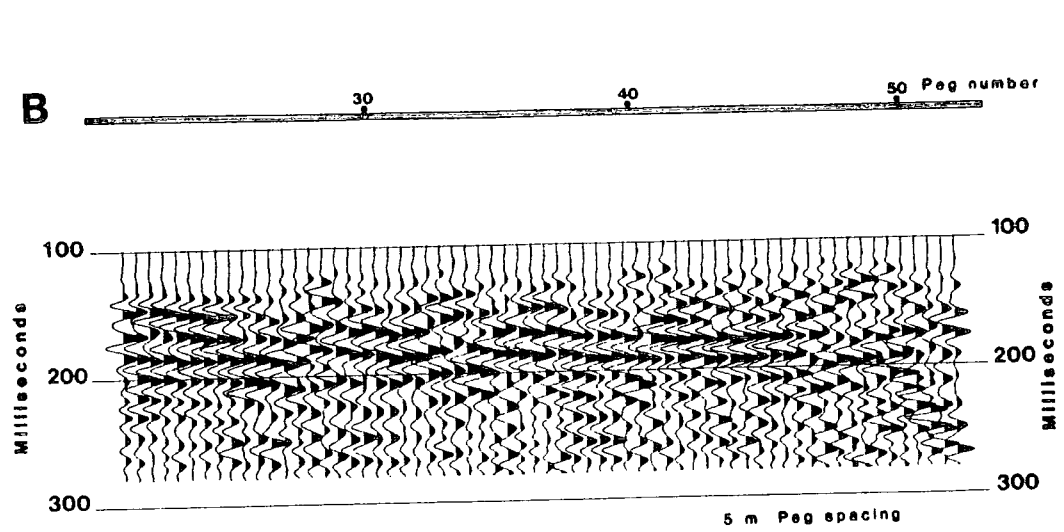

HIGH THORNE Line 2

Processing Sequence

Band pass	35/50/100/120 Hz
Normal moveout correction	
Geometric spreading correction	Time (velocity) ** 2
Autostatics routine	150(75) +/- 6 msec
Stack	
Band pass	35/50/100/120 Hz
Trace normalization	(energy)

Velocity profile

millisec	velocity (rms)
70	1750
120	2200
300	2500

Figure 7.13

High Thorn Line 3

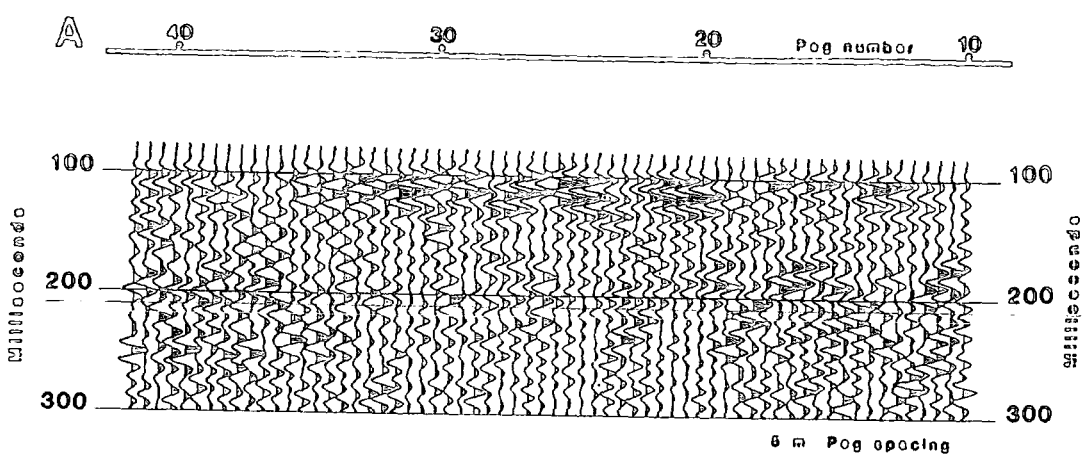

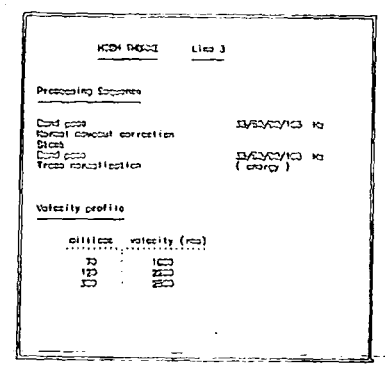

High Thorn Line 3

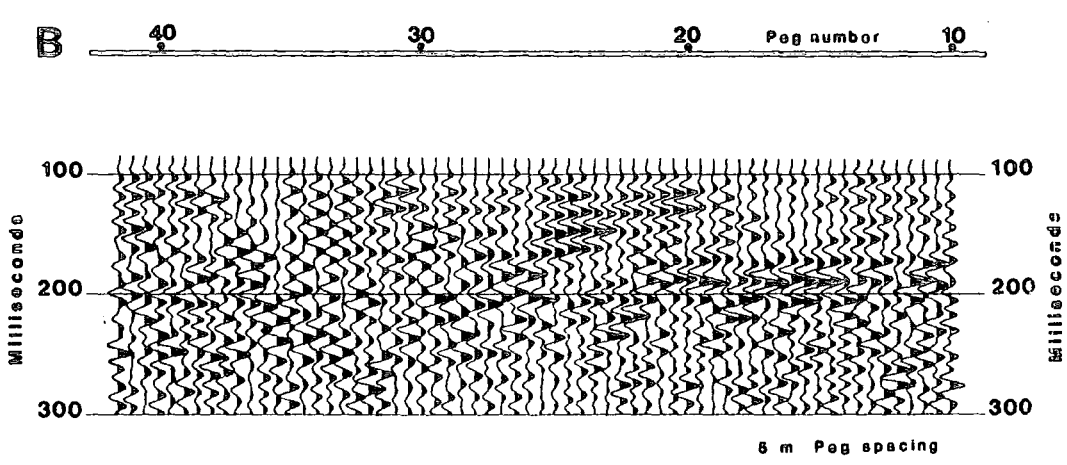

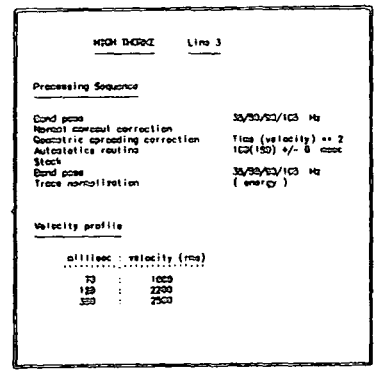

Figure 7.14

High Thorn Line 4

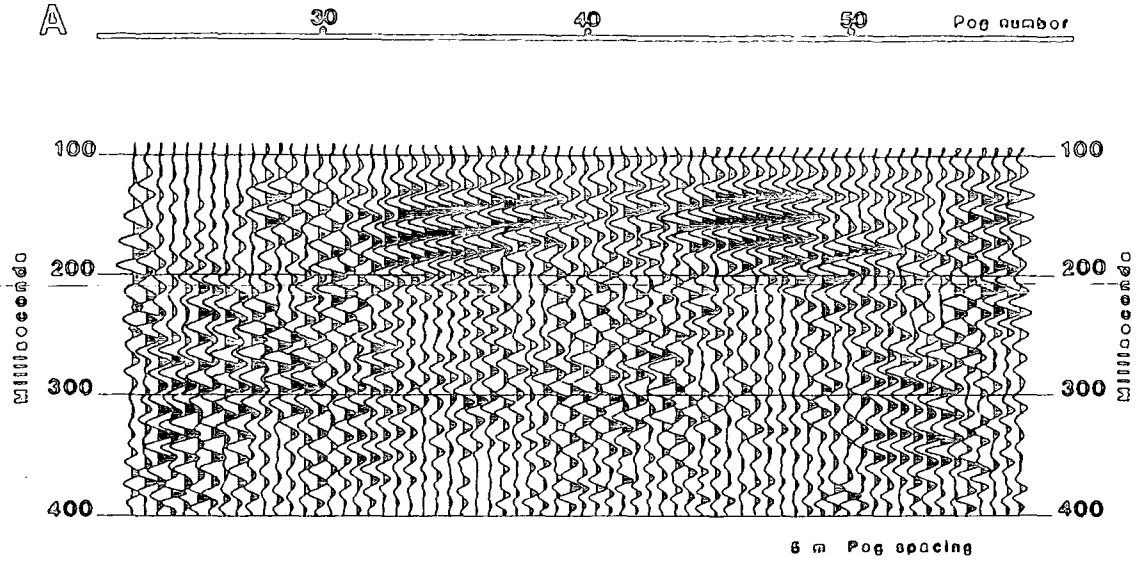

HIGH THORNE Line 4

Processing Sequence

Band pass	33/63/103 Hz
Normal moveout correction	
Geometric spreading correction	Tlog (velocity) ** 2
Autostatics routine	100(250) +/- 8 msec
Stack	
Band pass	33/63/103 Hz
Trace normalization	(energy)

Velocity profile

millisec	velocity (ms)
78	1809
128	2269
303	2503

High Thorn Line 4

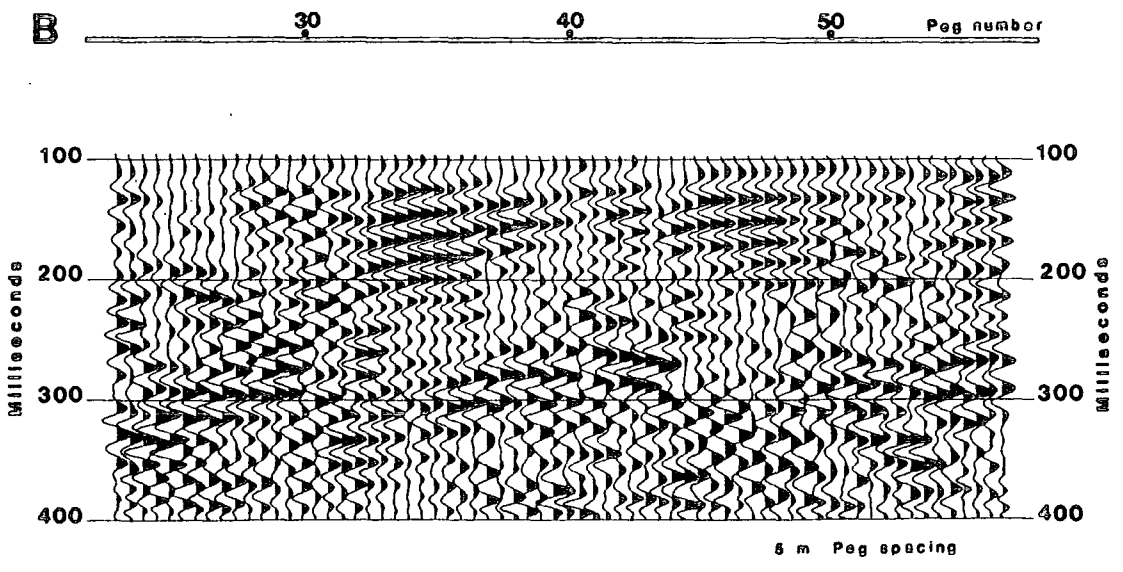

HIGH THORNE Line 4

Processing Sequence

Time varying band pass	103 msec (55/103) Hz 353 msec (40/63) Hz
Normal moveout correction	
Geometric spreading correction	Tlog (velocity) ** 2
Autostatics routine	150(250) +/- 8 msec
Stack	
Band pass	23/40/103/120 Hz
Trace normalization	(energy)

Velocity profile

millisec	velocity (ms)
78	1809
128	2269
303	2503

Figure 7.15

High Thorn Line 6

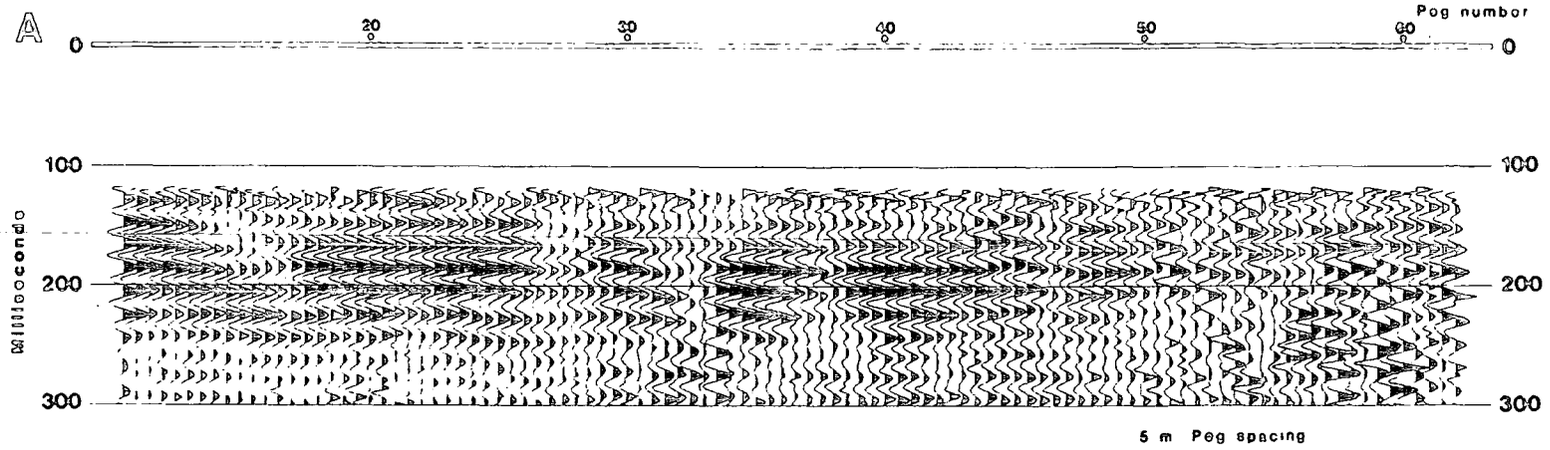

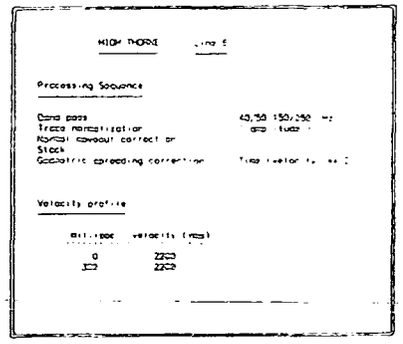

High Thorn Line 6

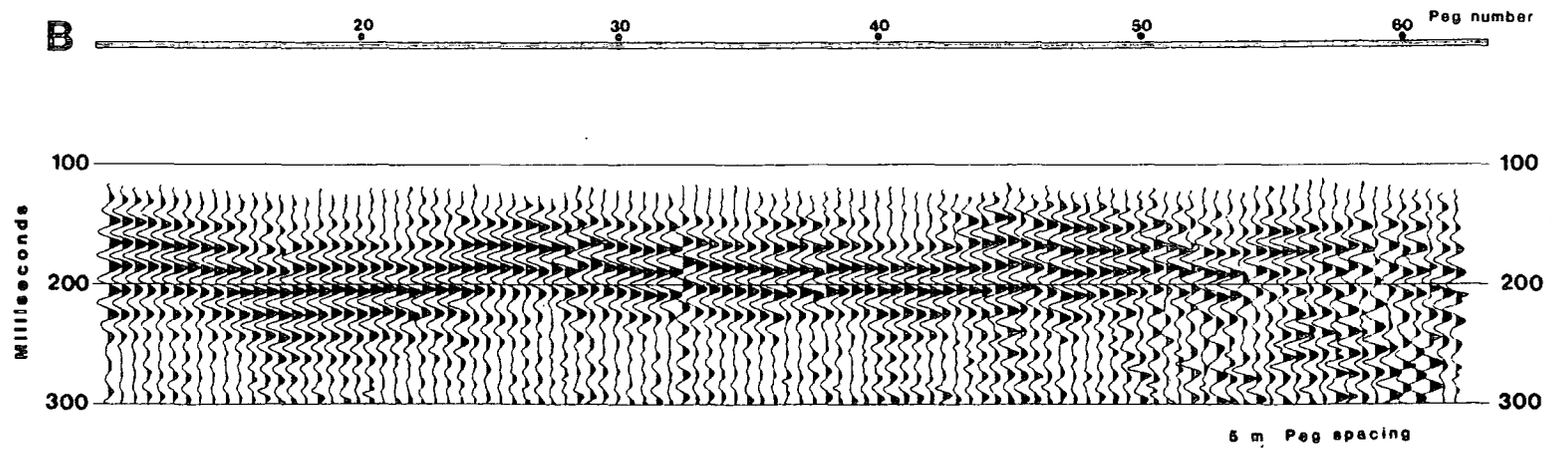

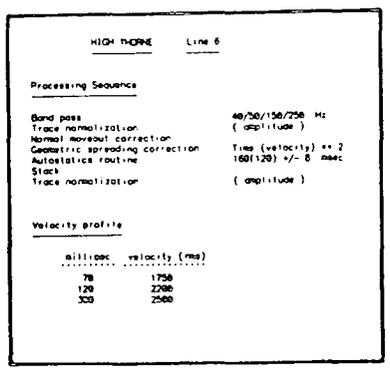

Figure 7.16

Line 6

Figure 7.21 displays the seismic section for line 6 plotted in such a way that it more truly reflects a true depth cross-section. The strong band of reflections from 140 to 220msecs depth convert to between 175 and 275m depth. This depth is again well below the Yard seam horizon at 45m. The strong lateral consistency of the reflections indicate that the data were acquired over an area of unworked ground, as indicated on the original plan (figure 7.1). The premise that the area of mine working may have extended north of the point indicated on the plan seems unfounded.

The perturbation in the reflections at peg 45 which is seen on both sections (figure 7.16), coincides with an area of faulting indicated on the old mine plans and from borehole logs. Although the fault throw is small at a depth of 50m, the throw may increase with depth and be a significant feature at around 250m, which is the depth of origin of the reflections.

Conclusions

The results of the trials at High Thorn are disappointing. Although some features seen on the reflection lines can be related to the boundaries of old mine workings, there does not appear to be any consistency.

The main reason for this is that the mine workings are too shallow to be directly imaged by the reflection technique. The mine workings are only 50m deep, whereas the shallowest reflections recorded originate from a depth of 150m. As a result

we are relying on the mine workings causing effects such as an increase in traveltime to a reflector and a decrease in data quality on reflections which originate from well below the mined horizon.

In the example given by Waters (1979) shown in chapter 2, the depth of the pillar and stall mining is 200m, well within the range of reflection depths recorded at High Thorn. Given such a situation at High Thorn, the reflection data would have yielded more useful information.

High Thorn

Line 1

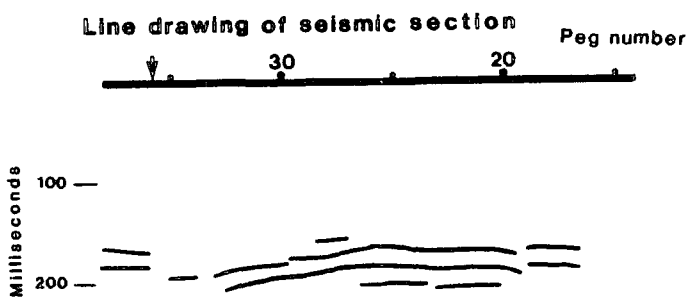

Line 2

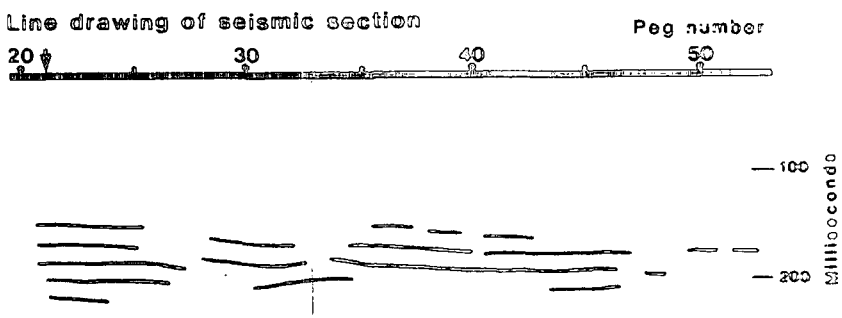

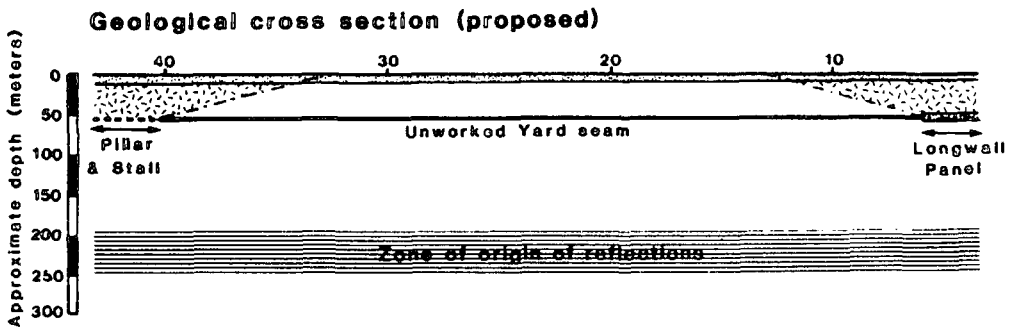

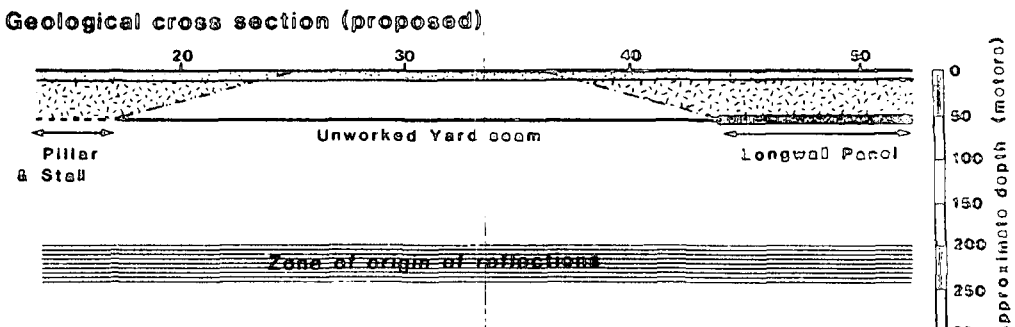

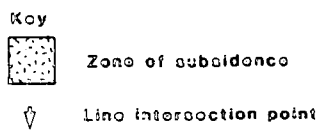

Figure 7.17

Figure 7.18

High Thorn

Line 3

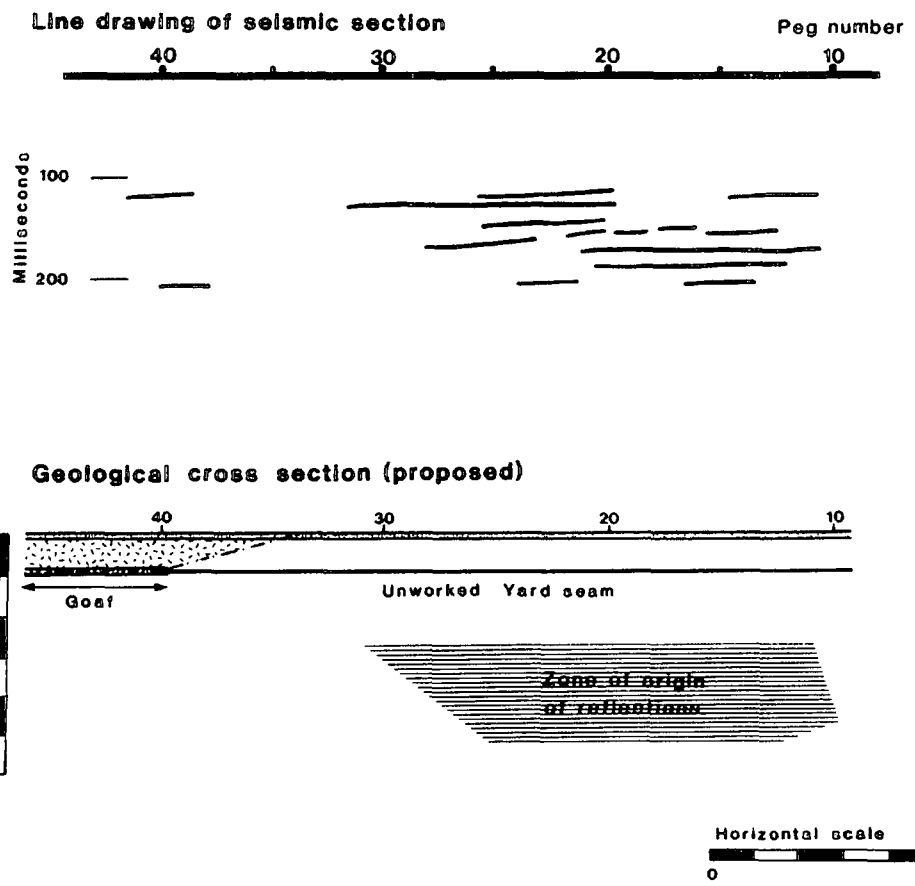

Figure 7.19

Line 4

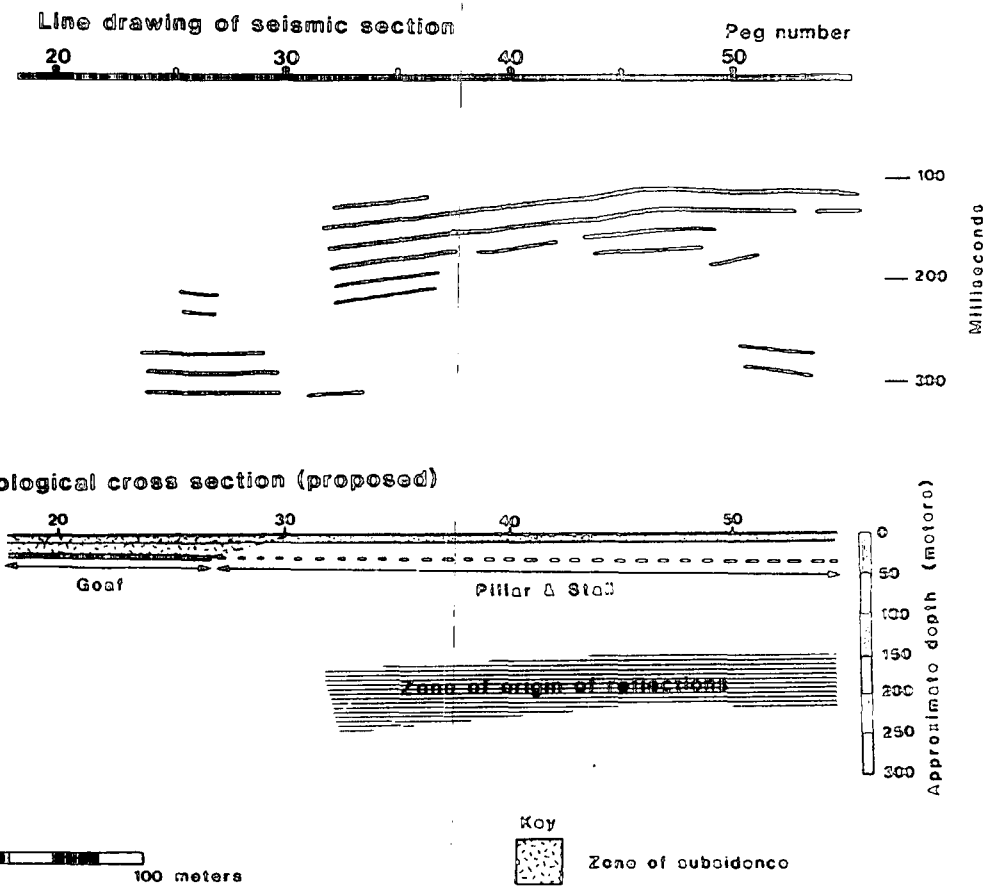

Figure 7.20

Horizontal scale
0 50 100 meters

Key
Zone of subsidence

High Thorn Line 6

Seismic section

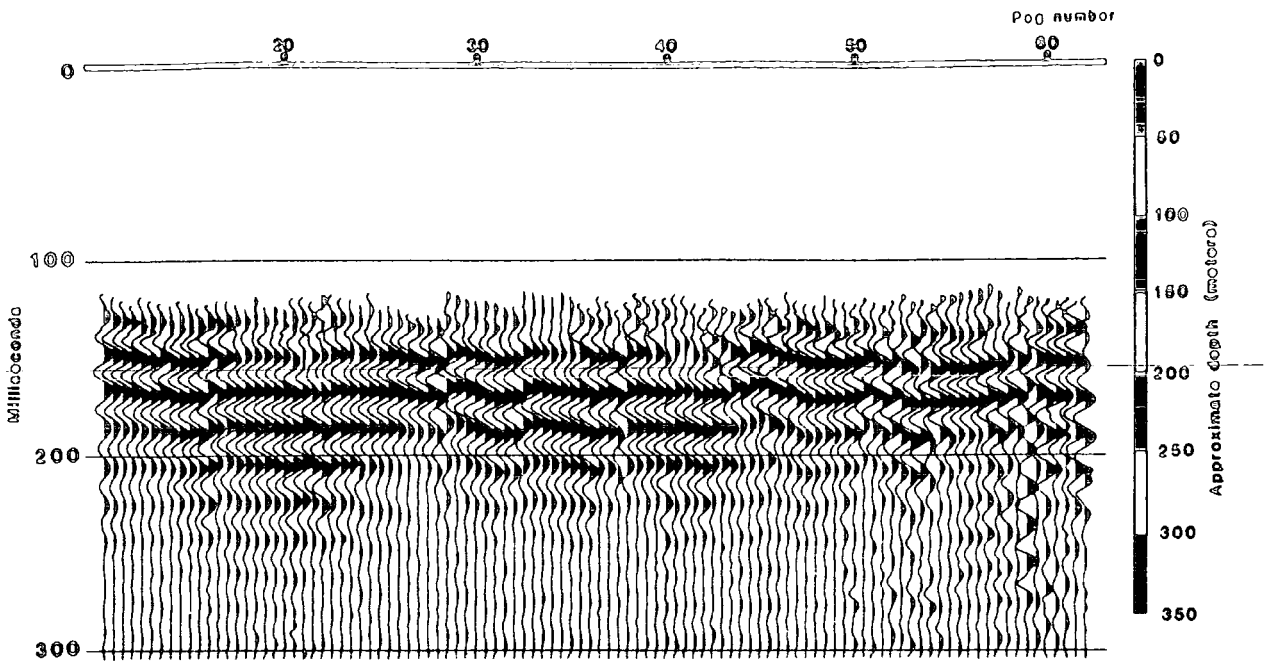

Geological cross section

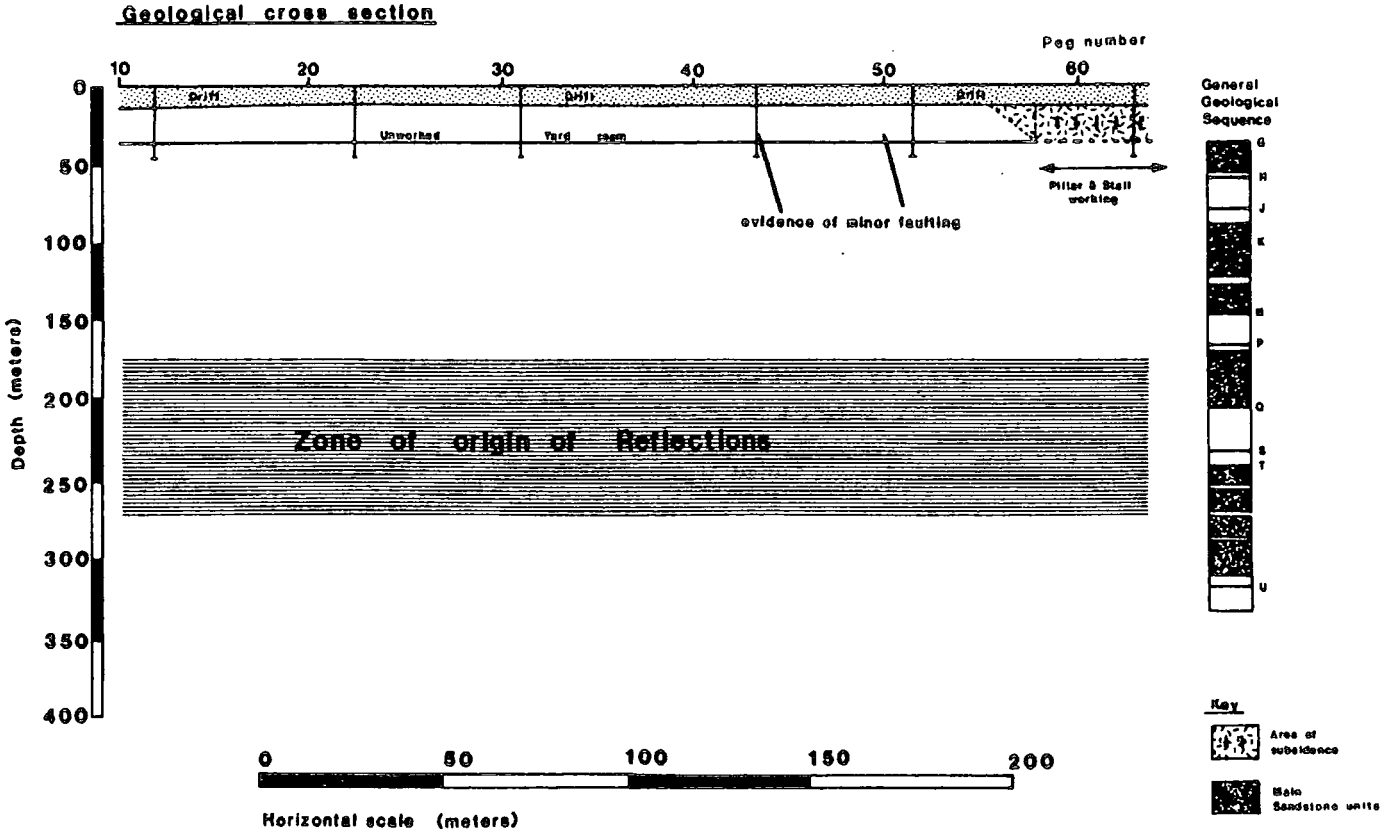

Figure 7.21

CHAPTER EIGHT

KEEKLE : SITE NO. 5

Keekle Extension site is situated on the Cumbrian Coalfield on the western flanks of the Lake District. The purpose of the reflection and refraction surveys at this prospective opencast site was to locate a major fault which acts as a boundary to the proposed opencast coal site, and to locate other minor faults within the Coal Measures.

The geology of the site and the surrounding area is displayed in figure 8.1. The surface geology in the area consists of Carboniferous and Permo-Triassic rocks. The Cumbrian Coalfield has a gentle westerly dip, off the central Lake District dome. The coalfield is transected by a series of normal faults with general north easterly and north westerly trends, these are Hercynian in origin. Some faults display later reactivation where they cut Permo-Triassic strata. The faults generally displace Permo-Triassic strata by 30m or less, although the same fault may displace the underlying Carboniferous strata by a much larger amount (Moseley, 1978).

The oldest rocks exposed in the vicinity of the site are the Lower Carboniferous (Dinantian) strata. These consist of a series of limestones and shales. Limestone horizons being locally up to 9m in thickness. Overlying the Dinantian is the Millstone Grit (Namurian) strata. The basal bed of the Namurian is the First Limestone which is locally an average of 14m in thickness (Eastwood, 1931). Overlying the limestone is the Hensingham Grit

Geology at Keekle Extension

Geological Plan

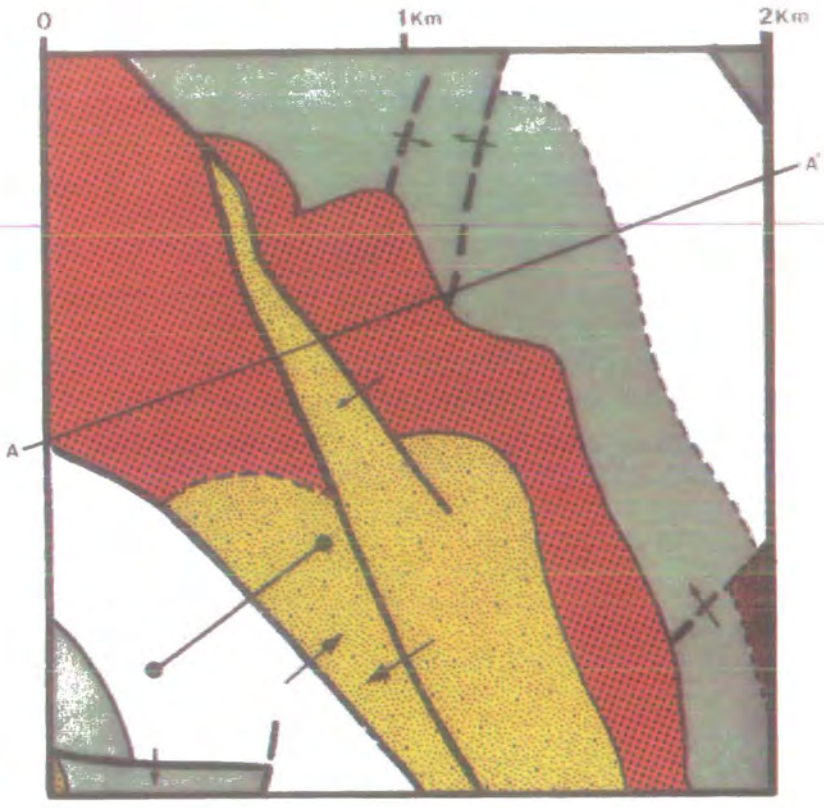

Seismic reflection line

Major fault

Generalized section

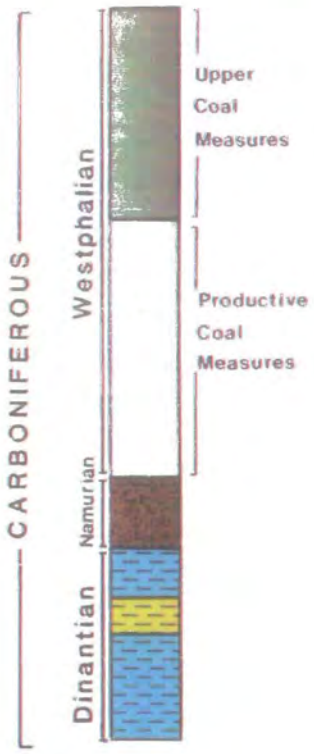

Cross Section

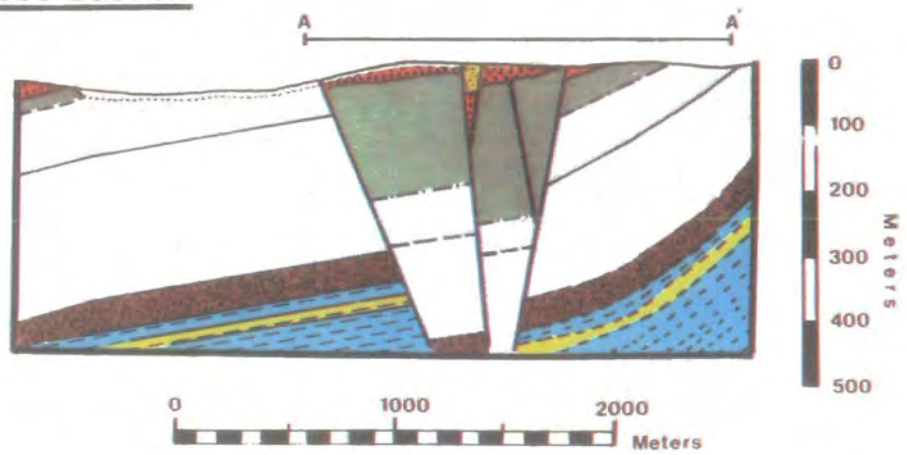

Information obtained from Geological Survey sheet 28 (Whitehaven)

Figure 8.1

series. This series consists of coarse sandstones, mudstones and thin limestone horizons.

Above the Namurian lie the Coal Measures (Westphalian), which can be divided into the Productive (Lower) and the Upper Coal Measures. The lithologies of the Westphalian, range from coarse sandstones to the finest of mudstones, the coal seams of economic importance being contained in a group of measures some 300 to 400m thick. The Westphalian locally exhibits a reddened appearance due to oxidation effects related to the pre-Permian land surface (Moseley, 1978).

Overlying the Carboniferous strata are the Permian and Triassic rocks. These are separated into the Brockram and the St Bees Sandstone. The Brockram is a basal breccia found along the fringes of the Lake District dome, and is a hard, well cemented rock. Its maximum recorded thickness locally is 26m, although it is generally much thinner. The overlying St Bees Sandstone is Triassic in origin and is a dull red, fine to medium-grained sandstone.

The fault of interest has an estimated Carboniferous throw of 220m (from BGS geological map no.28) and causes the Productive Coal Measures to lie adjacent to the downthrown Permo-Triassic strata (figure 8.1). The geological information given in figure 8.1 was obtained entirely from the BGS geological map of the Whitehaven area published in 1929. When we commenced our operations at this site, this was the only information available on the exact fault location in the area, as no drilling had been carried out by the Opencast Executive at that time.

8.1 P WAVE REFLECTION LINE

The site was first visited in September 1983, when the seismic reflection line was surveyed. Due to the long length of seismic line required, a 5m peg spacing was chosen for the survey. The location of the seismic reflection line was designed so that it straddled the proposed fault location given on the BGS map. From the geological map, the fault trend is given as NW-SE and should intersect the seismic reflection line at peg number 67. A detailed plan of the line location is given in figure 8.2, The drift cover along the seismic line is thin, varying from zero to 10m, generally only 3 to 5m thick.

Due to the improvement in data quality achieved at Hemscott North by the increased depth of burial of the source, it appeared imperative that at Keekle the explosive charge must be buried into rockhead. This required that shot holes had to be drilled for this survey. The departmental Victor Products waterflush drill was used for this task. Drilling was not an easy task, due firstly to boulders in the overburden, and secondly to the hardness of the rockhead. The cores displayed the characteristic reddening mentioned previously. The shot holes were only able to penetrate about 1m into rockhead (5 to 6m hole depth). After much effort twelve shot holes were drilled between pegs 37 and 79. It was hoped that this penetration would be sufficient to obtain high frequency data.

At each shot point, six 12 channel geophone spreads were laid out, with no geophone overlap between spreads. This produces an effective 72 channel common shot gather. The source used for the

KEEKLE EXTENSION

Location of seismic lines.

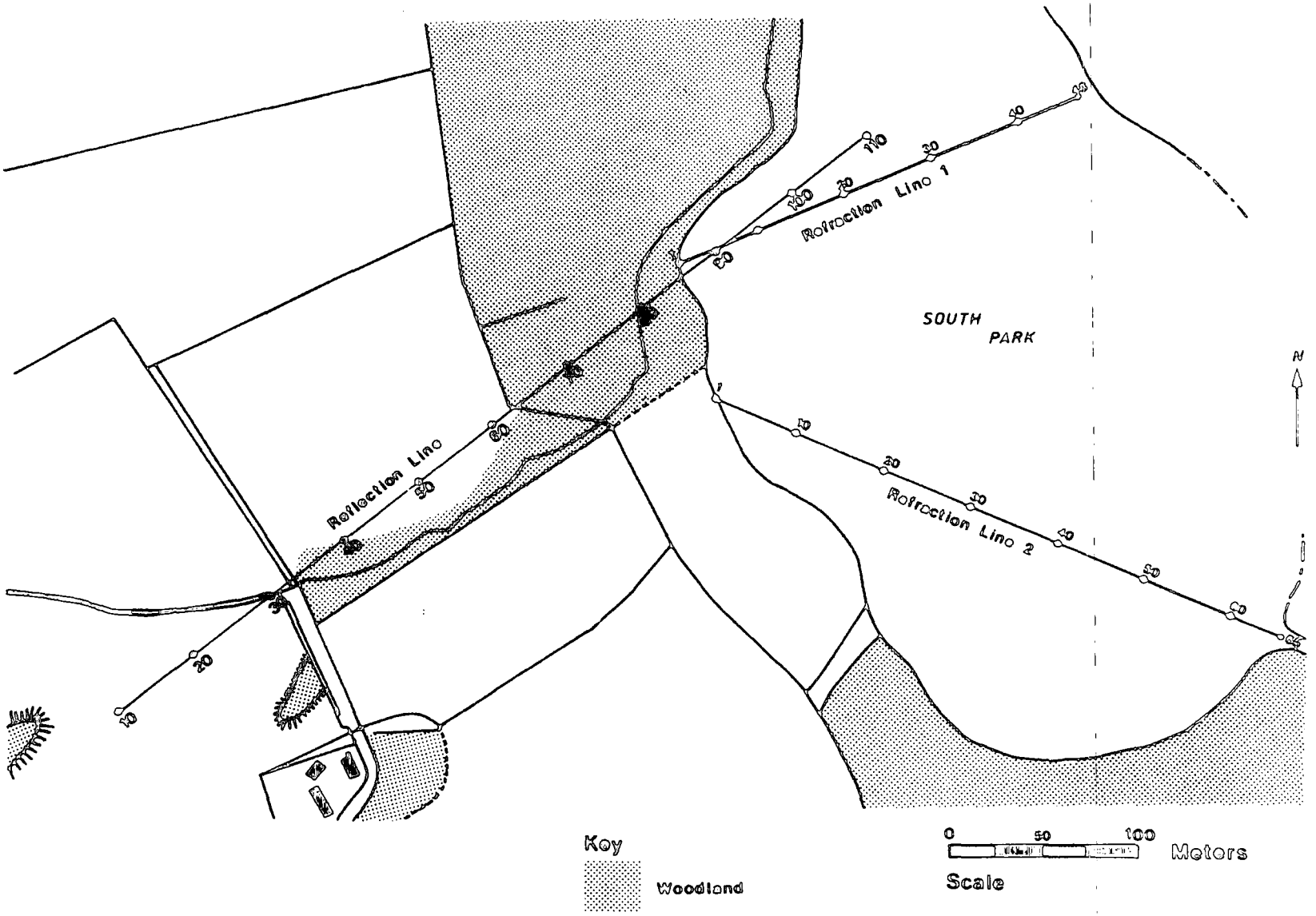

Figure 8.2

survey was a seismic detonator, exploded in rockhead. The data was recorded for 512msecs (0.5msec sampling frequency). A 100Hz high pass analogue filter was used on recording to remove ground roll on the field records. In total, 74 records were recorded on tape. Figure 8.3 displays the records obtained at shot point 79. No reflected energy was received below 300msecs, due to our low power (high frequency) P wave source. Subsequent data processing was carried out on the first 300msecs of data. Figure 8.4 displays the complete CSG as recorded. By the application of a time varying gain function to the field data one is able to observe the deeper reflections down to 300msecs (figure 8.5).

The first stage of data processing carried out on the data was to design a mute function to effectively remove the first break refraction arrivals from the data. No problems were encountered with reverberant refractions with this data, so a consistent mute function could be applied to every CSG. On figure 8.5, one can see that the traces with offsets close to the shot exhibit no coherent reflected arrivals. The short offset traces also exhibit clipping due to the saturation of the A/D converter. The inclusion of these traces in further processing would only impair the final section, so traces with offsets of zero to 20m were edited out of each CMP gather.

Great care was taken with the data to calculate the static corrections for this reflection line. A three-stage process was carried out on the data. Firstly the effects of the land surface elevation and shot depth variations along the line were calculated. The landsurface topography displays a gradual rise of 20m eastwards along the line. The effects of the elevation on

each shot to receiver raypath were calculated and removed down to a datum of 100m (aod), this is the land surface level at the western end of the line. Shot statics of +2.5 to -4msecs and geophone statics of -2 to -8msecs were applied to individual traces (shifts greater than 1/2 wavelength for 150Hz data). This process effectively removes the long wavelength statics. The second stage was to plot out the first break information from each shot point (figure 8.6). Any anomalous early/late arrivals can be clearly seen on the graph and a corresponding static shift applied. Less than ten traces required this treatment. This technique removes high amplitude, short wavelength statics. Thirdly any residual static effects can be removed by the addition of the CMP aligned statics routine to the processing sequence, restricting the maximum static shift to half a cycle of the predominant frequency. Figure 8.7 displays the CSG after the application of the first two of the above processes.

The next stage in the data processing sequence is the design of the band pass frequency filter. Figure 8.7 shows that ground roll modes are still present on the data at this stage, having not been effectively removed by the analogue field filter. Separate amplitude spectra were analysed for traces containing predominantly ground roll and reflections. Figure 8.8 displays typical results from these tests. Spectrum f1 originates from a ground roll trace, the peak frequency being 40Hz. Spectrum f2 originates from a trace solely containing reflections, and displays high frequencies ranging from 80 to 170Hz. The optimum filter must remove 40Hz ground roll, whilst retaining frequencies between 70 and 200Hz. Figure 8.9 shows the results of the application of the optimum band pass filter on the CSG. Trials

were also carried out using a time varying band pass filter on the data (figure 8.10). The philosophy behind using a time variant band pass filter is that it allows you to pass only the very highest frequencies for the near surface reflections, but gradually introduce lower frequencies into the data at later times to account for dispersion and absorption effects. This technique allows the deeper reflections to be enhanced whilst retaining optimum resolution of the near surface reflections. For the final section a band pass filter was applied pre-stack whilst a time varying band pass filter was applied post-stack.

The common shot gathers were then re-sorted into common mid point gathers. The resultant fold of cover varied from a maximum of 10 in the centre of the line to 2 at the ends (figure 8.11).

The calculation of the stacking velocities was carried out by firstly band passing the data, then stacking with constant velocities between 2000 to 4000m/sec at 200m/sec increments. This technique was carried out on two segments of the line, and the velocity picks made (figure 8.12). Figure 8.13 displays the velocity profiles chosen. The velocity at zero time was tied to the refracted arrival velocity value. The velocity profiles are similar, so an average stacking velocity profile was used for the whole line.

A variety of pre-stack and post-stack deconvolution operators were applied to the data, none of which enhanced the data, causing only a decrease in the signal/noise ratio. Therefore this technique was not added to the processing sequence.

Keekle Reflection Line

Data as recorded in the field

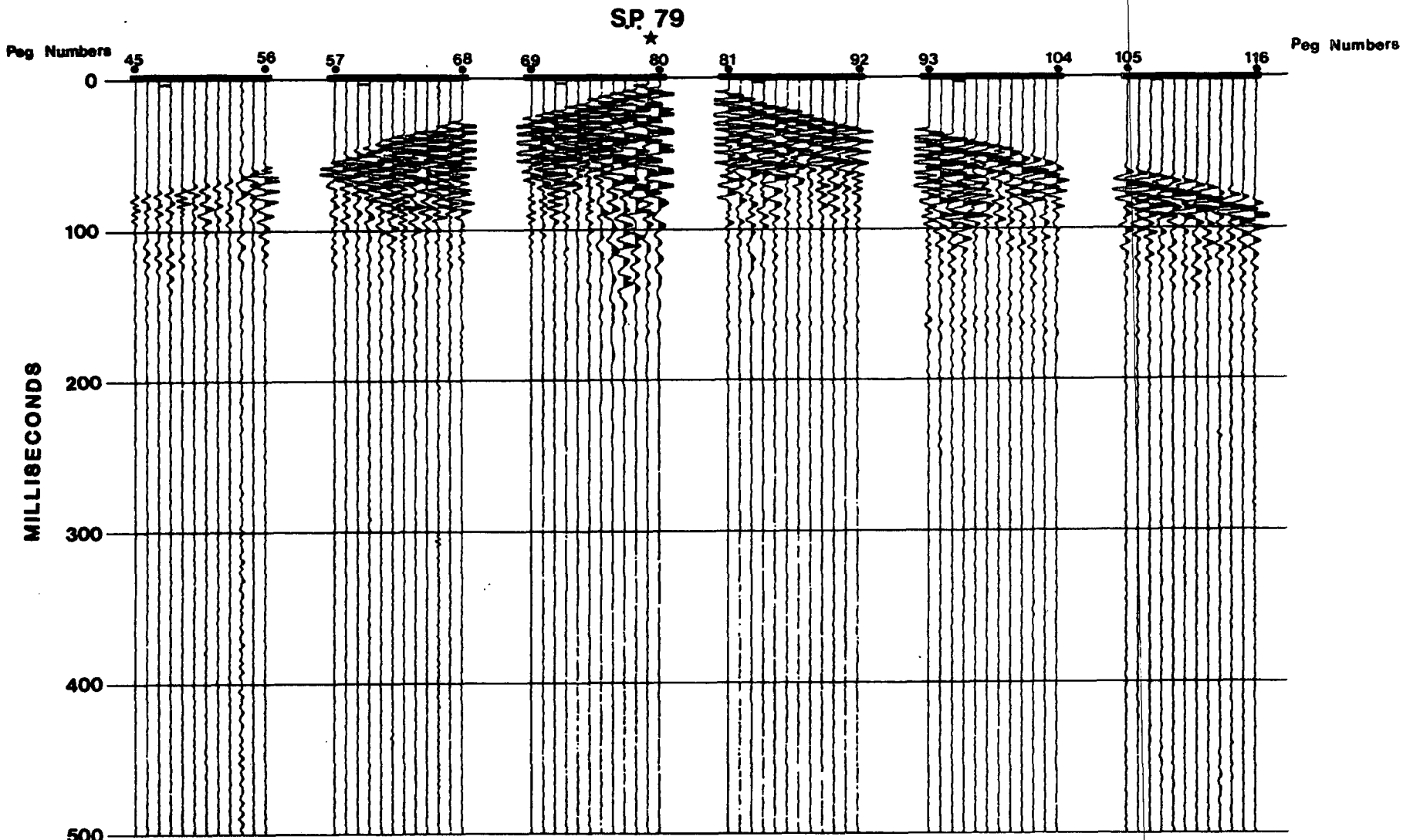

Six x twelve channel geophone spreads

Figure 8.3

Keekle Reflection Line

Common Shot Gather - as recorded

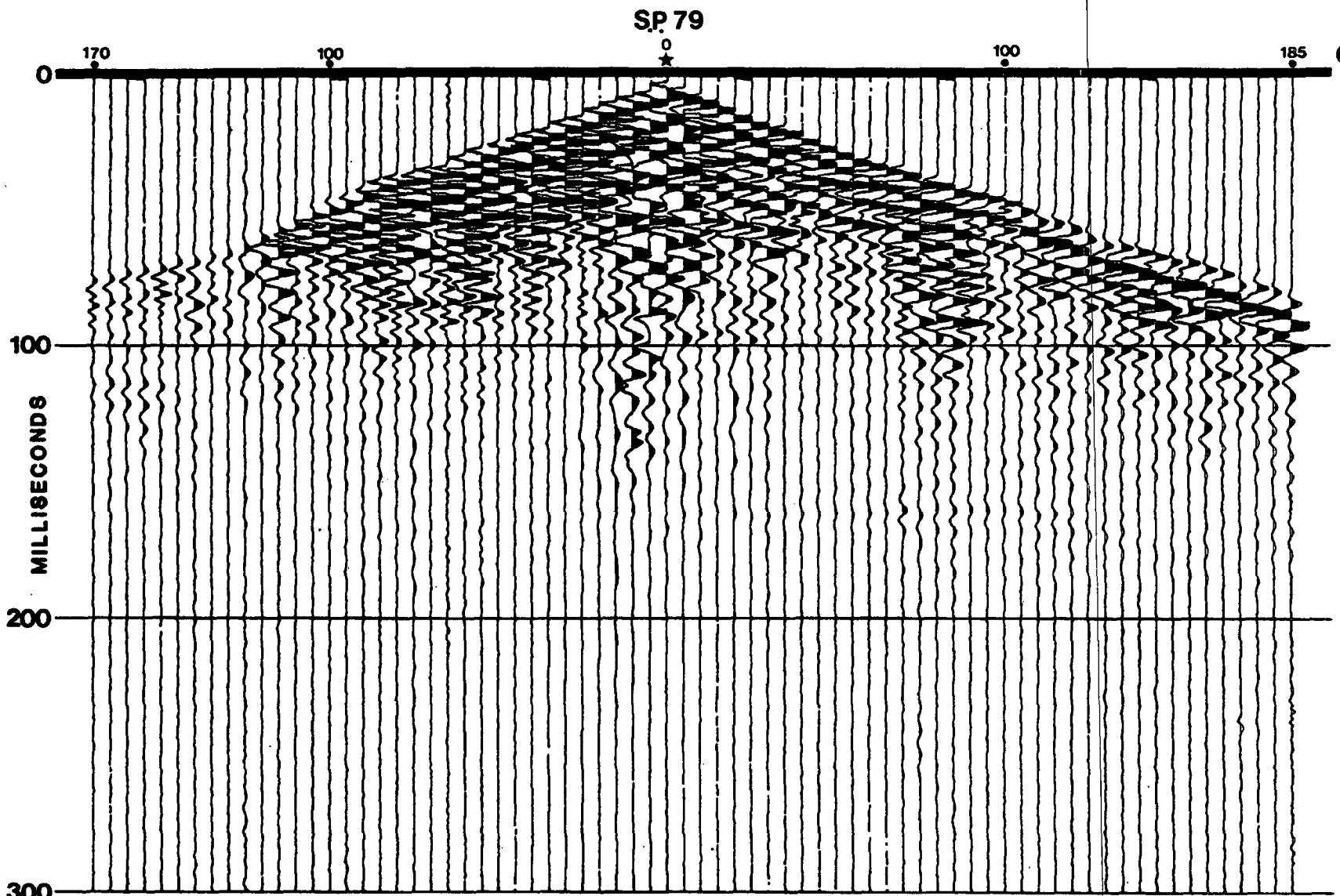

Figure 8.4

Keekle Reflection Line

Common Shot Gather - gain $\propto$ time^2 applied

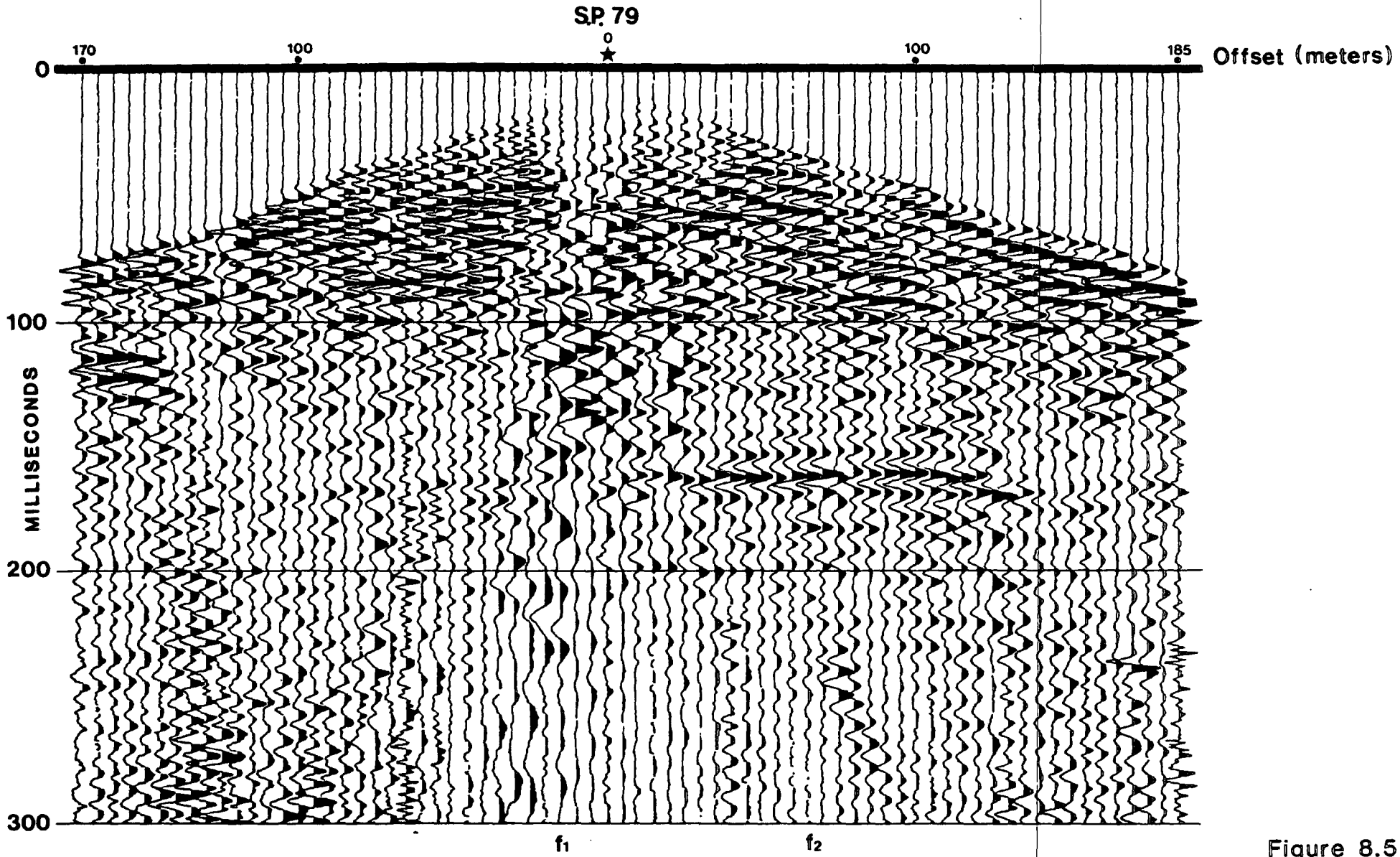

Figure 8.5

First Break Plot

Figure 8.6

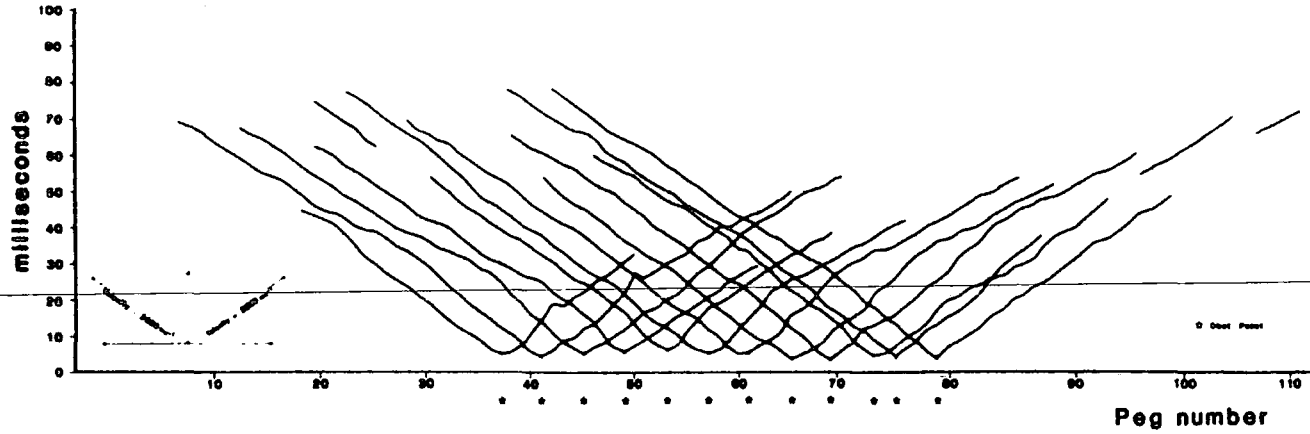

Fold of Cover of Reflection line

Figure 8.11

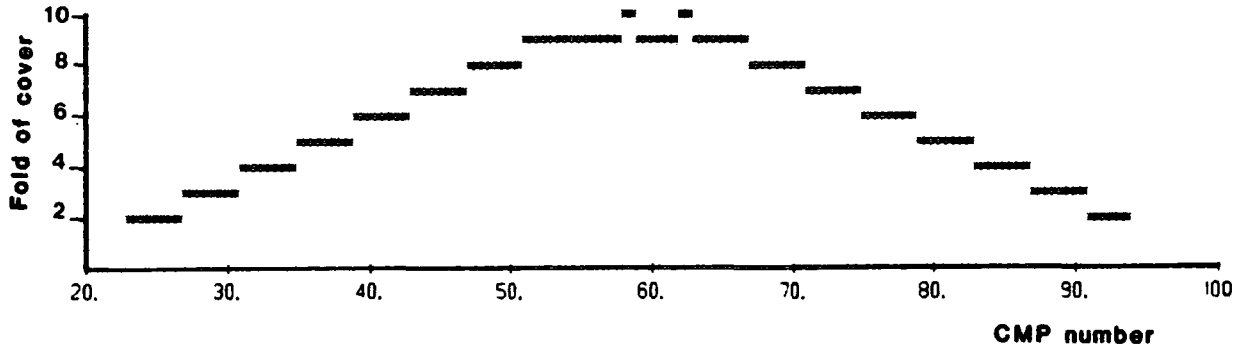

Stacking Velocity picks

Figure 8.13

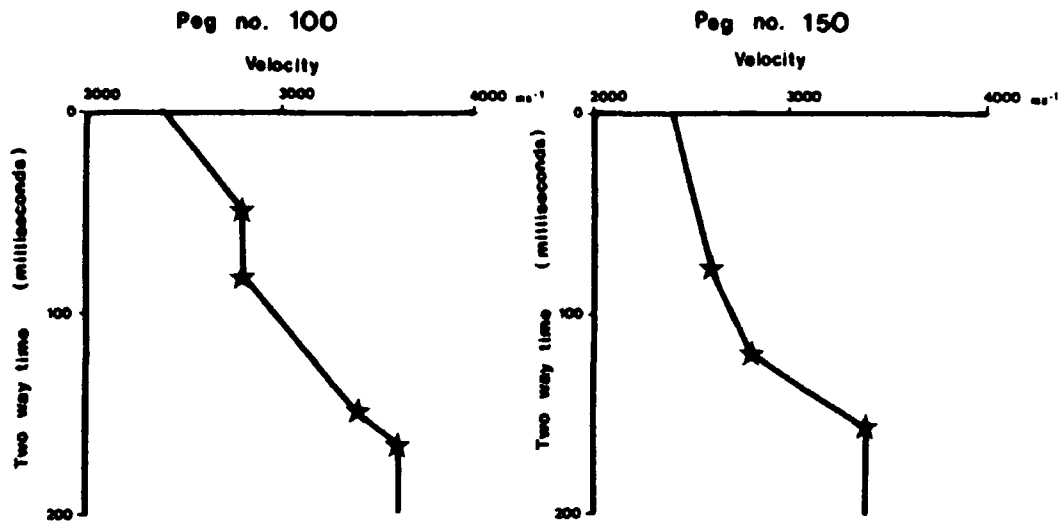

Keekle Reflection Line

Common Shot Gather - static shifts & mute applied

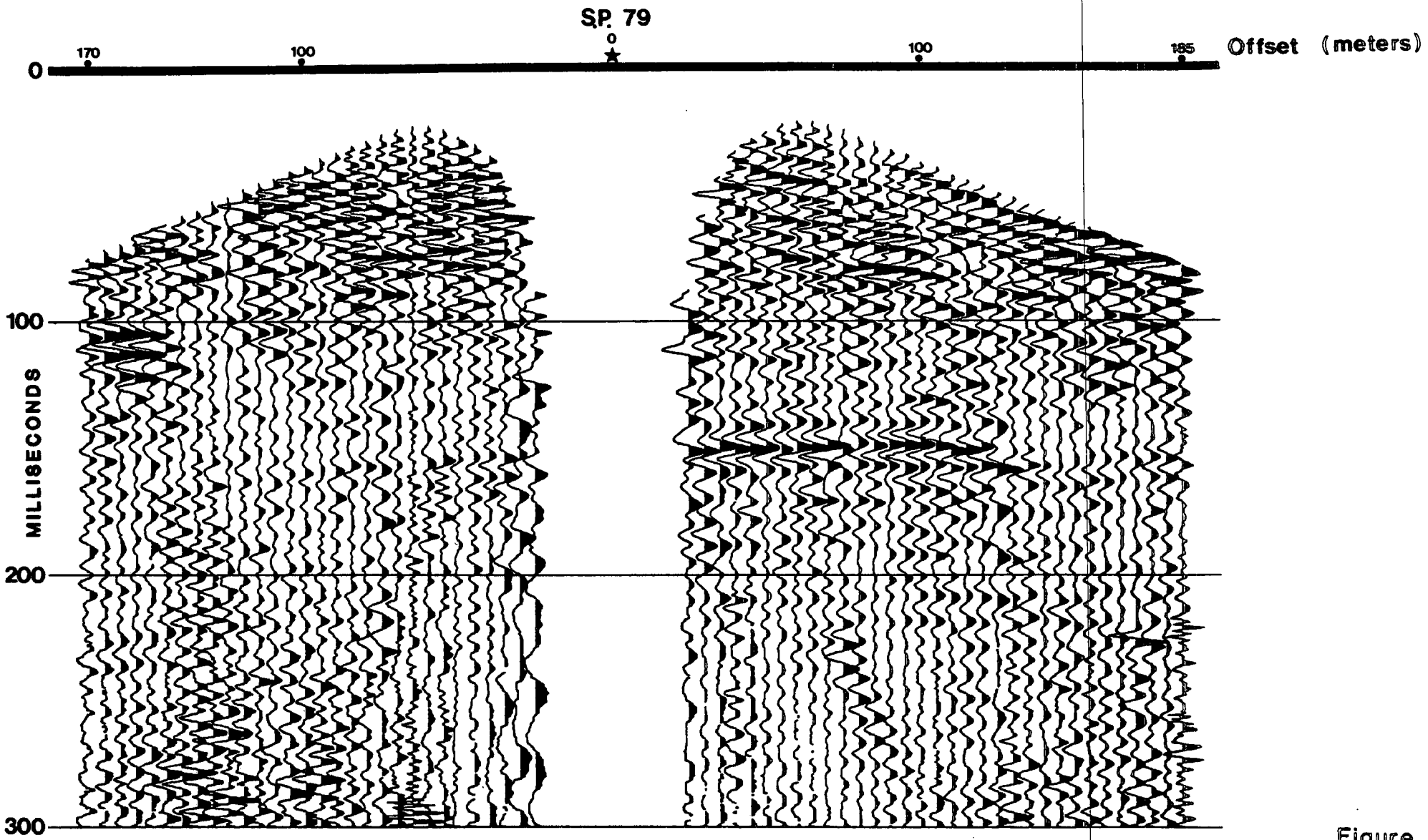

Figure 8.7

Keekle Reflection Line

AMPLITUDE SPECTRA

S.P. 79 offset 15m

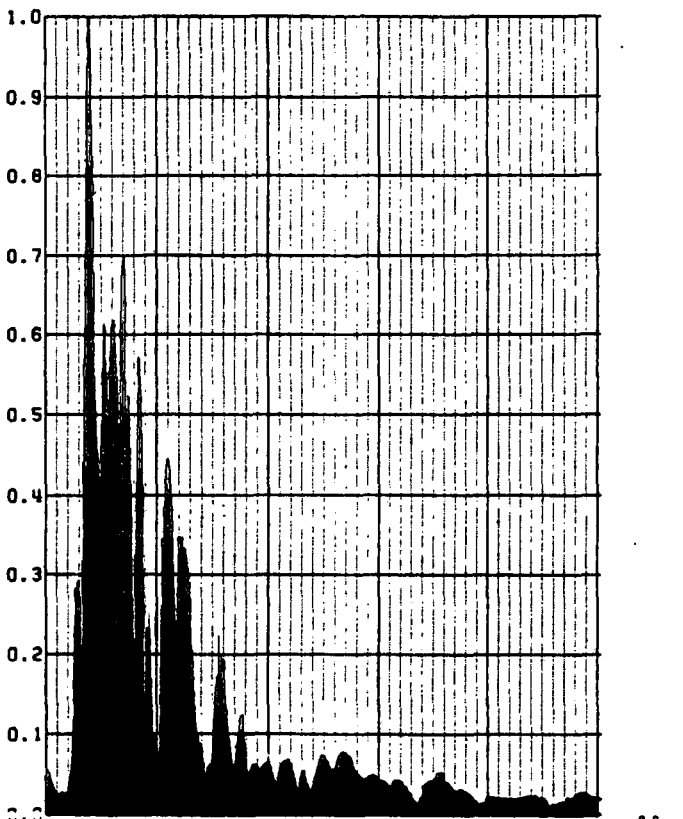

f_1

S.P. 79 offset 65m

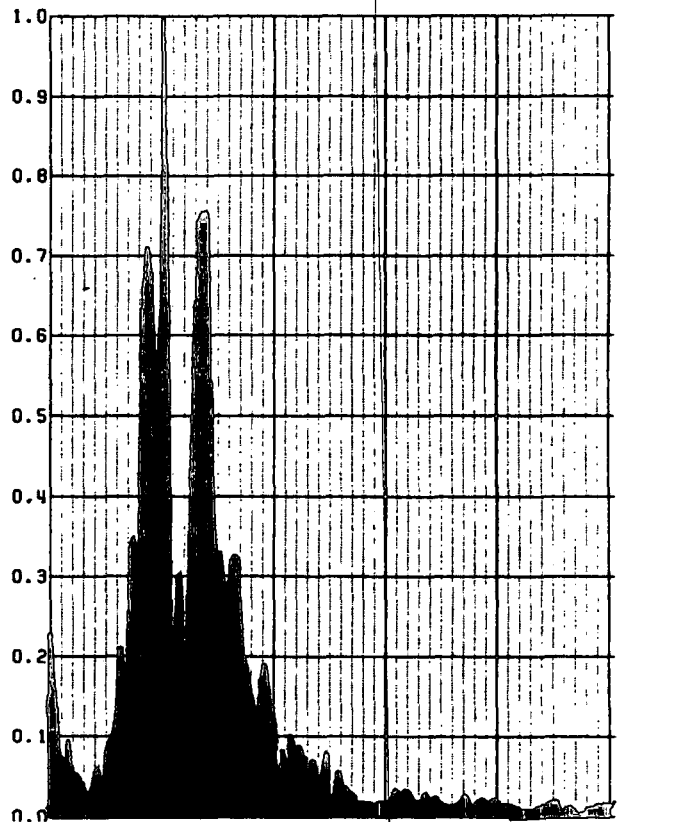

f_2

Figure 8.8

Keekle Reflection Line

Common Shot Gather - band pass filter applied

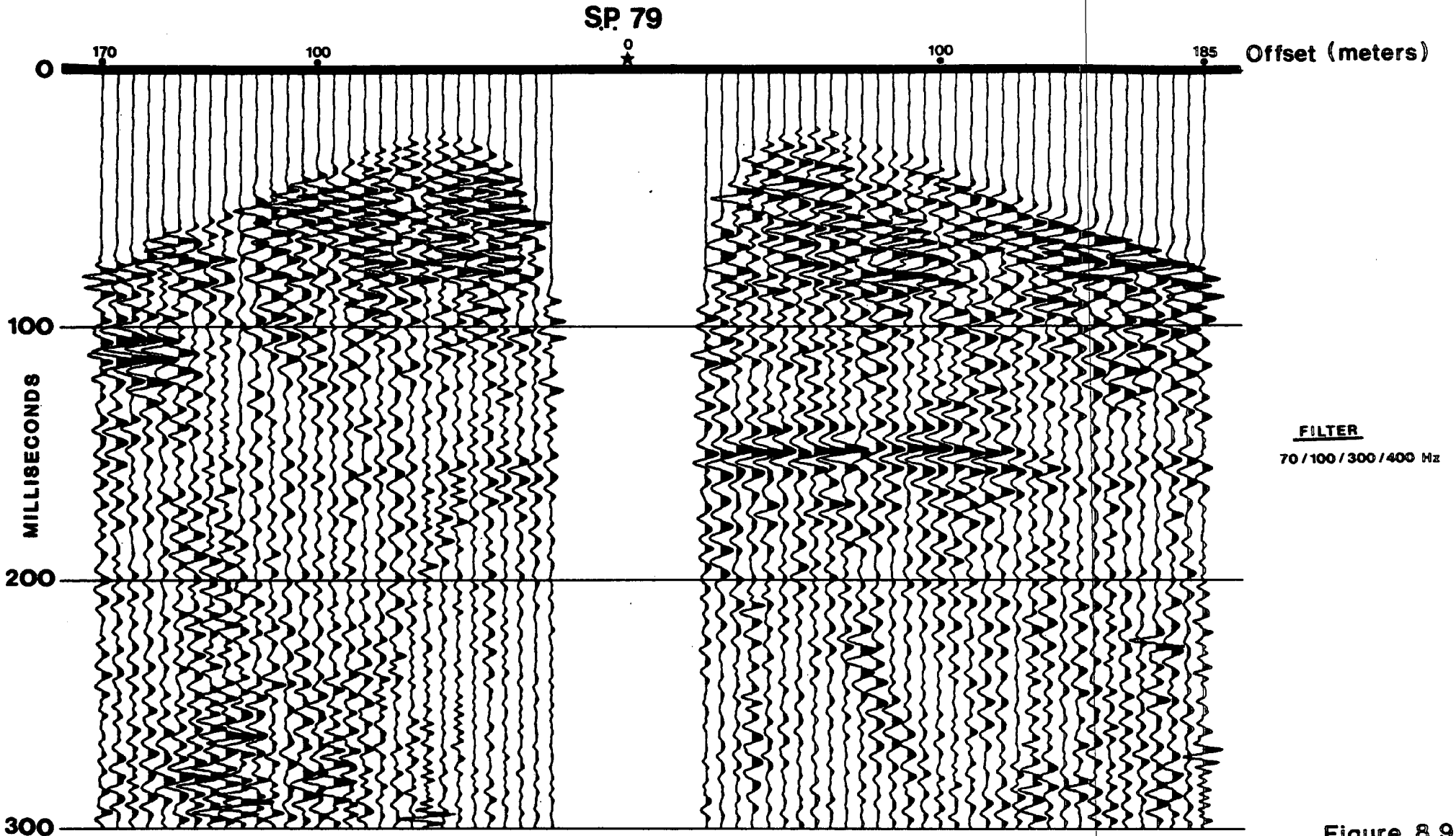

Figure 8.9

Keekle Reflection Line

Common Shot Gather - time variant band pass filter applied

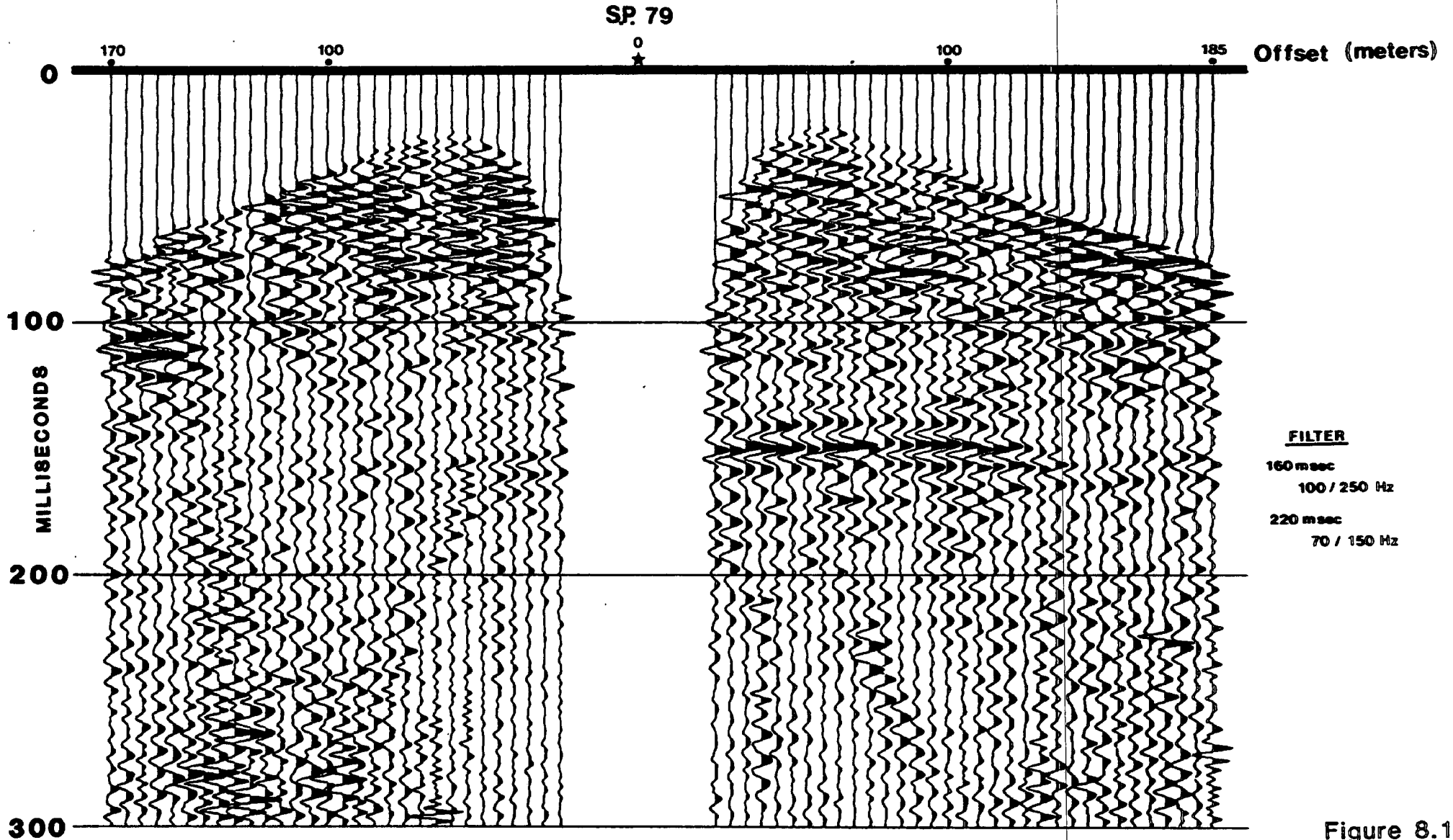

Figure 8.10

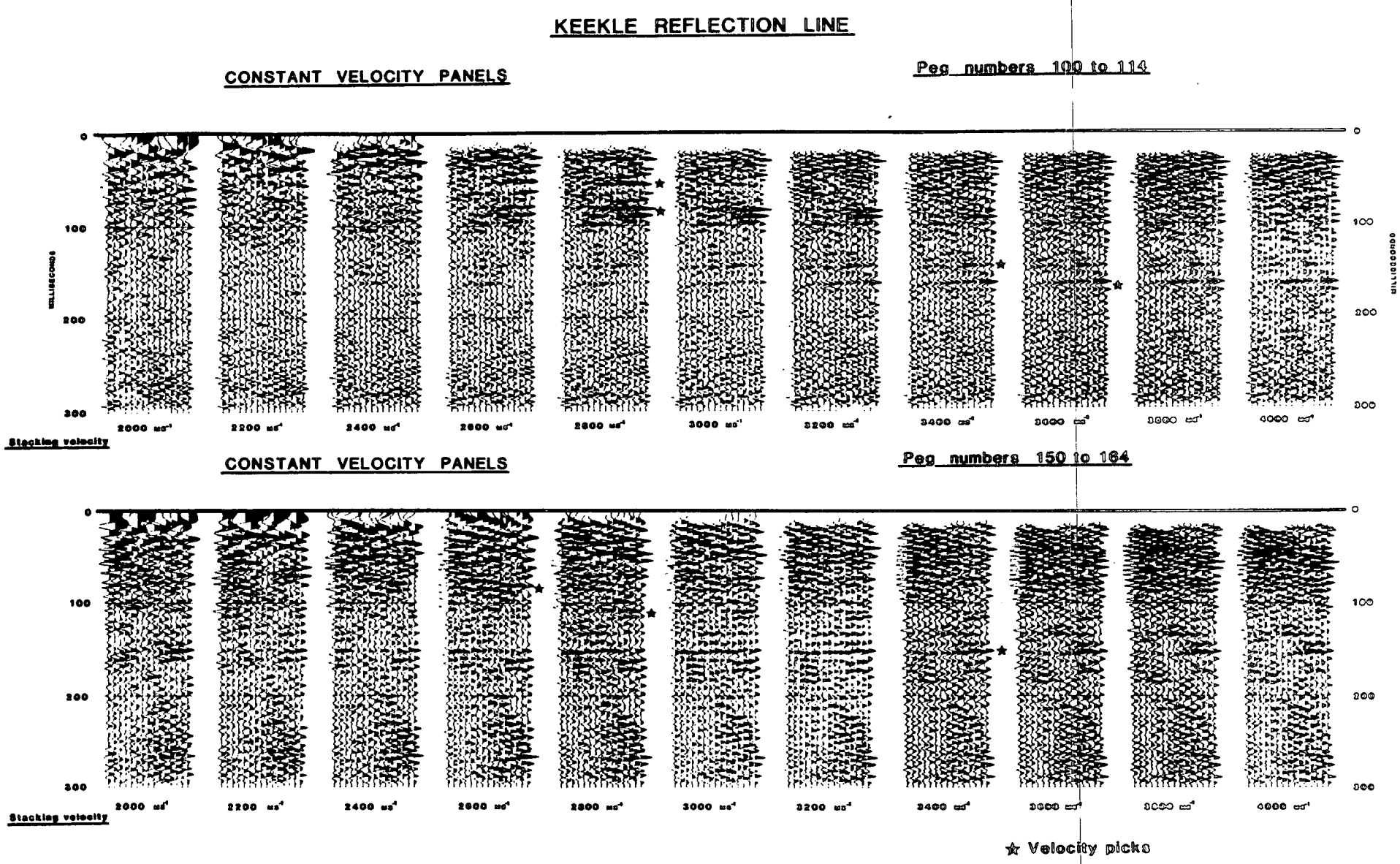
KEEKLE REFLECTION LINE
CONSTANT VELOCITY PANELS
Peg numbers 100 to 114
0
100
200
300
2000 ms⁻¹
2200 ms⁻¹
2400 ms⁻¹
2600 ms⁻¹
2800 ms⁻¹
3000 ms⁻¹
3200 ms⁻¹
3400 ms⁻¹
3600 ms⁻¹
3800 ms⁻¹
4000 ms⁻¹
Stacking velocity
CONSTANT VELOCITY PANELS
Peg numbers 150 to 164
0
100
200
300
2000 ms⁻¹
2200 ms⁻¹
2400 ms⁻¹
2600 ms⁻¹
2800 ms⁻¹
3000 ms⁻¹
3200 ms⁻¹
3400 ms⁻¹
3600 ms⁻¹
3800 ms⁻¹
4000 ms⁻¹
Stacking velocity
☆ Velocity picks

Figure 8.12

Figure 8.14 displays the final seismic reflection section produced for Keekle Extension. The section displays high frequency data with bands of reflection events clearly apparent, although few between 0 to 150msecs display any lateral consistency across the seismic section. Figure 8.15 was produced to display the true relative amplitudes of reflection events on the seismic section. Clearly the strongest events occur between pegs 50 and 65, with a strong event at 70msecs between pegs 75 and 80. There is also a deep event at 170msecs laterally consistent between pegs 50 and 90. Few reflections occur around peg 40.

Interpretation

The interpretation of the Keekle Extension reflection line is shown in figure 8.16. The subsurface structure is one which is highly faulted, with normal faults separating blocks of solid geology of varying dips. Overall the strata exhibit a general apparent dip towards the south west. An attempt has been made to define the fault positions and dips, although it it difficult tracing the faults at depth. Between pegs 40 and 46 there is a zone where no coherent reflections occur, This may be due to a near surface feature impairing the data quality.

Overlaid onto the seismic interpretation is the geological interpretation by the Opencast Executive based solely on borehole information. Up to peg 80 both techniques come to similar conclusions regarding the near surface. Beyond peg 80 the seismic interpretation suggests two near vertical faults not apparent on the borehole interpretation.

KEEKLE REFLECTION LINE

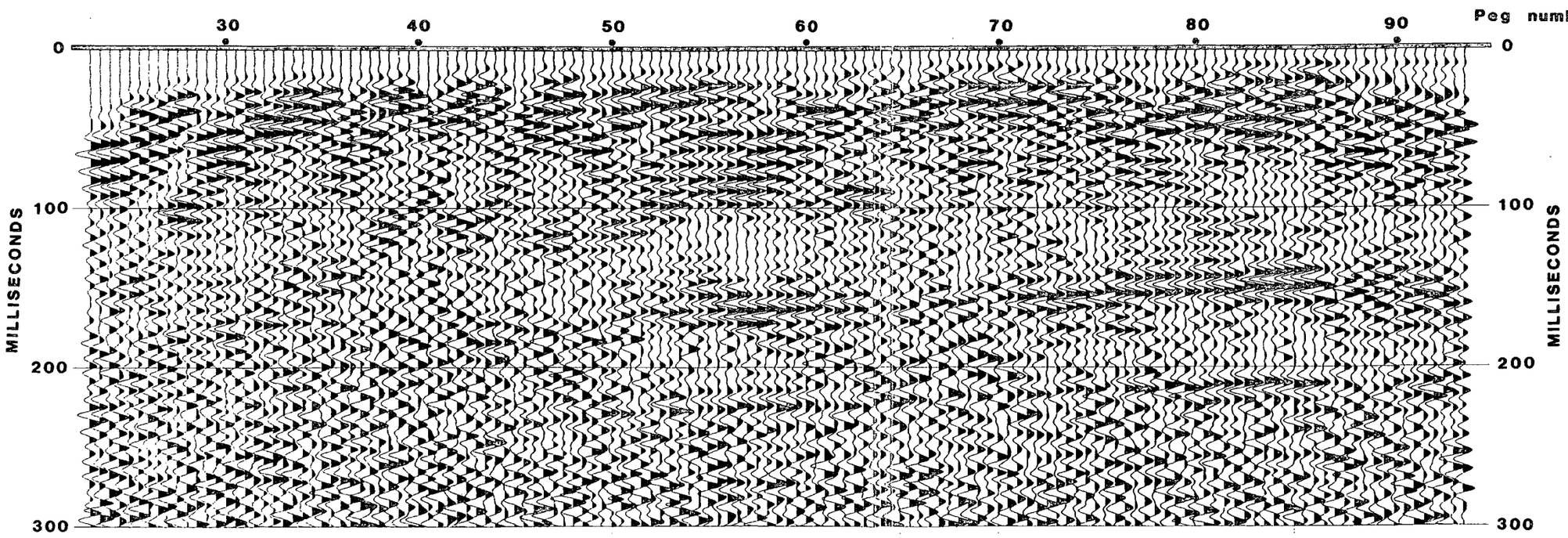

PROCESSING SEQUENCE

Band Pass
40/70/150/200 Hz

Trace equalisation
(energy)

Normal moveout correction

Autostatics
maximum shift : 3msec

Stack

Time variant band pass
100 msec (80/150 Hz)
220 msec (65/120 Hz)

100 mSec A.G.C. applied

TIME	VRMS	VINT
0.000	2.400	2.400
0.050	2.700	3.000
0.100	2.800	2.944
0.150	3.400	4.750
0.185	3.600	5.192

Figure 8.14

KEEKLE REFLECTION LINE

TRUE AMPLITUDE PLOT

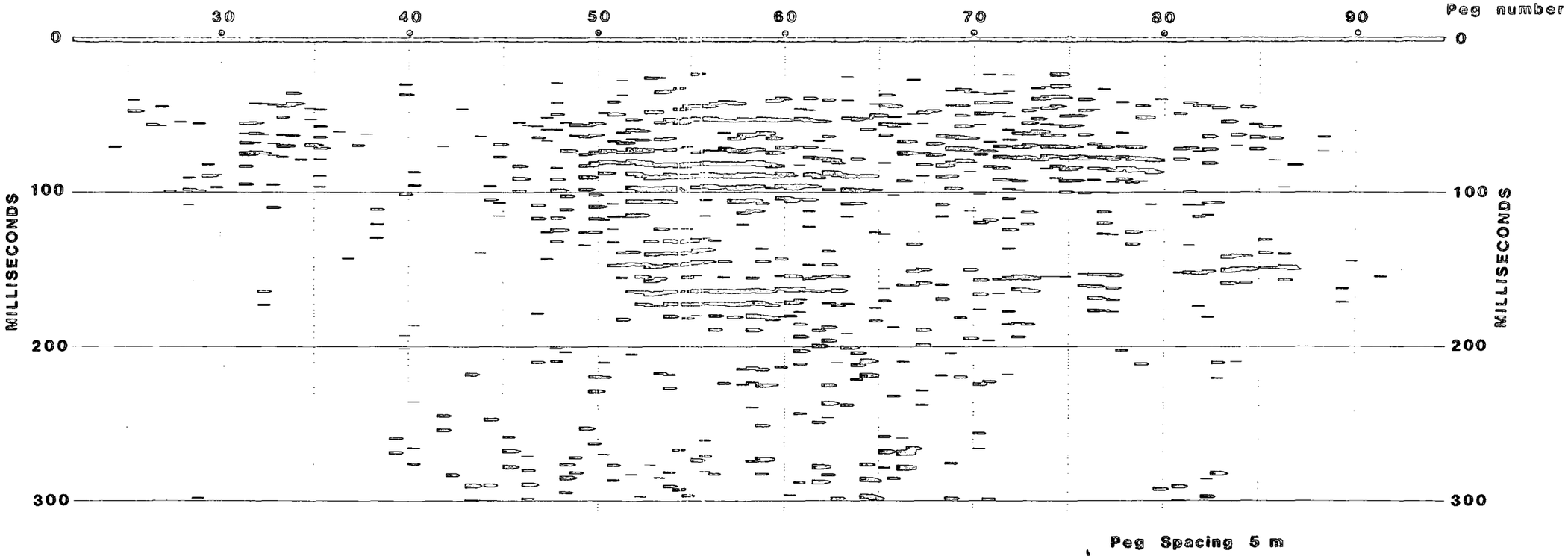

Figure 8.15

Neither the seismic nor the borehole interpretation allows for the presence of the boundary fault in its assumed location from the geological map (figure 8.1). Therefore the fault position on the map must be incorrect, the true fault location being some distance eastward. The seismic interpretation displays a consistent character up to peg 86, where a near vertical fault is interpreted. Whether or not this could be the boundary fault is unclear, as it occurs at the extreme eastern end of the line.

If the geological cross-section (figure 8.1) is correct, the Permo-Triassic strata would appear at rockhead on the downthrown side of the boundary fault. One would expect a change in the character of the seismic section if the shots and receivers were on the Permian Brockram. Up to peg 86 this appears not to be the case. Therefore if this is so, we must still be on Carboniferous strata up to peg 86.

Using the velocity function obtained from the velocity analysis, the section can be re-plotted so that the vertical and horizontal scales are approximately equal (figure 8.17). The section now displays true dips.

The seismic section shows three bands of reflections. Firstly between 0 to 120msecs (0 to 170m depth), originating from the Productive Coal Measures, which exhibit a typical cyclic sequence. The seismic wavelength through these measures is approximately 20m. Therefore the thin coal seams would not be resolved on the seismic data. The reflections would originate from thick sandstones within the sequence. Between 120 and 150msecs (170 to 220m depth) there is a quiet zone of poor reflections. This

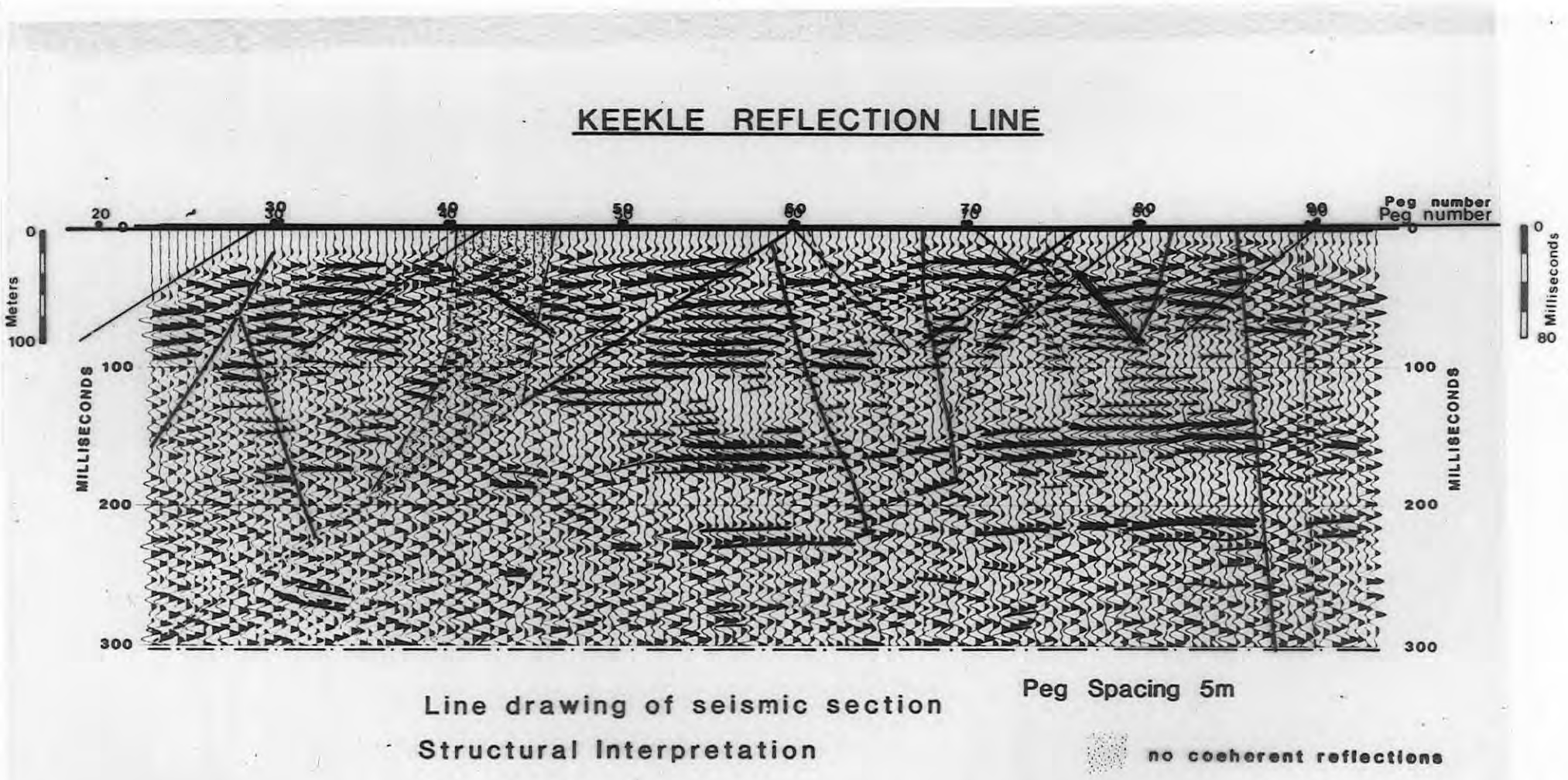
KEEKLE REFLECTION LINE
20
30
40
50
60
70
80
90
Peg number
Peg number
0
Meters
100
MILLISECONDS
100
200
300
0
80 Milliseconds
Line drawing of seismic section
Structural Interpretation
Peg Spacing 5m
no coeherent reflections
Interpretation of fault positions using borehole information only
conversion velocity
2500 m/sec

Figure 8.16

Keekle Extension
True depth section

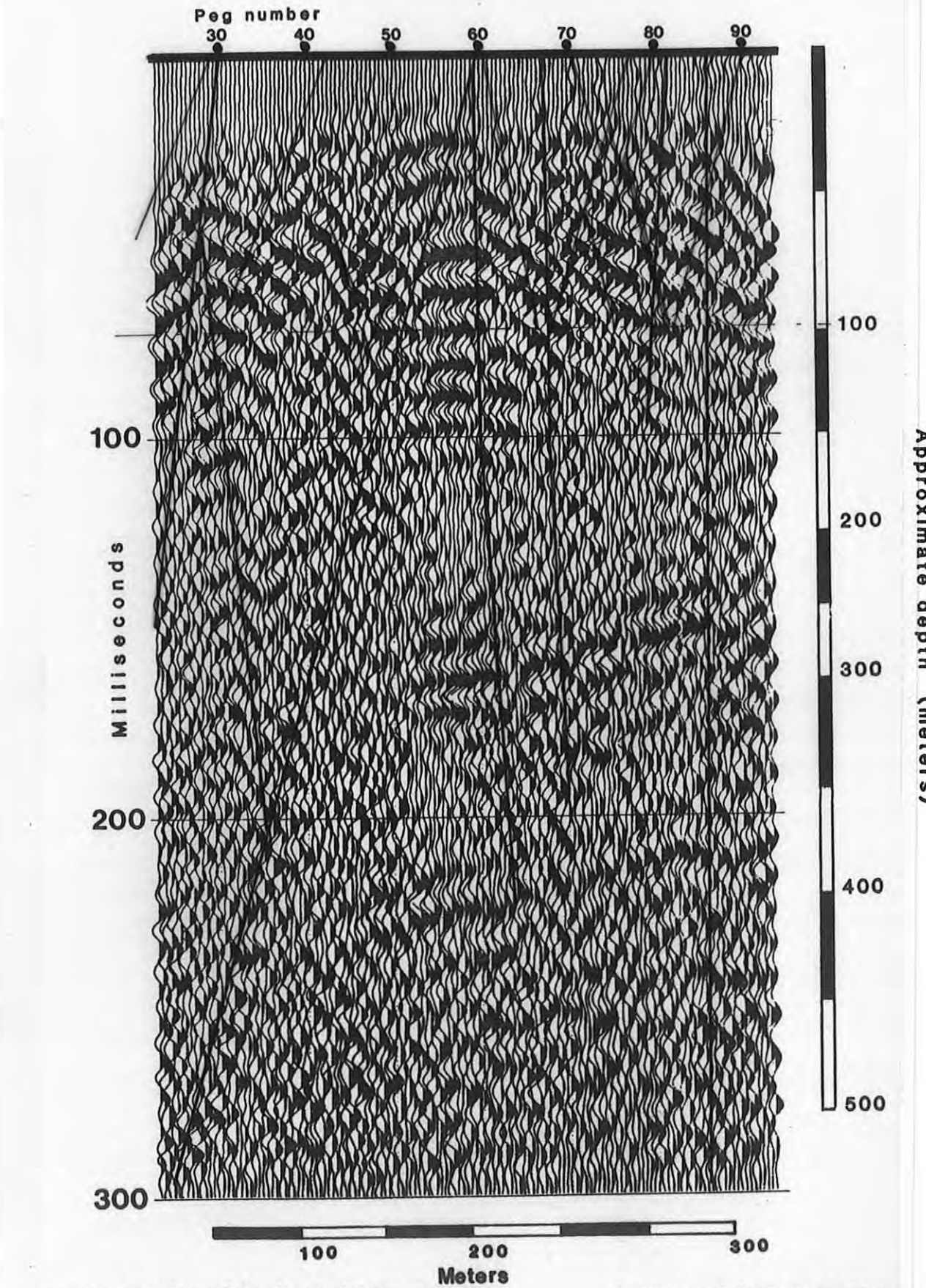

Interpretation of fault positions and dips using borehole information only.

Structural Interpretation

Figure 8.17

corresponds to the grits of the Namurian, where one would not expect large reflection coefficients to occur. Below 150msecs (220m) there are two strong reflection events at 170 and 220msecs (280 and 360m depth). These probably originate from the First and Second Limestones at the base of the Namurian and within the Dinantian sequence.

The original objective of the survey, to locate the boundary fault, has not been realised. This is due to the fact that the fault must be located further eastwards than previously thought.

It was originally hoped that the seismic line would have extended further eastwards than it did. This was due in the main to the problems encountered in drilling the shot holes into the very hard rockhead. A considerable amount of the available time was lost due to this.

8.2 P WAVE REFRACTION LINES

The site was re-visited in May 1984, when an attempt was made to extend the survey eastwards. Due to the fact that other projects were being undertaken at different sites at this time, time constraints did not allow us to extend the reflection line. As a result only P wave refraction surveys could be undertaken. It was hoped that these surveys would at least reveal the position of the boundary fault at rockhead.

Two P wave refraction surveys were carried out. One along the trend of the seismic line, the other in a NE-SW direction (figure 8.2). The data were acquired using 1oz explosive charges buried

at a depth of 1.5m in the overburden and 5m peg spacing was used for the surveys. Only two days were allotted for this work.

Figures 8.18 and 8.19 show the raw field data and the velocity analyses carried out on the data. The results from line 1 show a dramatic uniformity in refractor velocity across the line, displaying a velocity of 2404m/sec. Line 2 displays a significant break in refractor velocity at peg 20. West of peg 20 the refractor velocity is 2745m/sec. East of peg 20 the refractor velocity is 2308m/sec, which would correspond to the refractor velocity found on line 1.

Figure 8.20 shows the final interpretations of the refraction data at this site. The Generalized Reciprocal Method (Palmer 1980), was used for the interpretation. Line 1 shows an apparent ridge in rockhead at peg 30. This depth change is not well constrained due to the lack of time spent in carefully monitoring the overburden velocity over the whole line. The ground conditions were not consistent as there was a bog between pegs 21 and 25. Line 2 displays a consistent overburden thickness of 7m. There is a significant change in refractor velocity at peg 20.

The anomaly at peg 20 on line 2 is along strike from the near vertical fault interpreted at peg 87 on the reflection line. Therefore these two features are probably defining the same structure (figure 8.21). Whether or not this fault is the hypothetical boundary fault is uncertain at present, as it lies outside the present prospective opencast boundary limits, so no drilling has been carried out in this area.

Keekle Extension Line 1 P wave

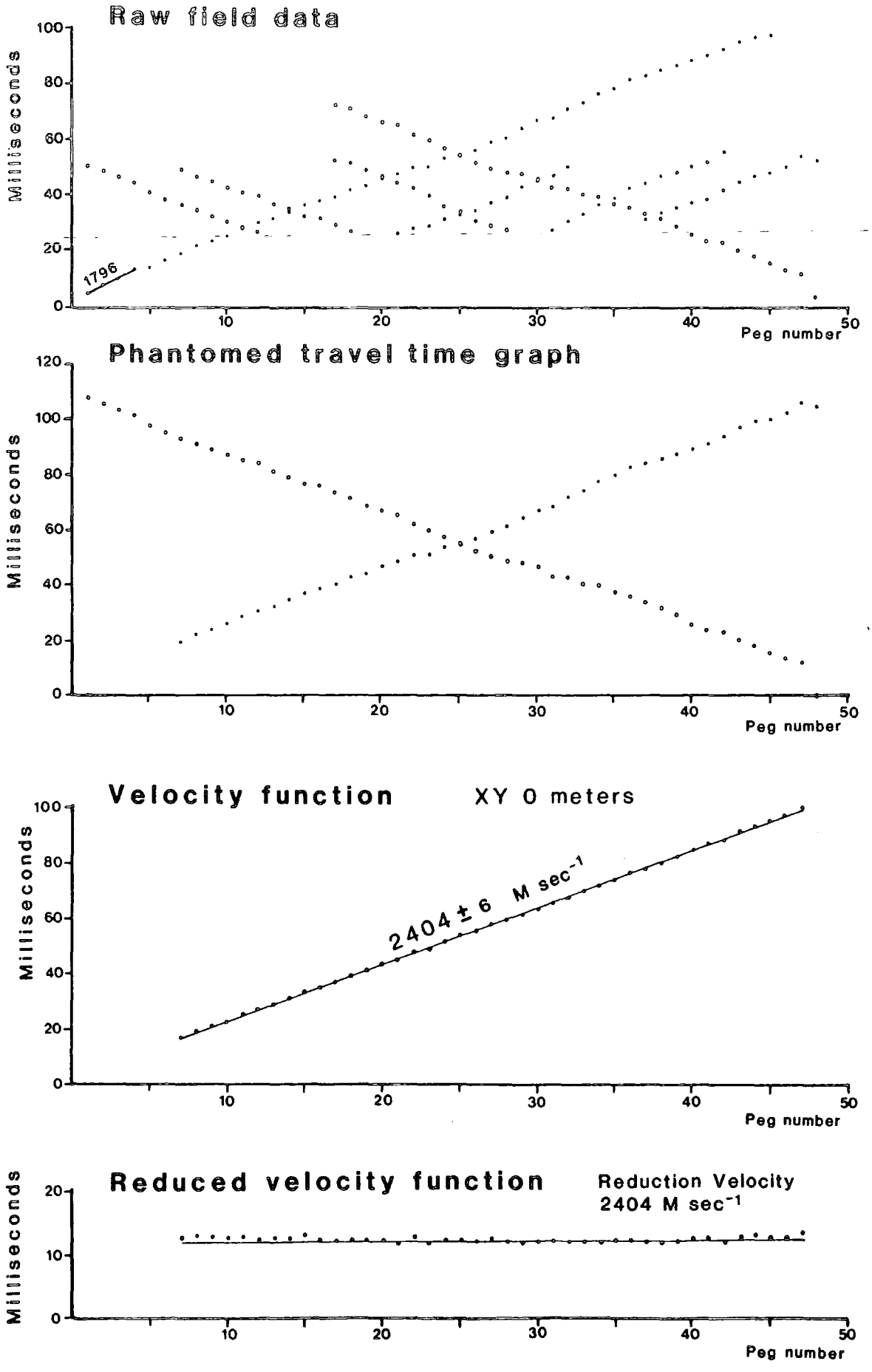

Peg spacing 5 meters

Figure 8.18

Keekle Extension Line 2 P wave

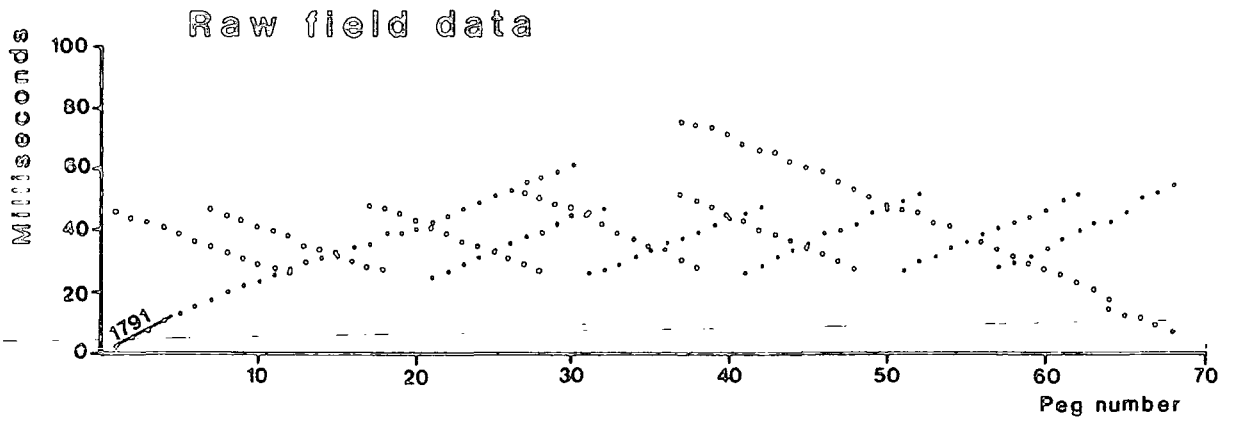

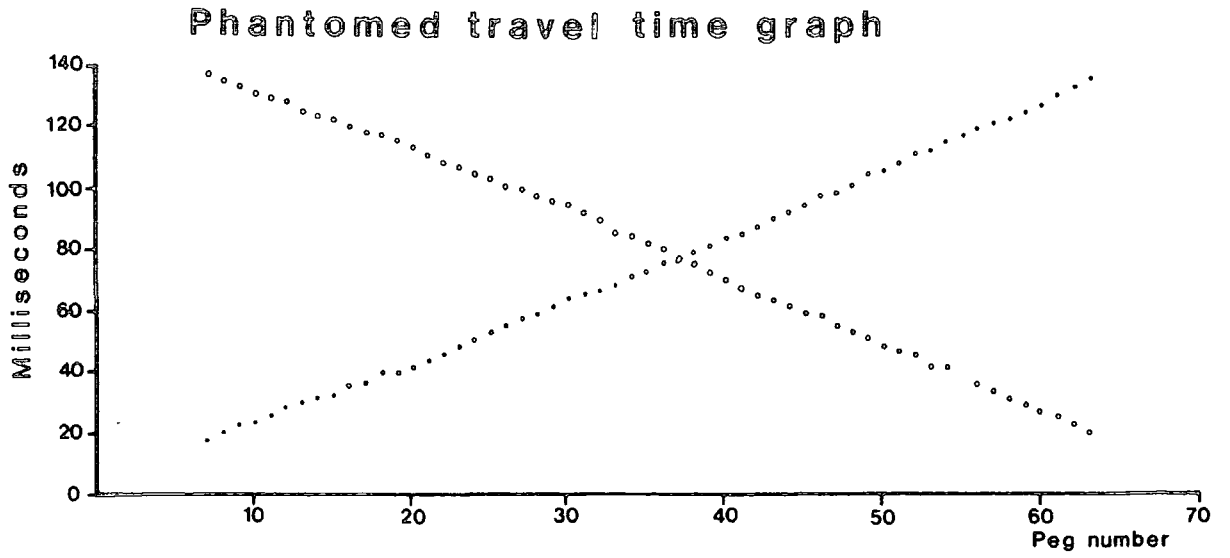

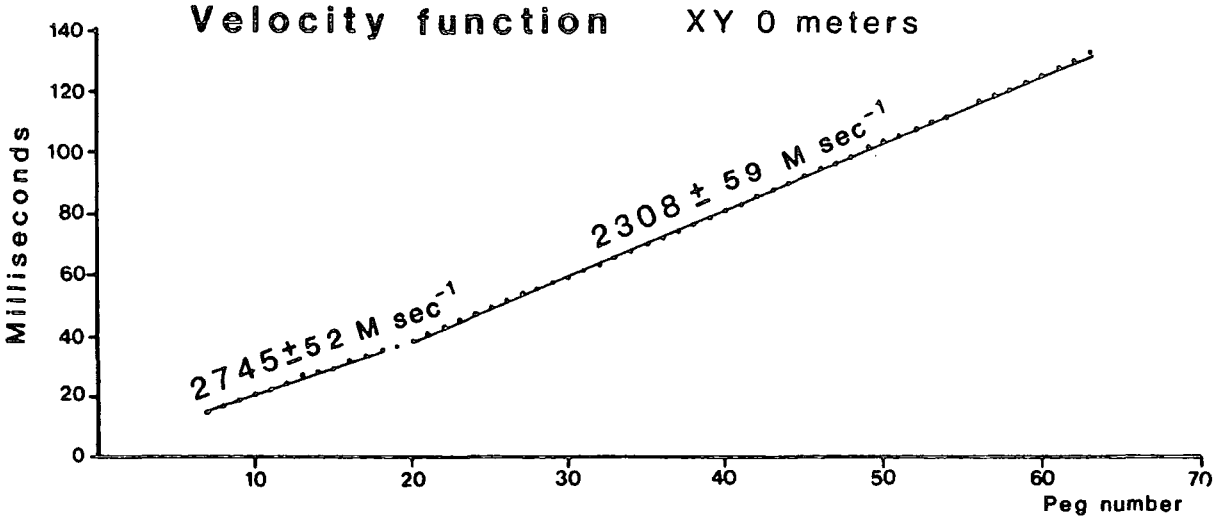

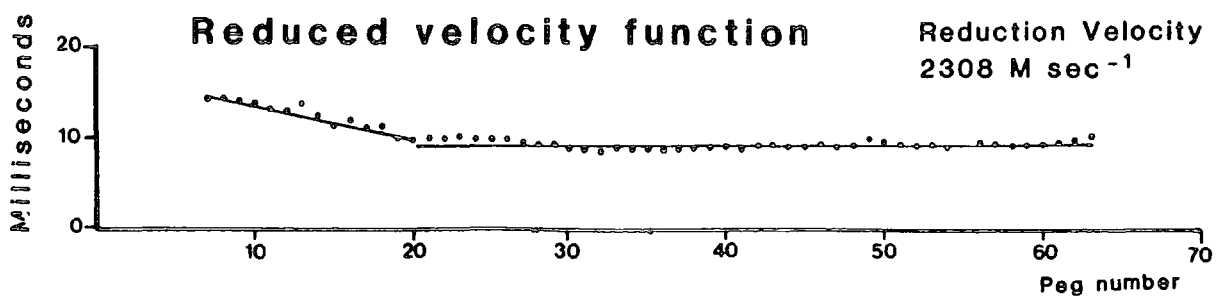

Peg spacing 5 meters

Figure 8.19

Keekle Extension Interpretations

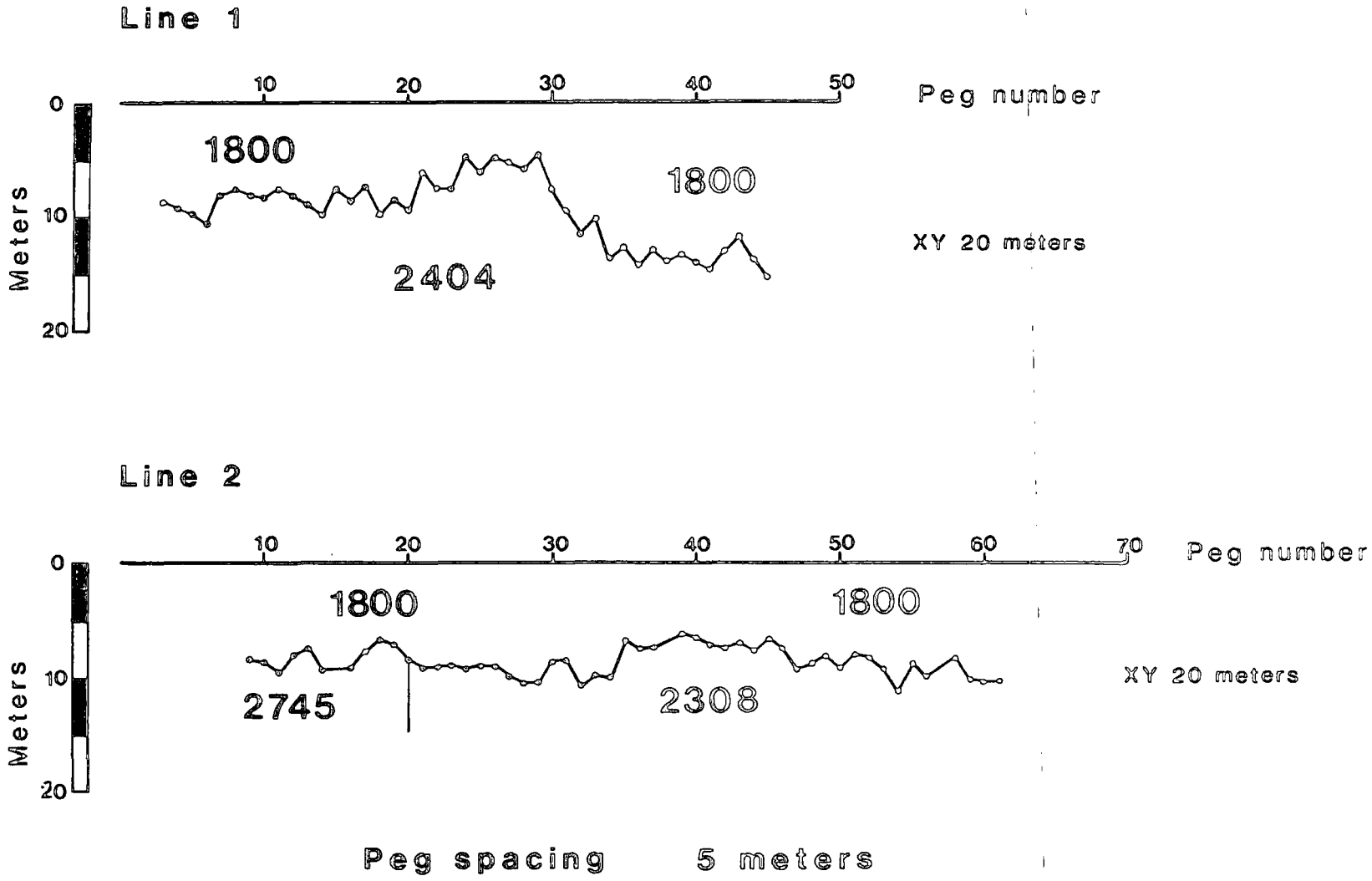

Figure 8.20

Interpretation of Refraction Results

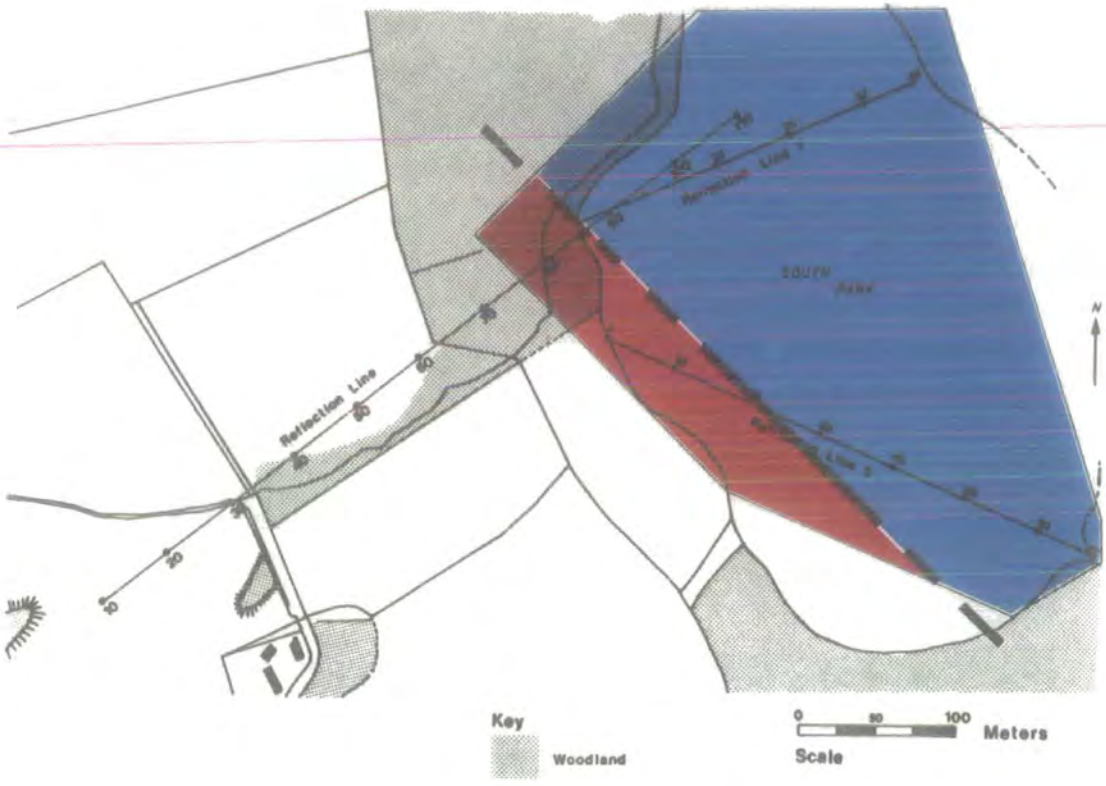

Refractor Velocity 2300 to 2400 m/sec

Refractor Velocity >2700 m/sec

★ Vertical Fault seen on Reflection Line

Figure 8.21

CHAPTER NINE

STOBSWOOD : SITE NO. 6

Stobswood is a prospective opencast coal site situated near the village of Tritlington in Eastern Northumberland. The site is located on the extreme north western edge of the Northumberland coalfield.

The problem under investigation at this site is the accurate location of a major fault which crosses the northern part of the site. This fault is the western extension of the Grange Moor Fault that was first studied at Hemscott North. The Grange Moor Fault is one of series of major faults found in the Northumberland coalfield. It has a NE-SW trend at Stobswood and downthrows the Carboniferous strata toward the south. In the central area of the Stobswood site, the fault location is accurately known from borehole information gathered on a dense 60m grid pattern. The fault plane has a dip of 50 degrees towards the south east, and has a large unknown throw. The fault would form a boundary to any prospective opencast working.

The site was first visited in September 1984. The objective at this site is to locate the fault precisely along strike to the west and east of the central area where there is little or no borehole information available. Two seismic lines were laid out for this purpose; both were investigated using P and S wave refraction techniques (figure 9.1).

STOBSWOOD

Location of seismic refraction lines

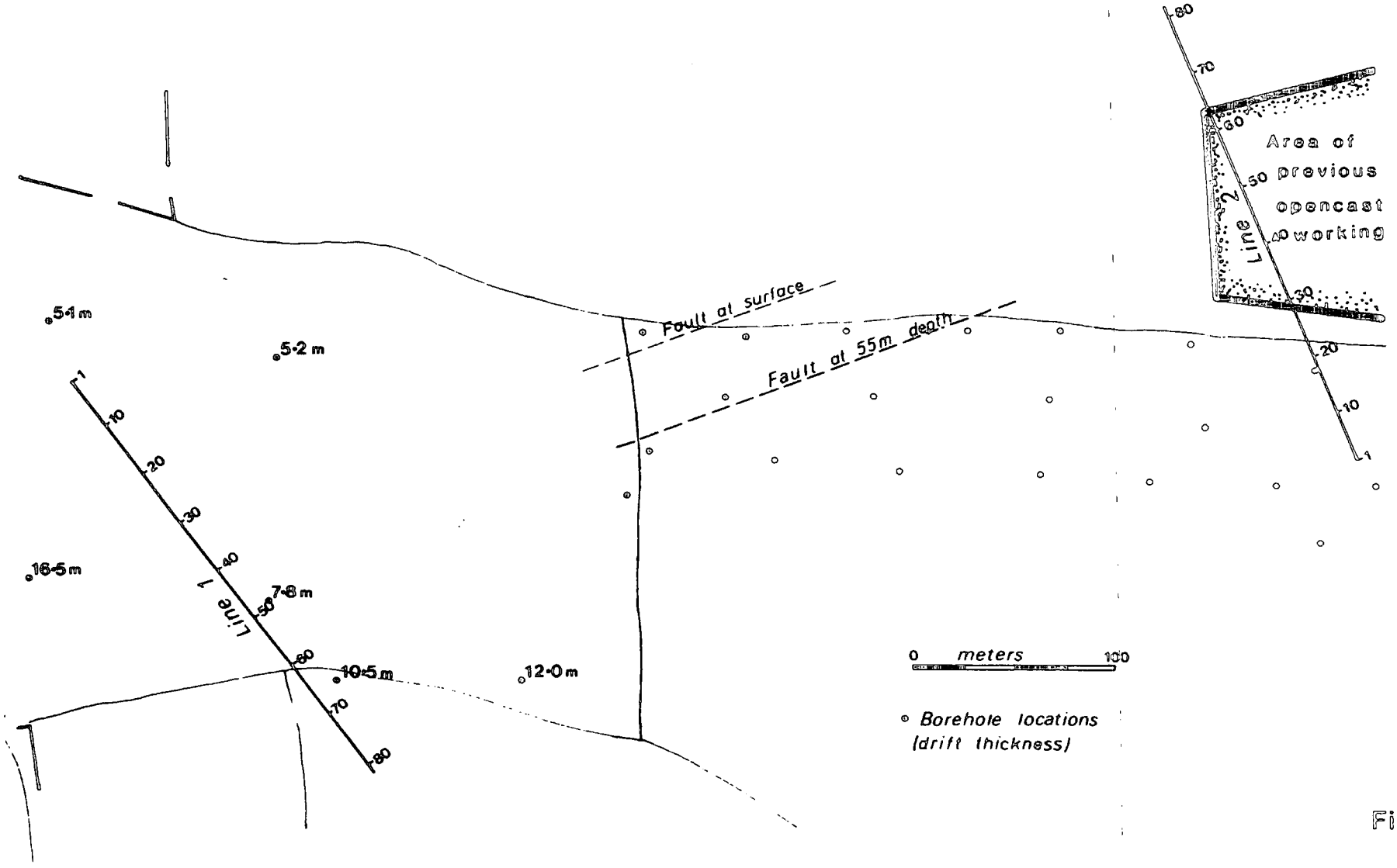

Figure 9.1

Line 1

Line 1 was laid out at this site using a 3m peg spacing perpendicular to the estimated fault trend, to the west of the central area.

P Wave Data

The P wave source was an explosive charge (1/4oz to 2oz) buried at a depth of 1.5m in the glacial drift.

12 channel records were acquired using a variety of shot to geophone offsets from zero to 120m, with a shot spacing of 30m. Data were acquired in both the forward and reverse directions. Figures 9.2 and 9.3 show the P wave field records recorded along line 1. The field records display an extremely complex set of first arrivals. There is no consistent refractor along the line. The refracted arrivals tend to be overtaken by a deeper higher velocity refractor or die out, especially in the central area of the line. Also high velocity refracted arrivals continue into lower velocity segments. The most complex first arrival patterns occur between pegs 30 to 50.

Where both the forward and reverse refracted first arrivals can be assumed to originate from the same refractor, using criteria such as apparent velocity, intercept time and end to end times as a guide, the Generalized Reciprocal Method (Palmer,1980) was used on the reversed data for interpretation. When no overlap exists between the forward and reverse arrivals, a dipping planar layer interpretation technique was used on the data. Single ended

Field Records

Line 1 P wave

FORWARD SHOTS

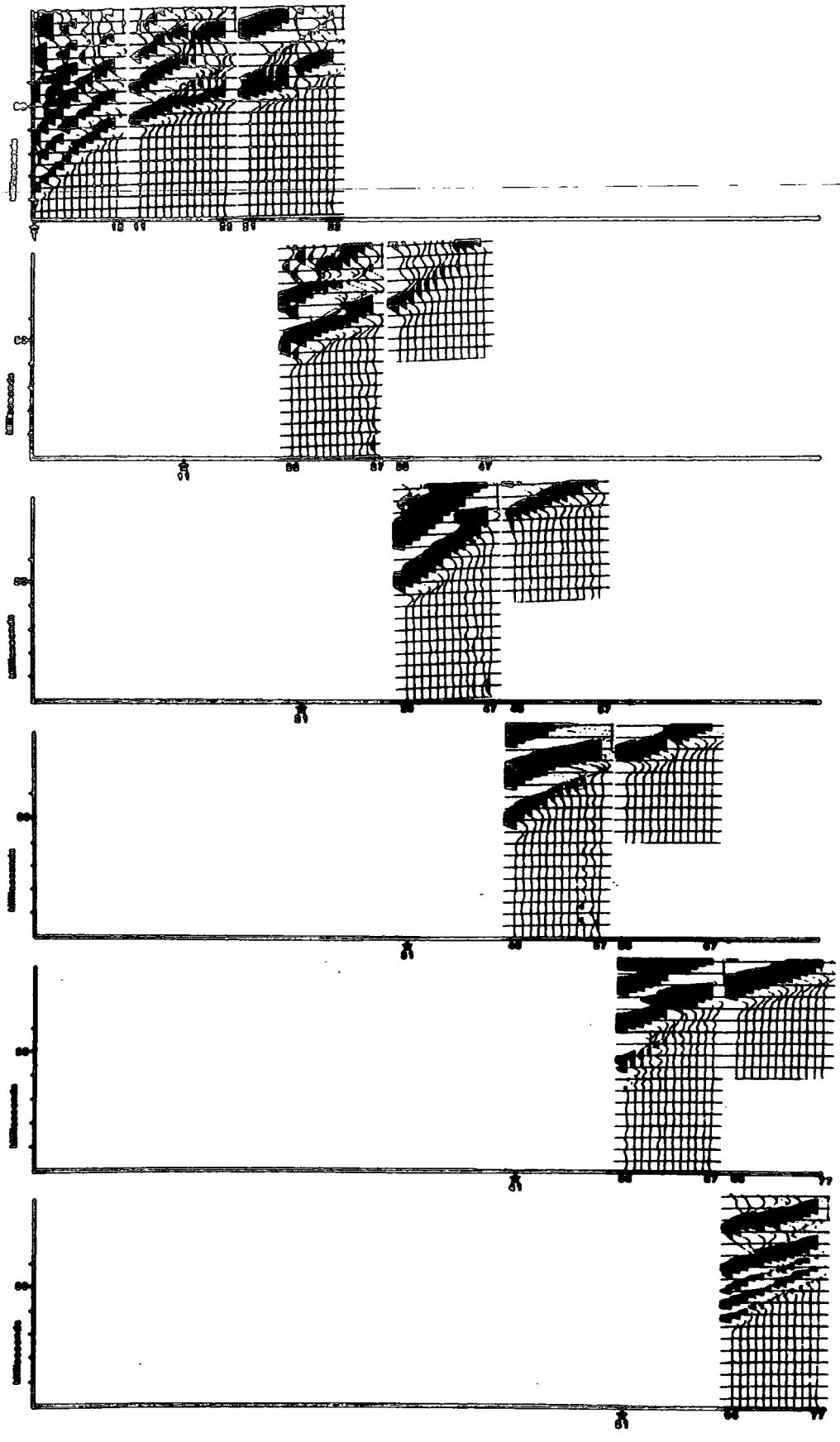

← Peg numbers →

Figure 9.2

Field Records

Line 1 P wave

REVERSE SHOTS

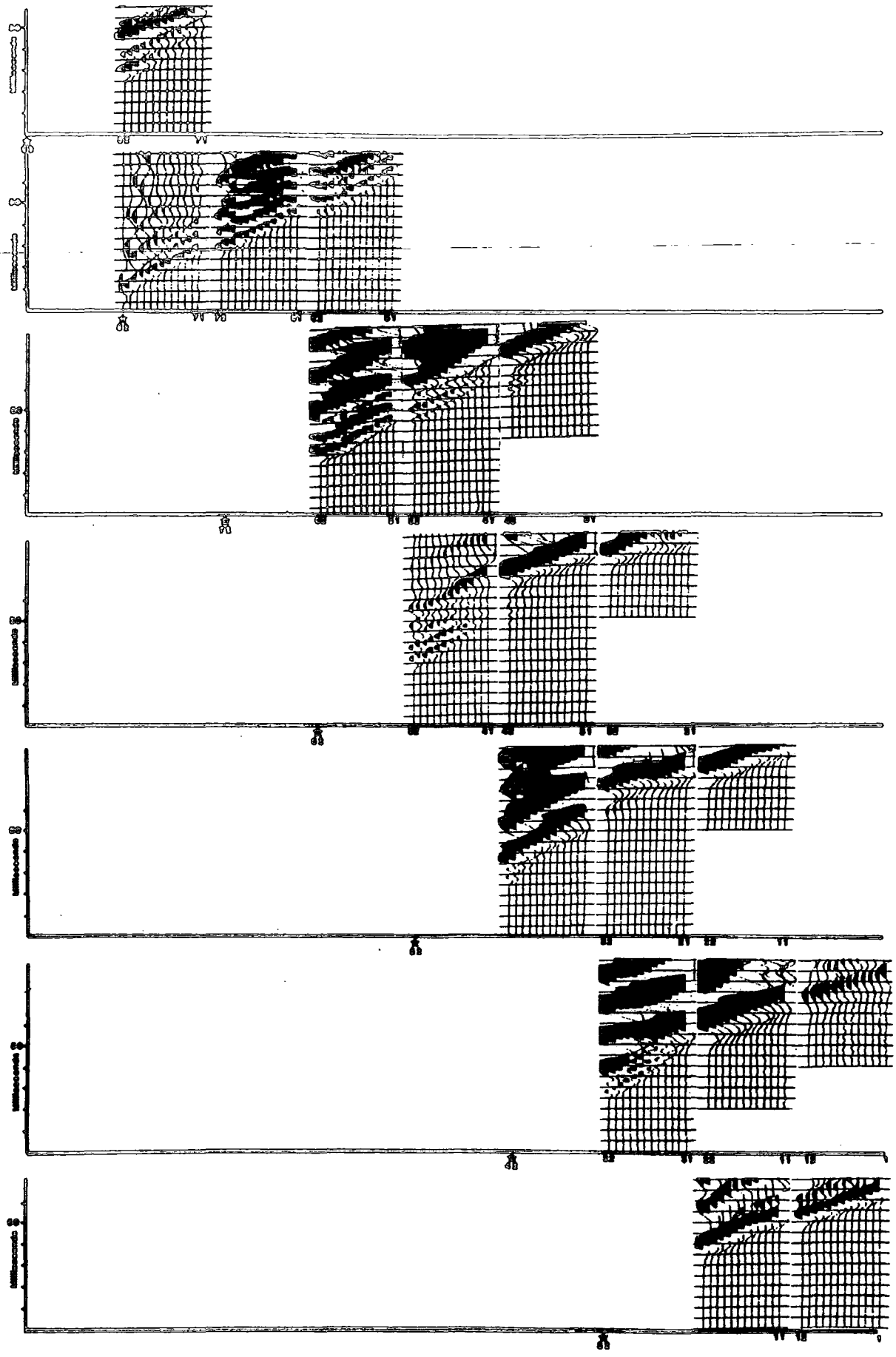

← Peg numbers →

Figure 9.3

intercept times were also used to estimate the depth of the boundary between the overburden and the first refractor.

Figure 9.6 displays the final seismic model produced to account for the intricate first arrival patterns seen on line 1. The model is complicated: it displays two distinct regions. Between pegs 10 and 30 a simple two-layer model fits the data, with a layer of P wave seismic velocity 1042m/sec overlying a refractor of velocity 2543m/sec at a depth of 13m. This boundary is deeper than the rockhead boundary depth given in the borehole logs, and is probably the base of weathering of the sandstone at rockhead. Between Pegs 40 and 80 a very different model is required. A three-layer model is needed to explain the complex first arrivals recorded in this area. The upper boundary between the 1050m/sec surface layer and the underlying 1826 to 2074m/sec refractor at a depth of 4 to 6m appears to be coming from within the drift layer (from borehole information). This boundary also gives rise to high frequency first arrivals on the field records. This boundary is probably the top of the water table, i.e. the boundary between dry and wet unconsolidated material. The presence of water has a significant effect on the P wave velocity through unconsolidated material.

The rockhead boundary (as given in the borehole logs) appears to be transparent to the P wave refraction technique. This result has been seen at other sites.

The deep refractor (2821m/sec) at a depth of 40m could only be defined using a planar dipping layer model. It appears too deep to be the base of weathering of the sandstone at rockhead, so it

must therefore originate from a sandstone deeper within the Carboniferous sequence.

Due to the very complex arrival patterns seen between pegs 30 to 40, some of which may even be diffractions, no structure can be defined in this region. Therefore the fault location can only be pinpointed within a 30m wide zone using the P wave refraction technique at this site.

S Wave Data

Line 1 was also surveyed using the S wave refraction technique. Short offset refraction spreads were recorded along the line to determine the near surface velocity structure and the optimum shot to first geophone offset required for profiling. Figure 9.4 displays the results of this initial survey.

The near surface velocity structure appears simple from the graphs (figure 9.4). There is a direct velocity of about 100m/sec through the surface soil layer. The underlying refractor (around 300m/sec) corresponds to the glacial drift layer. Beyond offsets of 27m a refractor of around ~~100~~ 1000 m/sec is recorded on the field records. The depth of this refractor varies from 5m at the northern end of the line to between 12m and 13m at the southern end. These depths show good agreement with the depths to rockhead recorded by the boreholes in the vicinity of line 1. Therefore one can conclude that the S wave refraction technique is picking up the rockhead boundary as a refractor. An optimum profiling offset of 30m was also determined from these graphs.

Stobswood Line 1 S-wave

Near offset spreads

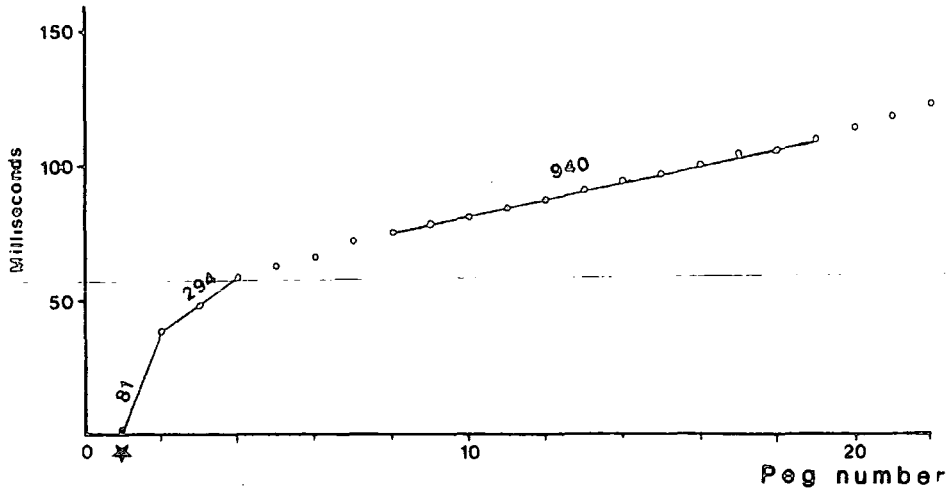

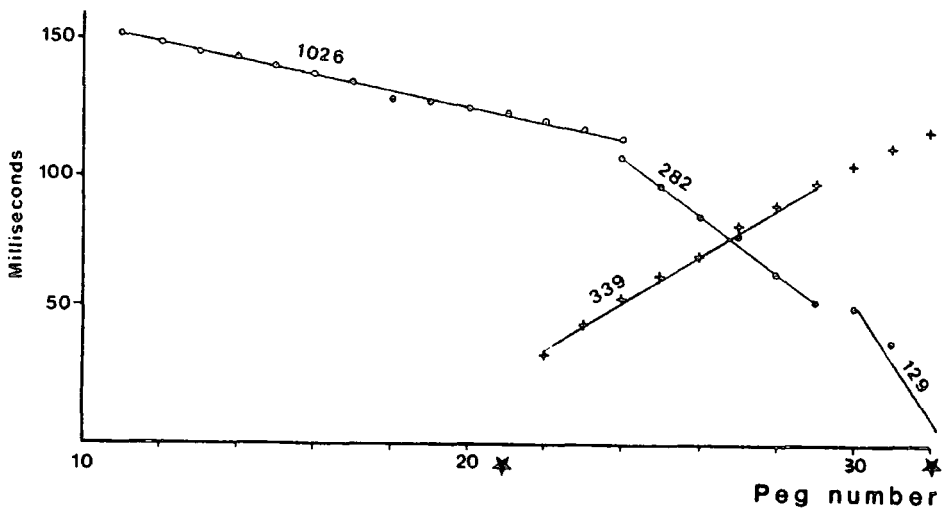

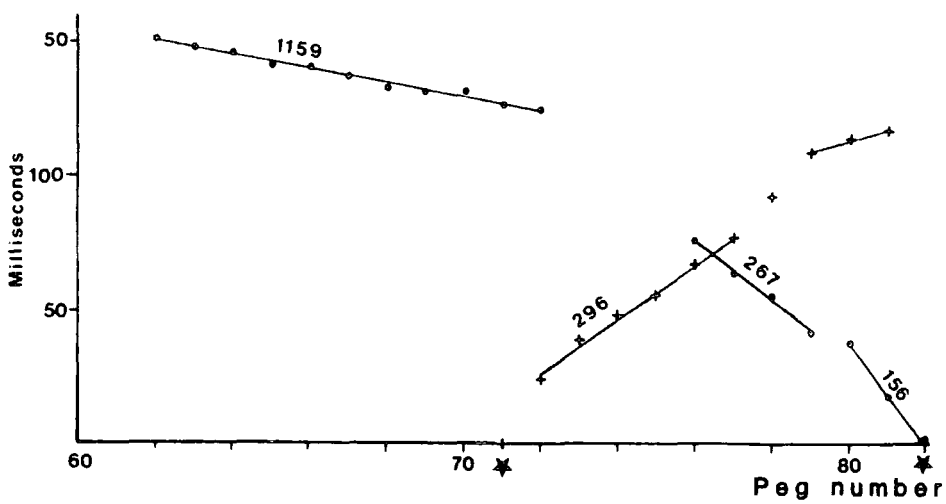

Models

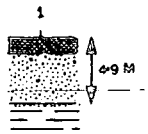

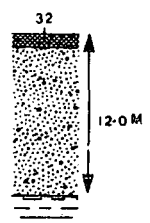

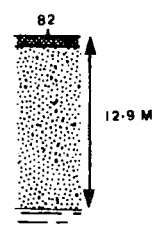

★ Shot point

Velocities in M/sec

Figure 9.4

The line was profiled in both the forward and reverse directions to obtain complete coverage of the rockhead refractor along the line. From this, a phantomed traveltime graph was produced (figure 9.5). Using the phantomed travel time graph, the GRM was used for the interpretation. The velocity function graph (figure 9.5) displays two distinct linear segments of 906m/sec in the north and 1002m/sec in the south, separated by a zone of relatively low velocity (706m/sec) between pegs 25 and 40.

From velocity and refractor depth considerations, the calculated optimum XY spacing for the generation of the time depth function varied from 0.7 to 3m. As the XY value could only be increased by increments of 3m, in the final analysis an XY spacing of zero was used. The time depth graph (figure 9.5) reveals a rapid increase in the depth to the rockhead boundary between pegs 25 and 32 (assuming the overburden velocity is near constant).

Before the time depth values were depth-converted the effect of the low velocity (100m/sec) soil layer was subtracted from the time depth values, using a curve produced by interpolation of half intercept times calculated from the near offset spreads (figure 9.5). The depth to rockhead was then accurately calculated and found to range from 5m in the north to 13m in the south (figure 9.6), as with the short offset spreads. There was a rapid increase in depth around peg 30, agreeing with the borehole information in the area (figure 9.1).

The exact fault position appears unclear and can only be determined within a 36m wide zone of low refractor velocity between pegs 26 and 38. The rapid increase in drift thickness

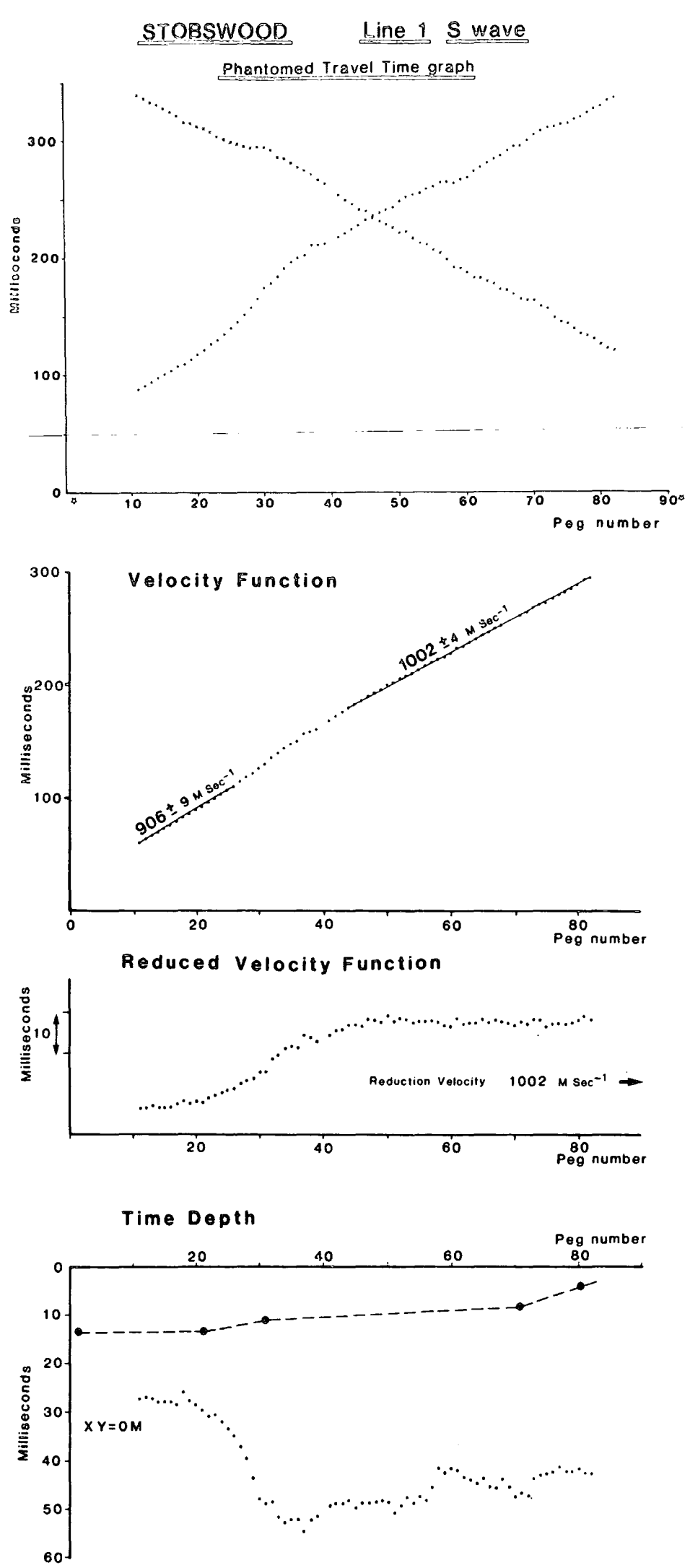

Peg spacing 3 meters

Figure 9.5

Stobswood Line 1

Interpretation

S-Wave

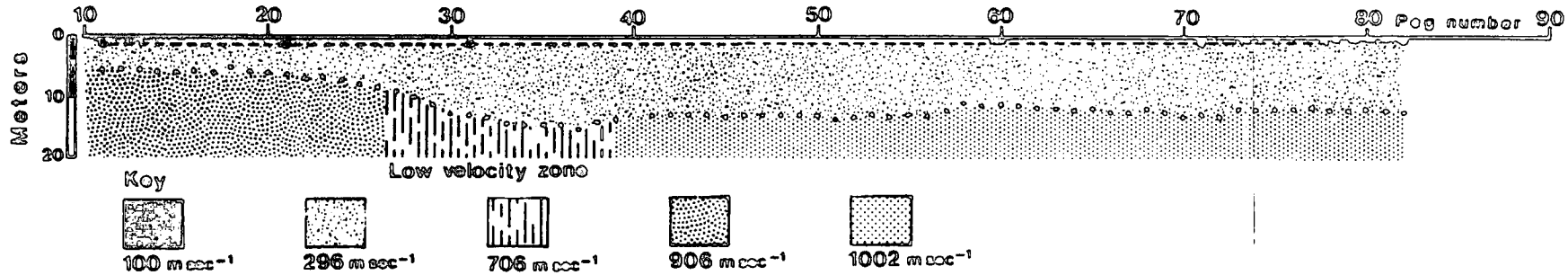

Peg spacing 3 meters

P-Wave

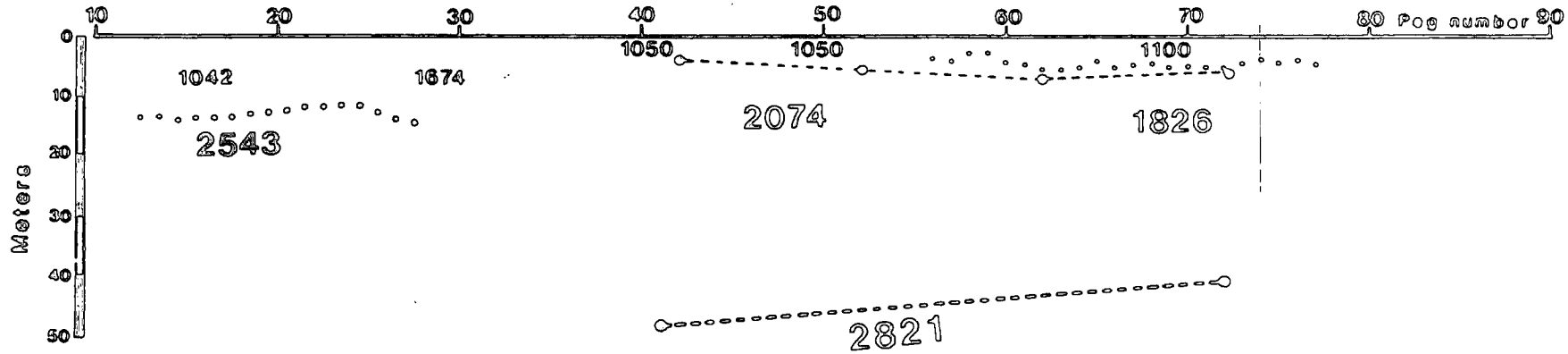

Figure 9.6

around peg 30 may be a fault-related feature, caused by differential erosion of the rockhead because of the different lithologies found at rockhead on both sides of the fault.

The fault may not be a simple single fracture, but may be a series of fault planes occurring in a zone, as is seen at Hemscott North.

The S wave technique displays a much simpler final result than the P wave technique along the same line (figure 9.6). To the P wave technique the rockhead boundary appears transparent. This results in a complicated first arrival pattern which requires much effort in interpretation before the first break information can be fully understood. The S wave technique on the other hand simply profiles rockhead and defines the S wave velocity of the rock below this boundary, thus making the identification of the fault position a much simpler procedure.

Line 2

Line 2 is situated to the east of the central area where the fault location is accurately known. The line was shot using both the P and S wave refraction techniques. Figure 9.1 shows the line crossing an area where the ground has been previously opencast. This information was not known when the seismic line was laid out and shot, or when the data was first analysed.

P Wave data

As with line 1, a 3m peg spacing was used for the survey using a variety of offsets (in light of the complex results from line 1). From the field records it was found that beyond a shot to geophone offset of 24m only one refracted arrival was seen. The data were acquired using a 90m shot to first geophone offset. By analysing the direct arrival on the field records, a velocity for the overburden of 1187m/sec was calculated.

The line was profiled in both the forward and reverse directions and the resultant phantomed traveltime graph is shown in figure 9.7. The data were analysed using the GRM. The velocity function graph shows a fluctuating refractor velocity across the seismic line. The refractor velocity increases from 1613m/sec in the south to 2858m/sec in the north (figure 9.7).

The time depth function (figure 9.7) shows a very large anomaly, indicating a large fluctuation in the depth to the refractor (assuming the overburden velocity is constant). This result was difficult to understand when the data were first analysed because the presence of the old opencast area was not known. It seemed impossible to fit the results to a structural model such as we see on line 1. When the presence of the old workings was known, the results became simpler to understand. It appears that the refraction results are simply picking out the base of the old workings, which are now backfilled with unconsolidated material.

STOBSWOOD Line 2 P wave

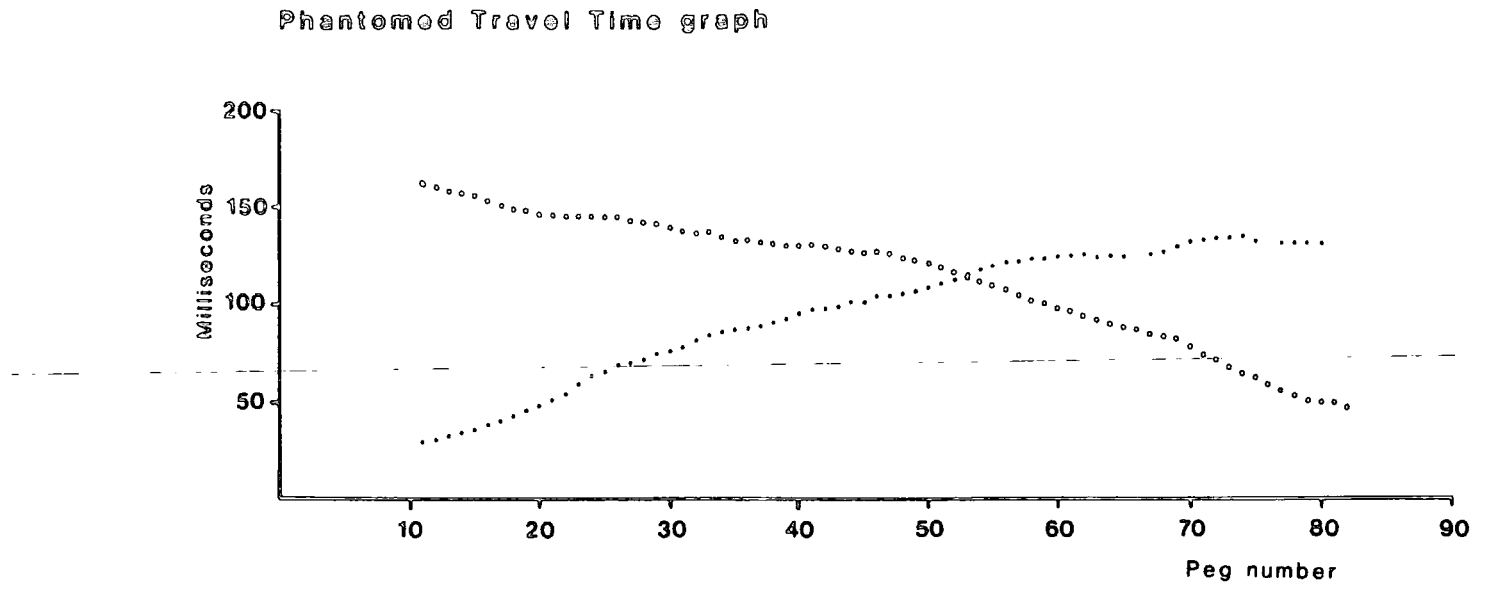

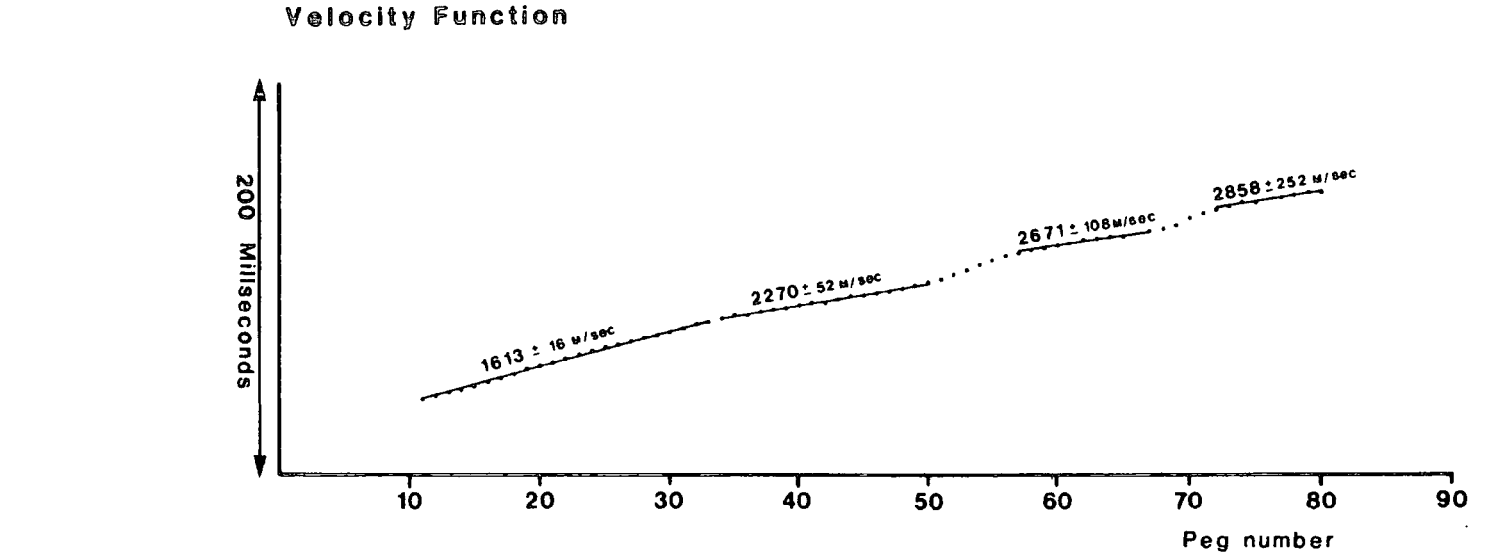

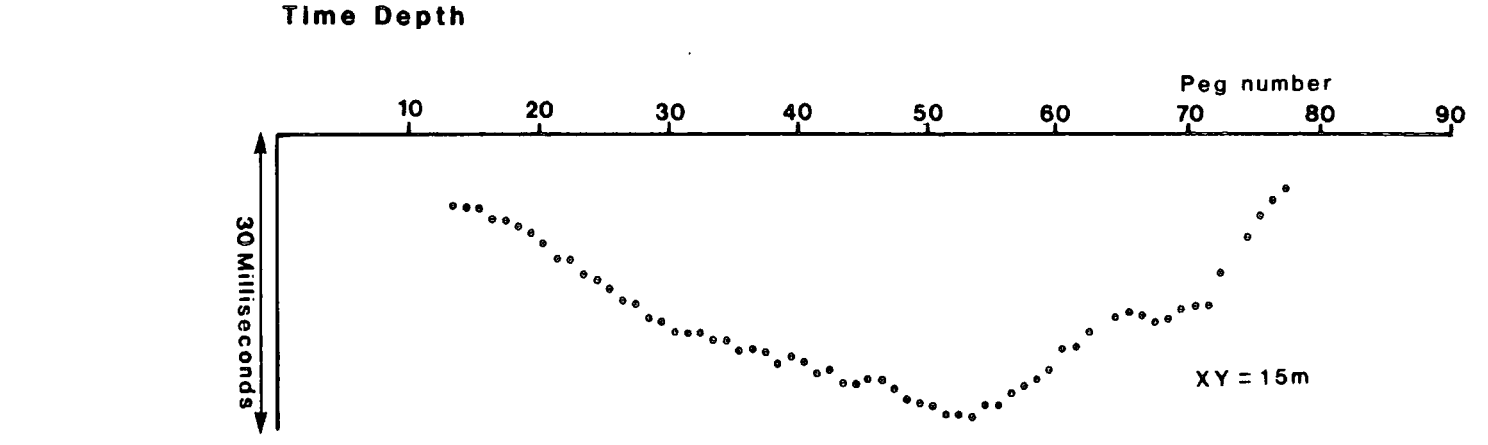

3m Peg spacing

Figure 9.7

The time depth function was calculated by incrementally increasing the XY value to produce a variety of functions. The optimum value of 15m was chosen because it gave the maximum amplitude to the function. This is a good way to determine the optimum value when you are dealing with a V-shaped depression (Palmer, 1980). Using the overburden velocity, refractor velocities and the time depth values the data were depth-converted. The resultant depth values are tied into borehole at peg 18, which gave the depth to the old workings of 10.5m at this point. The maximum depth of the old workings calculated from the seismic data is 36m. Borehole information from the vicinity gives a maximum depth of 25 to 30m.

Using a depth of 36m and the known overburden and refractor velocities, the optimum XY spacing can be calculated using Snell's law. From this, the optimum XY value can be seen to fluctuate between 20 to 40m, much larger than the value used in the analysis. This discrepancy can be attributed to the lack of knowledge that we have of the overburden velocity. The seismic velocity may vary quite considerably in the backfill material due to its inhomogeneity. The velocity would also increase with depth due to consolidation. The depth of the old workings calculated from the seismic refraction results is not well constrained. Although the amplitude may be in error, the overall cross-sectional shape of the area is quite accurate.

Figure 9.8 also shows a schematic cross section of the old workings and its relation to the geological structure. Near surface coal seams have been exploited south of the Grange Moor Fault. Once the fault was reached the excavation would have been

Stobswood Line 2

Seismic interpretation

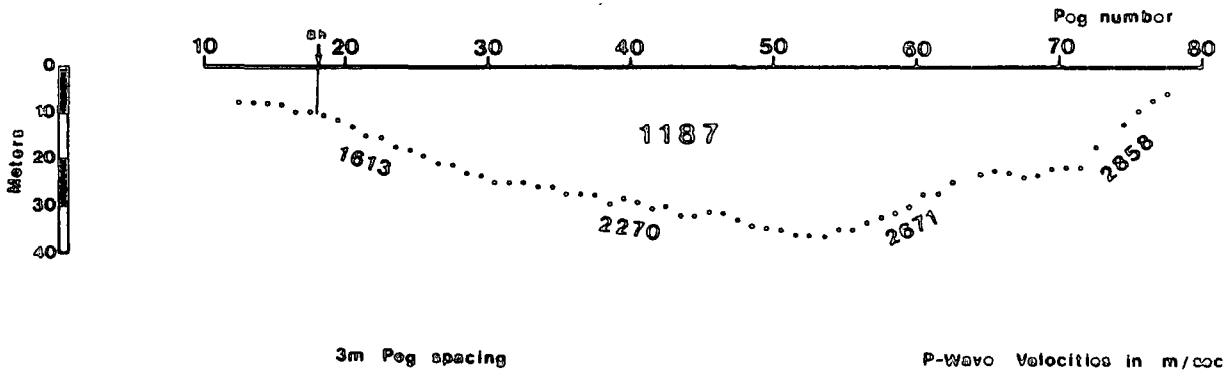

3m Pog spacing

P-Wave Velocities in m/sec

Schematic structural cross section

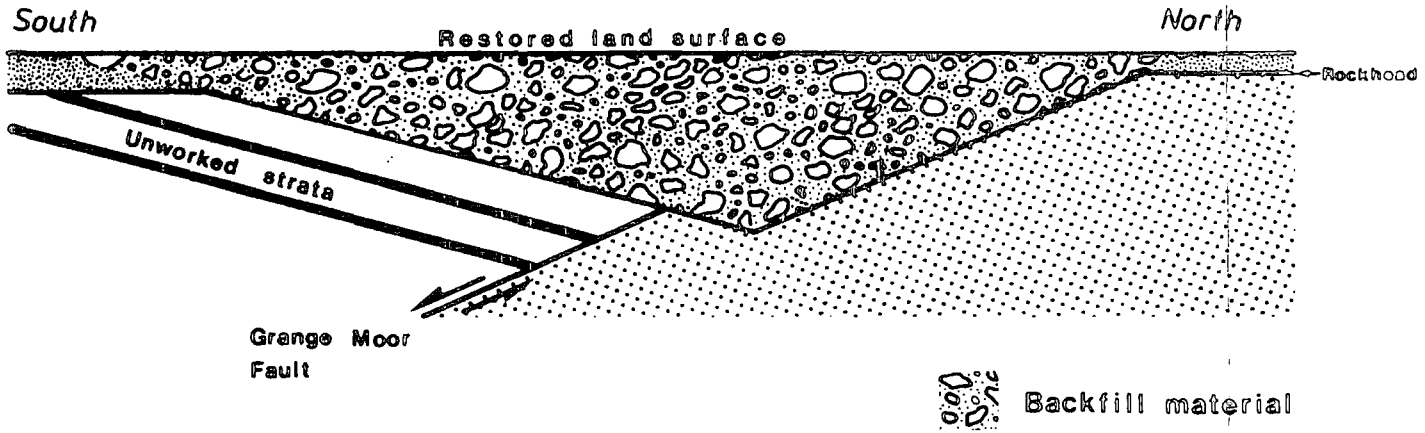

Figure 9.8

terminated, and the area backfilled. It is difficult to determine the exact position of the Grange Moor fault with this structure. The fault can only be located by using the refractor velocities to indicate a lithological change each side of the fault. The determination of refractor velocites beneath such a severe depression is unreliable (Sjogren,1984).

S Wave data

Line 2 was also shot using the S wave technique. When the source and receivers were located around peg 1, clear first arrivals were seen on the field records. As soon as the source and receivers crossed the field boundary around peg 20 (figure 9.1), the first arrival amplitudes completely died out. At the time this was attributed to the fact that the source was now standing on a ploughed field, where ground coupling was very poor. In hindsight knowing of the presence of the old workings, a more significant reason is the highly attenuating nature of the backfill material on the shear waves.

CHAPTER TEN

MARLEY HILL : SITE NO 7

Marley Hill prospective opencast coal site is located near the villages of Sunniside and Tanfield, Tyne and Wear, 8.5km south west of the City of Newcastle. The site lies near the famous Causey Arch.

Marley Hill was in the very early stages of exploration when it was first visited by the seismic team in April 1984. The primary objective at Marley Hill was to determine whether seismic refraction techniques could be used in advance of drilling to determine the thickness of superficial (drift) deposits at a prospective opencast site. The presence of very thick drift deposits at a site can seriously affect the overburden/coal ratio, and may make a site uneconomic.

The target coal seams at Marley Hill are the Low Main/Top Brass Thill coal seams which are joined to form a thick coal unit in this area of the East Durham Coalfield. Also underlying these coal seams is the Lower Brass Thill seam. The Low Main coal seam is overlain by a thick (30m) sandstone unit known as the "Low Main Post". This is one of the most areally persistant sandstones in the Durham coalfield. The unit is generally made up of a fine to medium grained sandstone, (Fielding, 1982).

This area of the Durham Coalfield has been economically exploited for many centuries, particularly since the seventeenth century. Nearby wooden wagonways date from the 1640s. Therefore

there must be a considerable amount of uncharted old mine workings in the target coal seams in the area. Nevertheless because of the thickness of the target coal seams, the presence of old mine workings would not necessarily make the site uneconomic.

10.1 P WAVE REFRACTION LINES. (NORTHERN AREA)

The only information available on the drift thickness at Marley Hill prior to the preliminary P wave surveys was based on an area to the east of the site, where gravel had been exploited for economic purposes. In this area the drift thickness was recorded as being around 40m.

With this information in mind, previous experience at Hemscott North showed us that our S wave source did not emit enough power to penetrate drift thicknesses exceeding 30m. Therefore preliminary surveys were carried out using the P wave refraction technique. Larger than usual peg spacings of 9m and 15m were used in the first instance in anticipation of a thick drift cover. The first surveys were carried out in the northern area of the site.

The main conclusion drawn from the results of the preliminary P wave surveys was that overall the area displays a three-layer near surface P wave velocity structure (figure 10.1). The layers can be summarised as follows.

Layer 1 displays a P wave velocity of 800 to 1200m/sec, at a variety of thicknesses (depending on area) of 5 to 20m.

Layer 2 displays a fluctuating P wave velocity of 1350 to

Identification of lithology by seismic velocity
Typical results from Marley Hill

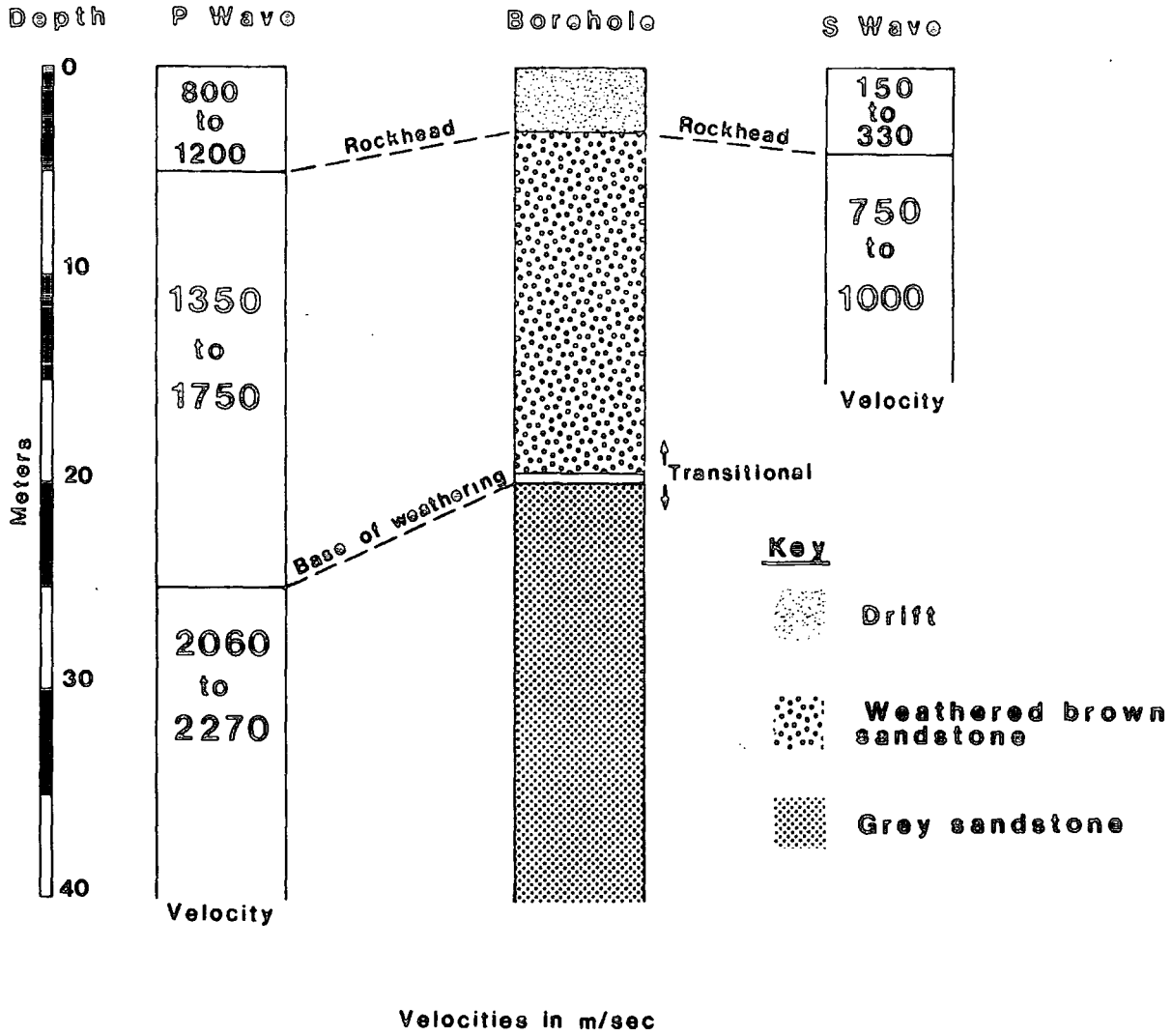

Figure 10.1

1750
~~1608~~m/sec. The base of this layer is found at approximately 20 to 50m (depending upon the area). The base of layer 2 usually runs sub-parallel to the base of layer 1.

Layer 3 displays a narrow band of P wave velocities from 2060 to 2270m/sec.

The only area which displays significantly different results to these above is discussed separately.

Analysing the above velocity structure, and using the limited previous knowledge of drift thickness and P wave velocity values from other sites, one would assume that the drift/rockhead boundary corresponds to the boundary between seismic layers 2 and 3. That is, layer 2 exhibits a P wave velocity which indicates an unconsolidated material. Therefore any estimate of drift thickness based on the seismic results alone, would be founded on the depth to the top of seismic layer 3.

After the preliminary P wave seismic lines had been processed, drilling had also progressed at the site. Therefore the results of the preliminary surveys could now be compared to the available borehole logs. Figure 10.2 shows the results of a P wave refraction survey carried out along line N2. The results are compared to a cross-section derived from borehole information. The P wave velocity structure conforms to the model outlined previously, displaying a three-layer structure. When one compares the seismic results directly with the borehole cross-section, it becomes obvious that the drift/rockhead boundary correlates with the boundary between seismic layers 1 and 2, not as originally

Marley Hill (Northern area)

Line 2

Geological cross section (from borehole information)

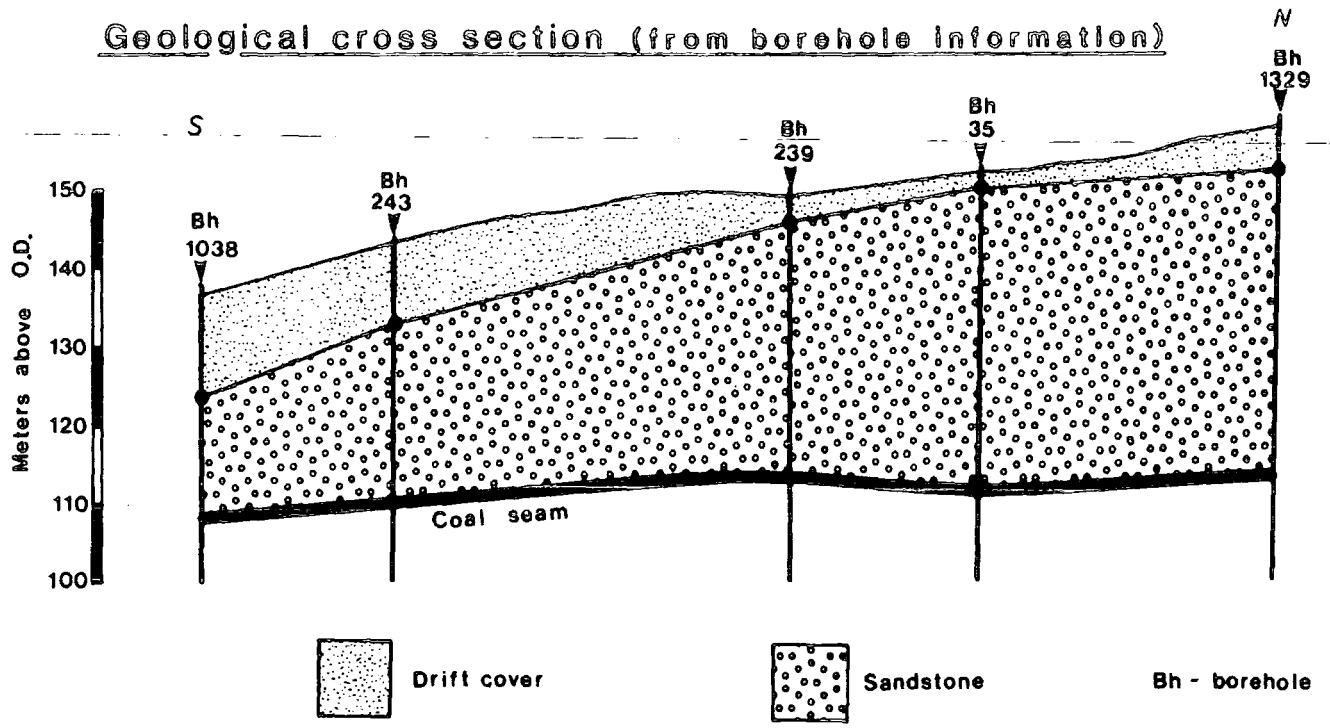

P wave velocity-depth section

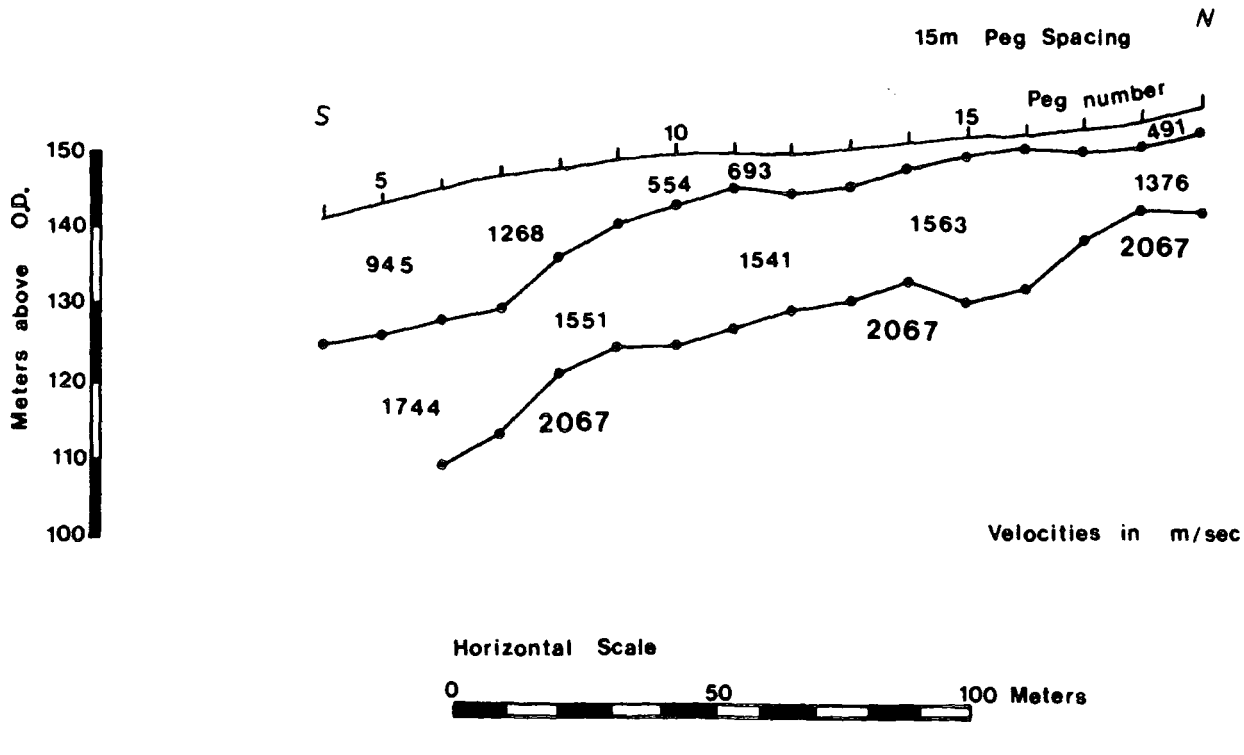

Horizontal Scale

0 50 100 Meters

Figure 10.2

assumed between layer 2 and 3. It is also apparent that the drift cover is much thinner than previous information led us to believe.

Over most of the Marley Hill site, rockhead is made up of the thick (30m) sandstone unit overlying the Low Main coal seam. It becomes apparent that the sandstone exhibits severe weathering below rockhead, (identified in the borehole logs as "soft sandstone"). This zone of weathering significantly lowers the P wave velocity from that of the "fresh rock". The boundary between seismic layers 2 and 3 marks the base of the "zone of weathering". Because this boundary runs sub-parallel to the drift/rockhead boundary (boundary of seismic layer 1 and layer 2), this causes an ambiguity in the identification of the rockhead boundary at this site using the P wave results alone, without some borehole information available for comparison.

S wave surveys were then carried out along the previous seismic lines. The S wave results were compared to the P wave data. Figure 10.1 shows that the S wave results display a two-layer velocity structure. The boundary correlates with the rockhead boundary. One interesting fact is that the P wave velocity ratio between drift and rockhead is around 1:1.9, whereas the S wave ratio is around 1:4. In light of the advantageous velocity contrast, and the economics of using the cheap S wave technique to obtain the same information as the expensive P wave technique, further surveys were carried out in the southern (Andrews House) area using the S wave technique.

P Wave Line N1

As stated previously the results of one P wave survey deviated from the typical model. These are the results found along seismic line N1.

Figure 10.3 displays the traveltime graphs recorded at line N1. Originally a reverse traveltime graph was built up using a 9m peg spacing in anticipation of a thick drift cover. The 9m peg spacing traveltime graph displays a three-layer structure. The direct wave is only recorded from peg 10. The first refractor becomes a first arrival at shot to geophone offsets greater than 20m. A second deeper refractor was recorded when a large (180m) shot to geophone offset was used. The Generalized Reciprocal Method (Palmer,1980) was used to calculate accurate refractor velocities. The first refractor has a velocity of 2050+/-60m/sec. The deep refractor displays a P wave velocity of 2637+/-50m/sec. A second reversed refraction survey was carried out using a 3m peg spacing to accurately tie down the direct (drift) velocity (figure 10.3). The results of the 3m survey show that the overburden exhibits an anomalously low P wave velocity in this area. In fact, the P wave velocities recorded along line N1 are the lowest P wave drift velocities encountered throughout all our surveys carried out during this project. Detailed reversed refraction spreads were then shot using a 1m peg spacing and a seismic detonator as a source (figure 10.3). The results of the 1m survey show that the drift can be sub-divided into two layers. A thin surface layer (soil layer), which exhibits a P wave velocity of around 250m/sec. This layer is underlain by a thicker layer (6 to 8m) exhibiting a P wave velocity of 350m/sec. Figure 10.4

MARLEY HILL Line N1

P wave

Travel Time graphs

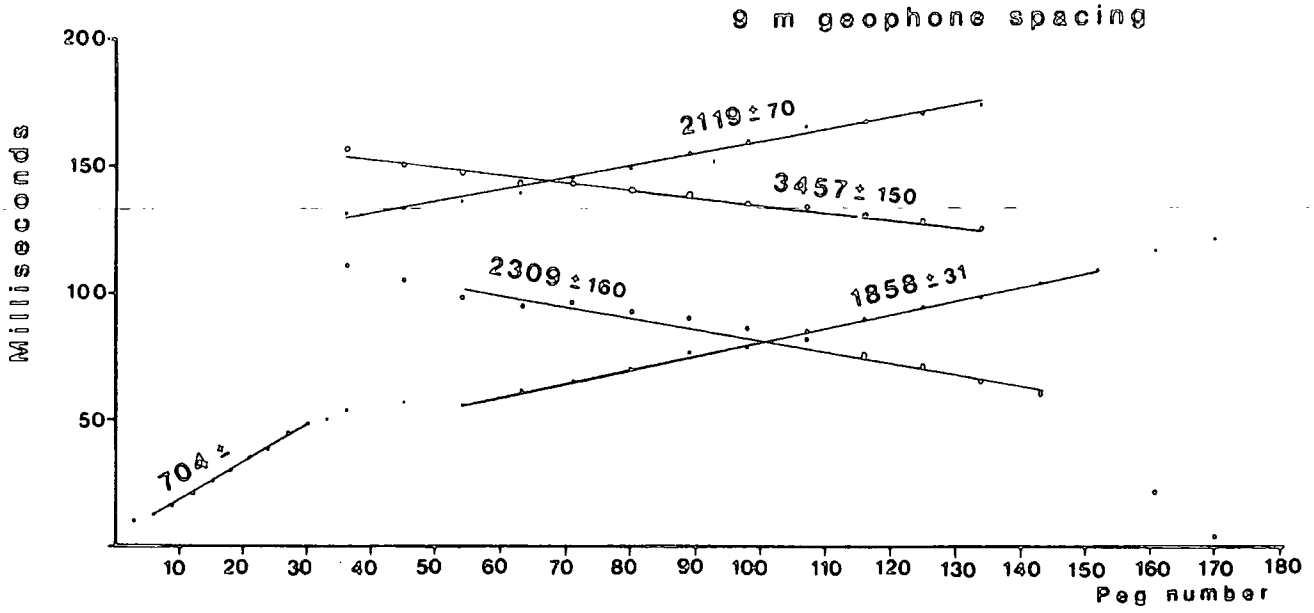

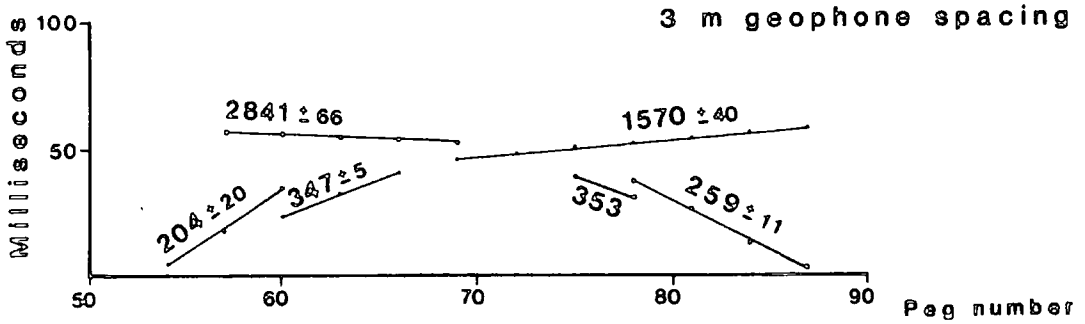

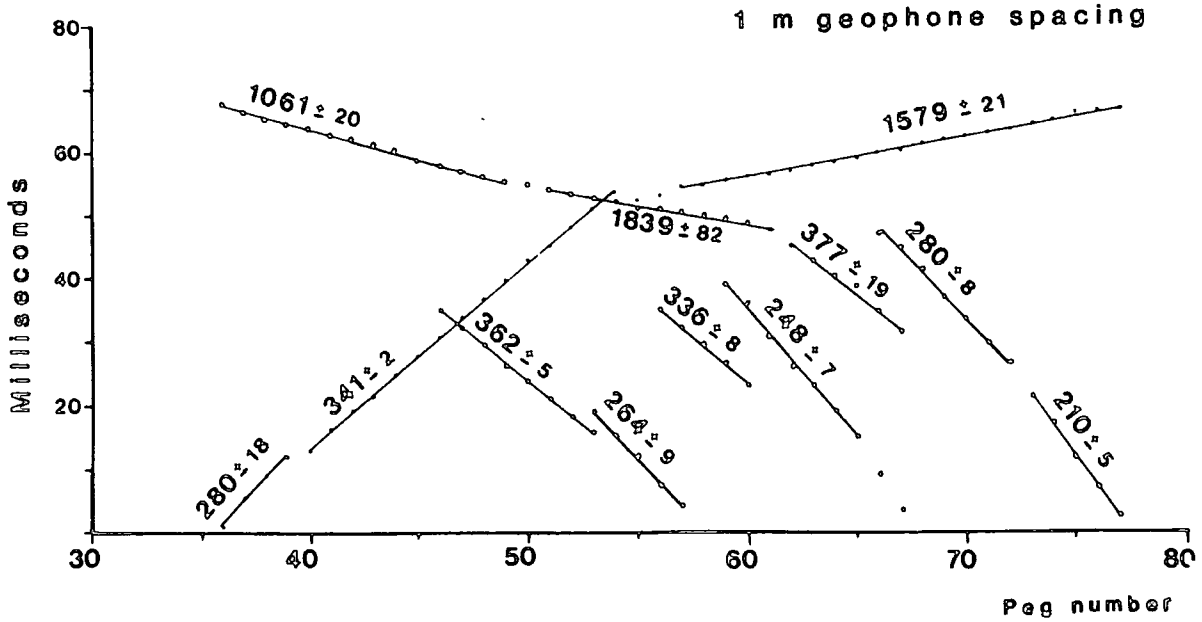

Peg spacing 1 meter

Figure 10.3

Marley Hill Line N1

P-wave data

Raw data

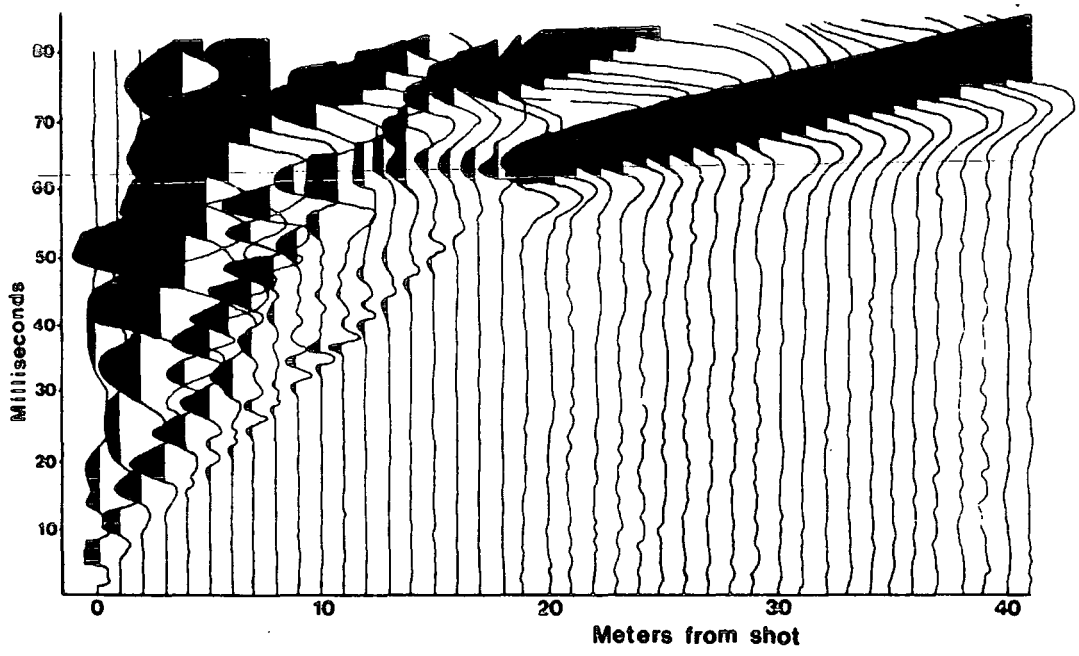

Interpretation

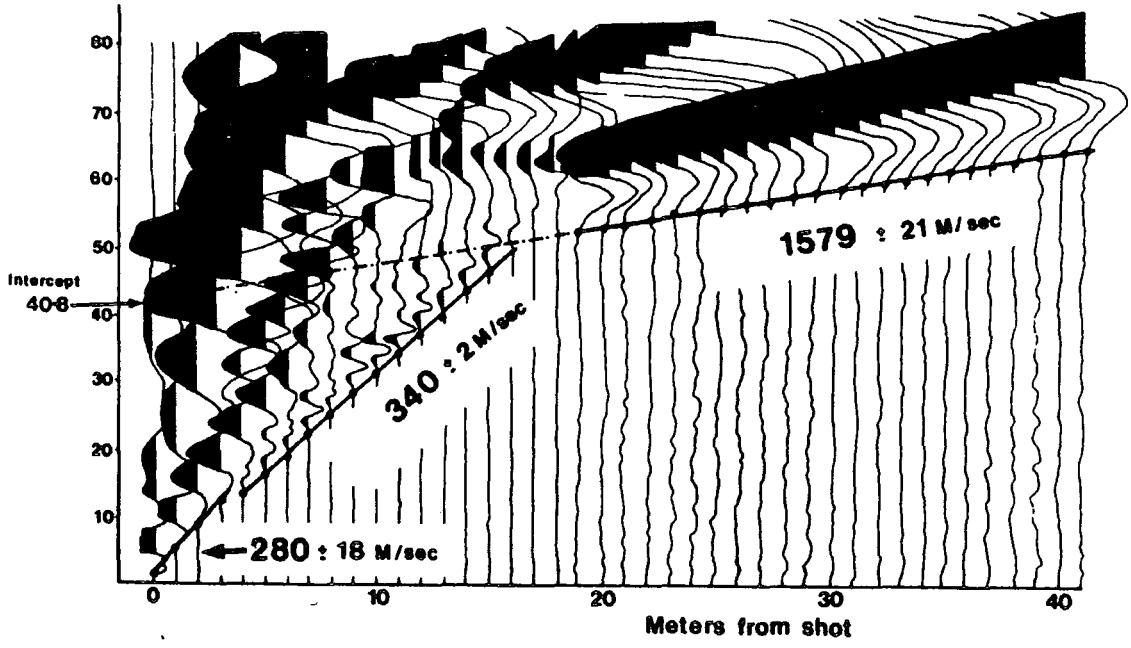

Figure 10.4

displays a complete set of seismograms (42 channels) shot from Peg 36 using a 1m peg spacing. The distinct two-layer structure of the drift can be seen from the two separate arrivals (280m/sec and 340m/sec). The strong refracted arrival originating from rockhead is clearly displayed.

Figure 10.5 displays the interpretation of all the P wave refraction data acquired along line N1. The rockhead boundary is interpreted as being at a depth of 6 to 8.5m. The deeper refractor lies at a depth of 45 to 60m. Because Line N1 lies in a topographic low, the deep refractor lies beneath the base of drilling at Marley Hill. Therefore no direct comparison can be made with the borehole logs. The origin of this refractor is probably a deeper sandstone unit within the Carboniferous sequence. Figure 10.6 displays the location of line N1, along with drift thickness values determined from nearby boreholes. It can be seen that the P wave refraction results consistently underestimate the depth to rockhead by some 3.5m. This can be explained by the fact that a drift velocity of 350m/sec was used in the depth conversion of the time depth data. It is not unreasonable to assume that the drift would display an increase in P wave velocity with depth, due to compaction. Assuming that the depth to the refractor determined by drilling is correct, the calculated time depth values from the survey show that the average P wave drift velocity is 466m/sec. If one assumes a linear increase in velocity with depth, (Dobrin, 1976) a function such as:

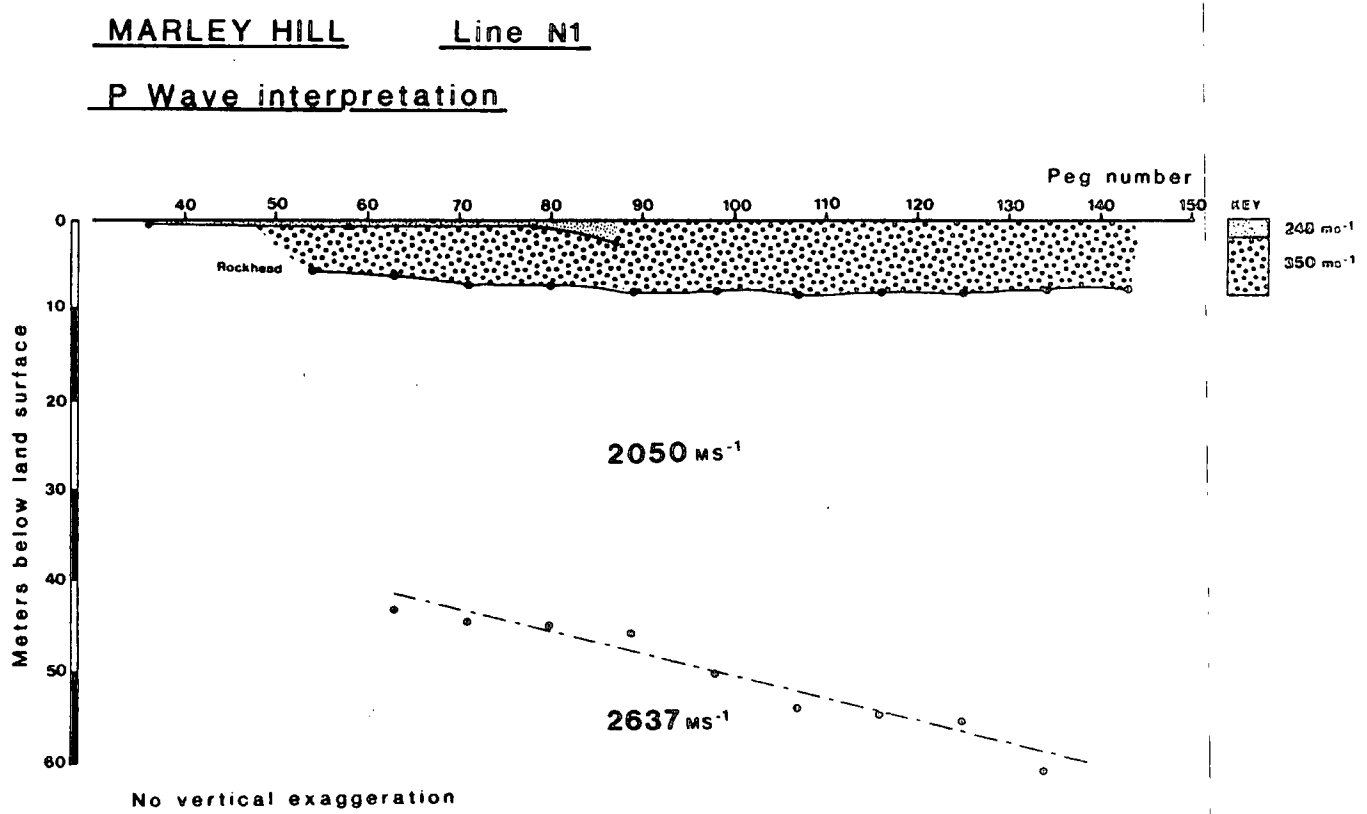
MARLEY HILL
Line N1
P Wave interpretation
Peg number
40
50
60
70
80
90
100
110
120
130
140
150
KEY
240 ms-1
350 ms-1
Rockhead
2050 MS-1
2637 MS-1
Meters below land surface
0
10
20
30
40
50
60
No vertical exaggeration

Figure 10.5

$$V = Vo + K.Z$$

V = velocity at depth z

Vo = velocity at zero depth

K = constant

can be employed to represent the increase of velocity with depth. Values such as Vo=340m/sec and K=22sec would produce the correct depth estimate for line N1.

One interesting fact concerning the anomalously low P wave velocity through the drift, is that nearby was the site of an old coke works (now demolished). Apparently tar obtained as a by-product of the coking process was disposed of by pouring it away over the embankment above the location of line N1 (figure 10.6). Tar beds were encountered in some of the nearby boreholes. It may be that tar has impregnated the drift in this area of the site, causing a significant lowering of its P wave velocity.

10.2 S WAVE REFRACTION LINES, SOUTHERN AREA (ANDREWS HOUSE)

In the southern region of the site (Andrews House area), boreholes that have been drilled in this area reveal an inconsistent thickness of the overburden. These fluctuations indicate the presence of glacial drift channels which have cut into Carboniferous strata at rockhead during the ice age. These erosional channels have been subsequently infilled by glacial depositional material. Drift thicknesses in the Andrews House

Marley Hill (Northern area)

Locations of P wave refraction lines N1 & N2

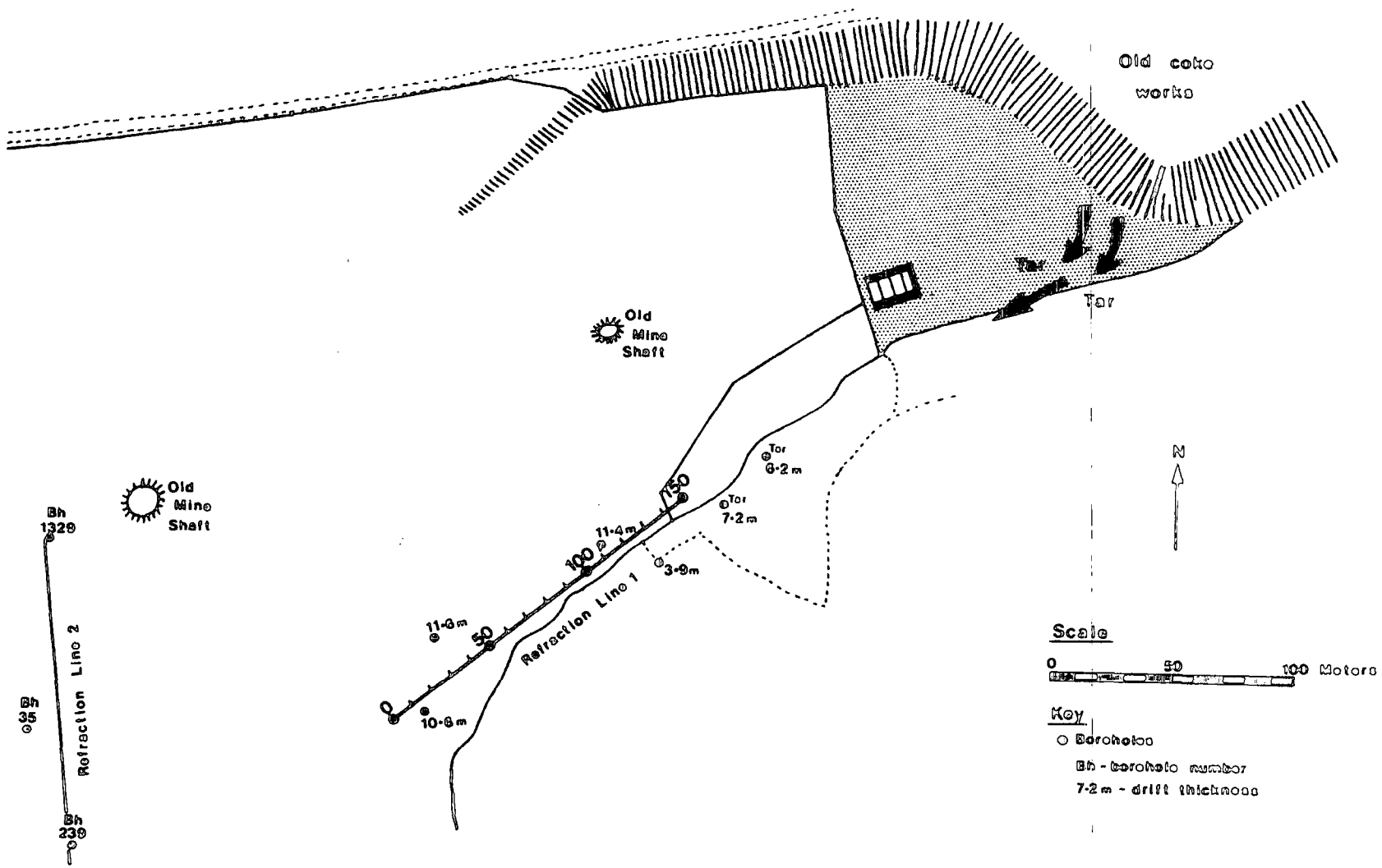

Figure 10.6

area vary from less than 5m to greater than 40m.

Figure 10.7 displays a contour map of the drift thickness in the Andrews House area compiled from the available borehole information. The two main features that can be clearly seen are a major east-west channel which deepens westward and narrows and shallows to the east, and also a north-south less deep "hanging valley" which extends under Andrews House (derelict).

It was thought that the severe rockhead topography in this area would be a good test of the S wave refraction technique's ability to determine the drift thickness. Therefore three S wave refraction lines were shot in the Andrews House area (figure 10.8). Line 1 crosses the north-south valley; lines 2 and 3 traverse the main east-west channel.

Using the data available from 44 boreholes in the Andrews House area, a perspective block diagram was drawn using the SurfaceII graphics package (Sampson, 1975), available on the NUMAC computer system. The block diagram (figure 10.9) graphically displays the lack of correlation between the surface and sub-surface topography in this area. The area is viewed from the south west at an elevation of 20 degrees above the horizon. The plot has a four times vertical exaggeration to accentuate the sub-surface relief. The positions of the S wave refraction lines are plotted on the surface topography.

Refraction lines 1 and 2 have a 3m peg spacing whilst line 3 has a 2m peg spacing. Figures 10.10 , 10.11 and 10.12 display the traveltime graphs, velocity functions and time depth plots

Marley Hill (Andrews House area)

Depth to rockhead (from borehole information)

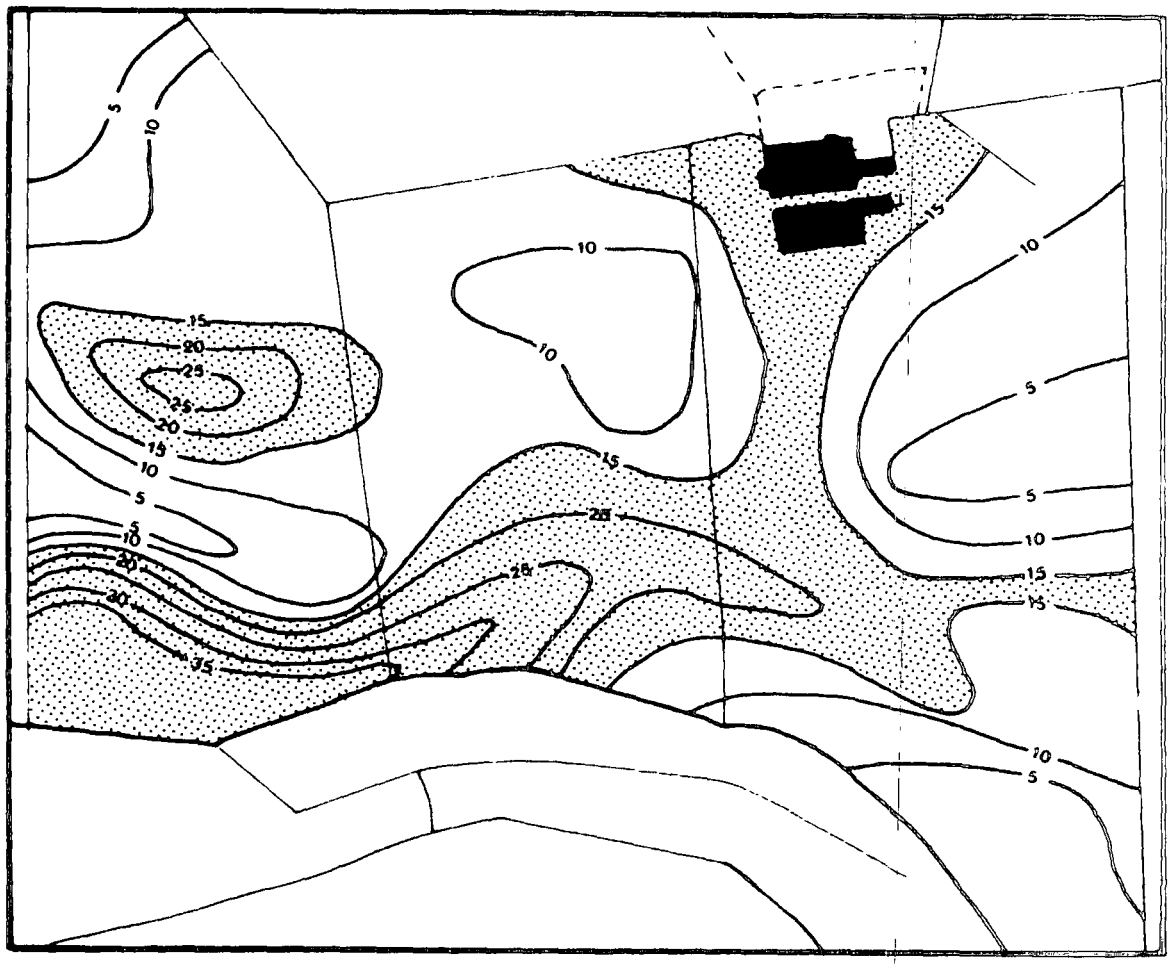

Key

Drift thickness greater than 15m

Figure 10.7

Marley Hill (Andrews house area)

Location of S wave lines

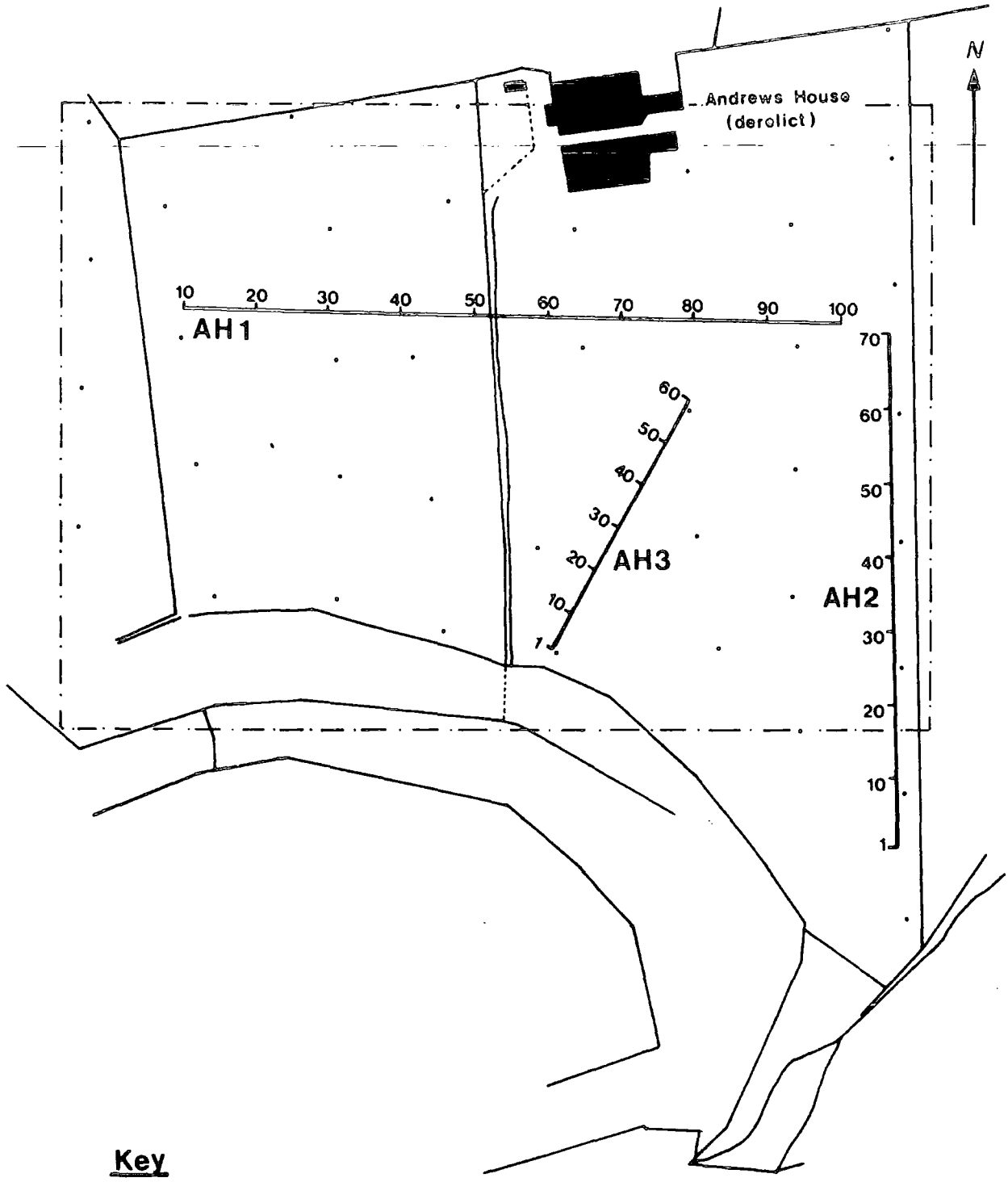

Key

- Borehole
- Area used in computer contouring

Scale

0 50 100

Meters

Figure 10.8

MARLEY HILL

Andrew's House area

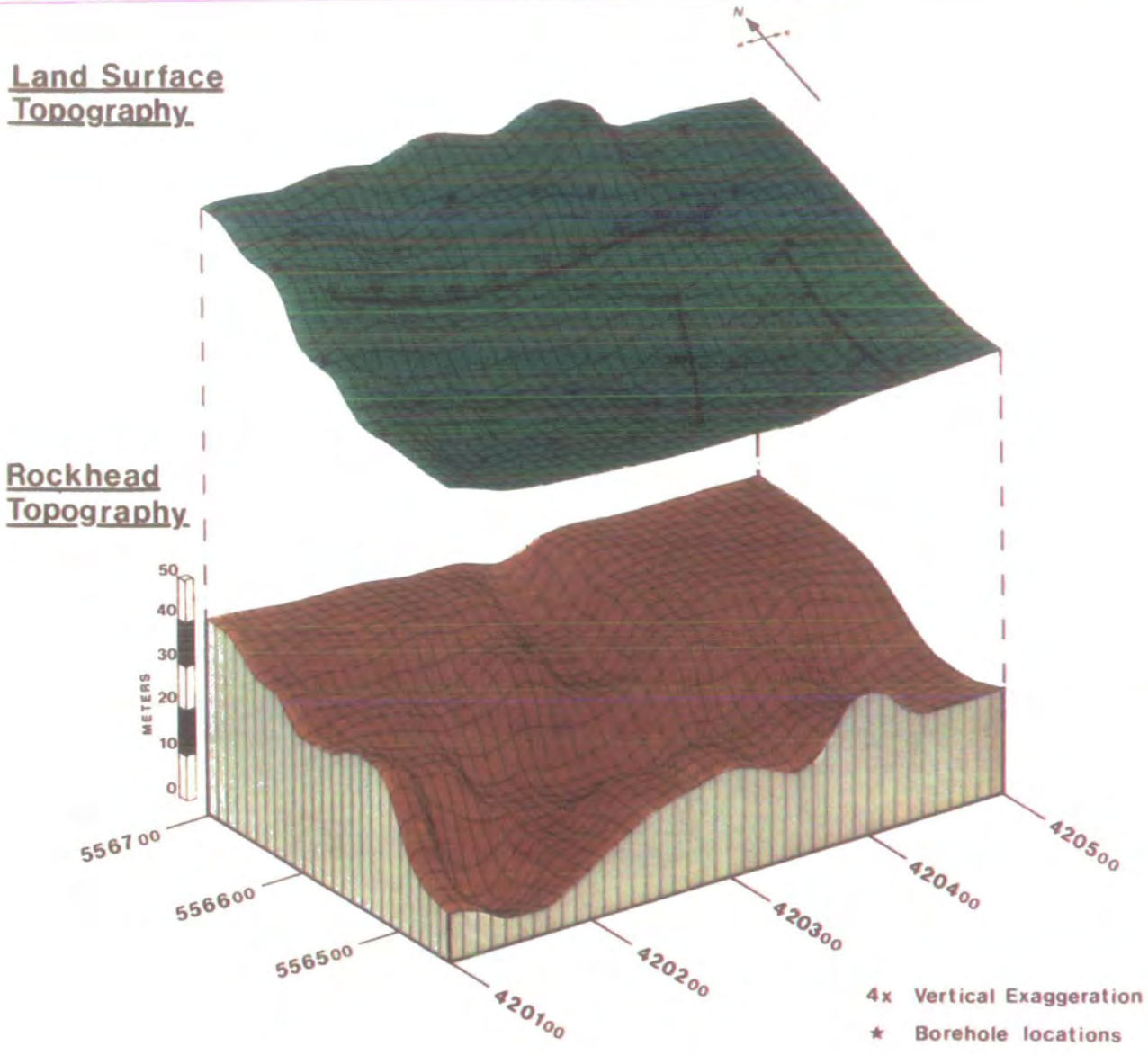

Surfaces generated using borehole information only

Figure 10.9

acquired along lines 1,2 and 3.

Line 1

On analysis of the traveltime graph (figure 10.10), a three-layer velocity structure is apparent. Layers 1 and 2 originate from the overburden. Layer 1 has a typical S wave velocity of between 140m/sec and 220m/sec, which corresponds to the thin surface soil layer. This is underlain by a thicker seismic layer of average S wave velocity of 328m/sec, which corresponds to the glacial drift material. Beyond a source to geophone offset of about 20m a single refracted arrival is recorded on the traveltime graph. This refracted arrival originates from rockhead. A phantomed traveltime graph is built up from the rockhead refraction arrivals displayed on the traveltime graph, in both the forward and reverse directions. The phantomed traveltime graph is then analysed using the Generalised Reciprocal Method (Palmer,1980), from which an accurate refractor velocity can be determined by plotting the velocity function.

The velocity function for line 1 displays a fluctuating S wave refractor velocity of between 743m/sec and 1333m/sec. These high S wave velocities indicate a solid rock refractor. The time depth function clearly displays the outline of the drift channel in the increase of the time depth values to a maximum value over the axis of the drift channel. The time depth of the near surface soil layer is also plotted. This is calculated by interpolation between half intercept times calculated along the survey. For an accurate determination of the drift thickness, the effect of the near surface low velocity "soil" material has to be calculated and

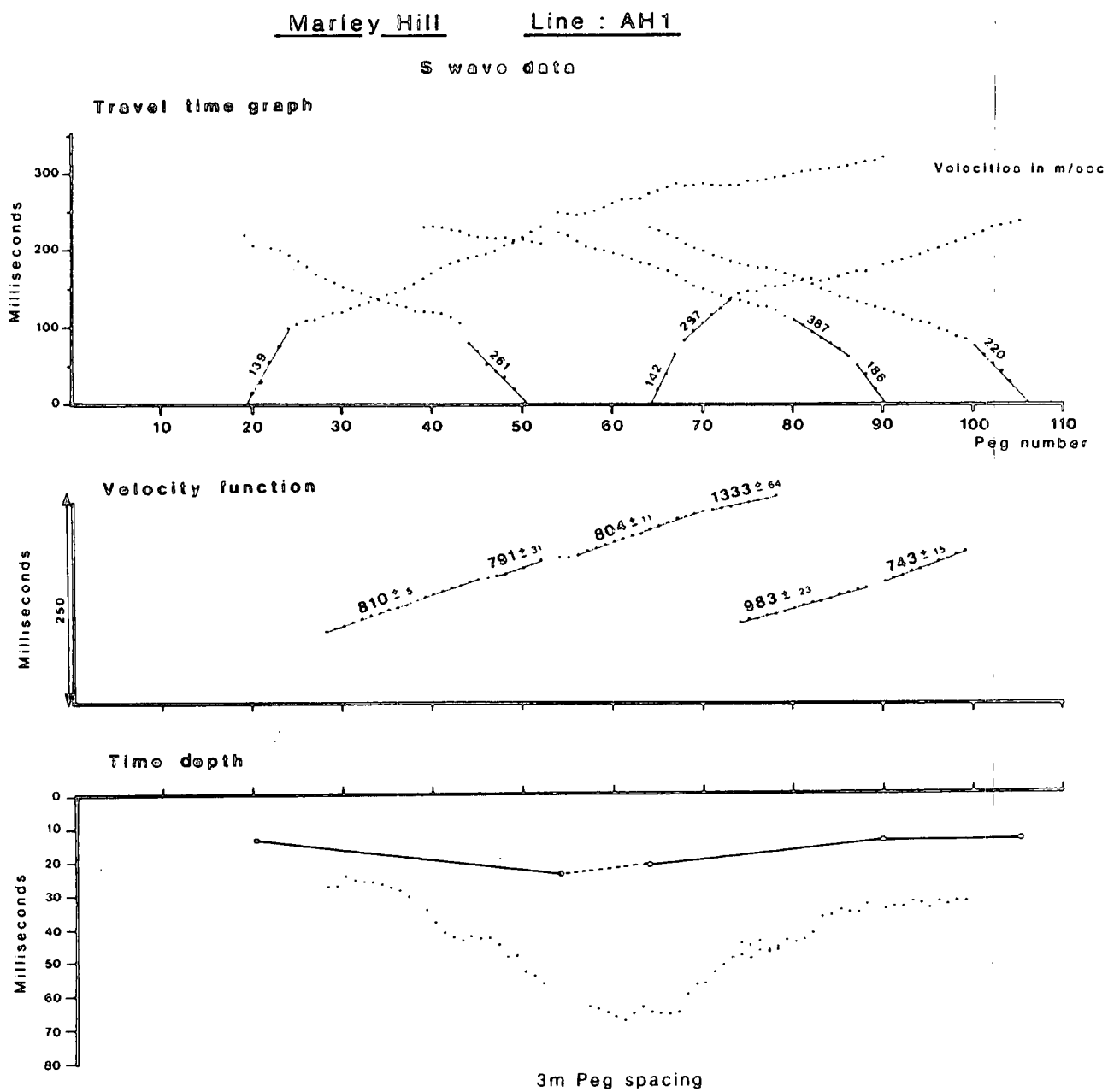
Marley Hill
Line : AH1
S wave data
Travel time graph
Velocities in m/sec
Milliseconds
300
200
100
0
139
261
142
297
387
186
220
10
20
30
40
50
60
70
80
90
100
110
Peg number
Velocity function
Milliseconds
250
810 ± 5
791 ± 31
804 ± 11
1333 ± 64
983 ± 23
743 ± 15
Time depth
Milliseconds
0
10
20
30
40
50
60
70
80
3m Peg spacing

Figure 10.10

subtracted from the time depth to the base of the drift.

Line 2

The traveltime graphs for line 2 (figure 10.11) display similar characteristics to line 1. Again the overburden can be sub-divided into two seismic layers. A phantomed traveltime graph was built up in the same manner as line 1, and analysed using the GRM. The velocity function graph displays a consistent refractor velocity between 836m/sec and 916m/sec, except for a small low velocity zone in the centre of the line around peg 40. The time depth graph again shows the general outline of the drift channel in the increase in the time depth values over the axis of the drift channel.

Line 3

The traveltime graph for line 3 (figure 10.12) again displays a similar form to the previous lines. A phantomed traveltime graph was built up from the data set using the parallelism of the refracted events. Some difficulty was encountered in distinguishing the direct and refracted arrivals southward from peg 70. This is due to the steep away dip of the sub-surface refractor at this point, which results in a low "apparent velocity" of the refractions. The apparent velocity is not much greater in value than the 350m/sec drift arrival.

The velocity function displays a fluctuating refractor velocity, from a central low velocity area of 385 to 950m/sec at the ends of the line. The shape of the drift channel is not

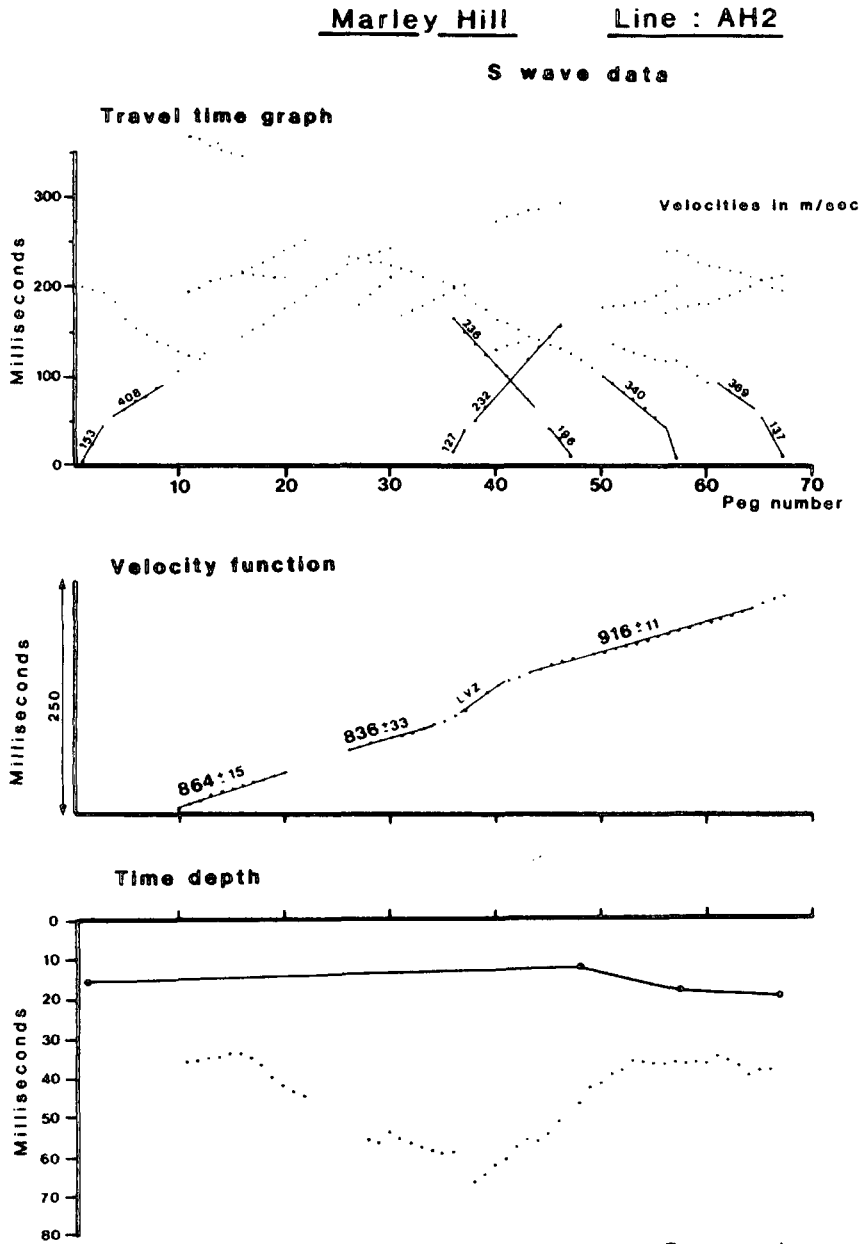

Figure 10.11

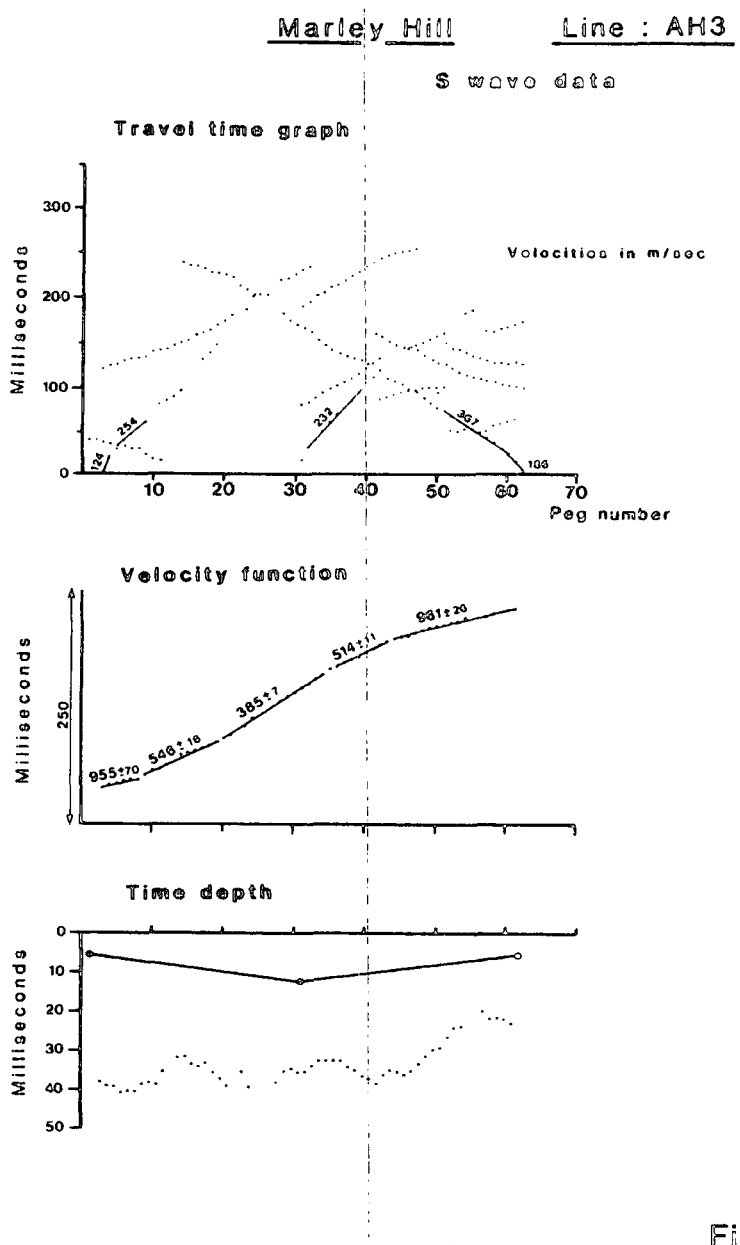

Figure 10.12

apparent on the time depth plot. This is due to the fact that the low refractor velocities encountered in the central part of the line result in different conversion factors required for the depth conversion of the time depth values along the survey.

Geological Interpretation of the S Wave Lines

Using the time depth values and conversion velocities calculated from the overburden and refractor velocities, the data were depth converted. The effect of the thin near surface "soil" layer was subtracted from the time depth values of the rockhead refractor.The thickness of the glacial drift layer could then be calculated; hence the shape of the drift channel can be outlined. The final interpretations are displayed in figure 10.13.

line 1

The shape of the glacial channel is clearly outlined by the S wave refraction technique. The maximum depth of the glacial drift calculated using the refraction technique is 18m, which agrees exactly with nearby borehole information. The depth of the drift at the western end of the line also shows good agreement with the borehole information. At the eastern end, the depth of the drift calculated by refraction is at a level 2m deeper than nearby boreholes predict.

The rockhead refractor velocity is consistently greater than 750m/sec over all the line. This indicates that we are dealing

with rockhead over all the line, even over the axis of the drift channel.

Line 2

The shape of the drift channel is not clearly outlined along line 2. There is a low refractor velocity between pegs 36 and 43. At peg 42 the seismic depth to the refractor is 9m. A borehole at peg 42 gives a log of 9m of boulder clay underlain by a layer of gravel and clay to a depth of 16.8m. This gravel base is not seen from other boreholes along the line. Therefore it would seem that the deep east-west channel has a gravel fill along its axis. From the seismic results it would seem that over the axis of the channel the gravel acts as a refracting boundary, and gives a low velocity zone. The width of the zone is 21m, this being the inferred width of channel along line 2. The severity of the cross-sectional shape of the channel at this location is also borne out by the contour plot (figure 10.6). The severe nature of the channel topography cannot be imaged by the refraction technique.

To the southern and northern ends of the line, where high refractor velocities confirm we are observing rockhead, the seismic depth to the refractor agree with nearby borehole information to within plus or minus 2m.

Line 3

From the contour plot (figure 10.6) the main east-west drift channel appears wider and deeper along line 3 compared to line 2. The interpretation of the seismic results confirms this. The general shape of the drift channel is outlined, although the low (409m/sec) refractor velocity may again signify that over the axis of the channel the boulder clay/gravel fill boundary may be acting as a refractor. At the ends of the seismic line the seismic results show an overburden thickness some 2m deeper than nearby boreholes indicate.

The accurate determination of the drift thickness not only relies upon the accurate determination of the overburden velocities, but also the accurate determination of the thickness of the near surface "soil" layer (150m/sec). As this boundary cannot be profiled without some considerable extra effort in the data acquisition stage, some approximation must be made. This is achieved by interpolation between half intercept times determined from near offset records along the seismic line. This interpolation may introduce a small error in the depth estimate. Also an average value of the overburden velocity is used in the depth conversion for computational ease.

The S wave technique overall is accurate in the determination of the drift thickness in the Andrews House area. A fourth seismic line was attempted in the south west corner of the survey area over the thick drift cover. This had to be aborted due to the fact that our low power S wave source did not emit enough

Marley Hill (Andrews house area)

Interpretation of S wave lines

Line : AH1

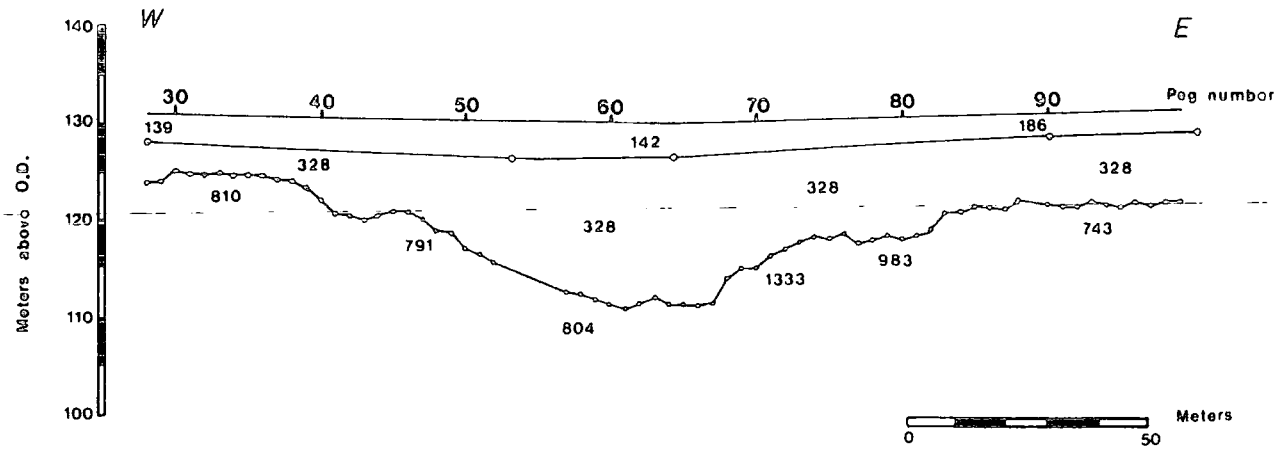

Line : AH2

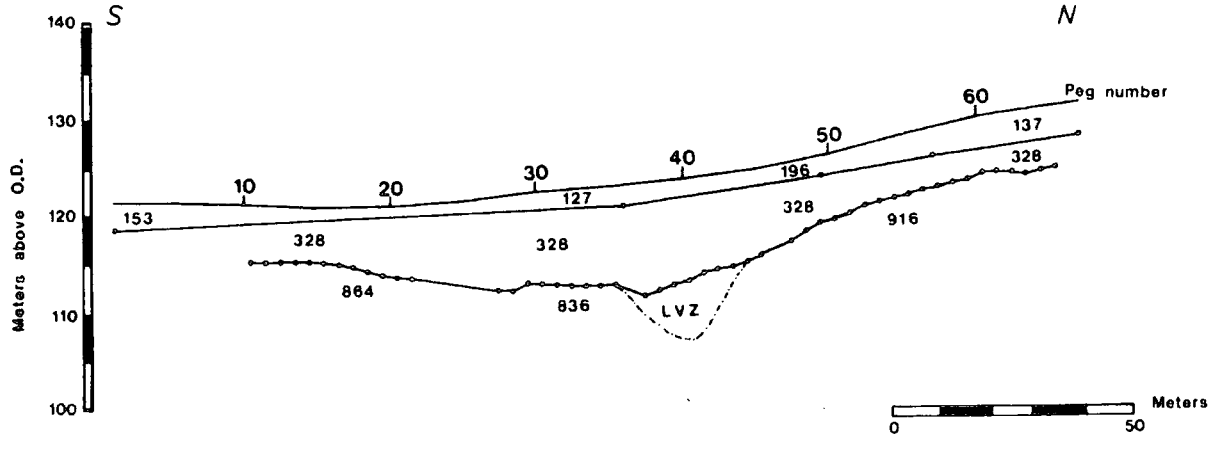

Line : AH3

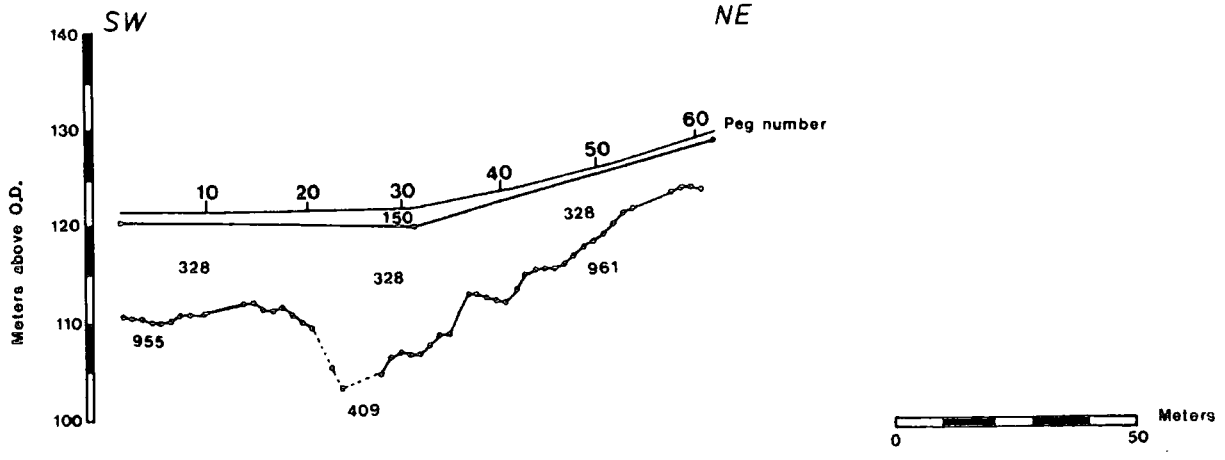

2X Vertical exaggeration

Figure 10.13

power for pickable refracted arrivals to be recorded from rockhead when the drift thickness exceeded 30m. The severe rockhead topography may also have contributed to this. There comes a point when there are steep refractor dips present, when no refracted arrivals will be recorded at the surface (Sjogren, 1984).

CHAPTER ELEVEN

CONCLUSIONS

Over the three year duration of this project, fifteen exploration sites have been visited. At seven of the sites comprehensive multi-line P and S wave refraction or P wave reflection surveys were carried out, the results from which are shown in this thesis. The project tackled a variety of geological problem areas of particular relevance in opencast exploration. A great deal of experience was gained from the results, enabling the assessment of the potential of seismic surveys as a tool in shallow coal exploration.

Seismic Refraction

The seismic refraction technique, using both P and Sh waves, has been used to locate faults, estimate drift thicknesses, locate drift channels, and to pinpoint areas of previous opencast excavation.

Faults in the Carboniferous strata can be located in two ways. Firstly by observing a change in refractor velocity along a profile caused by the fault juxtaposing two different lithologies at rockhead. Fault location by this method appears to be equally successful using either the P or S wave refraction technique when helpful conditions exist (Stanley moss, site 1 ; Stobswood, site 6). Secondly, faults can be located by observing a sudden change in the depth to a refractor caused by a displacement of the strata due to faulting. The optimum conditions occur where a high

velocity, easily locatable refractor, such as a thick sandstone bed, is faulted. This type of phenomenon occurred at some lines at Barley hill (site 2) and along the refraction lines shot at Hemscott North (site 3). For imaging depth anomalies by the refraction technique, the Generalized Reciprocal Method (Palmer, 1980) was used to obtain optimum results. This method displays a marked improvement in the imaging of a fault step over the more commonly used Plus-Minus technique (Hagedoorn, 1957). The Plus-Minus technique however displays a greater ability to monitor subtle refractor velocity variations, due to the correct cancellation of time anomalies due to the very near surface.

Shear waves display a greater ability to image sharp depth anomalies than compressional waves. Figure 11.1 displays the results from one of the lines shot a Barley Hill (site 2). Note that no matter what interpretation technique is used on the P wave data, the final results do not image the fault step as well as the S wave results. This is due to the fact that the velocity contrast between consolidated and unconsolidated rock is much greater for S waves than for P waves. As a consequence of this, the critical angle for S waves is much smaller than for P waves given the same geological situation. This results in the assumptions made in the delay time interpretation method being truer for S waves than P waves. Also anomalous zones on the traveltime graph caused by diffractions are smaller if a high velocity contrast exists.

The refraction method is never going to be able to pinpoint faults with complete reliability. This was highlighted by a P wave reconnaissance survey carried out in Yorkshire. The

FAULT LOCATION USING SHALLOW REFRACTION SURVEYS

A FAULT INTERPRETED AS A STEP IN A REFRACTOR

FIELD EXAMPLE

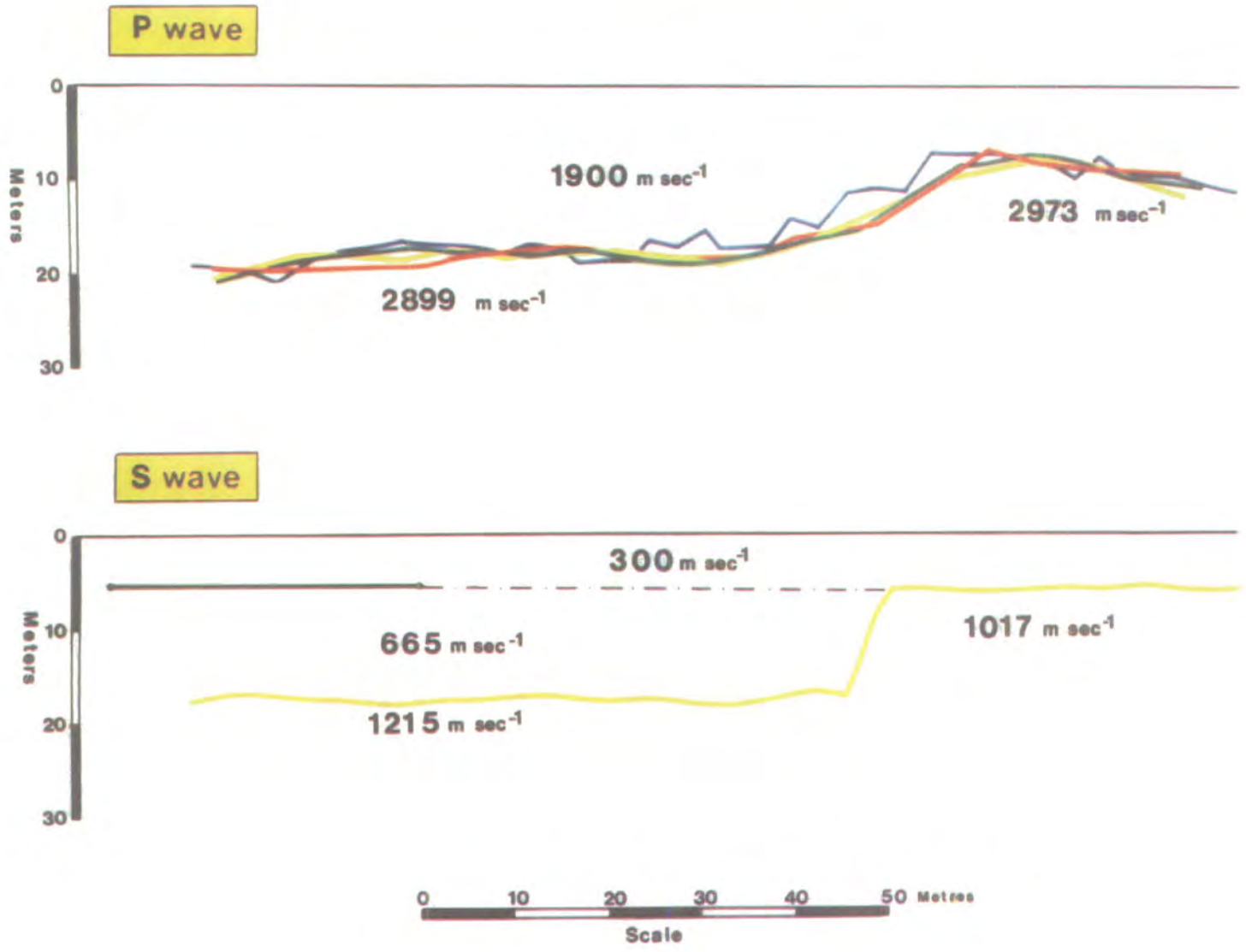

Figure 11.1

Site BH Line 4

refraction method failed to detect any anomaly over a fault with a 70m throw. This was due to the fact that the fault juxtaposed two large thicknesses of mudstone with the same P wave velocity. With no lithological contrast, a seismic anomaly could not be expected to be seen, either in velocity or depth. The P wave profile picked out the water-table along the line.

Both the P and S wave refraction techniques have also been used to estimate drift thicknesses at an exploration site (Marley Hill, site 7). This information is useful to the opencast geologist as it is used in the estimation of the overburden ratio. Marley Hill highlighted one of the problems of using P waves in this way. From the final results of a refraction profile, a cross-sectional image of the near surface velocity structure is obtained. One can only use the magnitude of the refractor velocity as a lithological indicator, if no borehole information exists. At Marley Hill a near surface P wave refractor of 1350 to 1750m/sec was encountered. This refractor was firstly assumed to be a layer in the drift due to its low seismic velocity. Subsequent drilling revealed the refractor to be a badly weathered sandstone horizon. Any depth estimate of rockhead based on P wave data alone would have been erroneous. S wave surveys at the same location gave a refractor velocity between 750 and 1000m/sec, a velocity value which indicates a consolidated rock. There is an overlap in the range of P wave velocities encountered for water saturated drift and weathered rockhead, as P wave velocity values range between 1400 and 1800m/sec for both types of strata. A P wave velocity greater than 2000m/sec is taken to indicate a consolidated rock. For S waves there exist distinct ranges of velocities for unconsolidated (150 to 400m/sec) and consolidated (650 to

1400m/sec) rocks. S waves are a much better lithological indicator than P waves for shallow refraction studies. It is thought that from the comparison of our drift depth estimates with known depths from borehole data, the refraction technique can estimate the depth to within about 10% of the true value.

The refraction technique was also used to profile the base of drift channels (Marley Hill, site 7). The S wave technique was used in preference to the P wave, due to the much smaller critical angle of the S wave compared to the P wave in a drift/bedrock situation. This enables the S wave technique to image the base of the channel better than the P wave technique. Also from some of the results the drift/bedrock boundary was transparent to the P wave refraction technique. The boundary was a hidden layer, due to the poor velocity contrast found between the water saturated drift and the weathered rockhead.

The problem with S wave surveying using portable equipment is one of penetration. Using our acquisition equipment drift cover of greater than 25m was unable to be penetrated even after stacking many hammer blows. If greater penetration is required, a more powerful, but less mobile S wave source would need to be developed. P waves have essentially unlimited penetration because the size of explosive charge can be easily increased.

The seismic refraction technique has also been used to detect areas of previous opencast excavation (Barley Hill, site 2 ; Stobswood, site 6). The detection of the old opencast workings is a relatively easy task using the P wave refraction technique. This is due to the large P wave velocity contrast seen between the

backfill material and the underlying bedrock. At both the sites where old opencast areas occurred, the P wave refraction lines located the edge of the mined area with great precision. Problems are encountered when using the S wave technique for such a target. This is due to the strong absorption of the shear waves in the unconsolidated material and weak coupling of the source to the ground surface.

Seismic Reflection

The fundamental problem with shallow seismic reflection surveys on land, is that surface waves (ground roll) and refracted energy occur within the same time-distance window where the shallow reflections are recorded. Figures 2.12 and 2.13 highlight this problem. This is further compounded when reverberant refractions are encountered (figure 3.6). Ground roll causes most problem when it is of high velocity and is highly dispersive, which occurs when the overburden is thin and a high percentage of the ground roll travels at around the shear wave velocity of the bedrock.

Seismic reflection data quality can be improved by drilling deeper shot holes into rockhead, as seen at Hemscott North and Keekle (sites 3 and 5). For small scale surveys envisaged for the opencast industry this would cause the method to become uneconomic.

The boulder clay drift cover encountered at all our reflection sites (except Keekle, site 5) exhibits very poor transmission characteristics for seismic waves. It is a high absorption medium, absorbing the high frequencies much sought after in

shallow reflection exploration. At the sites where boulder clay was found, little or no seismic energy above 100Hz was recorded. This causes the final section to lack resolution and character which is required for detailed interpretation. At Keekle (site 5) where the drift cover was thin and the shots were exploded in rockhead, seismic energy up to 170Hz was recorded, the final section lending itself to more detailed interpretation.

From the results of our reflection work no reflections from depths shallower than 100m were able to be recorded, except at Keekle where reflections from around 70m were seen. The average seismic wavelength that was recorded was around 35m, except for Keekle where the wavelength was less than 20m. The resolving power of the method in theory is approximately half the seismic wavelength.

At Hemscott North (site 3) the target of our investigation was a large fault found in the Northumberland coalfield (Grange Moor Fault). The thick drift encountered at this site caused presented problems to the P wave reflection technique. The drift cover caused absorption of seismic energy particularly at high frequencies. On one of the seismic lines (line 1), reflectors were seen from around 180 to 240m depth. The fault zone was clearly seen at these depths, although this is below the depth range of interest of the Opencast Executive.

The results of the single reflection line shot at Barley Hill were poor. This was due to the fact that the ground roll recorded was of a high velocity and amplitude. The recording system was unable to detect any small amplitude, high frequency reflections

from within the high amplitude ground roll cone, due to the recording systems limited dynamic range. The line was recorded on the lowest coal seams found in the Upper Coal Measures in the North East, the reflection data being shot over a grit and shale sequence where high acoustic impedances might not be expected.

The P wave reflection line shot at Keekle in Cumbria (site 5) produced the best quality section recorded during this project. This was due to the fact that the drift cover at this site was thin and the shots were exploded in an unweathered bedrock with good transmission characteristics. Shallow reflections were seen from around 70 to 380m depth. Unfortunately the very shallow reflections from the Coal Measures were very intermittent, due to the highly faulted nature of the geology. High amplitude deeper reflections from around 280m were also recorded, these were thought to originate from limestones at the base of the Namurian. The Coal Measures at Keekle consist of a series of alternating thin beds which are highly faulted. The beds may be too thin and the geology too complex to cause significant energy to be reflected at the seismic wavelength.

At High Thorn (site 4), the purpose of our surveys was to use the P wave reflection technique to try to detect the position of the boundaries of old deep mine workings. The results of the surveys were inconclusive, although some features seen on the final sections could be related to boundaries between worked and unworked strata, there was no consistency. The reason for this, is that the mine workings are too shallow at 50m, with the shallowest reflections seen at the site coming from 150m depth. Therefore the workings could not be detected directly, but only

indirectly by observing the effect of old workings has on reflections from deeper horizons.

At the onset of this project it was hoped to use shear wave reflection as an exploration tool. Many field tests were carried out at a variety of exploration sites, but no shear wave reflections were ever observed. The field records only showed a highly dispersive cone of Love waves occurring after the shear wave refraction arrivals. If any reflections exist within the cone of Love waves then they would have to be extracted from the data by a sophisticated processing technique. In theory, shear wave reflection could be used to profile the overburden/bedrock boundary as this would present a large acoustic impedance to shear waves.

APPENDIX A

3 LAYER SHALLOW REFRACTION MODEL

Seismic Earth Model

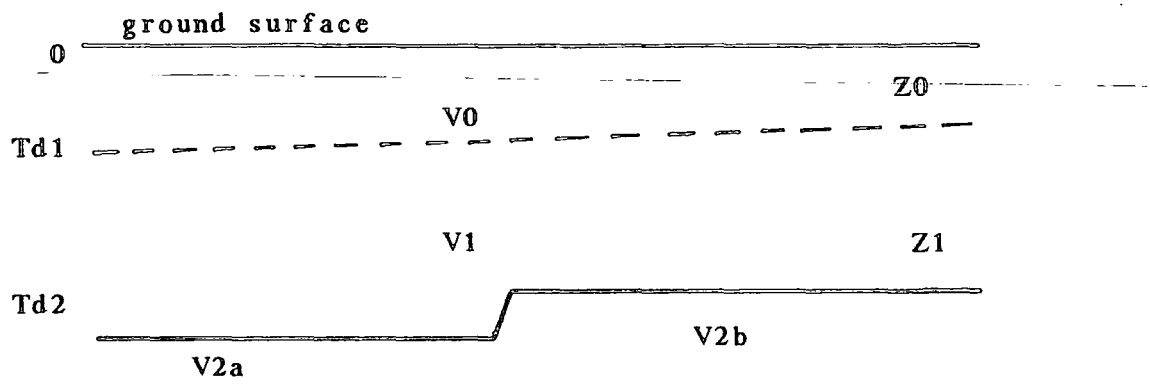

Td - Time. Depth values(msec) V - Velocity(m/sec) Z - Depth(meters)

Values of Td1

These values are usually obtained from short offset refraction spreads, used to monitor the very near surface velocity structure. These surveys can yield time depth values, but usually half intercept times are used to obtain Td1 values at the shot points. Intermediate values over the whole line at each peg are obtained by interpolation.
In shallow refraction surveys, the V0 layer is regarded as being the very near surface "soil" layer and must be taken into account due to low seismic velocity.

Values of Td2

These values are obtained from analysis of complete data sets of forward and reversed first break picks from the top of the V2 refractor. Time depth values are calculated using either the plus-minus method (Hagedoorn, 1959) or the generalized reciprocal method (Palmer, 1980). This refractor will be the target refractor, a sudden depth change found in this refractor may be used as a fault indicator.

Values of V0

This value is found by plotting a traveltime graph of the direct wave from short offset spreads, the velocity value being the reciprocal of the gradient to the best fit line through the data points.

Value of V1

This value is determined by using the plus-minus method on data from short offset refraction spreads, where data reversal exists. When no reversal exists, then simple dipping layer analysis is carried out to determine the average refactor velocity.

Values for V2

This is the velocity value of the target refractor, a lateral change in velocity along this refractor may be used as a fault indicator. Velocity analysis is carried out by using the plus-minus method on reversed "first break" picks from refracted arrivals from this horizon.

DEPTH CONVERSION OF TIME DEPTHS

Stage 1

Values of Z0 are calculated by multiplying the values of Td1 by the conversion velocity Vcon1:

$$Vcon1 = \frac{V0 \cdot V1}{\sqrt{V1^2 - V0^2}} \qquad Z0 = Td1 \times Vcon1$$

Stage 2

The time depth value of the V0 layer is recalculated with respect to the V2 layer i.e. the time depth that the ray refracting from the V2 layer takes to go through the V0 layer. This is different to the calculated value of Td1 due to the different raypaths involved.

$$Vcon2 = \frac{V0 \cdot V2}{\sqrt{V2^2 - V0^2}} \qquad Td1(apparent) = \frac{Z0}{Vcon2}$$

Stage 3

Subtract the value of Td1(apparent) from the calculated value of Td2. This gives Td(t), the time depth thickness of V1.

Stage 4

Using the value of Td(t) and the conversion velocity, the thickness of the Z1 layer can be calculated.

$$Vcon3 = \frac{V2 \cdot V1}{\sqrt{V2^2 - V1^2}} \qquad Z1 = Vcon3 \times Td(t)$$

Stage 5

To determine the depth to the V2 layer, the values of Z0 (stage 1) and Z1 (stage 5) are added together.

Rapid method

Assume the recalculation of the time depths in stage 2 is insignificant. This may be due to a thin V0 layer, or the fact that the V0 layer has a much lower velocity than either V1 or V2, so there is no significant difference in raypaths through the V0 layer for refractions from V1 and V2 layers.
In this case complete stage 1, then just subtract Td1 from Td2 and go to stage 4.

APPENDIX B

REFRACTION PROGRAMS

A set of four fortran programs perform the Generalized Reciprocal Method (Palmer, 1980) on a set of refraction data. The program uses a data file containing the peg number, forward time and reverse time for refraction picks from the same refractor. The data file also contains the Peg spacing and the Reciprocal Time for the refraction line.
After running each program the data file is updated with new information. The programs output graphs in the form of EASYPLOT data files, so that individual plots may be stored and later plotted using a variety of scales.
The programs are entitled : RECIPV RECIPP RECIPD RECIPL

RECIPV - This program calculates the velocity function for a given range of XY spacings. The program outputs a graph file of the results, along with a file of a reduced velocity plot.

RECIPL - This program carries out linear regression on a set of data points and outputs values of the best fit velocity gradient and intercept.

RECIPP - This program calculates the Time Depth values for a given range of XY spacings.

RECIPD - This program depth converts the time depth values. and outputs a graph of the results.

Example of Data file for RECIPV

```
STANLEY MOSS                    - Project name
 62                             - No. of forward & reverse readings (msec)
3.0                             - Peg Spacing (meters)
    0.0      0.0                - Time shifts to forward & reverse values
31.0    30.0    107.5
32.0    30.5    105.5           - Peg no.,Forward time, Reverse time (msec)
 | |     | |     | |
 | |     | |     | |
58.0    69.0    71.5
  200.0                         - Reciprocal Time (msec)
5                               - No. of iterations of XY
   0.0      60.0       6       - Graph parameters Xmin Xmax Nxdiv
   0.0     100.0      10       -                  Ymin Ymax Nydiv
 2000.0                         - Reduction velocity
```

Example of data file for RECIPP

The data file same as above except for the addition of the following values on the end of the file, and erasure of the reduction velocity.

```
2000.0  3000.0  2000.0    - Refractor Velocity Between the Peg Nos.
  20.0    30.0            - Peg Numbers (Pa & Pc)
```

Example of data file for RECIPD

```
STANLEY MOSS                    - Name
     3.0                        - Peg spacing
 50                             - No. of readings
     1.0     10.0
     2.0     10.2
     3.0     10.3
      |       |                 - Peg no. & Time depth
      |       |                           values
      |       |
   50.0      20.0
 1000.0    1200.0               - Vd1 & Vd2 values
   25.0                         - Peg a
 2000.0    2500.0  3000.0      - Vr1, Vr2 & Vr3 values
   20.0 40.0                    - Peg b & c
```

Values of Vd,Vr & Peg apply to the model described below.

Refractor Velocity Model

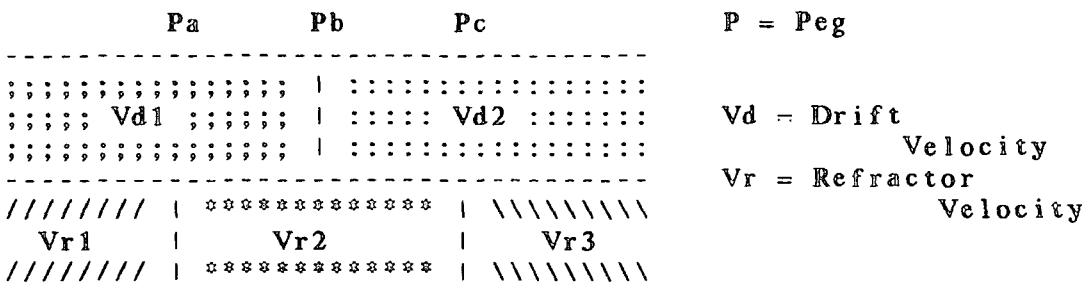

Running the programs

RUN RECIPV 5=Data1 6=PLOT1 7=Out 8=Plot2

Data - Input Data File
Plot1 - Easyplot file of Graph of Velocity Function values
Plot2 - Easyplot file of Graph of Reduced Velocity Function Values
Out1 - Numerical file of Velocity Function Values

RUN RECIPL 5=Out 6=Results

Out1 - Input Data File from RECIPV (edited to contain relevant data points).
Results - Output File containing Results of Least Squares Analysis

RUN RECIPP 5=Data2 6=Plot2 7=Out2

Data2 - Input Data File (amended version of Data1)
Plot2 - Easyplot File of Graph of Time Depth values
Out2 - Numerical Data File of Time Depth values

RUN RECIPD 5=Out2 6=Plot3 7=Out3

Out2 - Input data file from RECIPP (amended)
Plot3 - Easyplot file of Graph of depth values
Out3 - Numerical Data file of depth values

Program - RECIPV

```
C      RECIPROCAL METHOD VELOCITY FUNCTION
C      BY       P. J. BRABHAM  1984
C
       DIMENSION PEG(100),F(100),R(100),TV(10,100),PEGN(10,100),
      *NAME(20),TVD(10,100),FM(100),RM(100),TRED(10,100),DUMP(10)
C
       READ(5,5) NAME
     5 FORMAT(20A1)
C
C      N = THE NUMBER OF FORWARD / REVERSE VALUES
C
       READ(5,10)N
    10 FORMAT(I4)
C
C      PEGSPA = GEOPHONE PEG SPACING  ( METERS)
C
       READ(5,15) PEGSPA
       15 FORMAT(F4.1)
C
C      READ IN ANY TIME SHIFTS TO THE FORWARD AND REVERSE TIMES
C      ( E.G.  ZERO CROSSINGS TO 1ST BREAKS  MINUS CORRECTION)
C
       READ(5,18)CORF,CORR
    18 FORMAT(2F8.2)
       CORF=CORF/1000.0
       CORR=CORR/1000.0
C
C      READ IN THE VALUES OF THE PEG NO. FORWARD AND REVERSE TIMES
C
       DO 50 I=1,N
       READ(5,20)PEG(I),FM(I),RM(I)
       F(I)=(FM(I)/1000.0)+CORF
       R(I)=(RM(I)/1000.0)+CORR
       IF(FM(I).EQ.0.0)F(I)=0.0
       IF(RM(I).EQ.0.0)R(I)=0.0
    20 FORMAT(F5.1,2F8.2)
    50 CONTINUE
C
C      READ IN THE VALUE OF THE RECIPROCAL TIME  (RECIP)
C
       READ(5,60)RECIP
    60 FORMAT(F8.2)
       RECIP=RECIP/1000.0
C
C      READ IN THE NUMBER OF XY INCREMENTS REQUIRED
C
       READ(5,70)KO
    70 FORMAT(I2)
C
C      READ IN THE GRAPH PARAMETERS
C
       READ(5,80)XMIN,XMAX,NXDIV
       READ(5,80)YMIN,YMAX,NYDIV
    80 FORMAT(2F8.2,I8)
```

```
      READ(5,82)REDV
   82 FORMAT(F8.1)
C
C     THIS IS THE END OF THE DATA INPUT
C     NOW
C     CALCULATE THE VELOCITY FUNCTION
C
      DO 120 L=1,KO
      LT=L-1
      DO 100 J=1,N
      I=J-LT
      IF (I.LT.1)GOTO 100
      TV(L,J)=(F(J)-R(I)+RECIP)/2.0
      PEGN(L,J)=(PEG(I)+PEG(J))/2.0
      IF (F(J).EQ.0.0)TV(L,J)=0.0
      IF (R(I).EQ.0.0)TV(L,J)=0.0
  100 CONTINUE
  120 CONTINUE
C
C     THIS IS THE END OF THE CALCULATION
C     NOW
C     WRITE OUT THE EASYPLOT FILE  & REDUCED VELOCITY FILE
C
      WRITE(6,200)NAME
      WRITE(8,201)NAME,REDV
  200 FORMAT(13H &OPTS HEAD=',20A1,28HRECIPROCAL METHOD VELOCITY',)
  201 FORMAT(13H &OPTS HEAD=',20A1,17HREDUCED VELOCITY ,F8.1,6H M/S',)
      WRITE(6,205)
      WRITE(8,205)
  205 FORMAT(20H  XLAB='PEG NUMBER',)
      WRITE(6,210)
      WRITE(8,210)
  210 FORMAT(22H  YLAB='MILLISECONDS',)
      WRITE(6,220)XMIN,XMAX,NXDIV
      WRITE(8,220)XMIN,XMAX,NXDIV
  220 FORMAT(7H  XMIN=,F8.2,6H,XMAX=,F8.2,7H,NXDIV=,I4,1H,)
      WRITE(6,230)YMIN,YMAX,NYDIV
      WRITE(8,230)YMIN,YMAX,NYDIV
  230 FORMAT(7H  YMIN=,F8.2,6H,YMAX=,F8.2,7H,NYDIV=,I4,1H,)
      WRITE(6,240)
      WRITE(8,240)
  240 FORMAT(27H  PSIZE=0.5,XLEN=16,YLEN=8,,15HNY=1,GRID='NO',)
      WRITE(6,250)
      WRITE(8,250)
  250 FORMAT(43H  LETSIZ=0.2,PLOT='SCAT',NSYMB=3,DEV='VDU',)
      WRITE(6,255)
      WRITE(8,255)
  255 FORMAT(34H  XAXFMT='JF4.0*',YAXFMT='JF4.0*',)
      WRITE(6,260)
      WRITE(8,260)
  260 FORMAT(5H &END)
      DO 300 L=1,KO
      DUMP(L)=0.0
  300 CONTINUE
      DO 310 L=1,KO
      LT=L-1
      DO 320 J=1,N
      I=J-LT
      IF(I.LT.1)GOTO 320
      IF (TV(L,J).EQ.0.0)GOTO 320
```

```
C
C      APPLY A DC SHIFT TO THE XY INCREMENTS TO MAKE GRAPH READABLE
C
       TVD(L,J)=(TV(L,J)+(LT*0.017))*1000
       IF(DUMP(L).EQ.0.0)DUMP(L)=PEGN(L,J)
       TRED(L,J)=TV(L,J)-(((PEGN(L,J)-DUMP(L))*PEGSPA)/REDV)
       TRED(L,J)=(TRED(L,J)+(LT*0.006))*1000
C
C      OUTPUT IN MILLISECONDS
C
       WRITE(6,350)PEGN(L,J),TVD(L,J)
       WRITE(8,350)PEGN(L,J),TRED(L,J)
  350  FORMAT('    ',F8.2,',',F8.2,',')
  320  CONTINUE
  310  CONTINUE
C
C      OUTPUT A NUMERICAL DATA FILE FOR REFERENCE PURPOSES
C
       WRITE(7,400)
  400  FORMAT(27H  VELOCITY FUNCTION RESULTS,//)
       WRITE(7,410)
  410  FORMAT(40H  OUTPUT COMPATIBLE WITH LESTSQ ANALYSIS,//)
       WRITE(7,420)NAME
  420  FORMAT(20A1)
       WRITE(7,430)
  430  FORMAT(9H N ( I5 ))
       WRITE(7,440)PEGSPA
  440  FORMAT(F4.1)
C
C      PRINT OUT THE PEG NO & VELOCITY FUNCTION VALUES
C
       DO 450 L=1,KO
       LT=L-1
       DO 460 J=1,N
       I=J-LT
       IF(I.LT.1)GOTO 460
       IF(TV(L,J).EQ.0.0)GOTO 460
       TV(L,J)=TV(L,J)*1000
       WRITE(7,444)PEGN(L,J),TV(L,J)
  444  FORMAT(F5.1,F8.2)
  460  CONTINUE
  450  CONTINUE
       STOP
       END
```

Program - RECIPL

```
C   LEAST SQUARES ANALYSIS OF REFRACTION DATA
C   AMENDED FOR USE WITH RECIPROCAL METHOD
C   BY  P. J. BRABHAM      1983
C
      DIMENSION PEGN(100),TTIME(100),PDIST(100),NAME(20),TIMEL(20)
      READ(5,5) NAME
    5 FORMAT(20A1)
C
C   N  = THE NUMBER OF DISTANCE (METERS) & TIMES (MILLISECS)
```

```
C    PS = PEG SPACING (METERS)
C
        READ(5,10) N
   10   FORMAT(I5)
        READ(5,15) PEGSPA
   15   FORMAT (F5.1)
C
C    READ IN THE PEG NO. AND TRAVEL TIME
C
        DO 30 J = 1,N
        READ(5,20) PEGN(J),TTIME(J)
        TTIME(J)=TTIME(J)/1000.0
   20   FORMAT (F5.1,F8.2)
   30   CONTINUE
C
C   CONVERT PEG NUMBER TO DISTANCE (METERS)
C
        DO 60 J = 1,N
        PDIST(J) =(PEGN(J) * PEGSPA) - PEGSPA
   60   CONTINUE
C
C   END OF DATA INPUT
C   NOW
C   INITIALISE VARIABLES TO ZERO
C
        SUMX = 0.0
        SUMXSQ = 0.0
        SUMY = 0.0
        SUMYSQ = 0.0
        SUMXY = 0.0
C
C SUMMATION
C
        DO 100 I = 1,N
        SUMX = SUMX + PDIST(I)
        SUMXSQ = SUMXSQ + (PDIST(I) * PDIST(I))
        SUMY = SUMY + TTIME(I)
        SUMYSQ = SUMYSQ + (TTIME(I) * TTIME(I))
        SUMXY = SUMXY + (PDIST(I) * TTIME(I))
  100   CONTINUE
C
C    SUMMATIONS ARE COMPLETE
C    NOW CARRY OUT
C    LEAST SQUARES ANALYSIS  FOR  GRADIENT AND INTERCEPT
C
        DENOM = (N * SUMXSQ) - (SUMX * SUMX)
        AT = (N * SUMXY) - (SUMX * SUMY)
        BT = ((SUMXSQ * SUMY) - (SUMX * SUMXY))
        GRAD = AT / DENOM
        VEL = 1.0 / GRAD
        YINT = BT / DENOM
C
C     CALCULATE LEAST SQUARES  VALUES
C
        T1 = ((GRAD * PDIST(1)) + YINT)*1000
        TN = ((GRAD * PDIST(N)) + YINT)*1000
        YINT = YINT * 1000
C
C    VELOCITY AND INTERCEPT VALUES ARE CALCULATED
C    NOW CALCULATE ERRORS
```

```
C
      AE = ((N * SUMXY) - (SUMX * SUMY))**2
      BE = (N * SUMXSQ) - (SUMX * SUMX)
      DE = N * SUMYSQ
      CE = SUMY * SUMY
      FSIGY = DE - CE - (AE/BE)
      SIGY = SQRT(FSIGY / (N * N))
C
C  STANDARD ERROR OF GRADIENT
C
      SEB = ((N - 2) * ((N * SUMXSQ) - (SUMX * SUMX)))**0.5
      SER = (N * SIGY) / SEB
      SERVEL = (SER / GRAD )*VEL
C
C THIS IS THE STANDARD ERROR OF THE VELOCITY
C-------------------------------------------------------------------------
      ESEB = ((SEB * SEB) * N)**0.5
      ESER = ((N * SIGY * SUMXSQ)**0.5) / ESEB
      ESER = ESER * 1000
C
C ESER - THIS IS THE STANDARD ERROR OF THE INTERCEPT
C NOW WRITE OUT THE RESULTS
C
      WRITE(6,180)
  180 FORMAT(///'++++++++++++++++++++++++++++++++++++++++++++++'/////)
      WRITE(6,190) NAME
  190 FORMAT('      SITE : ',20A1/'      *******'//)
C
      WRITE(6,195)
  195 FORMAT('INPUT UNITS      DISTANCE : METERS     TIME : MILLISECONDS')
      WRITE(6,200) PEGSPA
  200 FORMAT(/'PEG SPACING : ',F5.1,'  METERS'//)
C
  210 FORMAT('PEG NUMBER     DISTANCE           TIME    ',/)
      WRITE (6,210)
C
      DO 230 I= 1,N
      TMIL=TTIME(I)*1000
      WRITE(6,220) PEGN(I),PDIST(I),TMIL
  220 FORMAT(F5.1,F15.1,F18.2)
  230 CONTINUE
C
      WRITE(6,250)
  250 FORMAT(///,'LEAST SQUARES REGRESSION LINE'/'--------------'//)
      WRITE(6,260) GRAD,SER
  260 FORMAT('GRADIENT  =    ',F10.6,'  +/- ',F10.6//)
C
      WRITE(6,280) VEL,SERVEL
  280 FORMAT('VELOCITY  =    ',F10.2,'  +/- ',F10.2,'METERS PER SECOND',
     *//)
C
      WRITE(6,300) YINT,ESER
  300 FORMAT('INTERCEPT =    ',F10.2,'  +/- ',F10.2,'MILLISECONDS'///)
C
      WRITE(6,320)
  320 FORMAT('VALUES OF REGRESSION FIT'/'------------------------'/)
      WRITE(6,340) PEGN(1),T1
      WRITE(6,350) PEGN(N),TN
  340 FORMAT('PEG : ',F5.1,'  TIME : ',F8.2)
  350 FORMAT('PEG : ',F5.1,'  TIME : ',F8.2/////////)
```

```
C
      STOP
      END


      Program - RECIPP
      ----------------


C     RECIPROCAL METHOD TIME DEPTH FUNCTION
C     BY       P. J. BRABHAM  1984
C
      DIMENSION PEG(100),F(100),R(100),TP(10,100),PEGN(20,100),
     *NAME(20),TPD(10,100),FM(100),RM(100)
      READ(5,5) NAME
    5 FORMAT(20A1)
C
C     N = THE NUMBER OF FORWARD / REVERSE VALUES
C
      READ(5,10)N
   10 FORMAT(I4)
C
C     PEGSPA = GEOPHONE PEG SPACING  ( METERS)
C
      READ(5,15)PEGSPA
   15 FORMAT(F4.1)
C
C     READ IN ANY TIME SHIFTS TO THE FORWARD AND REVERSE TIMES
C     ( E.G.  ZERO CROSSINGS TO 1ST BREAKS  MINUS CORRECTION)
C
      READ(5,18)CORF,CORR
   18 FORMAT(2F8.2)
      CORF=CORF/1000.0
      CORR=CORR/1000.0
C
C     READ IN THE VALUES OF THE PEG NO. FORWARD AND REVERSE TIMES
C
      DO 50 I=1,N
      READ(5,20)PEG(I),FM(I),RM(I)
      F(I)=(FM(I)/1000.0)+CORF
      R(I)=(RM(I)/1000.0)+CORR
      IF(FM(I).EQ.0.0)F(I)=0.0
      IF(RM(I).EQ.0.0)R(I)=0.0
   20 FORMAT(F5.1,2F8.2)
   50 CONTINUE
C
C     READ IN THE VALUE OF THE RECIPROCAL TIME  (RECIP)
C
      READ(5,60)RECIP
   60 FORMAT(F8.2)
      RECIP=RECIP/1000.0
C
C     READ IN THE NUMBER OF XY INCREMENTS REQUIRED
C
      READ(5,70)KO
   70 FORMAT(I2)
C
C     READ IN THE GRAPH PARAMETERS
C
      READ(5,80)XMIN,XMAX,NXDIV
```

```
      READ(5,80)YMIN,YMAX,NYDIV
   80 FORMAT(2F8.2,I8)
   90 FORMAT(F5.0)
C     READ IN THE REFRACTOR VELOCITIES VR1,VR2,VR3
      READ(5,94)VR1,VR2,VR3
   94 FORMAT(3F8.1)
      READ(5,96)STA1,STA2
   96 FORMAT(2F8.1)
C
C     THIS IS THE END OF THE DATA INPUT
C     NOW
C     CALCULATE THE TIME DEPTH FUNCTION
C
      DO 120 L=1,KO
      LT=L-1
      DO 100 J=1,N
      I=J-LT
      IF (I.LT.1)GOTO 100
      XY=(PEG(J)-PEG(I))*PEGSPA
      PEGN(L,J)=(PEG(J)+PEG(I))/2.0
      IF(PEGN(L,J).LE.STA1)VR=VR1
      IF(PEGN(L,J).GT.STA1.AND.PEGN(L,J).LE.STA2)VR=VR2
      IF(PEGN(L,J).GT.STA2)VR=VR3
      TP(L,J)=((F(J)+R(I))-(RECIP+(XY/VR)))/2.0
      IF(F(J).EQ.0.0)TP(L,J)=0.0
      IF(R(I).EQ.0.0)TP(L,J)=0.0
  100 CONTINUE
  120 CONTINUE
C
C     THIS IS THE END OF THE CALCULATION
C     NOW
C     WRITE TO DATA FILE FOR DEPTH CONVERSION
C
      WRITE(7,160)NAME
  160 FORMAT(20A1)
      WRITE(7,162)PEGSPA
  162 FORMAT(F8.2)
      WRITE(7,164)
  164 FORMAT(25H ** N NO.OF READINGS (I3))
C
C     WRITE OUT THE EASYPLOT FILE
C
      WRITE(6,200)NAME
  200 FORMAT(13H &OPTS HEAD=',20A1,30HRECIPROCAL METHOD TIME DEPTH',)
      WRITE(6,205)
  205 FORMAT(20H  XLAB='PEG NUMBER',)
      WRITE(6,210)
  210 FORMAT(22H  YLAB='MILLISECONDS',)
      WRITE(6,220)XMIN,XMAX,NXDIV
  220 FORMAT(7H  XMIN=,F8.2,6H,XMAX=,F8.2,7H,NXDIV=,I4,1H,)
      WRITE(6,230)YMIN,YMAX,NYDIV
  230 FORMAT(7H  YMIN=,F8.2,6H,YMAX=,F8.2,7H,NYDIV=,I4,1H,)
      WRITE(6,240)
  240 FORMAT(27H  PSIZE=0.5,XLEN=16,YLEN=8,,15HNY=1,GRID='NO',)
      WRITE(6,250)
  250 FORMAT(43H  LETSIZ=0.2,PLOT='SCAT',NSYMB=3,DEV='VDU',)
      WRITE(6,255)
  255 FORMAT(34H  XAXFMT='JF4.0*',YAXFMT='JF4.0*',)
      WRITE(6,260)
  260 FORMAT(5H &END)
```

```
C
      DO 310 L=1,KO
      LT=L-1
      DO 320 J=1,N
      I=J-LT
      IF(I.LT.1)GOTO 320
      IF (TP(L,J).EQ.0.0)GOTO 320
C
C     APPLY A DC SHIFT TO THE XY INCREMENTS TO MAKE GRAPH READABLE
C     OUTPUT IN MILLISECONDS
C
      TPD(L,J)=(TP(L,J)+(LT*0.008))*1000
      WRITE(6,350)PEGN(L,J),TPD(L,J)
      TO=TP(L,J)*1000
      WRITE(7,348)PEGN(L,J),TO
  348 FORMAT(2F8.2)
  350 FORMAT('    ',F8.2,',',F8.2,',')
  320 CONTINUE
  310 CONTINUE
      STOP
      END


      Program - RECIPD
      ----------------

C     RECIPROCAL METHOD TIME DEPTH FUNCTION -->  DEPTH CONVERSION
C     BY       P. J. BRABHAM  1984
C
      DIMENSION NAME(20),PEG(200),TD(200),PA(6),PB(6),VO(6),
     *QA(6),QB(6),VT(6),VDRIFT(200),VREF(200),VAV(200),DEPTH(200)
      READ(5,5) NAME
    5 FORMAT(20A1)
      READ(5,10)PEGSPA
   10 FORMAT(F8.2)
C
C     N IS THE NUMBER OF DEPTH VALUES
C
      READ(5,20)N
   20 FORMAT(I3)
C
C     READ IN THE VALUES OF THE PEG NO. & TIME DEPTH VALUE
C
      DO 50 I=1,N
      READ(5,30)PEG(I),TD(I)
      TD(I)=TD(I)/1000
   30 FORMAT(2F8.2)
   50 CONTINUE
C
C     READ IN THE LAYER 1 VELOCITIES
C
      READ(5,94)VD1,VD2
   94 FORMAT(2F8.1)
      READ(5,96)P1
   96 FORMAT(F5.1)
C
C     READ IN THE LAYER 2 VELOCITIES
C
      READ(5,110)VR1,VR2,VR3
  110 FORMAT(3F8.1)
```

```
      READ(5,115)P2,P3
  115 FORMAT(2F5.1)
C
C     THIS IS THE END OF THE DATA INPUT
C     NOW
C     CALCULATE THE  DEPTH  VALUE
C
      DO 180 I=1,N
      IF(PEG(I).LE.P1)VDRIFT(I)=VD1
      IF(PEG(I).GT.P1)VDRIFT(I)=VD2
      IF(PEG(I).LE.P2)VREF(I)=VR1
      IF(PEG(I).GT.P2.AND.PEG(I).LE.P3)VREF(I)=VR2
      IF(PEG(I).GT.P3)VREF(I)=VR3
C
C     CALCULATE V AVERAGE
C
      A=VDRIFT(I)*VREF(I)
      B=SQRT((VREF(I)**2)-(VDRIFT(I)**2))
      VAV(I)=A/B
C
C     CALCULATE THE DEPTH
C
      DEPTH(I)=VAV(I)*TD(I)
  180 CONTINUE
C
C     THIS IS THE END OF THE CALCULATION
C     NOW
C     WRITE OUT THE EASYPLOT FILE
C
      WRITE(6,200)NAME
  200 FORMAT(13H &OPTS HEAD=',20A1,26HRECIPROCAL METHOD  DEPTH',)
      WRITE(6,205)
  205 FORMAT(20H  XLAB='PEG NUMBER',)
      WRITE(6,210)
  210 FORMAT(22H  YLAB='MILLISECONDS',)
      WRITE(6,220)
  220 FORMAT(33H  XMIN=****,XMAX=****,NXDIV=****,)
      WRITE(6,230)
  230 FORMAT(33H  YMIN=****,YMAX=****,NYDIV=****,)
      WRITE(6,240)
  240 FORMAT(27H  PSIZE=0.5,XLEN=16,YLEN=8,,15HNY=1,GRID='NO',)
      WRITE(6,250)
  250 FORMAT(43H  LETSIZ=0.2,PLOT='SCAT',NSYMB=3,DEV='VDU',)
      WRITE(6,255)
  255 FORMAT(34H  XAXFMT='JF4.0*',YAXFMT='JF4.0*',)
      WRITE(6,260)
  260 FORMAT(5H &END)
      DO 500 I=1,N
      WRITE(6,400)PEG(I),DEPTH(I)
  400 FORMAT(F8.2,2H,-,F5.2,1H,)
  500 CONTINUE
      STOP
      END
```

APPENDIX C

REFLECTION PROGRAMS

Tape Handling Programs for SEGD Land Data.

A suite of programs has been developed on NUMAC for the conversion of a SEG-D field tape from the Nimbus Tape support, to a SEG-Y CMP sorted tape which can be transferred to the Durham University Processing System for further processing to be carried out.
The program suite has the added ability of applying individual mutes and static shifts to each trace.

The programs are written in FORTRAN 77, so they need to be compiled via a suitable compiler. FORTRAN 77 was used because the sort program makes use of the direct access feature available, this speeds up the sorting process over conventional FORTRAN.

The tape handling suite comprises of four FORTRAN 77 programs:

TAPEDUMP - A program which removes the numerical data from a SEG-D tape, decodes the 2 byte quaXternary exponent numerical format of SEG-D. The program then outputs all the seismograms as a one dimensional array onto a temporary disk file.

SORTPROG - An interactive program which outputs a numerical data file which indexes the original file and record number of the field records into a common shot or common mid point sorted order.

The program works for a variety of acquisition geometries used throughout the fieldwork. The shot - receiver offset is calculated by the program. For each gather the records are sorted into ascending offset value. Numerical values for the individual mute and static shift values can also be applied via the program.

EDITSORT - This is an interactive program which allows the editing of the SORT data file. Information can be added to the SORT data file to apply an offset dependent mute function or static shifts. The program also allows for the editing out of the data set of unwanted traces, based on individual file and record number, or files with a common offset or with a common original file number.

SEGDSEGYMS - A program which uses the numerical dump of digital Seismogram sample values output by TAPEDUMP, plus the SORT data file from SORTPROG.

The program outputs a SEG-Y tape sorted into either CSGs or CMPs, depending upon the SORT file.

A SEG-Y header block is written onto the start of the tape (copied directly from file SEGYHED).

The digital seismogram values are written sequentially onto the tape, applying mutes and static shifts as directed by the SORT data file.

If the data file contains zeros then a zero file is written onto tape.

Information such as offset, gather number and number in the gather are written into the record header block.

Running the Programs

1. TAPEDUMP

RUN TAPEDUMP 7=*T* 6=-DATA 9=*SINK*

T - A SEG-D field tape mounted on a 1600 bpi tape drive and rewound to start of tape.
-DATA - A temporary file where all the digital data on the tape is dumped (this requires a large temporary file space).
SINK - Input/Output unit VDU terminal.

2. SORTPROG

RUN SORTPROG 6=*SINK* 7=SORTDATA

SORTDATA - The SORT data file.

Questions need to be answered in the running of this program. You should be armed with the answers, this is the data required :

a. Sampling frequency of seg-d data
b. Survey peg spacing (meters)
c. Number of common shot files taken.
d. Peg no. of shot & Peg no. of 1st geophone for each file.
e. Offset dependent mute function values.

3. SEGDSEGYMS

RUN SEGDSEGYMS 2=SEGYHED 5=SORTDATA 6=*SINK* 7=-DATA 8=*OUT*

SEGYHED - A SEG-Y tape header block which is copied and written to the start of the SEG-Y tape.
OUT - A virgin tape mounted onto a tape drive (1600 bpi).

Example of a SORT data file (SORTDATA)

Two CMPs or CSGs, each with 6 fold data

```
2                                          - Digital samples per sec
21   1   0   0    0    0    0             - Individual trace information
21   2   0   0    0    0    0                   (see below)
21   3   0   0   35    0    0
21   4   3   5   55  120    0
21   5   2   9   75  128    0
21   6   7   1   95  139    0
22   1   0   0    0    0    0
22   2   0   0    0    0    0
22   3   0   0   40    0    0
22   4   3   6   60  122    0
22   5   2  10   80  130    0
22   6   7   2  100  143    0
 0                                         - end of file marker
```

Column 1 = CMP/CSG number
Column 2 = Record No. in CMP/CSG
Column 3 = Original Shot File No.
Column 4 = Record No. in Original File
Column 5 = Shot-receiver offset (meters)
Column 6 = Mute Function Value
Column 7 = Static Shift value

Program - TAPEDUMP

```
C     ************************************************************
C     This program reads a SEG-D field tape mounted on a drive
C     (Unit 7).
C     The program then decodes the digital seismogram values by
C     masking the 2nd, 3rd, & 4th bits on the tape.
C     The data is then written to a temporary disk file (Unit 6)
C     Unit 9 is a VDU terminal
C     This program is written in FORTRAN 77.
C     ************************************************************
C
C     PROGRAM BY P.BRABHAM (1984)
C
      INTEGER*2 A, ILEN, SEIS, CRAP, CRAP2
      DIMENSION A(1034), SEIS(1024,12)
      CRAP=24576
      CRAP2=4096
      IREC=1
      IRLEN=2056
      OPEN(UNIT=6,ACCESS='DIRECT',RECL=IRLEN,FORM='UNFORMATTED')
      WRITE(9,*)'HOW MANY SHOT FILES ARE ON THIS TAPE ? (Integer)'
      WRITE(9,*)'-------------------------------------'
      READ(9,*)ITAPE
C
C    DO LOOP FOR THE NUMBER OF SHOT FILES ON THE SEG-D TAPE
C
      DO 100 J=1,ITAPE
C
C    WIND TAPE OVER THE HEADER BLOCK
C
      ILEN = 5
      CALL CNTRL('FSR 1', ILEN, 7)
C
C     EXECUTE DO LOOP TO READ IN 12 FILES
C
      DO 20 L = 1, 12
        ILEN = 2068
        CALL READ(A, ILEN, 0, LNUM, 7)
        DO 10 I = 1, 1024
          M = I + 10
          SEIS(I,L) = A(M)
C
C    CORRECT DATA INTO AN UNDERSTANDABLE FORM BY MASKING OUT THE SECOND
C    THIRD AND FOURTH BITS ON THE TAPE
C
          IF (SEIS(I,L) .GT. 1023) SEIS(I,L) = SEIS(I,L) - CRAP
          IF (SEIS(I,L) .LT. 0) SEIS(I,L) = SEIS(I,L) + 1
          IF (SEIS(I,L) .LT. - 1024) SEIS(I,L) = SEIS(I,L) + CRAP2
 1000   FORMAT(F6.1)
   10   CONTINUE
        WRITE(UNIT=6,REC=IREC) (SEIS(JK,L),JK=1,1024)
        IREC=IREC+1
   20   CONTINUE

C
```

```
C    SKIP THE END OF FILE MARKER SO THAT TAPE IS READY TO READ NEXT
C    SEISMOGRAM
C
       ILEN=5
       CALL CNTRL('FSR 1',ILEN,7)
       WRITE(9,*) 'File ',J,' has been written to disk'
  100    CONTINUE
       CLOSE(UNIT=6)
       STOP
       END
```

PROGRAM - SORTPROG

```
C
C      **********************************************************************
C      This program will produce a data file that will sort the
C      field data into either CSGs or CMPs.
C      Original data shot as 12 channel records
C      The program is interactive
C      The program is written in FORTRAN 77
C      **********************************************************************
C
       IMPLICIT INTEGER(A - Y)
       DIMENSION FILENO(1000), RECNO(1000), CDPNO(1000), OFF(1000),
      1          CDPNO2(1000,40), OFF2(1000,40), FILEN2(1000,40),
      2          RECNO2(1000,40),MO(100),MT(100),EOFF(100),
      3          SHOTS(1000)
C
C     ----------------------PROGRAM INTRODUCTION-------------------------
C
       WRITE (6,*)' ††††††††††††††††††††††††††††††††††††††††'
       WRITE (6,*)'  Welcome to the cdp sort program !'
       WRITE (6,*)'  Answer the questions put to you,'
       WRITE (6,*)'  All input numbers are integers.'
       WRITE (6,*)' ††††††††††††††††††††††††††††††††††††††††'
       WRITE (6,*)'      '
       WRITE (6,*)'      '
       WRITE (6,*)'      '
       WRITE (6,*)' Do you want to sort the data into '
       WRITE (6,*)'      '
       WRITE (6,*)' Common Shot Gathers        (input 0)'
       WRITE (6,*)'      '
       WRITE (6,*)' Common mid point gathers  (input 1)'
       WRITE (6,*)'      '
       READ (6,*) SORT
       WRITE (6,*)'      '
       WRITE (6,*)'      '
       WRITE (6,*)'      '
       WRITE (6,*)'      '
       WRITE (6,*)'      '
       WRITE (6,*)'      '
       WRITE (6,*)'      '
       WRITE (6,*)'      '
       WRITE (6,*)' Shooting Technique'
       WRITE (6,*)' ------------------'
       WRITE (6,*)'      '
       WRITE (6,*)' Which one of these techniques is employed ?'
```

```
      WRITE (6,*)'      '
      WRITE (6,*)'         ----> increasing Peg no.'
      WRITE (6,*)' (0) '
      WRITE (6,*)'       Shot Point        1st geo         Last geo'
      WRITE (6,*)' -----*----------------*--------------*-----------'
      WRITE (6,*)' (1) '
      WRITE (6,*)'       Shot Point        Last geo        1st geo'
      WRITE (6,*)' -----*----------------*--------------*-----------'
      WRITE (6,*)'      '
      WRITE (6,*)'  ie.   For geophone nos. > Peg nos'
      WRITE (6,*)'        Last geo offset > 1st geo offset  input 0'
      WRITE (6,*)'        Last geo offset < 1st geo offset  input 1'
      WRITE (6,*)'      '
      WRITE (6,*)'      '
      READ (6,*)SWITCH
C-----------------------------------------------------------------------
C
C     ----------------INPUT DATA-----------------------------------------
C
      WRITE (6,*)'How many digital samples make 1 msec on tape'
      READ (6,*) NSAMP
      WRITE(7,1) NSAMP
    1 FORMAT(I3)
      WRITE (6,*)'  What is the Peg spacing of this survey ? (meters)'
      READ (6,*) PGSPAC
      WRITE (6,*)'  How many shot files are there ?'
      READ (6,*) NOSHOT
      WRITE (6,*)'.....................................................'
C
      NONE=0
      CDPMIN = 1000
      CDPMAX = 1
      IF(SORT.EQ.0)GOTO 5
      DO 20, J = 1, NOSHOT
        WRITE (6,*)' What is the peg no. of the shot in file ', J,
     1 ' ? (integer)'
        READ (6,*) ISN
        SHOTS(J)=ISN
        WRITE (6,*)' What is the peg no. of the  first  geophone in this
     & file ?'
        READ (6,*) ISG
C
C     -------CALCULATE CDP & OFFSET FOR 12 CHANNELS IN SHOT GATHER------
C
        DO 10 I = 1, 12
          K = ((J - 1)*12) + I
          IF(SWITCH.EQ.1)GOTO 11
          CDPNO(K) = ISN + ISG + I - 1
          OFF(K) = (ISG - ISN + I - 1) * PGSPAC
          OFF(K)=ABS(OFF(K))
        GOTO 12
   11     CDPNO(K) = ISN + ISG - I + 1
   13     OFF(K) = (ISG - ISN - I + 1) * PGSPAC
          OFF(K)=ABS(OFF(K))
   12     FILENO(K) = J
          RECNO(K) = I
          IF (CDPNO(K) .LT. CDPMIN) CDPMIN = CDPNO(K)
          IF (CDPNO(K) .GT. CDPMAX) CDPMAX = CDPNO(K)
   10   CONTINUE
   20 CONTINUE
      GOTO 22
```

```
    5  DO 120, J = 1, NOSHOT
         WRITE (6,*)' What is the peg no. of the shot in file ', J,
       1 ' ? (integer)'
         READ (6,*) ISN
         SHOTS(J)=ISN
         WRITE (6,*)' What is the peg no. of the  first  geophone in this
       & file ?'
         READ (6,*) ISG
C
C   -------CALCULATE SHOT NO.& OFFSET FOR 12 CHANNELS IN SHOT GATHER------
C
   21    DO 110 I = 1, 12
           K = ((J - 1)*12) + I
           CDPNO(K) = ISN
         IF (SWITCH.EQ.1)GOTO 113
           OFF(K) = (ISG - ISN + I - 1) * PGSPAC
         GOTO 112
  113      OFF(K) = (ISG - ISN - I + 1) * PGSPAC
  112      FILENO(K) = J
           RECNO(K) = I
           IF (CDPNO(K) .LT. CDPMIN) CDPMIN = CDPNO(K)
           IF (CDPNO(K) .GT. CDPMAX) CDPMAX = CDPNO(K)
  110    CONTINUE
  120 CONTINUE
C
C   ---------------INPUT DATA-----------------------------------
C
   22 WRITE(6,*)'Do you want an offset dependant mute function?'
      WRITE(6,*)'(yes=1, no=0)'
      READ(6,*)YN
      IF(YN.EQ.0)GOTO 23
      WRITE(6,*)'how many offsets do you want to mute?'
      READ(6,*)OFN
      DO 24 I=1,OFN
      WRITE(6,*)'Input offset value', I,'&time to mute until (msec)'
      READ(6,*)MO(I)
      READ(6,*)MT(I)
   24 CONTINUE
   23 WRITE(6,*)'Do you want to edit out specific offsets ?'
      WRITE(6,*)'(yes=1, no=0)'
      READ(6,*)YN2
      IF(YN2.EQ.0)GOTO 29
      WRITE(6,*)'How many offsets do you want to edit out ?'
      READ(6,*)ENO
      DO 25 I=1,ENO
      WRITE(6,*)'Input offset ',I,' you want to edit (Meters)'
      READ(6,*)EOFF(I)
   25 CONTINUE
C
C   -------SORT INTO ASCENDING CDP ( ASCENDING OFFSETS )------------
C
C            ------INITIALISE SOME ARRAYS------
C
   29 DO 40 , J = 1,1000
        DO 30 , I = 1, 40
          CDPNO2(J,I) = 0
          OFF2(J,I) = 0
          FILEN2(J,I) = 0
          RECNO2(J,I) = 0
   30   CONTINUE
```

```
 40 CONTINUE
    NORECS = NOSHOT * 12
    END = NORECS + 1
    CDPEND=CDPMAX+1
    CDPVAL = CDPMIN - 1
    KMAX = 0
 45 I = 0
    K = 0
 50 CDPVAL = CDPVAL + 1
 60 K = K + 1
 70 I = I + 1
    IF (CDPVAL .EQ.CDPEND) GO TO 90
    IF (I .EQ. END) GO TO 45
    IF (CDPNO(I) .EQ. CDPVAL) GO TO 80
    GO TO 70
 80 J = CDPNO(I)
    CDPNO2(J,K) = J
    OFF2(J,K) = OFF(I)
    FILEN2(J,K) = FILENO(I)
    RECNO2(J,K) = RECNO(I)
    IF (K.GT.KMAX) KMAX = K
    GO TO 60
C
C -----NOW SORT THE OFFSETS INTO ACENDING ORDER----------
C
 90 J=CDPMIN-1
    CDPFIN=CDPMAX+1
200 J=J+1
    IF(J.EQ.CDPFIN.AND.SORT.EQ.1)GOTO 500
    IF(J.EQ.CDPFIN.AND.SORT.EQ.0)GOTO 888
    FLAG=1
    IF(SORT.EQ.0)GOTO 198
    WRITE(6,*)'CDP being processed  *',J,'*'
    GOTO 210
198 WRITE(6,201)J
201 FORMAT(1H+,'SHOT NO BEING PROCESSED',I3)
210 K=1
220 N=K+1
    IF(K.EQ.KMAX.AND.FLAG.EQ.0)GOTO 200
    IF(K.EQ.KMAX)GOTO 210
    IF(OFF2(J,K).GT.1.AND.OFF2(J,N).LT.1)GOTO 300
    IF(OFF2(J,K).GT.OFF2(J,N))GOTO 300
    FLAG=0
230 K=K+1
    GOTO 220
300 STORE1=OFF2(J,K)
    OFF2(J,K)=OFF2(J,N)
    OFF2(J,N)=STORE1
    STORE2=CDPNO2(J,K)
    CDPNO2(J,K)=CDPNO2(J,N)
    CDPNO2(J,N)=STORE2
    STORE3=FILEN2(J,K)
    FILEN2(J,K)=FILEN2(J,N)
    FILEN2(J,N)=STORE3
    STORE4=RECNO2(J,K)
    RECNO2(J,K)=RECNO2(J,N)
    RECNO2(J,N)=STORE4
    FLAG=1
    GOTO 210
500 DO 610 , J = CDPMIN, CDPMAX
```

```
        DO 605 , I =1,KMAX
      COUNT=I
      MF=0
C
C  ---------WRITE OUT THE MUTE FUNCTION VALUE IF APPLICABLE-------
C
  502 DO 520 A=1,OFN
      IF(OFF2(J,I).EQ.MO(A))MF=MT(A)
  520 CONTINUE
C
C  ----------EDIT OUT THE TRACE IF OFFSET IS NOT REQUIRED----------
C
  503 DO 504 B=1,ENO
      IF(OFF2(J,I).EQ.EOFF(B))GOTO 506
  504 CONTINUE
      GOTO 510
  506 FILEN2(J,I)=0
      RECNO2(J,I)=0
  510 WRITE (7,601) J,COUNT, FILEN2(J,I), RECNO2(J,I),
     1OFF2(J,I),MF,NONE
  601 FORMAT(I4,I3,I3,I3,I4,I4,I4)
  605   CONTINUE
  610 CONTINUE
      GOTO 619
  888 DO 910 , J = CDPMIN, CDPMAX
        DO 905 , I =1,KMAX
      COUNT=I
      MF=0
C
C  ---------WRITE OUT THE MUTE FUNCTION VALUE IF APPLICABLE-------
C
  582 DO 580 A=1,OFN
      IF(OFF2(J,I).EQ.MO(A))MF=MT(A)
  580 CONTINUE
C
C  ----------EDIT OUT THE TRACE IF OFFSET IS NOT REQUIRED----------
C
  803 DO 804 B=1,ENO
      IF(OFF2(J,I).EQ.EOFF(B))GOTO 806
  804 CONTINUE
      GOTO 810
  806 FILEN2(J,I)=0
      RECNO2(J,I)=0
  810 DO 807 A=1,NOSHOT
      IF (J.EQ.SHOTS(A))SHFLAG=1
  807 CONTINUE
      IF(SHFLAG.EQ.0) GOTO 904
C
      WRITE (7,901) J,COUNT, FILEN2(J,I), RECNO2(J,I),
     1OFF2(J,I),MF,NONE
  901 FORMAT(I4,I3,I3,I3,I4,I4,I4)
  904 SHFLAG=0
  905   CONTINUE
  910 CONTINUE
C
C ---------WRITE THE ZERO TO MARK THE END OF THE DATA SET----------
C
  619 WRITE(7,620)NONE
  620 FORMAT(I4)
      IF(SORT.EQ.0)GOTO 2000
```

```
C ---------WRITE SOME LINE DIAGNOSTICS-------------------------------
C
      NCDP=CDPMAX-(CDPMIN-1)
      WRITE(6,*)' '
      WRITE(6,*)'*********************************************'
      WRITE(6,*)' '
      WRITE(6,*)' SURVEY DIAGNOSTICS'
      WRITE(6,*)' ------------------'
      WRITE(6,*)'   There are ',NORECS,'seismograms'
      WRITE(6,*)'   There are ',NCDP,' possible cdps.'
      WRITE(6,*)'   from cdp nos ',CDPMIN,' to ',CDPMAX
      WRITE(6,*)'   With a fold of cover of ',KMAX
      WRITE(6,*)'     '
      WRITE(6,*)'Note: CDP nos. are twice true value due to value'
      WRITE(6,*)'      having to be an integer.'
      IF(YN.EQ.0)GOTO 710
      WRITE(6,*)'   Mute Function'
      WRITE(6,*)'   -------------'
      WRITE(6,*)'   offset        time (msec)'
      DO 700 I=1,OFN
      WRITE(6,*)MO(I),'    ',MT(I)
  700 CONTINUE
  710 WRITE(6,*)' '
      WRITE(6,*)'*********************************************'
      GOTO 3000
C
C ---------WRITE SOME LINE DIAGNOSTICS-------------------------------
C
 2000 NCDP=CDPMAX-(CDPMIN-1)
      WRITE(6,*)' '
      WRITE(6,*)'*********************************************'
      WRITE(6,*)' '
      WRITE(6,*)' SURVEY DIAGNOSTICS'
      WRITE(6,*)' ------------------'
      WRITE(6,*)'   There are ',NORECS,'seismograms'
      WRITE(6,*)'   Minimum shot no  ',CDPMIN
      WRITE(6,*)'   Maximum shot no  ',CDPMAX
      WRITE(6,*)'   Maximum no of traces from one shot point ',KMAX
      WRITE(6,*)'     '
      IF(YN.EQ.0)GOTO 1710
      WRITE(6,*)'   Mute Function'
      WRITE(6,*)'   -------------'
      WRITE(6,*)'   offset        time (msec)'
      DO 1700 I=1,OFN
      WRITE(6,*)MO(I),'    ',MT(I)
 1700 CONTINUE
 1710 WRITE(6,*)' '
      WRITE(6,*)'*********************************************'
 3000 STOP
      END
```

Program - EDITSORT

```
C     ****************************************************
C     This program is the edit program for the sort
C     File produced by SORTPROG
C     Unit 5  = The sort data file
C     Unit 6  = Terminal
```

```
C     Unit 7  = Edited sort data file
C     ********************************************************
C
      IMPLICIT INTEGER(A-Z)
      DIMENSION CDP(2000),TRACE(2000),FILE(2000),RECORD(2000),
     &OFFSET(2000),MUTE(2000),STATIC(2000),
     &EF(100),EFL(100),EIF(100),ETR(100),EOFF(100),
     &SF(100),ST(100),STATF(100),
     &O(100),M(100)
      NONE=0
      NUM=0
      READ(5,10)RATE
   10 FORMAT(I3)
    2 READ(5,1)C
      IF(C.EQ.0)GOTO 9
    1 FORMAT(I4)
      NUM=NUM+1
      GOTO 2
    9 REWIND (5)
      READ(5,11)RATE
      WRITE(7,11)RATE
   11 FORMAT(I3)
      DO 8 I=1,NUM
   12 READ(5,14)CDP(I),TRACE(I),FILE(I),RECORD(I),OFFSET(I),MUTE(I),
     &STATIC(I)
   14 FORMAT(I4,I3,I3,I3,I4,I4,I4)
    8 CONTINUE
   22 DO 20 I=1,30
      WRITE(6,*)'  '
   20 CONTINUE
      WRITE(6,*)'Editing & Static application '
      WRITE(6,*)'----------------------------'
      WRITE(6,*)' '
      WRITE(6,*)'Do you want to edit or insert static shifts ?'
      WRITE(6,*)'edit (enter 1)   static (enter 2)  mute (enter 3)'
      WRITE(6,*)'exit program and write out file (4)'
      READ(6,*)CHOICE
      GOTO(50,2000,4000,5000)CHOICE
   50 DO 53 I=1,30
      WRITE(6,*)'  '
   53 CONTINUE
      WRITE(6,*)' Do you want to edit a specific 12 channel file ? (1)'
      WRITE(6,*)' '
      WRITE(6,*)' Do you want to edit a specific trace ? (2)'
      WRITE(6,*)' '
      WRITE(6,*)' Do you want to edit a specific offset ? (3)'
      WRITE(6,*)' '
      READ(6,*)SWITCH
      GOTO(100,300,500)SWITCH
  100 WRITE(6,*)'How many files do yo want to edit ?'
      READ(6,*)N
      DO 108 J=1,N
      WRITE(6,*)'Enter the number of the file (integer)'
      READ(6,*)EF(J)
  108 CONTINUE
      DO 120 J=1,N
      DO 140 I=1,NUM
      IF(FILE(I).EQ.EF(J)) CALL ZERO(I,FILE,RECORD,OFFSET,MUTE,STATIC)
  140 CONTINUE
  120 CONTINUE
```

```
      GOTO 22
  300 WRITE(6,*)'How many individual traces do you want to remove ?'
      READ(6,*)N
      DO 320 I=1,N
      WRITE(6,*)'Input the file number and trace number'
      WRITE(6,*)'within that file'
      READ(6,*)EFL(I)
      READ(6,*)ETR(I)
  320 CONTINUE
      DO 340 J=1,N
      DO 360 I=1,NUM
      IF(FILE(I).EQ.EFL(J).AND.RECORD(I).EQ.ETR(J)) CALL ZERO (I,FILE,RE
     &CORD,OFFSET,MUTE,STATIC)
  360 CONTINUE
  340 CONTINUE
      GOTO 22
  500 WRITE(6,*)'How many offset do you want to edit out ?'
      READ(6,*)N
      DO 520 I=1,N
      WRITE(6,*)'Input the offset (meters)'
      READ(6,*)EOFF(I)
  520 CONTINUE
      DO 540 J=1,N
      DO 560 I=1,NUM
      IF(OFFSET(I).EQ.EOFF(J)) CALL ZERO(I,FILE,RECORD,OFFSET,MUTE,STATI
     &C)
  560 CONTINUE
  540 CONTINUE
      GOTO 22
 2000 DO 2002 I=1,30
      WRITE(6,*)' '
 2002 CONTINUE
      WRITE(6,*)'Do you want to apply a static shift ? (1)'
      WRITE(6,*)' '
      WRITE(6,*)'or add/subtract a number to an already existing'
      WRITE(6,*)'static ?  (2)'
      WRITE(6,*)' '
      READ(6,*)SC
      DO 2003 I=1,30
      WRITE(6,*)' '
 2003 CONTINUE
      WRITE(6,*)'Do you want to apply the static to a'
      WRITE(6,*)'specific 12 channel file (1) ?'
      WRITE(6,*)' '
      WRITE(6,*)'Do you want to apply a static '
      WRITE(6,*)'to a specific trace (2) ?'
      WRITE(6,*)' '
      READ(6,*)STATC
      GOTO(2010,2500)STATC
 2010 WRITE(6,*)'How many files do you want to apply ?'
      READ(6,*)N
      DO 2020 J=1,N
      WRITE(6,*)'Enter the number of the file '
      READ(6,*)SF(J)
      WRITE(6,*)'the static shift'
      READ(6,*)STATF(J)
 2020 CONTINUE
      DO 2100 J=1,N
      DO 2150 I=1,NUM
      IF(FILE(I).EQ.SF(J).AND.SC.EQ.1)CALL STATA(I,J,STATIC,STATF)
```

```
      IF(FILE(I).EQ.SF(J).AND.SC.EQ.2)CALL STATB(I,J,STATIC,STATF)
 2150 CONTINUE
 2100 CONTINUE
      GOTO 22
 2500 WRITE(6,*)'How many files do you want to apply ?'
      READ(6,*)N
      DO 2520 J=1,N
      WRITE(6,*)'Enter the number of the file '
      READ(6,*)SF(J)
      WRITE(6,*)'the trace no within the file'
      READ(6,*)ST(J)
      WRITE(6,*)'and the static shift'
      READ(6,*)STATF(J)
 2520 CONTINUE
      DO 2600 J=1,N
      DO 2650 I=1,NUM
      IF(FILE(I).EQ.SF(J).AND.ST(J).EQ.RECORD(I).AND.SC.EQ.1)CALL STATA(
     &I,J,STATIC,STATF)
      IF(FILE(I).EQ.SF(J).AND.ST(J).EQ.RECORD(I).AND.SC.EQ.2)CALL STATB(
     &I,J,STATIC,STATF)
 2650 CONTINUE
 2600 CONTINUE
      GOTO 22
 4000 DO 4002 I=1,30
      WRITE(6,*)'  '
 4002 CONTINUE
      WRITE(6,*)'Application of an offset dependant mute function'
      WRITE(6,*)'------------------------------------------------'
      WRITE(6,*)'  '
      WRITE(6,*)'How many offsets do you want to mute ?'
      READ(6,*)N
      DO 4020 J=1,N
      WRITE(6,*)'Input the offset (meters) & mute length (msecs)'
      READ(6,*)O(J)
      READ(6,*)M(J)
 4020 CONTINUE
      DO 4100 J=1,N
      DO 4150 I=1,NUM
      IF(O(J).EQ.OFFSET(I))MUTE(I)=M(J)
 4150 CONTINUE
 4100 CONTINUE
      GOTO 22
 5000 DO 5001 I=1,NUM
      WRITE(7,5014)CDP(I),TRACE(I),FILE(I),RECORD(I),OFFSET(I),MUTE(I),
     &STATIC(I)
 5014 FORMAT(I4,I3,I3,I3,I4,I4,I4)
 5001 CONTINUE
      WRITE(7,5002)NONE
 5002 FORMAT(I4)
      DO 5004 I=1,40
      WRITE (6,*)'  '
 5004 CONTINUE
      WRITE(6,*)'*** Data file written to unit 7 ***'
      DO 5005 I=1,20
      WRITE (6,*)'  '
 5005 CONTINUE
      STOP
      END
C
      SUBROUTINE ZERO(I,FILE,RECORD,OFFSET,MUTE,STATIC)
```

```
C      ***************
       IMPLICIT INTEGER (A-Z)
       DIMENSION FILE(200),RECORD(200),OFFSET(200),MUTE(200),STATIC(200)
       FILE(I)=0
       RECORD(I)=0
       OFFSET(I)=0
       MUTE(I)=0
       STATIC(I)=0
       RETURN
       END
C
       SUBROUTINE STATA(I,J,STATIC,STATF)
C      ****************
       INTEGER STATIC,STATF
       DIMENSION STATIC(200),STATF(200)
       STATIC(I)=STATF(J)
       RETURN
       END
C
       SUBROUTINE STATB(I,J,STATIC,STATF)
C      ****************
       INTEGER STATIC,STATF,ADD
       DIMENSION STATIC(200),STATF(200)
       ADD=STATIC(I)
       STATIC(I)=STATF(J)+ADD
       RETURN
       END
```

Program - SEGDSEGYMS

```
C      ************************************************************************
C      This program takes the digital data arranged in the original
C      field shooting order on a temorary disk file (Unit 7)
C      The first N samples of each trace can be zeroed to remove
C      refractions
C      The MUTE time is given in milliseconds
C      A +ve or -ve static shift can be applied to individual traces
C      -ve time shift toward time origin
C      The shift is in samples
C      The data is sorted into the order given in the SORT data file
C      (Unit 5)
C      Data outputed as a sorted SEG-Y tape on unit 8
C
C      This program is written in FORTRAN 77 using direct access
C      statements
C      ************************************************************************
C      PROGRAM BY P.BRABHAM (1984)
C
       INTEGER CDPN,CDPF,FN,FREC,OFFSET,RNO
       INTEGER*2 SEIS
       DIMENSION SEIS(1024),RSEIS(1024)
C
C      WRITE THE TAPE HEADER ONTO THE SEGY TAPE
C      ----------------------------------------
       CALL HEDA(2,8)
C
```

```
C      READ IN THE NO OF SAMPLES IN 1 MILLISECOND
C      ------------------------------------------
       READ(5,80)INSAMP
   80  FORMAT(I3)
C
C      CALCULATE SAMPLING FREQUENCY IN MICROSECS FOR HEADER
C      ---------------------------------------------------
       SF=(1/INSAMP)*1000
       ISF=INT(SF)
C
C      READ IN THE SORT PARAMETERS FROM UNIT 5
C      --------------------------------------
C        CDPN = Number of the CDP
C        CDPF = Record number within the CDP (smallest offset is trace 1)
C          FN = File number on the original SEG-D tape
C        FREC = Record number in the file ( 1 to 12 )
C      OFFSET = Shot to Geophone offset (meters)
C         RNO = Record number in the data file (Unit 7)
C       IMUTE = Trace zeroed from start to IMUTE msecs
C       ISTAT = Static shift -ve shift toward time zero
C               (*shift in samples * )
C
       ICOUNT=-1
C
C      OPEN FILE
C     * 2056 USED INSTEAD OF 2048 NUMAC FRIG FACTOR *
C      NUMAC BUG MAY BE RECTIFIED AT SOME DATE
C      Dont worry if program crashes, it took 3 weeks to
C      sort this one out
C
       IRECL=2056
       OPEN (UNIT=7,ACCESS='DIRECT',FORM='UNFORMATTED',RECL=IRECL)
C
  100  READ (5,10) CDPN,CDPF,FN,FREC,OFFSET,IMUTE,ISTAT
       ICOUNT=ICOUNT+1
   10  FORMAT(I4,I3,I3,I3,I4,I4,I4)
       RNO=(((FN-1)*12)+FREC)
       XSTAT=ISTAT/INSAMP
       IMUTES=INT(IMUTE+XSTAT+0.5)
C
C      GET THE RIGHT RECORD OFF UNIT 7 IF NO RECORD EXISTS THEN WRITE
C      A ZERO RECORD
C
       IF (CDPN .EQ. 0)GO TO 500
       IF (FN .EQ. 0 .AND. FREC .EQ. 0 ) GO TO 210
       WRITE(6,*)'**  Trace ',RNO,'  =   File  ',FN,'  trace  ',FREC
       READ(UNIT=7,REC=RNO) (SEIS(JK),JK=1,1024)
       DO 199 I=1,1024
       RSEIS(I)=SEIS(I)
  199  CONTINUE
C
C   ** APPLY THE MUTE IF REQUIRED ( IMUTE IN MILLISECONDS )
C   ** NOTE IMUTE IS IN MSECS
C
       IF(IMUTE.EQ.0)GOTO 200
       CALL MUTE(RSEIS,IMUTE,INSAMP)
C
C   ** APPLY THE STATIC SHIFT IF REQUIRED -VE SHIFT TRACE MOVED TOWARD ZERO
C   **  NOTE -->     *ISTAT IS IN MILLISECONDS*
C
```

```
  200 IF(ISTAT.EQ.0)GOTO 205
      CALL STATIC(RSEIS,ISTAT,INSAMP)
  205 ITY=1
      CALL SEGY(RSEIS,CDPN,CDPF,ITY,OFFSET,FN,FREC,ISF,IMUTES)
      GO TO 100
C
C     WRITE THE ZERO TRACE
C
  210 WRITE(6,*) '00   Zero  Trace    00 '
      DO 300 I=1,1024
      SEIS(I)=0
      RSEIS(I)=0.0
  300 CONTINUE
      ITY=2
      CALL SEGY(RSEIS,CDPN,CDPF,ITY,OFFSET,FN,FREC,ISF,IMUTES)
      GO TO 100
  500 WRITE(6,*)'ALL ',ICOUNT,' FILES HAVE BEEN WRITTEN TO TAPE'
      STOP
      END
C
      SUBROUTINE SEGY(SEIS,CDPN,CDPF,ITY,OFFSET,FN,FREC,ISF,IMUTES)
C     ****************
      INTEGER CDPN,CDPF,OFFSET,FN,FREC
      INTEGER*2 IHDR(120),ILEN
      DIMENSION ARRAY(1084),SEIS(1024)
      INTEGER HED(60)
      EQUIVALENCE (ARRAY(1),HED(1)),(HED(1),IHDR(1))
      DO 5 J=1,1084
5     ARRAY(J)=0.0
      DO 10 L=1,60
10    HED(J)=0
      DO 15 J=61,1084
   15 ARRAY(J)=SEIS(J-60)
C
      HED(3)=FN
      HED(4)=FREC
      HED(6)=CDPN
      HED(7)=CDPF
      HED(10)=OFFSET
      IHDR(15)=ITY
      IHDR(54)=0
      IHDR(56)=0
      IHDR(57)=IMUTES
      IHDR(58)=1024
      IHDR(59)=ISF
C
       ILEN=4*1024+240
       CALL WRITE(ARRAY,ILEN,0,LNUM,8)
      RETURN
      END
C
      SUBROUTINE HEDA(NIN, NOUT)
C     ****************
C     HEADER BLOCK TRANSFERS
C
      IMPLICIT INTEGER*2(I)
      DIMENSION TPHEDA(800)
      INTEGER TPHEDB(100)
C
C     READ THE EBCDIC HEADER
```

```
C
      ILEN = 3200
      CALL READ(TPHEDA, ILEN, 0, LNUM, NIN)
C
C     READ BINARY HEADER
C
      ILEN = 400
      CALL READ(TPHEDB, ILEN, 0, LNUM, NIN)
C
C     WRITE EBCDIC HEADER
C
      ILEN = 3200
      CALL WRITE(TPHEDA, ILEN, 0, LNUM, NOUT)
C
C     WRITE BINARY HEADER
C
      ILEN = 400
      CALL WRITE(TPHEDB, ILEN, 0, LNUM, NOUT)
      RETURN
      END
C
      SUBROUTINE STATIC(PSEIS,ISTAT,INSAMP)
C     ******************
      DIMENSION TSEIS(1024),PSEIS(1024)
      ISTATS=ISTAT
      WRITE(6,*)'++ Static shift ',ISTATS,'   samples  ++'
      IF(ISTATS.LT.0)GOTO 1040
      DO 1010 I=1,ISTATS
      TSEIS(I)=0.0
 1010 CONTINUE
      ISTART=ISTATS+1
      DO 1020 J=ISTART,1024
      K=J-ISTATS
      TSEIS(J)=PSEIS(K)
 1020 CONTINUE
      GOTO 2000
 1040 ISTATS=ABS(ISTATS)
      L=1024-ISTATS
      DO 1050  I=1,L
      K=I+ISTATS
      TSEIS(I)=PSEIS(K)
 1050 CONTINUE
      K=1024-ISTATS+1
      DO 1070 I=K,1024
      TSEIS(I)=0.0
 1070 CONTINUE
 2000 DO 2010 I=1,1024
      PSEIS(I)=TSEIS(I)
 2010 CONTINUE
      RETURN
      END
C
      SUBROUTINE MUTE(ASEIS,IMUTE,INSAMP)
C     ***************
      DIMENSION ASEIS(1024)
      NSAMP=IMUTE*INSAMP
      WRITE(6,*)'++ Mute 0 to ',IMUTE,' msecs = ',NSAMP,'  samples'
      DO 3000 I=1,NSAMP
        ASEIS(I)=0.0
 3000 CONTINUE
```

```
C
C     PUT A 7 SAMPLE COSINE TAPER ON AFTER THE MUTED SECTION
C
      J=NSAMP+1
      ASEIS(J)=ASEIS(J)*0.1736
      J=NSAMP+2
      ASEIS(J)=ASEIS(J)*0.342
      J=NSAMP+3
      ASEIS(J)=ASEIS(J)*0.50
      J=NSAMP+4
      ASEIS(J)=ASEIS(J)*0.6427
      J=NSAMP+5
      ASEIS(J)=ASEIS(J)*0.7660
      J=NSAMP+6
      ASEIS(J)=ASEIS(J)*0.8660
      J=NSAMP+7
      ASEIS(J)=ASEIS(J)*0.9396
      J=NSAMP+8
      ASEIS(J)=ASEIS(J)*0.9848
      RETURN
      END
```

APPENDIX D

TAPE FORMATS

The Nimbus DMT-911 digital magnetic tape recorder in conjunction with the Nimbus ES-1210F seismograph, was used throughout the duration of this project to record the seismic data. The digital recorder records the data in the SEG-D, de-multiplexed, IBM compatible format on 1600bpi, 9 track, 1/2" tape. The tape can be directly transferred onto tape drives on the NUMAC main frame computer at Durham University. The SEG-D format comprises of individual files containing 12 channels of seismic data, the files are separated by an end of file marker. Each file comprises of a 32 byte general file header that includes an automatically assigned sequential file number and a constants entry, this is followed by an inter-block gap, then the individual records. Each record comprises of a 20 byte trace header (unique to SEG-D format). The trace header precedes each channel's data, the header and the data are recorded as one data block. The DMT-911 sets no information into the trace header except the file number.

General Tape layout

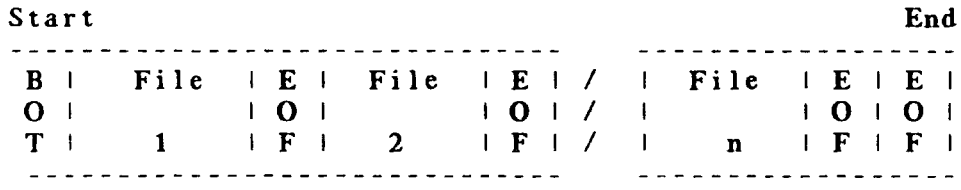

Individual file format

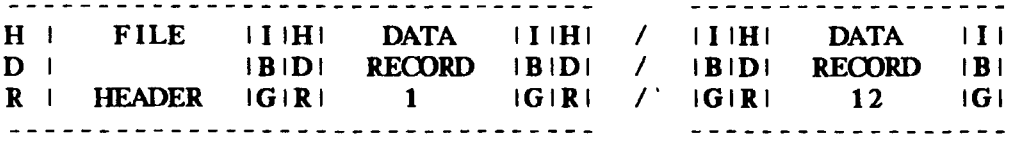

BOT - Beginning of tape marker EOF - End of file marker
IBG - Inter-block gap HDR - Trace header

Number Format

The Nimbus ES-1210F seismograph records 1024 samples per trace, each sample recorded on 10 bits, thus giving a sample value range from an integer value of -512 to +512.

The digital sample values are recorded in a 2 byte quaternary exponent form.

Bit	(msb) 0	1	2	3	4	5	6	(lsb) 7
1st byte	S	C2	C1	C0	Q1	Q2	Q3	Q4
2nd byte	Q5	Q6	Q7	Q8	Q9	Q10	Q11	Q12

The digital sample value is expressed as:

$$S.\ QQQQ,QQQQ,QQQQ,\ \times 4^{CCC} \times 2^{MP}$$

S is the sign bit.

For the ES-1210F seismograph, Q11 & Q12 are set to zero.

Q1 represents 2^{1} and Q2 represents 2^{2} etc.

C2, C1, C0 is always set to 6, so that the radix point is forced to the right of Q12 to permit processing of each datapoint as a 12 bit, one's complement integer.

MP is set to zero in the general header.

Decoding the sample value

When the SEG-D field tape is read on NUMAC the digital sample values will appear as meaningless numbers as NUMAC is trying to read the bits as a two's complement integer value. The number needs to be decoded, this is done by masking bits 2, 3 and 4 (the C values).

The FORTRAN 77 routine which does this is;

```
IF (NUMBER .GT. 1023) NUMBER = NUMBER - 24576
IF (NUMBER .LT.    0) NUMBER = NUMBER + 1
IF (NUMBER .LT.-1024) NUMBER = NUMBER + 4096
```

This decodes the numerical values to an integer range of -512 to +511.

REFERENCES

ACKERMANN H.D., PANKRATZ L.W. & DANSEREAU D., (1986)
Resolution of ambiguities of seismic refraction traveltime curves.
Geophysics, Vol. 51 No. 2, (Feb.86), p223-235

ANSON W.W. & SHARP J.I., (1960)
Surface and rock-head relief features in the northern part of the Northumberland coalfield.
University of Durham, Dept. of Geography, Research series No. 2

BAREFOOT M.J., (1978)
Geology applied in opencast working.
In. Industrial Geology, Ed. Knill J.L.
Oxford University Press, (1978).

BARFORD N.C., (1967)
Experimental Measurements : Precision, Error and Truth
Addison-Wesley Publishing Co. Ltd., (1967), 143pp

BARNETT J.A.M, FAIRBAIRN C.M, HOLT J.M, WARD W.A. & WESTERMAN A.R, (1986)
The balance between primary and short path multiple energy in coal measures reflection data : The evidence from British coalfields.
Paper at 48th meeting of E.A.E.G., Belgium, 3-6th June 1986.

BUSH J., (1985)
A short history of high technology in opencast mining surveying.
Land & Mineral Surveyor, Vol. 3, (January 1985).

CHESTER D.N., (1982)
"An initial investigation into shallow seismic surveying for opencast coal exploration".
(M. Sc. Dissertation, University of Durham).

DAMPNEY C.N.G. & WHITELY R.J., (1980)
Velocity determination and error analysis for the seismic refraction method.
Geophysical Prospecting, Vol. 28, (1980), p1-17.

DANKBAAR J.W.M., (1983)
High resolution shallow seismics.
Paper at, 53rd annual meeting of S.E.G., Las Vegas, Nevada September 11-15th 1983.

DAVIS A.M. & SCHULTHEISS P.J., (1980)
Seismic signal processing in engineering site investigation - A case history.
Ground Engineering, Vol. 13 No. 4 (1980), p44-48.

DAVISON D.J., (1977)
Opencast coal mining in the United Kingdom and its role in the mining industry.
Mining Engineer, Vol. 137 (November 1977), p215-221.

DE VOOGD N. & STAUDT CHR., (1982)
Research on the coal beneath the Netherlands II - Geological/Geophysical Reconnaissance
Geologie en Mijnbouw, 61 (1982), p359-365

DISON I. & WHITWORTH K.R., (1985)
Downhole logging - Extracting information from boreholes.
Colliery Guardian, August 1985, p400-408.

DOBRIN M.B., (1976)
Introduction to Geophysical Prospecting (3rd edition).
Mc Graw-Hill, (1976).

DOMZALSKI W., (1956)
Some problems of shallow refraction investigations.
Geophysical Prospecting, Vol. 4 (1956), p140-166.

DOORNENBAL J.C. & HELBIG K., (1983)
High resolution reflection seismics on a tidal flat in the Dutch Delta - acquisition, processing and interpretation.
First Break, May 1983, p9-20, E.A.E.G.

EASTWOOD T., DIXON E.E.L., HOLLINGSWORTH S.E. & SMITH B., (1931)
The geology of the Whitehaven and Workington District, Explanation of sheet 28, Geological survey of England & Wales.
H.M.S.O., (1931).

EDELMANN H.A.K. & HELBIG K., (1983)
Some aspects of field layout for shear wave surveys.
Paper at 53rd S.E.G. meeting, Las Vegas, Nevada, Sept.11-15th 1983

EDELMANN H.A.K. & SCHMOLL J., (1983a)
Seismic measurements with horizontally polarized shear waves.
Natural Res. & Develop., Vol. 18 (1983) 23S, p44-66.

EDELMANN H.A.K. & SCHMOLL J., (1983b)
Shear wave seismics - The fundamentals.
Prakla Seismos report 1+2/83, Prakla Seismos, Hannover, (1983).

EVISON F.F., (1956)
The seismic determination of Young's modulus and Poisson's ratio for rocks in situ.
Geotechnique, Vol. 6 (1956), p118-123.

FIELDING C.R., (1982)
"Sedimentology and stratigraphy of the Durham coal measures and comparisions with other British coalfields".
(Ph. D. Thesis, University of Durham).

FOWLER A., (1935)
The Geology of the Country around Rothbury, Amble and Ashington. Explanation of sheets 9 & 10, Memoirs of the Geological Survey of England & Wales.
H.M.S.O., (1935).

GARDENER L.W., (1939)
An areal plan of mappling subsurface structure by refraction shooting.
Geophysics, Vol. 4 (1939), p247-259.

GARDENER L.W. (1967)
Refraction seismograph profile interpretation,
In. Seismic Refraction Prospecting, Ed. Musgrave A.W.,
Soc. of Exploration Geophysicists, Tulsa, (1967), p338-347.

GILBERT K.A., (1984)
"Studies of the coal measures using shallow seismic refraction and resistivity methods".
(B. Sc. Dissertation, University of Durham).

GOOSENS R, (1985)
Exploration in the U.K.
Colliery Guardian, August 1985, p331-334.

GOULTY N.R., (1983)
Seismic surveying over Bunter sandstone.
First Break, July 1983, p17-23, E.A.E.G.

GOULTY N.R. & BRABHAM P.J., (1984)
Seismic refraction profiling in opencast exploration.
First Break, May 1984, p26-34, E.A.E.G.

GOULTY N.R., DALEY T.E., WALTERS K.G. & EMSLEY D.B., (1984)
Location of dykes in coalfield exploration.
First Break, December 1984, p15-21, E.A.E.G.

GREEN R., (1974)
The seismic refraction method - a review.
Geoexploration, Vol. 12 (1974), p259-284.

GREENHALGH S.A., SUPRAJITNO M., & KING D.W., (1986)
Shallow seismic reflection investigations of coal in the Sydney basin.
Geophysics, Vol. 51 No. 7 (July 1986), p1426-1437

GREAVES R.J., (1984)
Coal prospect evaluation using high-resolution reflection seismology-a case study.
Geophysics:The leading edge of exploration, October 1984, p44-47

HAGEDOORN J.G., (1957)
The Plus-Minus method of interpreting seismic refraction lines.
Geophysical Prospecting, Vol. 7 (1957), p158-182.

HALES F.W., (1958)
An accurate graphical method for interpreting seismic refraction lines.
Geophysical Prospecting, Vol. 6 (1958), p285-294.

HARMAN P., (1981)
High resolution seismic reflection techniques in the coal industry.
Austrailian Coal Geology, Vol. 3 Pt. 1 (1981), p3-14.

HASBROUCK W.P. & PADGET N, (1982)
Use of shear wave seismics in evaluation of strippable coal resources.
Utah Geological & Mineral Survey, Bulletin 118 (1982), p203-210.

HATHERLY P.J. & NEVILLE M.J., (1986)
Experience with the Generalized Reciprocal Method of seismic refraction interpretation for shallow engineering site investigation
Geophysics, Vol. 51 No. 2 (Feb.86), p255-265.

HAWKINS L.V., (1961)
The Reciprocal method of routine shallow seismic refraction investigations.
Geophysics, Vol. 6 (1961), p806-819.

HELBIG K. & MESDAG C.S., (1982)
The potential of shear wave observations.
Geophysical Prospecting, Vol. 30 (1982), p413-431.

HUGHES V.J. & KENETT B.L.N., (1983)
The nature of seismic reflections from coal seams.
First Break, February 1983, p9-18, E.A.E.G.

HUNTER J.A, PULLAN S.E, BURNS R.A. GAGNE R.M. & GOOD R.L, (1984)
Shallow seismic reflection mapping of the overburden-bedrock interface with the engineering seismograph-some simple techniques.
Geophysics, Vol. 49 No. 8 (Aug.1984), p1381-1385.

KNAPP R.W. & STEEPLES D.W., (1986a).
High resolution common-depth-point reflection profiling : Instrumentation
Geophysics, Vol. 51 No. 2 (Feb.86), p276-282.

KNAPP R.W. & STEEPLES D.W., (1986b).
High resolution common-depth-point reflection profiling : Field acquisition parameter design.
Geophysics, Vol. 51 No. 2 (Feb.86), p283-294.

LANKSTON R.W. & LANKSTON M.M., (1986)
Obtaining multilayer reciprocal times through phantoming.
Geophysics, Vol. 51 No. 1 (Jan.86), p45-49.

LOVERIDGE M.M., (1981)
"Residual static corrections".
(M.Sc. Dissertation, University of Durham).

Mc CANN D.M., ANDREW E.M., & Mc CANN C., (1985)
Seismic sources for shallow reflection surveying.
Geophysical Prospecting, Vol. 33 (1985), p943-955.

MORRIS D.V. & ABBISS C.P., (1979)
Static modulus of Gault clay predicted from seismic tests.
Ground Engineering, Vol. 12 No. 8 (1979), p44-50.

MOSELEY F., (1978)
The Geology of the Lake District.
Yorkshire Geological Society, occasional publication No.3 (1978).

N.C.B., (1975)
Subsidence Engineers Handbook.
NCB publication, Hobart House, London, (1975).

NORTHWOOD E.J., (1967)
Errors in refraction interpretation.
In. Seismic Refraction Prospecting, Ed. Musgrave A.W.
Soc. of Exploration Geophysicists, Tulsa, U.S.A., (1967), p459-465

NUNN K.R. & BOZTAS M., (1977)
Shallow seismic reflection profiling on land using a controlled source.
Geoexploration, Vol.15 (1977), p87-97.

PALMER D., (1980)
The Generalized Reciprocal Method of Seismic Refraction Interpretation, Ed. Burke K.B.S.
Soc. of Exploration geophysicists, Tulsa, USA.

PALMER D., (1981)
An introduction to the Generalized Reciprocal Method of seismic refraction interpretation.
Geophysics, Vol. 46 No. 11 (Nov.1986), p1508-1518.

PALMER D., (1983)
Comment on "Curved raypath interpretation of seismic refraction data", by S.A. Greenhalgh and D.W. King.
Geophysical Prospecting, Vol. 31 (1983), p542-543.

POULTER M.J., (1982)
"The design and implementation of the Durham University seismic processing system".
(Ph.D. Thesis, University of Durham).

RAVENS J., (1983)
"Surface consistent static corrections".
(M.Sc. Dissertation, University of Durham).

ROCKWELL D.W., (1967)
A general wavefront method.
In. Seismic Refraction Prospecting, Ed. Musgrave A.W.
Soc. of Exploration Geophysicists, Tulsa, USA, (1967), p365-415.

ROGERS A.W., (1981)
Determination of static corrections.
In Developments in Geophysical Exploration Methods - 2.
Ed. Fitch A.A.
Applied Science Publishers Ltd., London. p1-36

RUTER H. & SCHEPERS R., (1978)
Investigation of the seismic response of cyclically layered Carboniferous rock by means of synthetic seismograms.
Geophysical Prospecting, Vol. 26 (1978), p29-47.

RUTER H. & SCHEPERS R., (1985)
Is it possible to increase the resolution in seismic exploration coal by using high frequency signals ?
Geophysical Prospecting, Vol. 33 (1985), p1160-1173

SAMPSON R.J., (1975)
Surface II Graphics System.
Kansas Geological Survey, Kansas, USA, 66044.

SCHLICKER H. & BONING G., (1981)
Reflection seismics and wireline coring : Two optimal systems for exploring the Saar coal deposit.
In Coal Exploration 3, Ed. G.O. Argall Jr., Papers in the 3rd international coal exploration symposium.
Calgary, Alberta, Canada, (August 1981).

SINGH S., (1986)
Reflection window mapping of shallow bedrock.
Geophysical Prospecting, Vol. 34 (1986), p492-507.

SJOGREN B., (1979)
Refractor velocity determination - cause and nature of some errors.
Geophysical Prospecting, Vol. 27 (1979), p507-538.

SJOGREN B., (1980)
The law of parallelism in refraction shooting.
Geophysical Prospecting, Vol. 28 (1980), p716-743.

SJOGREN B., (1984)
Shallow Refraction Seismics.
Cambridge University Press, (1984).

SPOONER J., BREWIS T., KENNEDY A., MARSHMAN R., ELLIS R., HINDE C., ROSIN N., BAILEY J. & CAMPBELL K., (1985).
Mining Annual Review 1985.
Mining Journal Ltd.

STUMPEL H., KAHLER S., MEISSNER R. & MILKEREIT B., (1984)
The use of seismic shear waves and compressional waves for lithological problems of shallow sediments.
Geophysical Prospecting, Vol. 32 (1984), p662-675.

TELFORD W.M., GELDART L.P., SHERIFF R.E. & KEYS D.A., (1976)
Applied Geophysics
Cambridge University Press, (1976), 860pp.

THORNBURGH H.R., (1930)
Wavefront diagrams in seismic exploration.
Bull. Am. Assoc. Petrol. Geol., Vol. 14 (1930), p185-200

VAN REIL W.J., (1965)
Synthetic seismograms applied to the seismic investigation of a coal basin.
Geophysical Prospecting, Vol. 13 (1965), p105-121.

WARD C.R., (1984)
Coal Geology and Coal Technology.
Blackwell Scientific Publications, (1984), 334pp.

WATERS K.H., (1978)
Reflection Seismology.
John Wiley & Sons Inc., (1978), 377pp.

WEIST B. & EDELMANN H.A.K., (1984)
Static corrections for shear wave sections.
Geophysical Prospecting, Vol. 32 (1984), p1091-1102

WOOLLETT R.W, (1985)
"A geophysical investigation of the Southern Uplands fault and adjacent igneous intrusions, New Cumnock, Ayrshire".
(B.Sc. Dissertation, University Of Durham).

ZIOLKOWSKI A., (1979)
Seismic profiling for coal on land.
In. Developments in Geophysical Exploration Methods - 1
Ed. A.A. Fitch.
Applied Science Publishers Ltd., London, (1979), p271-306.

ZIOLKOWSKI A. & LERWILL W.E., (1979)
A simple approach to high resolution seismic profiling for coal.
Geophysical Prospecting, Vol. 27 (1979), p360-393.

ZIOLKOWSKI A., (1981)
Seismic surveying in the British coalfields.
Mining Engineer, 234 (March 1981), p605-615

HOBBS R.W, (1985)
"Processing of a Multichannel Seismic Reflection Survey in the Hebridean Region with Special Emphasis on improvements in Velocity Analysis".
(Ph. D. Thesis, University of Durham).

MUNRO D.M, (1982)
FORTRAN 77
Edward Arnold, 1982